LAPPEENRANTA
UNIVERSITY OF TECHNOLOGY

*Antti Kosonen*

# POWER LINE COMMUNICATION IN MOTOR CABLES OF VARIABLE-SPEED ELECTRIC DRIVES − ANALYSIS AND IMPLEMENTATION

Supervisor      Professor Jero Ahola
Faculty of Technology
Department of Electrical Engineering
Lappeenranta University of Technology
Lappeenranta, Finland


Reviewers     D.Sc., Docent Marko Hinkkanen
Faculty of Electronics, Communications and Automation
Helsinki University of Technology
Helsinki, Finland

Professor Lauri Sydänheimo
Institute of Electronics, Rauma Research Unit
Tampere University of Technology
Tampere, Finland


Opponent     D.Sc., Docent Janne Väänänen
The Berggren Group
Helsinki, Finland

# ABSTRACT

Antti Kosonen

**Power line communication in motor cables of variable-speed electric drives − analysis and implementation**

Data transmission between an electric motor and a frequency converter is required in variable-speed electric drives because of sensors installed at the motor. Sensor information can be used for various useful applications to improve the system reliability and its properties. Traditionally, the communication medium is implemented by an additional cabling. However, the costs of the traditional method may be an obstacle to the wider application of data transmission between a motor and a frequency converter. In any case, a power cable is always installed between a motor and a frequency converter for power supply, and hence it may be applied as a communication medium for sensor level data.

This thesis considers power line communication (PLC) in inverter-fed motor power cables. The motor cable is studied as a communication channel in the frequency band of 100 kHz−30 MHz. The communication channel and noise characteristics are described. All the individual components included in a variable-speed electric drive are presented in detail. A channel model is developed, and it is verified by measurements. A theoretical channel information capacity analysis is carried out to estimate the opportunities of a communication medium.

Suitable communication and forward error correction (FEC) methods are suggested. A general method to implement a broadband and Ethernet-based communication medium between a motor and a frequency converter is proposed. A coupling interface is also developed that allows to install the communication device safely to a three-phase inverter-fed motor power cable. Practical tests are carried out, and the results are analyzed. Possible applications for the proposed method are presented. A speed feedback motor control application is verified in detail by simulations and laboratory tests because of restrictions for the delay in the feedback loop caused by PLC. Other possible applications are discussed at a more general level.

Keywords: Power line communication, motor cable, frequency converter, electric motor, channel model, condition monitoring, speed control, HomePlug

UDC 621.314.26 : 621.313.3 : 004.7 : 681.5

*"Make everything as simple as possible, but not simpler."*

*Albert Einstein (1879–1955)*

# ACKNOWLEDGEMENTS

Lappeenranta, September 2008

Antti Kosonen

# LIST OF PUBLICATIONS

I   A. Kosonen, M. Jokinen, V. Särkimäki, J. Ahola, and M. Niemelä, "Motor Feedback Speed Control by Utilizing the Motor Feeder Cable as a Communication Channel," in *Proc. of 18<sup>th</sup> International Symposium on Power Electronics, Electrical Drives, Automation and Motion (SPEEDAM)*, Taormina (Sicily), Italy, May 2006, pp. 131−136.

II   J. Ahola, A. Kosonen, J. Toukonen, and T. Lindh, "A New Approach to Data Transmission between an Electric Motor and an Inverter," in *Proc. of 18<sup>th</sup> International Symposium on Power Electronics, Electrical Drives, Automation and Motion (SPEEDAM)*, Taormina (Sicily), Italy, May 2006, pp. 126−130.

III   A. Kosonen, J. Ahola, and M. Jokinen, "Modelling the RF Signal Propagation in the Motor Feeder Cable," in *Proc. of Nordic Workshop on Power and Industrial Electronics (NORPIE)*, Lund, Sweden, June 2006, 5 p.

IV   A. Kosonen, M. Jokinen, J. Ahola, and M. Niemelä, "Real-Time Induction Motor Speed Control with a Feedback Utilizing Power Line Communications and Motor Feeder Cable in Data Transmission," in *Proc. of the 32<sup>nd</sup> Annual Conference of the IEEE Industrial Electronics Society (IECON)*, Paris, France, November 2006, pp. 638−643.

V   A. Kosonen, M. Jokinen, J. Ahola, and M. Niemelä, "Performance Analysis of Induction Motor Speed Control Method that Utilizes Power Line Communication," *International Review of Electrical Engineering (I.R.E.E.)*, Vol. 1, No. 5, November/December 2006, pp. 684−694.

VI   A. Kosonen, J. Ahola, and P. Silventoinen, "Measurements of HF Current Propagation to Low Voltage Grid through Frequency Converter," in *Proc. of the 12<sup>th</sup> European Conference on Power Electronics and Applications (EPE)*, Aalborg, Denmark, September 2007, 10 p., CD-ROM.

VII   A. Kosonen, M. Jokinen, J. Ahola, M. Niemelä, and J. Toukonen, "Ethernet-Based Broadband Power Line Communication between Motor and Inverter," *IET Electric Power Applications*, Vol. 2, No. 5, September 2008, pp. 316−324.

The publications are in the chronological order, in which they have been published. In this dissertation, these publications are referred to as Publication I, Publication II, Publication III, Publication IV, Publication V, Publication VI, and Publication VII.

# CONTENTS

# ABBREVIATIONS AND SYMBOLS

**Roman letters**

| | |
|---|---|
| $a$ | attenuation parameter |
| $c$ | distributed capacitance |
| $c_0$ | speed of light in vacuum |
| $d$ | path length |
| $e$ | added redundant symbols |
| $e_{era}$ | number of erasures |
| $e_{err}$ | number of errors |
| $f$ | frequency |
| $f_h$ | highest frequency |
| $f_l$ | lowest frequency |
| $f_{out}$ | output frequency |
| $f_r$ | resonance frequency |
| $f_{sw}$ | switching frequency |
| $g$ | distributed conductance, weighting factor |
| $h$ | impulse response |
| $i$ | index |
| $j$ | index |
| $k$ | index, message length, number of shift registers |
| $l$ | distributed inductance |
| $m$ | message bits, number of bits, state number |
| $n$ | code word length, index, noise signal, number of mod-2 summers |
| $n_n$ | nominal rotation speed |
| $r$ | distributed resistance, received signal |
| $r_b$ | bit rate |
| $s$ | injected signal |
| $t$ | time |
| $t_r$ | rising time |
| $v_p$ | propagation velocity |
| $x$ | data sequence |
| $\mathbf{x}$ | coefficient of IDFT |
| $y$ | output sequence |
| $\mathbf{A}$ | frequency dependent coefficient matrix |
| $B$ | bandwidth |
| $\mathbf{B}$ | frequency dependent coefficient matrix |
| $C$ | capacitance, channel capacity |
| $\mathbf{C}$ | frequency dependent coefficient matrix |
| $C_{coup}$ | high frequency capacitance of coupling interface |
| $C_{dudt}$ | high frequency capacitance of output filter |
| $C_{DC\ link}$ | high frequency capacitance of DC link |
| $C_{IGBT}$ | high frequency capacitance of IGBT |
| $C_{motor}$ | high frequency capacitance of motor |
| $C_n$ | nominal capacitance |
| $\mathbf{D}$ | frequency dependent coefficient matrix |

| | |
|---|---|
| $E_\mathrm{b}$ | bit energy |
| $\mathbf{H}$ | transfer function of communication channel |
| $\mathbf{I}_\mathrm{in}$ | input current |
| $I_\mathrm{n}$ | nominal current |
| $\mathbf{I}_\mathrm{out}$ | output current |
| $L$ | cable length, inductance |
| $L_\mathrm{coup}$ | high frequency inductance of coupling interface |
| $L_\mathrm{dudt}$ | high frequency inductance of output filter |
| $L_\mathrm{DC\,link}$ | high frequency inductance of DC link |
| $L_\mathrm{IGBT}$ | high frequency inductance of IGBT |
| $L_\mathrm{motor}$ | high frequency inductance of motor |
| $L_\mathrm{n}$ | nominal inductance |
| $N$ | length of data set, noise power |
| $N_0$ | noise energy |
| $P_\mathrm{n}$ | nominal power |
| $P_\mathrm{tx}$ | transmission power |
| $P_\mathrm{tx,tot}$ | total transmission power |
| $R_\mathrm{c}$ | code rate |
| $R_\mathrm{coup}$ | high frequency resistance of coupling interface |
| $R_\mathrm{dudt}$ | high frequency resistance of output filter |
| $R_\mathrm{DC\,link}$ | high frequency resistance of DC link |
| $R_\mathrm{IGBT}$ | high frequency resistance of IGBT |
| $R_\mathrm{motor}$ | high frequency resistance of motor |
| $S$ | signal power |
| $S_{11}$ | scattering parameter for power reflection coefficient at input port |
| $S_{12}$ | scattering parameter for power attenuation from output port to input port |
| $S_{21}$ | scattering parameter for power attenuation from input port to output port |
| $S_{22}$ | scattering parameter for power reflection coefficient at output port |
| $\mathbf{T}$ | transmission matrix |
| $T_\mathrm{n}$ | duration of noise symbol |
| $T_\mathrm{s}$ | duration of data symbol |
| $U_\mathrm{C}$ | collector voltage |
| $U_\mathrm{E}$ | emitter voltage |
| $U_\mathrm{G}$ | gate voltage |
| $\mathbf{U}_\mathrm{in}$ | input voltage |
| $\mathbf{U}_\mathrm{n,rx}$ | noise voltage at receiver end |
| $U_\mathrm{n}$ | nominal voltage |
| $\mathbf{U}_\mathrm{out}$ | output voltage |
| $\mathbf{U}_\mathrm{rx}$ | voltage at receiver end |
| $\mathbf{U}_\mathrm{s}$ | source voltage |
| $\mathbf{U}_\mathrm{tx}$ | voltage at transmitter end |
| $\mathbf{X}$ | coefficient of DFT |
| $\mathbf{Z}_0$ | characteristic impedance |
| $\mathbf{Z}_\mathrm{access}$ | access impedance |
| $\mathbf{Z}_\mathrm{C}$ | impedance of capacitor |
| $\mathbf{Z}_\mathrm{cable,open}$ | input impedance of cable with other end open |
| $\mathbf{Z}_\mathrm{cable,sc}$ | input impedance of cable with other end short-circuited |

| $\mathbf{Z}_{\text{IGBT,on}}$ | impedance of IGBT when it is on |
|---|---|
| $\mathbf{Z}_{\text{IGBT,off}}$ | impedance of IGBT when it is off |
| $\mathbf{Z}_{\text{in}}$ | input impedance |
| $\mathbf{Z}_{\text{in,tx}}$ | input impedance at transmitter |
| $\mathbf{Z}_{\text{load}}$ | load impedance |
| $\mathbf{Z}_{\text{L}}$ | impedance of inductor |
| $\mathbf{Z}_{\text{P}}$ | parallel impedance |
| $\mathbf{Z}_{\text{S}}$ | serial impedance |

**Greek letters**

| $\alpha$ | attenuation coefficient |
|---|---|
| $\beta$ | propagation coefficient |
| $\varphi$ | phase angle |
| $\gamma$ | propagation constant |
| $\boldsymbol{\mu}$ | complex permeability |
| $\mu'$ | real part of complex permeability |
| $\mu''$ | imaginary part of complex permeability |
| $\tau$ | delay in feedback loop |
| $\omega$ | angular frequency |
| $\boldsymbol{\Gamma}_{\text{R}}$ | reflection coefficient |

**Acronyms**

| ADSL | Asymmetric Digital Subscriber Line |
|---|---|
| AE | Acoustic Emission |
| AES | Advanced Encryption Standard |
| AM | Amplitude Modulation |
| ARQ | Automatic Repeat Request |
| ASIC | Application-Specific Integrated Circuit |
| ASK | Amplitude Shift Keying |
| AWGN | Additive White Gaussian Noise |
| BCH | Bose-Chaudhuri-Hocquenghem |
| BER | Bit Error Ratio |
| BPL | Broadband over Power Line |
| BPSK | Binary Phase Shift Keying |
| CATV | Cable Television |
| CD | Compact Disc |
| CEBus | Consumer Electronic Bus |
| CENELEC | Comité Européen de Normalisation Electrotechnique |
| CEPCA | Consumer Electronics Powerline Communication Alliance |
| CIFS | Contention Inter-Frame Space |
| CP | Cyclic Prefix |
| CSMA | Carrier Sense Multiple Access |
| CSMA/CA | Carrier Sense Multiple Access with Collision Avoidance |
| CSMA/CD | Carrier Sense Multiple Access with Collision Detection |
| CTP | Carrier Transmission over Power lines |
| DBPSK | Differential Binary Phase Shift Keying |

| | |
|---|---|
| DES | Data Encryption Standard |
| DFT | Discrete Fourier Transform |
| DMT | Discrete Multitone |
| DQPSK | Differential Quadrature Phase Shift Keying |
| DSL | Digital Subscriber Line |
| DSP | Digital Signal Processor |
| DTC | Direct Torque Control |
| DVB-T | Digital Video Broadcasting – Terrestrial |
| DVD | Digital Versatile Disc |
| EFG | End of Frame Gap |
| EIA | Electronic Industries Alliance |
| EMI | Electromagnetic Interference |
| EtherCAT | Ethernet for Control Automation Technology |
| ETSI | European Telecommunications Standards Institute |
| FEC | Forward Error Correction |
| FFT | Fast Fourier Transform |
| FSK | Frequency Shift Keying |
| FTP | File Transmission Protocol |
| HF | High Frequency |
| HTTP | Hypertext Transfer Protocol |
| HV | High Voltage |
| ICI | Inter-Carrier Interference |
| ICMP | Internet Control Message Protocol |
| IDFT | Inverse Discrete Fourier Transform |
| IFFT | Inverse Fast Fourier Transform |
| IGBT | Insulated Gate Bipolar Transistor |
| IGMP | Internet Group Management Protocol |
| IP | Internet Protocol |
| ISI | Inter-Symbol Interference |
| LAN | Local Area Network |
| LF | Low Frequency |
| LonWorks | Local Operation Networks |
| LTI | Linear Time-Invariant |
| LV | Low Voltage |
| MAC | Medium Access Control |
| MF | Medium Frequency |
| MV | Medium Voltage |
| OFDM | Orthogonal Frequency Division Multiplexing |
| OPERA | Open PLC European Research Alliance |
| PCC | Parallel Concatenated Codes |
| PE | Protective Earth |
| PHY | Physical Layer |
| PI | Proportional-Integral |
| PLC | Power Line Communication |
| PMSM | Permanent Magnet Synchronous Machine |
| PRP | Priority Resolution Period |
| PRS | Priority Resolution Signal |

| | |
|---|---|
| PSD | Power Spectral Density |
| PSK | Phase Shift Keying |
| PVC | Polyvinyl Chloride |
| PWM | Pulse Width Modulation |
| QAM | Quadrature Amplitude Modulation |
| QoS | Quality of Service |
| QPSK | Quadrature Phase Shift Keying |
| RCS | Ripple Carrier Signalling |
| RF | Radio Frequency |
| RIFS | Response Inter-Frame Space |
| RMS | Root Mean Square |
| ROBO | Robust OFDM |
| RS | Reed-Solomon |
| RSC | Recursive Systematic Convolutional |
| RTE | Real-Time Ethernet |
| SIR | Signal-to-Interference Ratio |
| SNR | Signal-to-Noise Ratio |
| TCP/IP | Transmission Control Protocol/Internet Protocol |
| TEM | Transverse Electromagnetic |
| TM | Tone Map |
| UDP | User Datagram Protocol |
| USB | Universal Serial Bus |
| WLAN | Wireless Local Area Network |

# 1  INTRODUCTION

During the last few decades, power line communication (PLC) has been widely applied both in electricity and indoor distribution networks in different kinds of applications. However, little attention has been paid to the research of industrial applications. This chapter highlights the background and motivation for the work carried out in this dissertation. First, the history of PLC is outlined. Next, some general aspects about the PLC are addressed. Then, a summary section is provided and the appended original publications are introduced. Finally, scientific contributions of this dissertation are discussed.

## 1.1  History of power line communication

According to Brown (1999), the idea of utilizing power lines for communication is a very old invention. In 1838, the first remote electricity supply metering for the purpose of checking the voltage levels of batteries at an unmanned site in the London-Liverpool telegraph system was proposed by Edward Davy (Fahie, 1883). In 1897, the first PLC patent on a power line signalling electricity meter was applied by Joseph Routin and C. E. L. Brown in Great Britain (Routin and Brown, 1897). In 1905, the remote reading of electricity meters using an additional signalling wire was patented by Chester Thoradson in the USA (Thoradson, 1905). In 1913, the first commercial products of electromechanical meter repeaters were launched.

In 1920, the carrier frequency transmission of voice over high voltage (HV) power lines was started. Carrier transmission over power lines (CTP) was of importance because of management and monitoring tasks, and on the other hand, at the beginning of electrification, there was no full-coverage telephone network available. The applied frequencies for CTP were 15−500 kHz, the lower frequency being limited because of the cost for coupling equipment. The size of the coupling capacitor for HV can be seen in Fig. 1.1. HV overhead lines were relatively good waveguides for CTP at these frequencies, and hence it was possible to bridge the enormous distance of 900 km with the transmission power of 10 W (40 dBm) under favourable circumstances. First, only amplitude modulation (AM) was applied, because it was a simple solution and optimal for voice transmission (Dostert, 2001).

Fig. 1.1: Coupling capacitors in the HV distribution network.

From 1930 onwards, ripple carrier signalling (RCS) was applied in the medium (MV) and low voltage (LV) networks. The main tasks were load distribution including the avoidance of extreme load peaks and smoothing of the load curve. In contrast to HV overhead lines, MV and LV networks were a poor medium because of a large number of branches. The transmission power had to be fitted according to the peak load of the network, because RCS worked in the low frequency range of approximately 125−3000 Hz. Hence, the transmission power was enormous, in practice around 0.1−0.5 % of the maximum apparent power transmitted by the network that corresponded the power levels of around 10−100 kW (70−80 dBm). The applied carrier frequencies enabled information to flow over transformers between MV and LV networks with minor attenuation. In addition, the data rates were low and the data transmission was unidirectional from the power supply company to the consumers. RCS was used to transmit digital information with amplitude shift keying (ASK) and frequency shift keying (FSK) methods. ASK was widely used, but FSK did not gain ground (Dostert, 2001).

The development of modulation methods and the use of higher frequencies in the carrier signal enabled higher data transmission rates and decreased the required transmission power. Also bidirectional data transmission was generalized. By the late 1980s and the early 1990s, quite sophisticated error control coding techniques and their subsequent implementation into low-cost microcontrollers within the hardware of PLC modems were proposed. Also the benefits of using power lines for data transmission indoors were considered along with the development of Internet. Several technologies that apply PLC were presented during the last few decades. These include, for example, X10, MELKO™, LonWorks, CEBus, INSTEON, and HomePlug®.

The X10 standard was developed by Pico Electronics in 1975. X10 is an international and open industry standard for communication among electronic devices used for home automation. It primarily uses LV power lines for signalling and control. The digital data is encoded onto a 120 kHz carrier that is transmitted as bursts during zero crossings of AC voltage in the mains network (X10, 2008). A single bit is transmitted at each zero crossing, and hence data rates of 100 bps and 120 bps are possible in 50 Hz and 60 Hz electric networks, respectively.

The Enermet MELKO™ system was published in 1984. It utilizes phase shift keying (PSK) modulation and the frequency band of 3025−4825 Hz for data transmission. With this configuration, the data transmission rate of 50 bps is possible in MV and LV distribution networks between a substation and measurement or control units. Because of the low frequency band, the carrier signal can pass through the distribution transformers. MELKO™ is also capable of bidirectional data transmission. The main applications are remote meter reading and load management.

The local operation networks (LonWorks) platform was created by Echelon in 1990 (Echelon, 2008). It is a robust, flexible, and expandable standard-based control networking platform, upon which manufacturers can build products and applications. The physical layer (PHY) signalling can be implemented over the media such as a twisted pair, a power line, fibre optics, and radio frequency (RF). The LonWorks enables information-based control systems in contrast to the previous command-based control systems. The LonWorks PLC technology offers data transmission rate of either 5.4 or 3.6 kbps depending on the frequency. Applications using LonWorks technology are, for example, lighting control, energy management, security, and home automation systems.

In 1984, the members of the Electronic Industries Alliance (EIA) identified the need for standards that include more capability than the standard X10 (EIA, 2008). The consumer electronic bus (CEBus) standard was released in 1992; it is also known as EIA-600. CEBus defines protocols for products to communicate through a power line, a twisted pair, a coaxial cable, infrared, RF, and fibre optics. The standard includes spread spectrum modulation on power lines in the frequency band of 100−400 kHz. CEBus is a packet-oriented, connectionless, and peer-to-peer network. It is intended for devices to transmit commands and data. CEBus is suitable mainly in indoor applications.

INSTEON is a home automation networking technology introduced by SmartLabs, Inc. in 2001. It is developed for domestic control and sensing applications. It is based on the X10 standard. INSTEON technology is a dual-band mesh topology enabling simple devices to be networked together using power lines and/or RF, and it is thereby less susceptible than other single band networks to the noise interferences. PLC uses the frequency of 131.65 kHz and binary phase shift keying (BPSK) modulation. INSTEON technology includes error detection and correction. It is backward compatible with X10 and offers an instantaneous data rate of about 12.9 kbps and a continuous data rate of 2.8 kbps. INSTEON devices are also peers, in which each device can transmit, receive, and repeat messages of the INSTEON protocol without any additional network devices or software. The main applications are, for example, control systems, home sensors, energy savings, and access control (INSTEON, 2008).

In the recent decade, the applied frequency bands have been extended from kilohertz to megahertz frequencies. The development of new processor, digital signal processing, and algorithm techniques have made it possible to apply more sophisticated modulation and error control coding methods in embedded systems. Both the extended frequency bands and new technologies have enabled broadband communication over power lines. Radio amateurs have protested against PLC because of using the same high frequency (HF) band as they do. Also the outdated regulations have slowed down the use of megahertz frequencies in PLC. However, the development of Internet has stimulated to invent new ways to transmit information to all households. Nowadays, the electricity network covers almost all households, and using the public electricity and indoor distribution networks for broadband communication has therefore gained ground. The suitable communication techniques have been intensively investigated; here, also the development of wireless communication is acknowledged. Power line channel

characteristics have also been widely researched, the study being now extended up to 30 MHz. Several application-specific integrated circuits (ASICs) have been developed for the broadband PLC systems. Only a few electricity distribution companies have started commercial activities to offer broadband Internet access through the power lines. However, the challenging price competition with other technologies, such as asymmetric digital subscriber line (ADSL) and cable television (CATV) technologies has halted PLC activities at least in Finland. In any event, the Internet access has to be delivered everywhere inside the households. In this case, in addition to PLC, there are two alternatives, wireless technologies or additional cablings. In 2001, a promising PLC technology, HomePlug 1.0, was specified for this purpose (HomePlug, 2004). In 2002, several HomePlug compliant home networking products were presented in the USA, and during the following year also in Europe. HomePlug 1.0 specification is described in detail in (Lee et al., 2003).

## 1.2  Background of power line communication

Generally, PLC means that the same electric cables used for power delivery are also applied in communication. The powering and signalling circuits are separated by a high-pass filter, called a coupling interface. The coupling interface makes it possible to connect different circuits with different voltage levels. For example, the application of this dissertation, the circuit of the motor power cable and communication act as their own, and these circuits have to be coupled by a coupling interface to enable PLC over the motor power cable. The communication signal is fed through the coupling interface to the mains electricity network. Generally, the carrier frequencies of communication are notably higher than the frequency used in the mains networks (50/60 Hz). Correspondingly, the voltage levels of communication are notably lower than in the mains electricity networks (230/115 V). The operational principle of PLC is illustrated in Fig. 1.2.
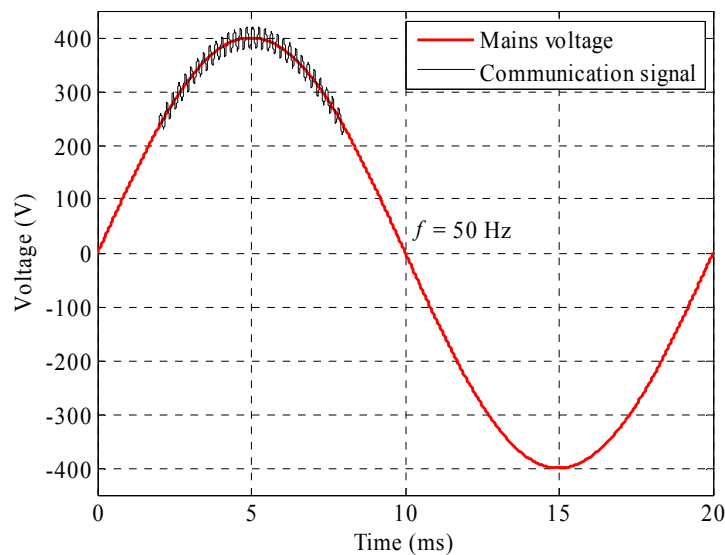


Fig. 1.2: Basic idea of PLC.

According to Hrasnica et al. (2004), PLC can be categorized based on the bandwidth. Narrowband PLC (<100 kbps) is applied in automation, meter reading, various control applications, and in a small number of voice channels. Correspondingly, broadband PLC (>2 Mbps) is applied in Internet access, multiple voice connections, transmission of video signals, high-speed data transmission, in-home networks, and narrowband services. On the other hand, PLC can also be categorized by its application environment as illustrated in Fig. 1.3 into HV and MV power supply networks ($U_n > 1$ kV), LV power supply networks ($U_n < 1$ kV), and in-home networks (Majumder and Caffery, 2004).
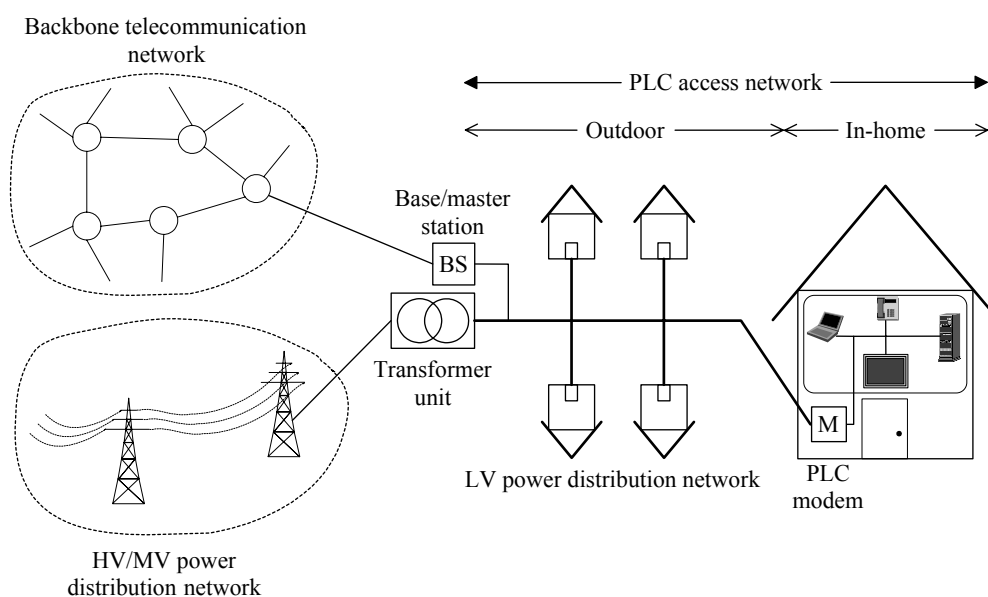


Fig. 1.3: Structure of a PLC access network (Hrasnica et al., 2004). In-home network includes, for example, computers, set-top-boxes, TVs, servers, and internet protocol (IP) phones.

The power distribution network is a very hostile environment for communication. The main problems are the signal multi-path propagation, impedance mismatches, noise, and both the time and frequency dependent impedance of the power supply network. The impedance mismatch causes signal reflection from the load, and together with multi-path propagation, they cause deep notches to the channel frequency response or several peaks to the channel impulse response. The impedance of a power supply network is time variant, because electric devices are randomly connected to the grid. Many electric devices, such as halogen lamps, microwave ovens, and other household appliances, cause noise to the electric distribution network. The most problematic noise scenario from the viewpoint of communication is impulsive noise. Impulsive noise is produced for example by switched-mode power supply units, fluorescent lamps, dimmers, and vacuum cleaners.

## 1.3 Background and motivation of thesis

In recent years, the development of PLC has mainly concentrated on the indoor applications in conventional residential buildings, and less attention has been paid to the research of industrial applications. However, PLC could revolutionize the usage of several exploitable on-line condition monitoring applications in industry in the future. Traditionally, separate

instrumentation cabling has been used for signalling. The cost of cabling may be between $60 and $6000 per meter installed in an industrial environment (Brooks, 2001). Thus, the price of these cablings can be a major obstacle to the wider adoption of on-line condition monitoring applications. Another alternative is to apply wireless methods, but floors, walls, metallic and moving parts can cause problems in industrial environments. These may question the reliability of wireless methods.

In industry, the number of electric motors is huge; for example, a forest products mill can contain thousands of electric motors (Ahola et al., 2005b). The motors are mainly used for producing torque that rotates some regulating unit, such as a pump, blower, compressor, or the like. All these units, motors included, may break down and lead to a production interruption. These occasions can be prevented by monitoring the condition of equipment and making the repair in advance before anything breaks down. However, condition monitoring requires various sensors to be installed at the motors (Lindh, 2003), generators or apparatuses, which are normally located near the process. The requirements of data transmission vary depending on the application. Requirements of data transmission for information of a few applications are gathered in Table 1.1.

Table 1.1: Requirements of data transmission for different kinds of information.

|  | On-line condition monitoring | Real-time control | Video | Voice |
|---|---|---|---|---|
| Throughput | + | ++ | +++ | ++ |
| Latency | + | +++ | ++ | ++ |
| Jitter | + | +++ | ++ | ++ |
| Reliability | + | +++ | ++ | ++ |

The sensor level data has to be transmitted out of the process, where it can be used and analyzed (Fig. 1.4). In the Finnish industry, the average LV power cable lengths are about 70−80 metres, but also cables with lengths of more than 200 metres are installed. These transmission distances lead to huge costs because of the additional cables required. However, the electric motors are powered by already installed power cables that can be used as a communication medium in addition to the power delivery. The installations will be considerably easier, because both the communication and powering are included in the same cables. The communication channel would be quite similar to a normal LV grid if the motors were supplied by the mains network. However, because of controllability, the motors in industry are nowadays increasingly supplied by inverters, and hence the communication channel differs totally from the normal LV network. In this dissertation, the main objective is to study the communication over inverter-driven motor power cables, its implementation and also the limitations of possible applications. In this thesis, the proposed method is termed 'motor cable communication'. The method can be utilized for two main applications, but also other targets are possible. The first one is the above-mentioned on-line condition monitoring and the second one motor control. Accurate motor control requires feedback information, such as the rotation speed or position angle of the rotor, from the motor to the controller. In this dissertation, instead of an additional feedback cable, the motor power cable is applied for this purpose.
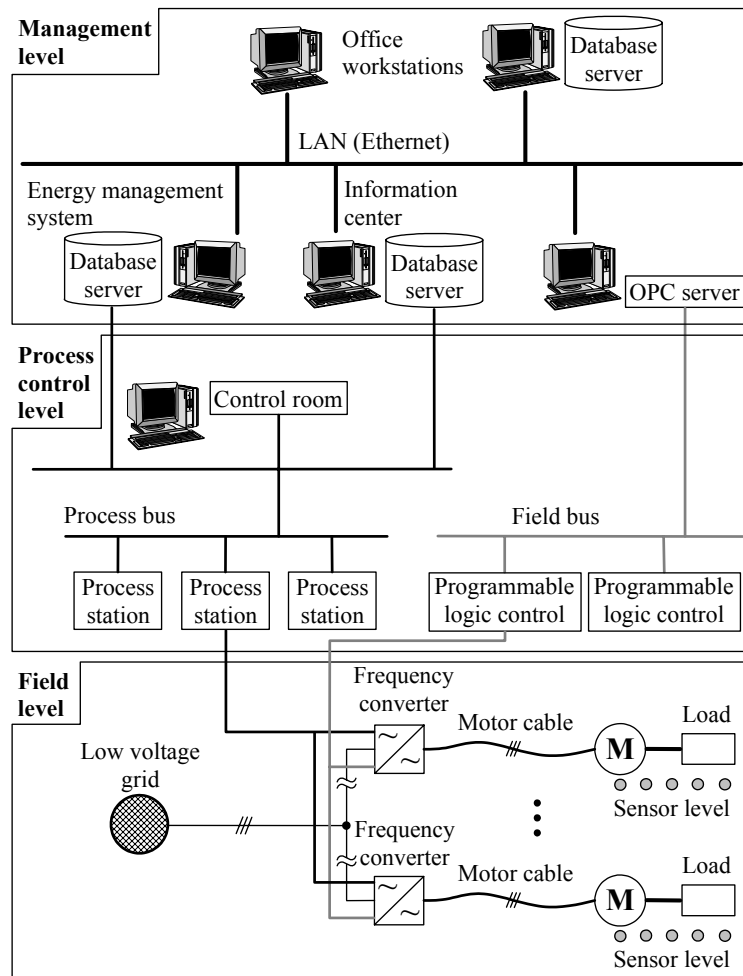
Fig. 1.4: Topology of an industrial information system concerning inverter-fed electric drives. Only the field level data transmission is studied in this thesis. At the field level, frequency converters are typically centralized, whereas the motors are located separately close to the loads or processes. It is advisable to implement the communication medium by common field and process buses down to the frequency converters, while separate communication media are required for the sensor level data.

In literature, only a few application-specific studies have focused on communication over a motor power cable in inverter-fed electric drives. In addition, these papers include only a PHY presentation. An on-line winding temperature monitoring system for an inverter-fed induction machine using its power cable as a communication medium is described in (Chen et al., 1994). The communication bandwidth is 9600 bps with the 3.5 MHz and 6.5 MHz FSK modulation frequencies used in the study. A motor cable is also used as a feedback channel for an encoder signal in the real-time control of a servosystem in (Coakley and Kavanagh, 1999). An FSK modulator is also applied with 15 V at 3.75 MHz or 6.25 MHz on the transmitter side. According to Coakley and Kavanagh (1999), with this configuration, it is possible to reach a communication rate above 40 kbps, but the paper does not define the length of the motor cable. In addition to these two papers, there are also a few ones that address PLC in a normal LV motor cable. The normal LV network and CENELEC frequencies are applied in (Ahola, 2003).

The papers (Liu et al., 2001; Wade and Asada, 2002; 2003) concentrate solely on servo systems, in which the DC bus lines are utilized in communication.

## 1.4 Outline of thesis

The doctoral dissertation studies communication over the motor power cables of variable-speed electric drives. In addition, the study focuses on the ways to implement PLC in an industrial environment. Two applications are studied, on-line condition monitoring and real-time motor control. These two have essentially different limitations regarding communication. Motor control is studied in a laboratory environment. On-line condition monitoring is studied by the throughput and latency analysis. In the dissertation, the measurement results are presented to verify the theories and the simulations.

The thesis is composed of a summary section and the appended original publications. The contents of the summary are divided into the following five chapters.

**Chapter 1** introduces the history of PLC from the early days to the present. Background and basic aspects of PLC are also presented. Finally, the chapter provides the background and motivation for the thesis and presents its scientific contributions.

**Chapter 2** is devoted to the study and modelling of channel characteristics. First, the proposed data transmission concept is described. A power line channel is divided into two parts: the communication channel and the noise source. The communication channel is further divided into individual parts that include only a single physical component. The HF characteristics of these components are studied based either on previous studies or on measurements. On the basis of these models, a channel model is formed and verified by measurements. The noise source and its characteristics are also described. Lastly, based on the channel characteristics, the information capacity of a communication channel is estimated.

**Chapter 3** suggests the methods to be used for communication over an inverter-fed motor power cable. First, the chapter introduces and summarizes the available PLC regulations in Europe. Next, a method that enables broadband communication over power lines is introduced. Suitable and effective techniques to battle against different errors occurring during the transmission are also described. Next, the background of HomePlug and its two specifications are discussed. The developed coupling interface for motor cable communication is presented and analyzed in detail. A few experimental tests are also carried out for the coupling interface to ensure its operation. Finally, a test modem for the laboratory tests is constructed, and extensive measurements are carried out. The measurement results include a throughput and a latency test.

**Chapter 4** presents potential applications where the proposed motor cable communication method can be utilized. Two main applications are discussed, but also a few other ones are mentioned. The first application is continuous on-line condition monitoring that usually requires sensors to be installed at the monitored device. The second application is real-time motor speed control that applies feedback signal in control.

**Chapter 5** is the final chapter before the appended publications. It presents the conclusions and makes suggestions for future work.

In the following, the contents of the appended seven publications are summarized, and the contribution of the author and the co-authors to them is reported. The co-authors not listed below have participated in the project co-operation. In addition, they have contributed to the

preparation of the publications by revision comments and suggestions. These publications comprise two articles published in international journals and five international conference papers.

**Publication I** concentrates on the characteristics of the laboratory test system and its restrictions. This system will be applied in the study of motor feedback speed control. The main idea is to utilize the motor power cable as a communication channel for the feedback signal in a variable-speed drive, in which it is normally implemented by an additional cabling. The statistical properties of the latency behaviour are studied and analyzed. The affecting factors for the latency are also determined. According to the latency characteristics, the limitations of a control system are discussed in brief. The main contribution of this publication is the study of the latency characteristics of the proposed PLC method.

The whole test system was constructed in the laboratory by the author and the co-author Mr. Jokinen. The author implemented the PLC devices to the test system. The Matlab® Simulink model for the dSPACE equipment was implemented by the co-author Mr. Jokinen and the necessary software for the Ethernet demo board by the co-author Mr. Särkimäki. The measurement was carried out by the author and the co-author Mr. Jokinen. The results were analyzed and the manuscript was mainly written by the author in co-operation with the co-authors Mr. Jokinen and Mr. Särkimäki.

**Publication II** introduces a method for communication through the motor power cable between an electric motor and a frequency converter. The channel and noise characteristics are described. The test environment used in PLC over the motor power cable is presented. Both the throughput and latency are measured and analyzed in these tests. The factors that have an effect on the channel characteristics are also presented. The main contribution of this publication is the analysis of extensive laboratory test results that describe the applicability of the proposed method in different electric drives.

The laboratory tests were carried out by the author. The analysis was done by the author and the co-author Professor Ahola. The author participated in the writing process of the publication with the co-author Professor Ahola.

**Publication III** focuses on the modelling of HF signal propagation in the motor power cable. It describes the application and the methods applied in the modelling. The publication studies the voltage amplification of a communication channel. It is shown that the voltage measurement of a channel can be carried out with the mains voltage off. If an output filter is used, the channel characteristics do not change irrespective of whether the motor is driven by an inverter or not. The simulation results are verified by measurements. The main contribution of this publication is the simulation model and its verification by practical measurements.

The contents of this publication are produced and written by the author.

**Publication IV** considers real-time induction motor speed control when the speed information of the motor is transmitted through the motor power cable as a feedback signal to the controller. This publication is a continuation of Publication I. The methods used in motor cable communication are presented. Two different standard compliant PLC modems are used in the laboratory tests. Only a proportional-integral (PI) controller is applied, and it is tuned to meet the same requirements in all cases. The dSPACE equipment is used as a speed controller, and the frequency converter only as a torque amplifier. Simulations are carried out with different fixed feedback delays. Step response, ramp, and loading tests are used to determine the performance of the proposed method. The simulation results are

verified by laboratory tests. The test results with a direct feedback loop (a separate signal cable) are kept as a reference material for conclusions. The main contribution of this publication is to study the limitations of the proposed method in a feedback speed control application.

The publication was mainly written by the author. The simulations were carried out and reported by the co-author Mr. Jokinen. The measurements were carried out by the author and the co-author Mr. Jokinen.

**Publication V** discusses the performance of the proposed induction motor speed control method that applies the motor power cable as a communication bus. This publication is an extended version of Publication IV. In addition to the material introduced in Publication IV, the publication presents the results of comparison tests. These results include the measurement with a commercial drive. The commercial drive is tested both in a sensorless and a feedback mode, and the results are compared with the ones carried out with the proposed method. The main contribution of this publication is the analysis of extensive laboratory tests that can be utilized when evaluating the applicability of the proposed method to a control application.

The preparation and measurement with the commercial drive were carried out by the author and the co-author Mr. Jokinen. The simulations were carried out and reported by the co-author Mr. Jokinen. The manuscript was mainly written by the author in co-operation with the co-author Mr. Jokinen.

**Publication VI** studies the HF current propagation in electric drives; especially the signal propagation from the motor power cable to the LV grid through the frequency converter. This is important, because the data transmission of the proposed method causes HF signal to the motor power cable. In this publication, conducted emissions and the effect of parasitic impedances on signal propagation are discussed. Different paths of a HF signal in electric drives are analyzed, and thereby the main stray capacitances of an electric drive are presented. The laboratory equipment and the tests are described. The results of the measured conducted noise are illustrated and analyzed. Both the common mode and differential mode noise current are measured with different HF signal couplings.

The measurements were carried out by the author in co-operation with the co-authors Professor Ahola and Professor Silventoinen. The contents of this publication are produced and written by the author.

**Publication VII** introduces in detail the proposed broadband PLC method between a motor and a frequency converter. The method is Ethernet based, and hence it is packet-based data transmission. The publication presents the previous articles on the topic. The communication channel is described; both the channel and noise characteristics and the channel information capacity analysis are presented. The data transmission system is described, that is, the adopted HomePlug specification and the developed coupling interface. The test equipment is constructed, and the obtained experimental results are reported; these include the results of the tests carried out with the patented coupling interface. Two applications, on-line condition monitoring and real-time motor control, are discussed.

The contents of this publication are mainly produced and written by the author. The patented coupling interface was developed in co-operation with the co-author Professor Ahola. A part of the chapter concerning motor control was written by the co-author Mr. Jokinen.

The author also has other publications on closely related topics. These publications are listed here but are not appended to this thesis, and are therefore not discussed in detail. These five publications are:

Ahola, J., Toukonen, J., Kosonen, A., Lindh, T., and Tiainen, R., "Ethernet to Electric Motor – via Mains Cable," in *Proc. of the 18th International Congress and Exhibition on Condition Monitoring and Diagnostic Engineering Management (COMADEM)*, Cranfield, UK, August/September 2005, pp. 525−534.

Ahola, J., Toukonen, J., Kosonen, A., Lindh, T., and Särkimäki, V., "Electric Motor Cable Communication Overcomes the Biggest Obstacle in On-line Condition Monitoring," in *Proc. of Condition Monitoring 2005 Conference (COMADIT)*, Cambridge, UK, July 2005, pp. 105−110.

Jokinen, M., Kosonen, A., Niemelä, M., Ahola, J., and Pyrhönen, J., "Disturbance Observer for Speed Controlled Process with Non-Deterministic Time Delay of Feedback Information," in *Proc. of the 38th Annual IEEE Power Electronics Specialists Conference (PESC)*, Orlando, Florida, USA, June 2007, pp. 2751−2756.

Konaté, C., Kosonen, A., Ahola, J., Machmoum, M., and Diouris, J. F., "Power Line Channel Modelling for Industrial Application," in *Proc. of the 12th IEEE International Symposium on Power-Line Communications and Its Applications (ISPLC)*, Jeju Island, Korea, April 2008, pp. 76−81.

Ahola, J., Ahonen, T., Särkimäki, V., Kosonen, A., Tamminen, J., Tiainen, R., and Lindh, T., "Design Considerations for Current Transformer Based Energy Harvesting for Electronics Attached to Electric Motor," in *Proc. of 19th International Symposium on Power Electronics, Electrical Drives, Automation and Motion (SPEEDAM)*, Ischia, Italy, June 2008, pp. 901−905.

The coupling interface presented in Publication VII has been patented domestically, and also an international patent application (patent pending) has been made. These are enumerated below:

Kosonen, A., and Ahola, J., "Laitteisto tiedonsiirron järjestämiseksi," Owner ABB Oy, Patent number FI118840B, Application number FI20050766, Grant date 31 March 2008. (In Finnish)

Kosonen, A., and Ahola, J., "Apparatus for Arranging Data Transfer," Applicant ABB Oy, Application number WO2006FI00255, Publication number WO2007010083, Application date 14 July 2006, Publication date 25 January 2007.

## 1.5 Scientific contributions

The scientific contributions of this dissertation are:

- Modelling the individual components of an inverter-controlled electric drive, and forming a channel model in the frequency band of 100 kHz−30 MHz (Chapter 2)

- Theoretical information capacity analysis of a communication channel (Chapter 2 and Publication VII)

- Generally applicable implementation of a motor cable communication system for LV inverter-fed electric drives (Chapter 3 and Publication VII)

- Performance analysis of a real-time induction motor speed control that applies the motor feeder cable as a feedback loop (Publications IV and V)

- Analysis of HF current propagation in a motor power cable in inverter-fed electric drives (Publications III and VI)

- Throughput and latency analysis of the proposed method (Publications II and VII)

- Latency behaviour analysis from the viewpoint of a real-time speed control application (Publication I)

- Implementation of a generally applicable coupling interface for inverter-fed electric drives (Chapter 3 and Publication VII)

# 2  COMMUNICATION CHANNEL

In this chapter, the applied communication channel is studied. First, the data transmission concept is introduced, and its general channel model is described. The channel HF characteristics are studied by dividing the channel into several individual components and studying their input impedance behaviours or attenuation in the case of a motor power cable. The input impedance of individual components is modelled based on the impedance measurement. The applied frequency band is $100\,\text{kHz}{-}30\,\text{MHz}$. The method for communication channel modelling is presented, and the channel model is constructed. The channel model is also verified by measurements. The noise characteristics are also studied. Finally, the channel capacity analysis is performed as a case study for the frequency band of $4.49{-}20.7\,\text{MHz}$ in an inverter-fed motor power cable.

## 2.1  Data transmission concept

The proposed data transmission concept is illustrated in Fig. 2.1. The concept can be simplified into the general model of a power line channel described in Fig. 2.2. The model consists of a channel and noise model. According to the model, the received signal $r(t)$ is given by:

$$r(t) = s(t) * h(t) + n(t),\qquad(2.1)$$

where $s(t)$ is the signal injected into the channel by the transmitter, $h(t)$ the impulse response of the channel, and $n(t)$ the noise signal at the receiver end. Generally, signal attenuation and noise are important elements in a communication system. Therefore, the channel and noise characteristics are studied next in detail. In order to simulate the communication channel and to design a communication system, a channel model is required.
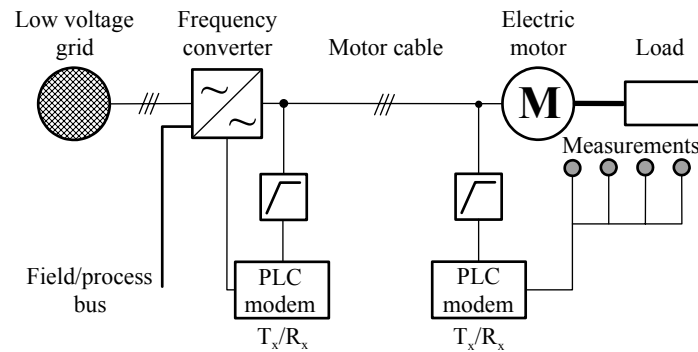


Fig. 2.1: Data transmission concept between an electric motor and a frequency converter. The motor power cable is used as a medium for PLC.
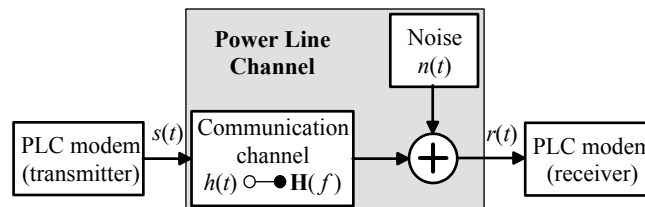


Fig. 2.2: General model of a power line channel, where $\mathbf{H}(f)$ is the transfer function of the channel.

## 2.2 Channel modelling in motor cable communication

In general, PLC channels are modelled in the frequency-domain by an echo model, the parameters of which are obtained by measurements (Phillips, 1999; Zimmermann and Dostert, 2002b). The analytic model discussed in (Zimmermann and Dostert, 2002b) describes complex transfer functions of typical power line networks. The signal components of the individual paths are combined by superposition. The frequency response of a PLC channel, which includes $N$ different paths, can be given by the weighting factor, attenuation, and delay portions for an individual path $i$ as follows:

$$\mathbf{H}(f) = \sum_{i=1}^{N} g_i \cdot \underbrace{e^{-\left(a_0 + a_1 f^k\right)d_i}}_{\substack{\text{attenuation} \\ \text{portion}}} \cdot \underbrace{e^{-j2\pi f\left(d_i / v_\text{p}\right)}}_{\substack{\text{delay} \\ \text{portion}}}, \tag{2.2}$$

where $g_i$ is the weighting factor for path $i$, $a_0$ and $a_1$ the attenuation parameters (derived from the measured transfer functions), $f$ the frequency, $k$ the exponent of the attenuation factor (0.5…1), $d_i$ the length of the path $i$, and $v_\text{p}$ the propagation velocity of the electromagnetic wave in the cable. However, in motor cable communication, the channel structure is simple and rather similar in different electric drives. The channel consists of similar components, and there are no branches. Thus, the typical frequency characteristics of individual components can be parameterized and estimated. Therefore, it is convenient to model the channel attenuation by two-port models, which are introduced for example in (Banwell and Galli, 2001; Esmailian et al., 2002). Generally, electric drives in industry are three-phase devices, and such are also the drives studied in this thesis. According to Ahola (2003), two-port modelling is not a problem, because mostly shielded and symmetrical LV power cables are installed nowadays as motor cables. The theoretical justification for applying two-port modelling of transmission lines in the case of three-phase symmetric cables is presented in (Papaleonidopoulos et al., 2005).

The transmission or chain parameter matrices can be applied to model the transfer function of a communication channel. The analysis is applicable to transverse electromagnetic (TEM) waves. A TEM wave has only transversal electric and magnetic fields, and no longitudinal fields. However, there is a small longitudinal electric field component because of the resistive losses. According to Paul (1994), the field structure can be kept almost TEM in spite of the small conductor losses. This is referred to as the quasi-TEM assumption. The relation between the input voltage $\mathbf{U}_\text{in}$ and the current $\mathbf{I}_\text{in}$, and the output voltage $\mathbf{U}_\text{out}$ and the current $\mathbf{I}_\text{out}$ can be described (Fig. 2.3) as follows:

$$\begin{bmatrix} \mathbf{U}_\text{in} \\ \mathbf{I}_\text{in} \end{bmatrix} = \begin{bmatrix} \mathbf{A} & \mathbf{B} \\ \mathbf{C} & \mathbf{D} \end{bmatrix} \begin{bmatrix} \mathbf{U}_\text{out} \\ \mathbf{I}_\text{out} \end{bmatrix}, \tag{2.3}$$

where $\mathbf{A}$, $\mathbf{B}$, $\mathbf{C}$, and $\mathbf{D}$ are the frequency dependent coefficient matrices.
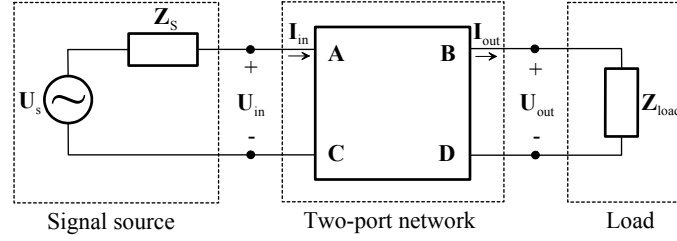
Fig. 2.3: Two-port network connected to a signal source and a load impedance. The signal source consists of a voltage source and a serially connected internal impedance.

The frequency dependent input impedance of the two-port network can be described as follows:

$$\mathbf{Z}_{\text{in}} = \frac{\mathbf{A}\mathbf{Z}_{\text{load}} + \mathbf{B}}{\mathbf{C}\mathbf{Z}_{\text{load}} + \mathbf{D}}, \tag{2.4}$$

where $\mathbf{Z}_{\text{load}}$ is the load impedance. The transfer function of the channel can be written as:

$$\mathbf{H} = \frac{\mathbf{U}_{\text{out}}}{\mathbf{U}_{\text{s}}} = \frac{\mathbf{Z}_{\text{load}}}{\mathbf{A}\mathbf{Z}_{\text{load}} + \mathbf{B} + \mathbf{C}\mathbf{Z}_{\text{load}}\mathbf{Z}_{\text{S}} + \mathbf{D}\mathbf{Z}_{\text{S}}}. \tag{2.5}$$

The transmission matrix of the motor cable can be written as:

$$\begin{bmatrix} \mathbf{A} & \mathbf{B} \\ \mathbf{C} & \mathbf{D} \end{bmatrix} = \begin{bmatrix} \cosh(\gamma L) & \mathbf{Z}_0 \sinh(\gamma L) \\ \dfrac{1}{\mathbf{Z}_0} \sinh(\gamma L) & \cosh(\gamma L) \end{bmatrix}, \tag{2.6}$$

where $L$ is the length of the cable, $\gamma$ the propagation constant, and $\mathbf{Z}_0$ the characteristic impedance of the cable. The propagation constant can be calculated as follows:

$$\gamma = \sqrt{(r + j\omega l)(g + j\omega c)} = \alpha + j\beta, \tag{2.7}$$

where $c$, $g$, $l$, and $r$ are the distributed capacitance, conductance, inductance, and resistance, respectively, and $\omega$ the angular frequency. $\alpha$ is the attenuation coefficient, and $\beta$ the propagation coefficient. According to Ahola (2003), these can be estimated for polyvinyl chloride (PVC) insulated LV motor cables as follows:

$$\alpha(f) = 0.5 \cdot 10^{-6} \cdot \left( f \cdot \frac{1}{\text{Hz}} \right)^{0.6} \frac{1}{\text{m}}, \tag{2.8}$$

$$\beta(f) = 2\pi f \sqrt{lc}. \tag{2.9}$$

The characteristic impedance can be written as:

$$\mathbf{Z}_0 = \sqrt{\frac{r + j\omega l}{g + j\omega c}}. \tag{2.10}$$

For a lossless ($r = 0$, $g = 0$) transmission line, (2.10) is simplified:

$$Z_0 = \sqrt{\frac{l}{c}} \,. \tag{2.11}$$

The serial and parallel impedances, $\mathbf{Z}_S$ and $\mathbf{Z}_P$, are illustrated as two-port models in Fig. 2.4.
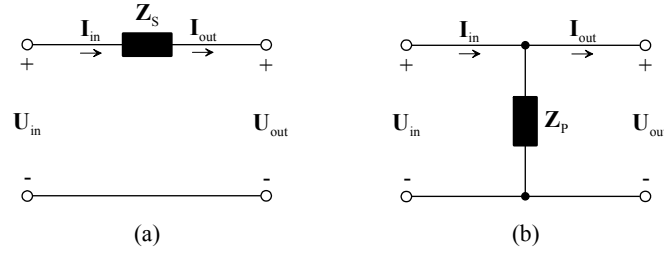


Fig. 2.4: Two-port models of impedances. (a) Serial impedance. (b) Parallel impedance.

According to Fig. 2.4, the transmission matrix for the serial impedance $\mathbf{Z}_S$ can be calculated as follows:

$$\begin{bmatrix} \mathbf{A} & \mathbf{B} \\ \mathbf{C} & \mathbf{D} \end{bmatrix} = \begin{bmatrix} 1 & \mathbf{Z}_S \\ 0 & 1 \end{bmatrix}, \tag{2.12}$$

and for the parallel impedance $\mathbf{Z}_P$:

$$\begin{bmatrix} \mathbf{A} & \mathbf{B} \\ \mathbf{C} & \mathbf{D} \end{bmatrix} = \begin{bmatrix} 1 & 0 \\ 1/\mathbf{Z}_P & 1 \end{bmatrix}. \tag{2.13}$$

The communication channel from the motor to the inverter consists of several network sections. Each section has to be described as a transmission matrix of its own. These sections are serially connected to each other. Generally, the transmission matrix $\mathbf{T}$ from the source to the load can be described by the chain rule:

$$\mathbf{T} = \prod_{i=1}^{n} \mathbf{T}_i \,, \tag{2.14}$$

where $n$ is the number of network sections. The channel model, which includes the components in an inverter-fed electric drive, can now be formed according to the chain rule. The model is illustrated in Fig. 2.5.
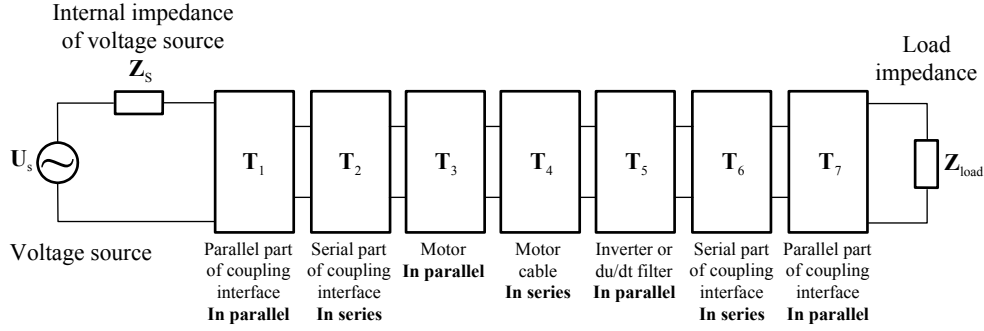
Fig. 2.5: Transmission-matrix-based channel model for an inverter-fed electric drive when the transmitter is at the motor end and the receiver at the inverter end.

## 2.3 Channel HF characteristics

The mains network is supplied by a transformer or a generator, while the pulse width modulation (PWM) inverter-fed power cable is supplied by semiconductor switching components, which results in completely different impedance characteristics (Chen et al., 1994). In motor cable communication, the motor power cable forms the medium for communication. The cable is terminated at both cable ends. At the inverter end, the cable is terminated by either an output filter (du/dt) or the output stage of an inverter, which may consist of insulated gate bipolar transistors (IGBTs) or thyristors, depending on the power rating of the electric drive. Correspondingly, at the other end, the cable is terminated by an electric motor. Both of these can be considered imperfect termination impedances, which lead to an impedance mismatch at the both cable ends. The impedance mismatches cause signal reflections, and thereby multi-path propagation. The PLC modems are also coupled to the three-phase motor power cable at the both ends by coupling interfaces. The reflection coefficient $\mathbf{\Gamma}_R$ at the cable end can be written:

$$\mathbf{\Gamma}_R = \frac{\mathbf{Z}_{load} - \mathbf{Z}_0}{\mathbf{Z}_{load} + \mathbf{Z}_0} .$$

(2.15)

The reflection coefficient $\mathbf{\Gamma}_R = 0$, if the load impedance of the transmission line is perfectly matched or the length of the transmission line is infinite. In other cases, part of the signal power is reflected back from the impedance mismatch. Next, all the individual components and their HF characteristics are described. From the viewpoint of PLC in the motor power cable, the frequency band of 100 kHz−30 MHz and signal coupling between two phases (L1, L2) are the most interesting ones. In practice, the low frequency (LF) band is 30−300 kHz, medium frequency (MF) band 300 kHz−3 MHz, and HF band 3−30 MHz. However, it is reasonable to talk only about the HF, because these frequencies can be used in practice for communication in the inverter-fed motor power cable.

The impedance measurements were carried out for the frequency band of 100 kHz−30 MHz by an HP 4194A impedance analyzer with an HP 41941A impedance probe kit. The measurement information was stored into 401 data points (frequency, absolute value, and phase) for each measurement. Only signal coupling (L1, L2) was applied in each measured and simulated case.

### 2.3.1 Electric motor

An electric motor acts as the termination impedance of a motor power cable, and therefore there is usually an impedance mismatch between the motor and the power cable. The input impedances of electric motors in the frequency-domain are discussed for instance in (Ahola 2003; Mirafzal et al., 2007). The disadvantage with the model presented in (Mirafzal et al., 2007) is that it is more complicated than the model introduced in (Ahola, 2003), because it describes the impedance characteristics of electric motors in the frequency band of 10 Hz−10 MHz. The model introduced in (Ahola, 2003) is adequate, because the model ranges over the frequency band used in motor cable communication. According to Ahola (2003), the input impedance model of an electric motor (Fig. 2.6) describes the main characteristics of electric motors in the HF band. In this band, the stray capacitances and leakage inductances have an effect on the input impedance of the motor. The input impedance behaves like a serial resonance circuit with signal coupling (L1, L2), and therefore it can be simulated with the model illustrated in Fig. 2.6. The HF parameters for different electric motors are listed in Table 2.1. The parameters are calculated according to the input impedance measurements. Most of these parameters are presented in (Ahola, 2003).
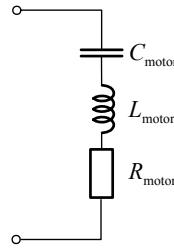


Fig. 2.6: Input impedance model of an electric motor (Ahola, 2003). The model can be applied in the frequency band of 100 kHz−30 MHz for signal coupling (L1, L2).

Table 2.1: Calculated parameters for the input impedance model of an electric motor in the frequency band of 100 kHz−30 MHz (Ahola, 2003). $I_n$, $U_n$, $P_n$, and $n_n$ are the nominal current, the nominal voltage, the nominal power, and the nominal rotation speed, respectively.

| Signal coupling (L1, L2) | | | | | | | | |
|---|---|---|---|---|---|---|---|---|
| Mf. | Type | $I_n$ (A) | $U_n$ (V) | $P_n$ (kW) | $n_n$ (rpm) | $C_{motor}$ (nF) | $L_{motor}$ (nH) | $R_{motor}$ (Ω) |
| Invensys | T-01F160L4/01 | 28.5 | 400 (Δ) | 15 | 1460 | 1.7 | 198 | 5 |
| ABB | M2AA160L4 | 30 | 400 (Δ) | 15 | 1455 | 0.8 | 127 | 12 |
| Strömberg | XHUR368G2B3 | 43 | 400 (Δ) | 22 | 1460 | 0.8 | 127 | 12 |
| ABB | M2BA200MLA4B3 | 56 | 400 (Δ) | 33 | 1473 | 1.4 | 266 | 5 |
| ABB | M3BP315MLA4B3 | 202 | 690 (Y) | 200 | 1486 | 7.2 | 412 | 3 |
| ABB | M2BA35532B3 | 410 | 400 (Δ) | 250 | 2980 | 7.7 | 329 | 2 |

### 2.3.2 Motor cable

Typically, the cables in variable-speed drives are three-phase symmetric ones and shielded because of electromagnetic interference (EMI) problems (Bartolucci and Finke, 2001). In the HF band, the cable attenuation is primarily caused by the PVC insulation material, which is both frequency and temperature dependent. Also the resistive losses of conductors, radiation losses, and coupling losses have an effect on attenuation. Typical LV power cable lengths are less than 100 m, but also lengths above 200 m are possible (Ahola, 2003). As mentioned in

Publication II, the main cable parameters that affect the performance of PLC are the characteristic impedance $\mathbf{Z}_0$, the attenuation coefficient $\alpha(f)$, and the cable length $L$. The characteristic impedance of the motor cable depends mainly on signal coupling, insulation material, its cross-sectional structure, and frequency. Typical characteristic impedances of power cables used in variable-speed drives are between 5 and 50 Ω.

According to Ahola (2003), the HF parameters of motor cables can be defined by input impedance measurements. The input impedance of a cable is measured both with the cable end open and short-circuited. Then, the characteristic impedance can be calculated as follows:

$$\mathbf{Z}_0 = \sqrt{\mathbf{Z}_{\text{cable,sc}} \mathbf{Z}_{\text{cable,open}}} \ , \tag{2.16}$$

where $\mathbf{Z}_{\text{cable,sc}}$ and $\mathbf{Z}_{\text{cable,open}}$ are the input impedances of the cable with other end short-circuited and open, respectively. Correspondingly, the propagation constant can be defined:

$$\gamma = \frac{1}{L} \arctan \sqrt{\frac{\mathbf{Z}_{\text{cable,sc}}}{\mathbf{Z}_{\text{cable,open}}}} \ . \tag{2.17}$$

The distributed inductance and capacitance can be solved applying the characteristic impedance and the propagation constant:

$$l = \frac{\text{Im}\{\mathbf{Z}_0 \gamma\}}{\omega} , \tag{2.18}$$

$$c = \frac{\text{Im}\{\mathbf{Z}_0 / \gamma\}}{\omega} . \tag{2.19}$$

In the case of a lossless and distortionless transmission line, the propagation velocity of the electromagnetic wave is:

$$v_{\text{p}} = \frac{1}{\sqrt{lc}} = \frac{\omega}{\beta} . \tag{2.20}$$

Some calculated values of different motor power cables are listed in Table 2.2.

Table 2.2: Characteristic impedance, propagation velocity proportion to the speed of light in vacuum $c_0$, distributed inductance, and distributed capacitance for MCMK type LV cables in the frequency band of 100 kHz−30 MHz (Ahola, 2003).

| Signal coupling (L1, L2) | | | | | |
|---|---|---|---|---|---|
| Mf. | Type | $Z_0$ (Ω) | $v_{\text{p}}/c_0$ | $l$ (nH/m) | $c$ (pF/m) |
| Reka | EMCMK 3x16+16 | 42 | 0.57 | 245 | 138 |
| Pirelli | MCCMK 3x35+16 | 27 | 0.64 | 141 | 190 |
| Pirelli | MCMK 3x70+35 | 25 | 0.63 | 132 | 213 |
| Reka | EMCMK 3x120+70 | 23 | 0.62 | 123 | 237 |

### 2.3.3 Output filter

An output filter, when used, acts as the termination impedance of a motor power cable at the other cable end. The output filter remarkably increases the magnitude of a serial impedance at the inverter end in the HF band because of the serial line inductances, and hence the effect of an inverter can be neglected. The input impedance model can be considered to be based on the serial and parallel shaped impedances. These impedances act as a function of frequency. Because of the high serial impedance in the HF band, only the parallel impedance is considered. There are no input impedance models available for the output filters of frequency converters in the HF band, which is the reason why this kind of a model has to be developed. The goal is to develop the input impedance model for an output filter and find its parameters according to measurements.

Two different output filters (du/dt) equipped with separated serial coils with an iron core for a three-phase drive are studied. The filters are intended for different sizes of three-phase supply currents (see Table 2.3). The filter manufactured by ABB includes the serial coils with parallel resistances, while the filter manufactured by Trafotek includes only the serial coils.

The developed input impedance model of an output filter is illustrated in Fig. 2.7. There are similarities with the model of an electric motor introduced in (Ahola, 2003). The topology of the model was formed according to the structure of an output filter and according to the resonance frequencies seen from the measurement. The capacitive and inductive components dominate the impedance. The parameters $L_{1,\text{dudt}}$ and $C_{1,\text{dudt}}$ form a parallel resonance circuit, $C_{1,\text{dudt}}$ and $L_{2,\text{dudt}}$ a serial resonance circuit, and $L_{2,\text{dudt}}$ and $C_{2,\text{dudt}}$ another parallel resonance circuit. The parameter $L_{1,\text{dudt}}$ acts as the mutual inductance between the adjacent windings and $C_{1,\text{dudt}}$ as the stray capacitance between the winding turns adjacent to two phases. The other components are not as clear. The parameters $L_{2,\text{dudt}}$ and $C_{2,\text{dudt}}$ may be caused by the paths including the coils, winding turns, the frame body of a filter, and the terminals of incoming wires. In addition, both the leakage inductances have their own serial resistances $R_{1,\text{dudt}}$ and $R_{2,\text{dudt}}$. The resistance $R_{3,\text{dudt}}$ (indicated by a dashed line in Fig. 2.7) is added because the ABB output filter has parallel resistances with the coils.
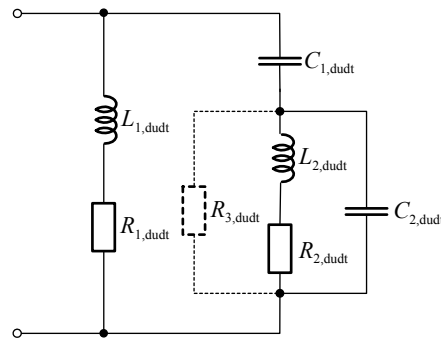


Fig. 2.7: Input impedance model of an output filter (du/dt). The model can be applied in the frequency band of 100 kHz−30 MHz for signal coupling (L1, L2).

The parameter values of a model can be defined according to the measurements. When the phase of the impedance is $\varphi \approx -90°$ or $\varphi \approx 90°$, the impedance can be estimated as capacitive or inductive, respectively. In addition, the magnitude of an impedance is known at a certain frequency, and hence the parameter values can be calculated according to:

$$\mathbf{Z}_{\mathrm{C}} = \frac{1}{\mathrm{j}2\pi f C}, \tag{2.21}$$

$$\mathbf{Z}_{\mathrm{L}} = \mathrm{j}2\pi f L, \tag{2.22}$$

where $C$ is the value of the capacitor and $L$ the value of the inductor. These parameters can be fitted together both at the serial and parallel resonance frequency according to:

$$f_{\mathrm{r}} = \frac{1}{2\pi\sqrt{LC}}. \tag{2.23}$$

The serial and parallel resonances occur, when the impedance changes from capacitive to inductive and vice versa, respectively. In addition, the structure of a model can be formed according to resonance frequencies. The amplitude of an impedance at the resonance frequency can be matched with the value of resistances.

The measurements for two output filters were performed in the frequency band of 100 kHz−30 MHz. According to the measurements, the model parameters (Table 2.3) were defined. The measured and modelled input impedances of two output filters are illustrated in Fig. 2.8 and Fig. 2.9.

Table 2.3: Calculated parameters for the input impedance model of an output filter (du/dt) in the frequency band of 100 kHz−30 MHz from the motor side. $L_{\mathrm{n}}$ is the nominal inductance.

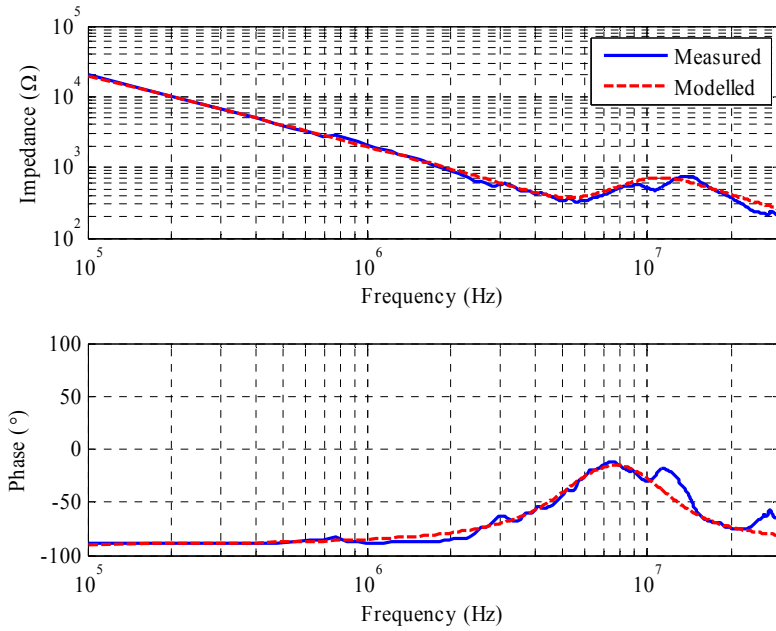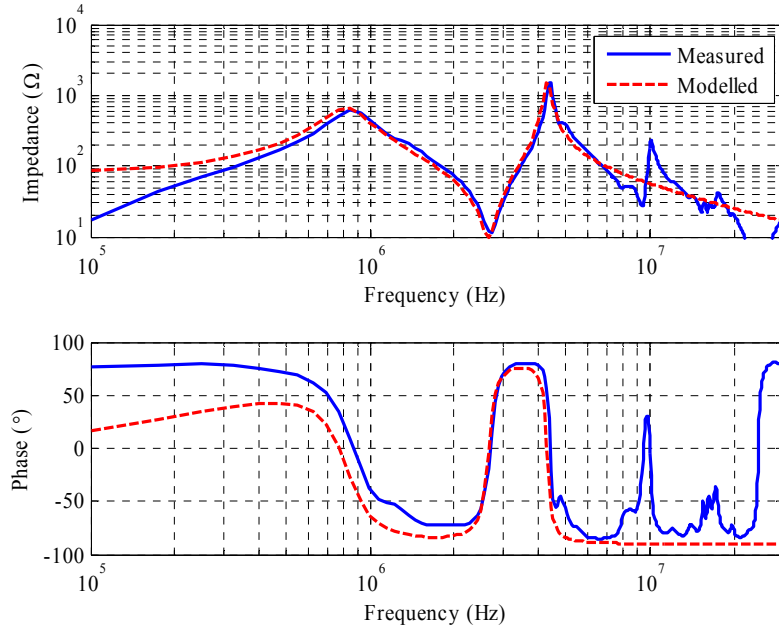| Signal coupling (L1, L2) | | | | | | | | | |
|---|---|---|---|---|---|---|---|---|---|
| Mf. | $I_{\mathrm{n}}$ (A) | $U_{\mathrm{n}}$ (V) | $L_{\mathrm{n}}$ (μH) | $L_{1,\mathrm{dudt}}$ (μH) | $R_{1,\mathrm{dudt}}$ (Ω) | $C_{1,\mathrm{dudt}}$ (pF) | $L_{2,\mathrm{dudt}}$ (μH) | $R_{2,\mathrm{dudt}}$ (Ω) | $C_{2,\mathrm{dudt}}$ (pF) | $R_{3,\mathrm{dudt}}$ (kΩ) |
| ABB | 28 | 380…690 | 130 | - | - | 80 | 8.8 | 200 | 30 | 1 |
| Trafotek | 650 | 500 | 35 | 43.7 | 80 | 800 | 2.7 | 3.5 | 540 | - |

Fig. 2.8: Measured and modelled input impedance and phase of an ABB output filter (du/dt) in the frequency band of 100 kHz−30 MHz with signal coupling (L1, L2). The parameters applied in the input impedance model are: $C_{1,\text{dudt}}$ = 80 pF, $L_{2,\text{dudt}}$ = 8.8 µH, $R_{2,\text{dudt}}$ = 200 Ω, $C_{2,\text{dudt}}$ = 30 pF, and $R_{3,\text{dudt}}$ = 1 kΩ.



Fig. 2.9: Measured and modelled input impedance and phase of a Trafotek output filter (du/dt) in the frequency band of 100 kHz−30 MHz with signal coupling (L1, L2). The parameters applied in the input impedance model are: $L_{1,\text{dudt}}$ = 43.7 µH, $R_{1,\text{dudt}}$ = 80 Ω, $C_{1,\text{dudt}}$ = 800 pF, $L_{2,\text{dudt}}$ = 2.7 µH, $R_{2,\text{dudt}}$ = 3.5 Ω, and $C_{2,\text{dudt}}$ = 540 pF.

The input impedance of both filters behaves in a similar way shown in Fig. 2.8 and Fig. 2.9. The differences are due to different sizes; the higher the power rating, the smaller mains frequency inductance. Hence, another parallel resonance frequency cannot be seen in the lower frequency band with the measurement of the ABB output filter, because it stays below the frequency of 100 kHz. The inductance values of output filters affect essentially the input impedances and the number of resonance frequencies seen in the HF band. The same model can be applied with different output filters (du/dt). The number of components in the model should be increased if all the resonance frequencies seen in Fig. 2.9 were to be modelled. In this thesis, this was not considered necessary.

### 2.3.4 Inverter

An inverter (when not using an output filter) acts as the termination impedance of a motor power cable. The inverter is more complicated to model than the above-introduced components, because it is an active one. Its input impedance of an output stage changes according to the states of the switches. However, the input impedance of an output stage can be described by two different cases with signal coupling (L1, L2). The first case is for the situation when two phases linked to the coupling interface are switched to the same potential of a DC link (Fig. 2.10a), and the second one when they are switched to different potentials (Fig. 2.11a). In the first case, the input impedance of an output stage is assumed to be equal with the impedance of the conducting switches that have the impedance of the non-conducting switches in parallel (Fig. 2.10b). In the second one, the impedance of a DC link capacitor has to be included in addition to the impedance of the conducting switches, and now the impedance of a non-conducting switch is in parallel with a DC link capacitor and a single conducting switch (Fig. 2.11b). However, there are also other possible routes in both cases, but the above-mentioned are the main ones. The IGBT includes a parallel freewheeling diode to allow current flowing when the IGBT is turned off. The communication signal cannot change the mode of a freewheeling diode. In this thesis, only an inverter that is equipped with IGBTs is studied. The effect of the input impedance of a non-conducting switch is also studied.
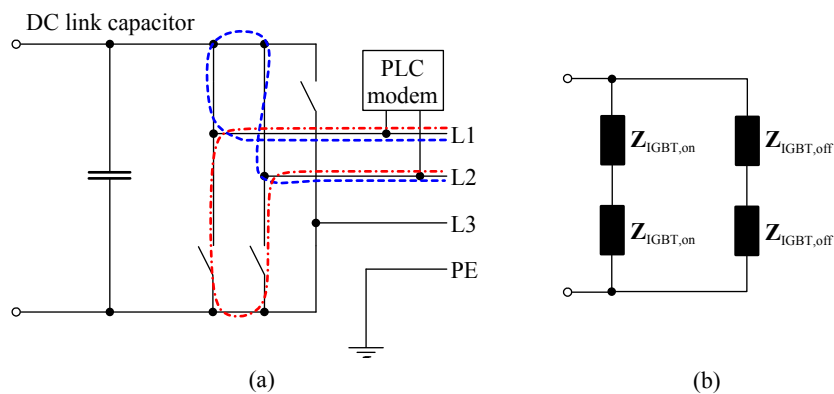


Fig. 2.10: Two phases linked to the coupling interface are switched to the same potential (state 1) of a DC link capacitor. (a) Switching state of an inverter and the paths for the HF current. (b) Input impedance model.
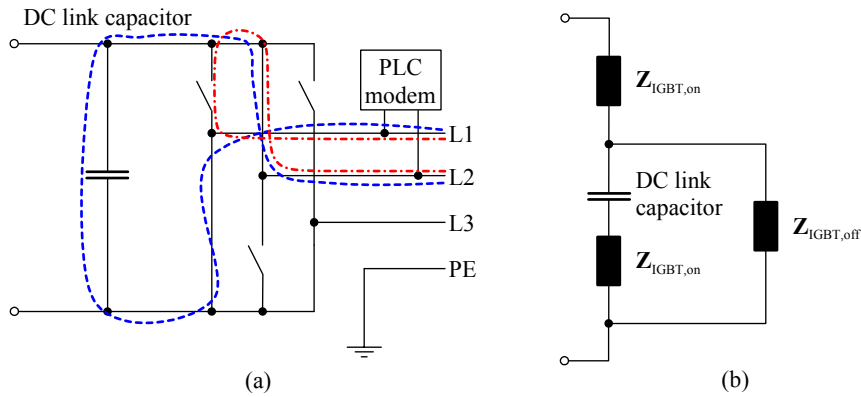
Fig. 2.11: Two phases linked to the coupling interface are switched to different potentials (state 2) of a DC link capacitor. (a) Switching state of an inverter and the paths for the HF current. (b) Input impedance model.

The input impedance model of a DC link capacitor is illustrated in Fig. 2.12. The model is identical to the model of an electric motor. The model is generally known and it is also illustrated for example in (Silventoinen, 2001). The parameter values of a model can be defined in the similar way as in the case of the output filters.
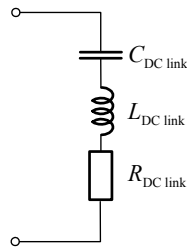


Fig. 2.12: Input impedance model of a DC link capacitor. The model can be applied in the frequency band of 100 kHz−30 MHz.

The measurement for the DC link capacitors of two frequency converters were performed for the frequency band of 100 kHz−30 MHz. The frequency converters under measurement were ABB ACS400 and ACS800. According to the measurement, the model parameters (Table 2.4) were defined. The measured and modelled input impedances of two DC link capacitors are illustrated in Fig. 2.13 and Fig. 2.14.

Table 2.4: Calculated parameters for the input impedance model of a DC link capacitor in the frequency band of 100 kHz−30 MHz. $f_{out}$ and $C_n$ are the output frequency and the nominal capacitance, respectively.

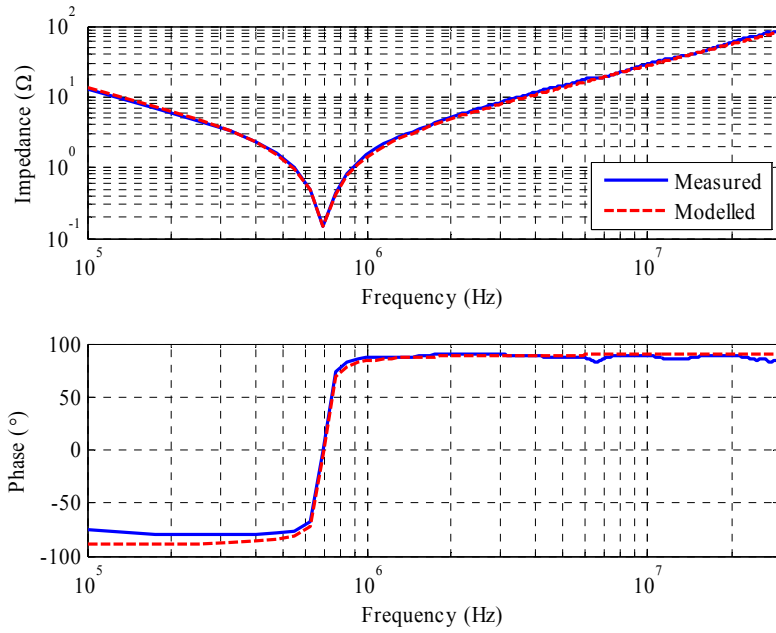| Mf. | Type | $U_n$ (V) | $I_n$ (A) | $f_{out}$ (Hz) | $C_n$ (µF) | $C_{DC\ link}$ (nF) | $L_{DC\ link}$ (nH) | $R_{DC\ link}$ (mΩ) |
|------|--------|-----------|-----------|----------------|------------|---------------------|---------------------|---------------------|
| ABB | ACS400 | 380…480 | 15.3 | 0…250 | 734 | 117 | 441 | 150 |
| ABB | ACS800 | 380…500 | 34 | 0…300 | 1030 | 400 | 400 | 100 |

Fig. 2.13: Measured and modelled input impedance and phase of a DC link capacitor (ACS400) in the frequency band of 100 kHz−30 MHz. The parameters applied in the input impedance model are: $C_{DC\ link}$ = 117 nF, $L_{DC\ link}$ = 441 nH, and $R_{DC\ link}$ = 150 mΩ.
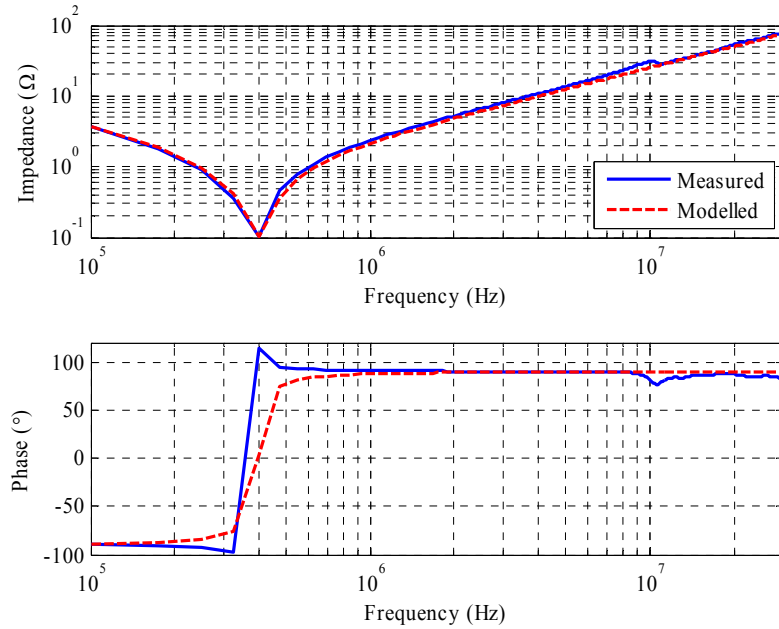


Fig. 2.14: Measured and modelled input impedance and phase of a DC link capacitor (ACS800) in the frequency band of 100 kHz−30 MHz. The parameters applied in the input impedance model are: $C_{DC\ link}$ = 400 nF, $L_{DC\ link}$ = 400 nH, and $R_{DC\ link}$ = 100 mΩ.

According to Fig. 2.13 and Fig. 2.14, the serial resonance frequency of the DC link capacitor of ACS800 is lower than the one of ACS400 because of the value of the capacitance. The size of the DC link capacitance mainly depends on the power class of an inverter. On the other hand, the power class of an inverter does not directly determine the size of a DC link capacitance, such as in (Sarén, 2005), in which the voltage source inverter with a small DC link capacitor is studied.

Different models of IGBTs are reviewed in (Sheng et al., 2000). These are divided into behavioural, numerical, and mathematical models. The models mainly illustrate the physical mechanisms and the behaviours of IGBTs. In this thesis, the input impedance model of an IGBT is developed into the HF band. The model is illustrated in Fig. 2.15, and the same model is also described in (Konaté et al., 2008). In Fig. 2.15a, the model describes the case when the switch is on, and in Fig. 2.15b, when it is off. The impedance of a conducting IGBT comprises a resistance and inductance; the resistance originates from the bonding wires and semiconductor, and the inductance mainly from the bonding wires. With the impedance of a non-conducting IGBT, in addition to the resistance and inductance, there is a serial capacitance. The capacitance is caused by the freewheeling diode, which is in parallel with the IGBT. In addition, there is also a capacitance between the collector and the emitter, when the IGBT is off. These capacitances enable the HF signal to propagate through the IGBT even if it is off. The parameter values of a model can be defined in the same way as in the case of the output filters.
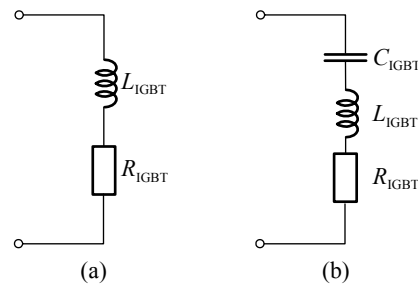


(a)           (b)

Fig. 2.15: Input impedance model of an IGBT. The model can be applied in the frequency band of 100 kHz−30 MHz. (a) IGBT is on. (b) IGBT is off.

The measured and modelled input impedances of an IGBT (conducting and non-conducting) are illustrated in Fig. 2.16 and Fig. 2.17. The IGBT under measurement was Semikron SKM75GB176D, which is used in frequency converter drives with the mains voltage of 575−750 V. The parameters in the model of an IGBT were as follows: $C_{IGBT} = 2.1$ nF, $L_{IGBT} = 123$ nH, and $R_{IGBT} = 300$ mΩ. According to Fig. 2.17, the impedance of an IGBT looks nearly similar above the frequencies of 7 MHz even if the switch is on or off, because the inductance and resistance dominate. The result is important, because it proves that the influence of a non-conducting IGBT on the construction of a channel model cannot be ignored. This effect on the HF current path is illustrated in Fig. 2.10a and Fig. 2.11a with the red lines. Hence, also the impedances of the non-conducting IGBTs are added to the input impedance models illustrated in Fig. 2.10b and Fig. 2.11b.
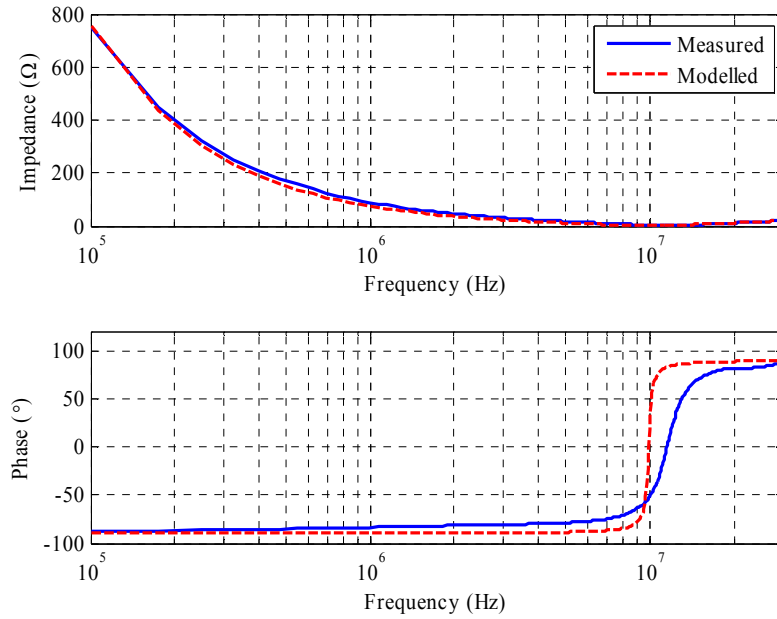
Fig. 2.16: Measured and modelled input impedance and phase of a non-conducting IGBT (Semikron SKM75GB176D) in the frequency band of 100 kHz−30 MHz. The ports of the IGBT were open. The parameters applied in the input impedance model are: $C_{IGBT}$ = 2.1 nF, $L_{IGBT}$ = 123 nH, and $R_{IGBT}$ = 300 mΩ.
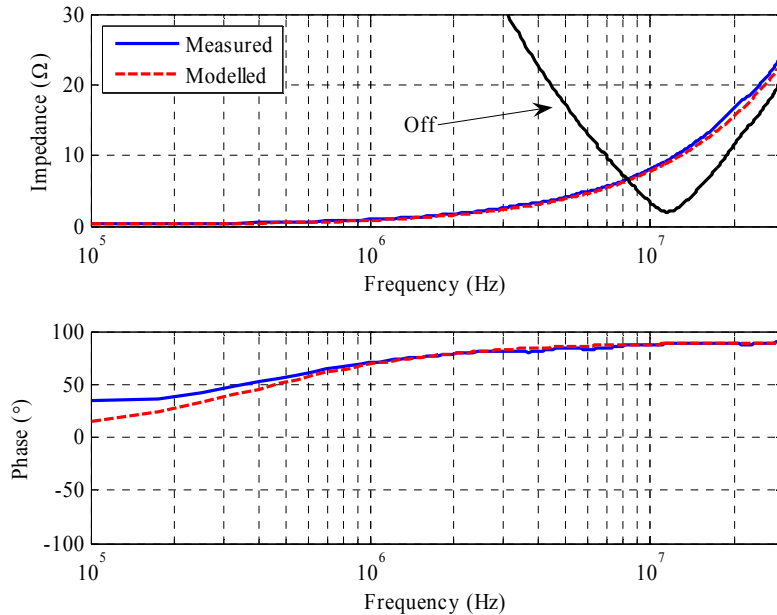


Fig. 2.17: Measured and modelled input impedance and phase of a conducting IGBT (Semikron SKM75GB176D) in the frequency band of 100 kHz−30 MHz. The parameters applied in the input impedance model are: $L_{IGBT}$ = 123 nH, and $R_{IGBT}$ = 300 mΩ. The collector, emitter, and gate voltages of

the IGBT were as follows: $U_C = 0.95$ V, $U_E = 0$ V, $U_G = 7$ V. The input impedance curve of a non-conducting IGBT is also included and marked as Off.

According to the input impedance models of a DC link capacitor and an IGBT, input impedance models can be formed for the states 1 and 2 of an inverter as illustrated in Fig. 2.10b and Fig. 2.11b, respectively. The modelled input impedances of an inverter are illustrated in Fig. 2.18 and Fig. 2.19. Both the cases, when non-conducting IGBTs are included into the model and when not, are modelled. According to Fig. 2.18 and Fig. 2.19, the non-conducting IGBTs add a parallel and serial resonance frequency into the input impedance. The resonance frequencies are located in the HF band, and hence they are very essential from the viewpoint of PLC. The input impedances vary between 0.6 and 300 Ω in the HF band and between 0.6 and 20 Ω in the lower frequency band. A different-size DC link capacitance changes only the location of the first serial resonance frequency in the case when two phases linked to the coupling interface are switched to different potentials of a DC link capacitor. Different IGBTs may also vary the locations of the resonance frequencies in the HF band.
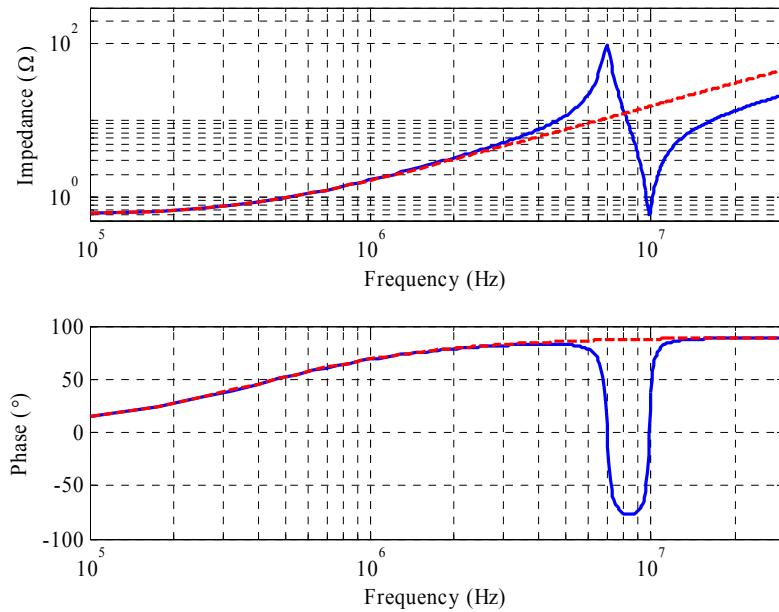


Fig. 2.18: Modelled input impedances and phases of an inverter in the frequency band of 100 kHz−30 MHz, when two phases linked to the coupling interface are switched to the same potential of a DC link capacitor. The solid line includes non-conducting IGBTs, but the dashed line does not. The model includes both the DC link capacitor (ACS400) and the IGBT (Semikron SKM75GB176D).

Fig. 2.19: Modelled input impedances and phases of an inverter in the frequency band of 100 kHz−30 MHz, when two phases linked to the coupling interface are switched to different potentials of a DC link capacitor. The solid line includes non-conducting IGBTs, but the dashed line does not. The model includes both the DC link capacitor (ACS400) and the IGBT (Semikron SKM75GB176D).
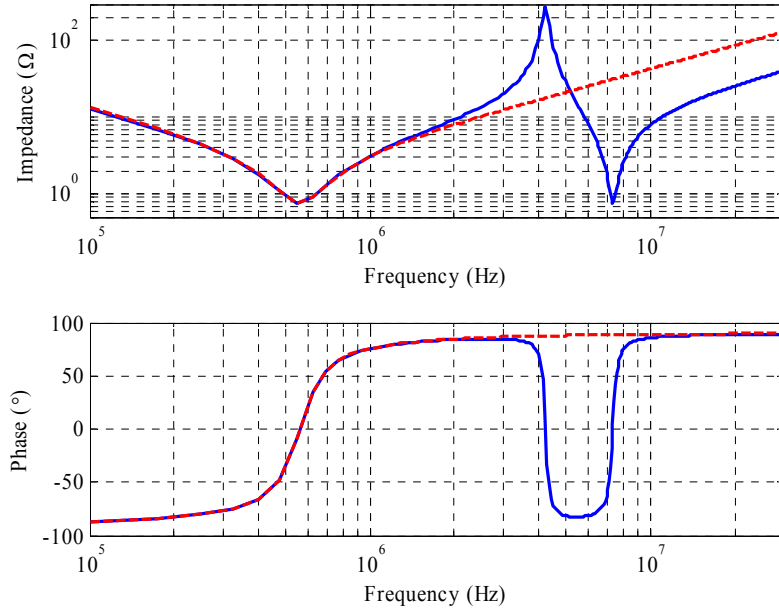
## 2.3.5  Coupling interface

The coupling interface forms the most important part of a PLC channel, because it is the only component that can be affected by the designer of the communication system. The coupling interface causes insertion and reception losses, which can generally be the most significant factors in the whole attenuation. The coupling interface is described in detail in section 3.5. Now, the input impedance model of a coupling interface is studied. The main components of a model are constructed according to the topology and the distributed ones according to the measurements. All the values are fitted by the measurement. The applied frequency band was 100 kHz−30 MHz. The topology of the developed coupling interface and its input impedance model are illustrated in Fig. 2.20.
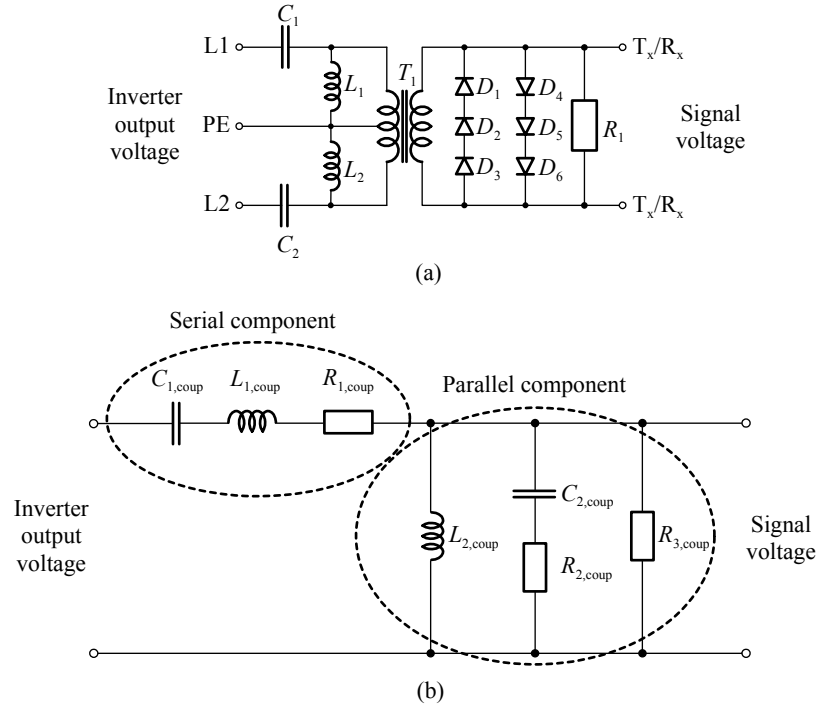
(a)



(b)

Fig. 2.20: Developed coupling interface. (a) Topology. (b) Input impedance model of a coupling interface. The model can be applied in the frequency band of 100 kHz−30 MHz.

The measured and modelled input impedances of a coupling interface for the serial and parallel components are illustrated in Fig. 2.21 and Fig. 2.22, respectively. The serial component was measured from the side of the output voltage of an inverter when the other end was short-circuited, and the parallel one from the side of the signal voltage when the other end was open. According to the measurement, the components in the model are as follows:

$$
\begin{cases}
C_{1,\text{coup}} = 374\,\text{pF (coupling capacitor)} \\
L_{1,\text{coup}} = 1.3\,\mu\text{H (leakage inductance of transformer)} \\
R_{1,\text{coup}} = 4.5\,\Omega\,\text{(winding resistance)} \\
L_{2,\text{coup}} = 1.5\,\mu\text{H (magnetizing inductance of transformer and inductors in parallel)} \\
C_{2,\text{coup}} = 56\,\text{pF (stray capacitance of winding turns of transformer, and diode bridge)} \\
R_{2,\text{coup}} = 15\,\Omega\,\text{(serial resistance of stray capacitance)} \\
R_{3,\text{coup}} = 10\,\text{k}\Omega\,\text{(load resistance)}
\end{cases}
$$

The values of the main components in the model differ slightly from the reported ones, but this is tolerable because ideal components were not used in the practical coupling interface. The model is kept as simple as possible, and hence it only includes the serial and parallel components of impedances as depicted in Fig. 2.20. According to Fig. 2.21 and Fig. 2.22, the serial resonance frequency is at 7.2 MHz and the parallel one at 17.3 MHz. The resonance frequencies can be moved by adjusting the values of components of the coupling interface.

Fig. 2.21: Measured and modelled input impedance and phase of a coupling interface for the serial component in the frequency band of 100 kHz–30 MHz. The parameters applied in the input impedance model are: $C_{1,coup} = 374$ pF, $L_{1,coup} = 1.3$ μH, and $R_{1,coup} = 4.5$ Ω.
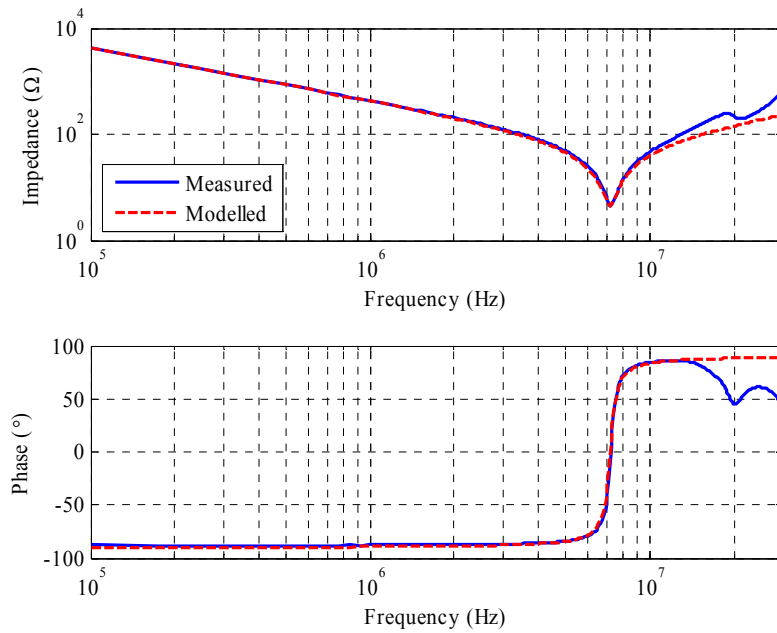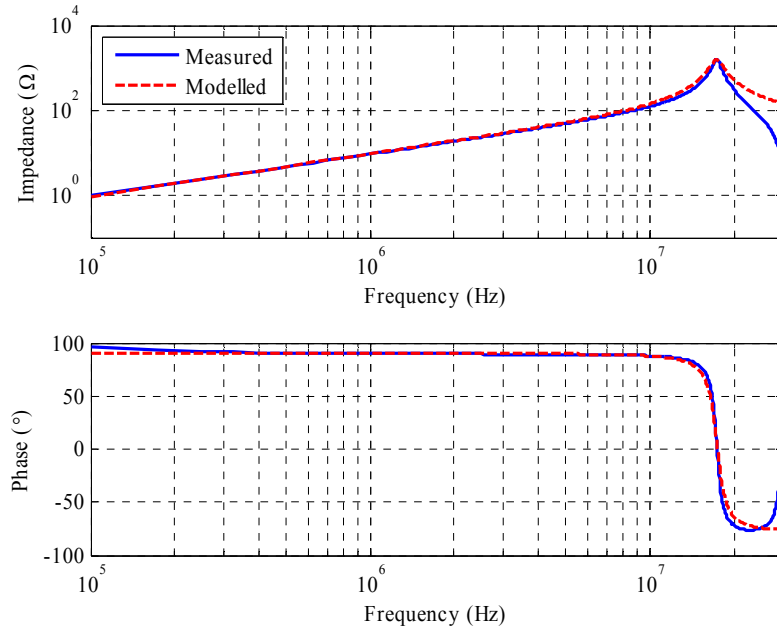


Fig. 2.22: Measured and modelled input impedance and phase of a coupling interface for the parallel component in the frequency band of 100 kHz–30 MHz. The parameters applied in the input impedance model are: $C_{2,coup} = 56$ pF, $L_{2,coup} = 1.5$ μH, $R_{2,coup} = 15$ Ω, and $R_{3,coup} = 10$ kΩ.

## 2.4 Channel model

The channel model can now be constructed by utilizing the developed input impedance models, forming two-port models for them according to (2.12) and (2.13), and concatenating them by the chain rule (2.14). The channel model is illustrated in Fig. 2.5. In order to verify the simulation results, the channel characteristics of the test drive were measured. The measurements were carried out for the frequency band of 100 kHz−30 MHz and signal coupling (L1, L2) by a network analyzer Agilent 4395A with a S-parameter test set device Agilent 87511A. The measurement information was stored into 401 data points including the frequency and the scattering parameters (or S-parameters) for each measurement. The source power was set to 10 dBm and the intermediate filter to the bandwidth of 30 kHz. To ensure the settling time of the filter and the detector circuit in the network analyzer, the sweep time was set to a second. The scattering parameters consist of four parameters; $S_{11}$ and $S_{22}$ are the power reflection coefficients at the input and output ports, respectively, while $S_{12}$ and $S_{21}$ are the power attenuation through the channel from the output port to the input port and vice versa, respectively.

If both the source and load impedances are equal, the power attenuation is equal to the voltage attenuation. Hence, both in the measurement and simulation, the source and load impedances were set to 50 Ω. The drive under test comprised an ABB 15 kW induction motor (4-pole), a 90-meter-long Pirelli MCCMK 3x35+16 motor cable, an ABB output filter (optional), an ABB ACS400 frequency converter, and the developed coupling interfaces at both cable ends. The measurements were carried out without the mains voltage on; this, however, does not affect the results when an output filter is included. This is shown in Publication III. On the other hand, the channel attenuation is almost impossible to measure with the mains voltage on when the output filter is not applied, because the channel attenuation would vary all the time resulting from the switching states of IGBTs. Hence, in this thesis, the channel attenuation is only simulated when the output filter is not used. The measured and simulated power amplification is illustrated in Fig. 2.23 when the output filter is applied in the test drive.

According to Fig. 2.23, the measured power amplification includes oscillation above 14 MHz frequencies. The oscillation frequency is too high to be considered cable oscillation. On the other hand, the cable oscillation is attenuated the more, the higher frequency is at issue, which has been presented in (Ahola, 2003). The cable length affects also the strength of cable oscillations. In practice, the cable oscillation is strongest at the LF band, but in this case, it is attenuated by the coupling interface. The strong oscillation and the differences between measured and simulated power amplifications above 14 MHz frequencies may be caused by the network analyzer. According to the measured result, the power attenuation still gets smaller when reaching the frequency of 30 MHz, but this cannot be true because of the signal attenuation of the motor power cable according to (2.8), which is illustrated in the form of dB/m in Fig. 2.24. According to Fig. 2.24, the 90-meter-long motor power cable attenuates about 6 dB more the signal of 30 MHz than the signal of 10 MHz.
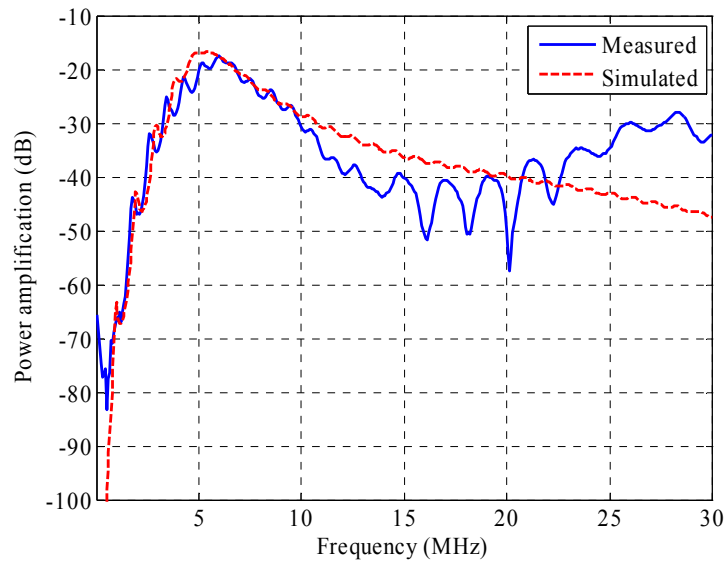
Fig. 2.23: Measured and simulated power amplification of the test channel from the motor to the inverter in the frequency band of 100 kHz−30 MHz. The drive under test comprised an ABB 15 kW induction motor (4-pole), a 90-meter-long Pirelli MCCMK 3x35+16 motor cable, an ABB output filter, an ABB ACS400 frequency converter, and the developed coupling interfaces at the both cable ends.
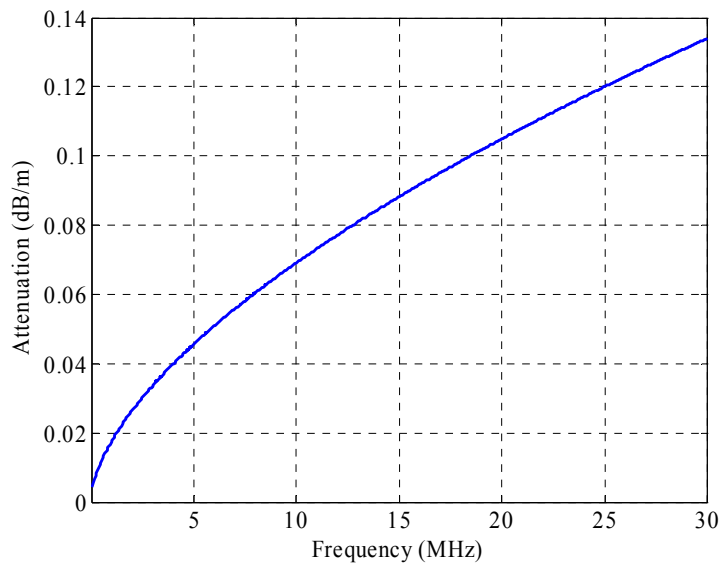


Fig. 2.24: Signal voltage attenuation per-unit length in the MCMK type LV power cable in the frequency band of 100 kHz−30 MHz.

The simulated power amplifications are illustrated in Fig. 2.25 for the both above-introduced switching states of IGBTs in the test drive when the output filter is not applied. The State 1 indicates the case, when two phases linked to the coupling interface are switched to the same potential, and the State 2, when they are switched to different potentials. According to Fig. 2.23 and Fig. 2.25, all the channels seem to be very similar until the frequency of 5 MHz. There is a

notch at the frequencies of 10 MHz and at 7 MHz in the cases of State 1 and State 2, respectively. These are caused by the serial resonance frequency in the input impedance of an inverter seen both in Fig. 2.18 and Fig. 2.19. There is about 2−15 dB difference above 5 MHz frequencies except near the notch frequencies in the channel attenuations between the cases when the output filter is used and when not. Near the notch frequencies, the difference may be even twice of that. Even if all the channel attenuation characteristics are near to each other, the main problem without the output filter is nevertheless the noise power at the inverter end. This result means that the output filter decreases both the HF signal attenuation and the HF noise power in the motor power cable.



Fig. 2.25: Simulated power amplifications of the test channel from the motor to the inverter in the frequency band of 100 kHz−30 MHz. The drive under test comprised an ABB 15 kW induction motor (4-pole), a 90-meter-long Pirelli MCCMK 3x35+16 motor cable, an ABB ACS400 frequency converter, Semikron SKM75GB176D IGBT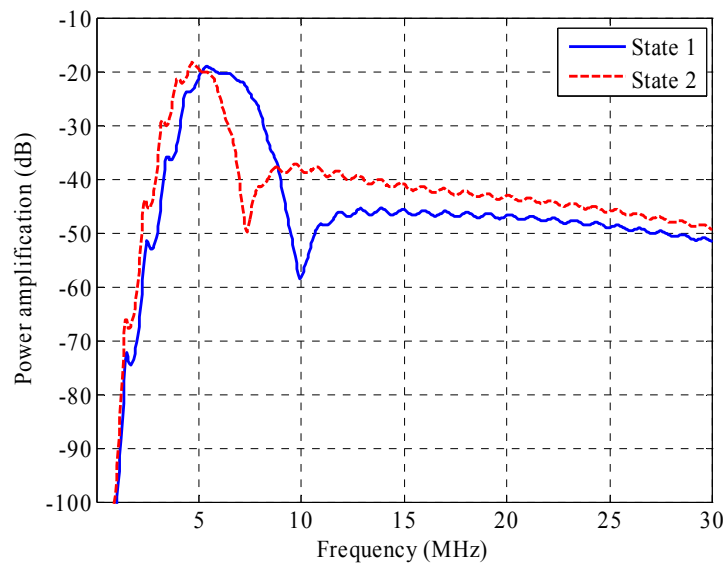s, and the developed coupling interfaces at the both cable ends. The State 1 indicates the case, when two phases linked to the coupling interface are switched to the same potential, and the State 2, when they are switched to different potentials.

## 2.5  Noise source

Not only the channel transmission characteristics, but also the interference scenario is important from the viewpoint of communication. In motor cable communication, this is naturally an issue that has to be taken into consideration. According to Götz et al. (2004), power lines do not represent an additive white Gaussian noise (AWGN) channel. According to Zimmermann and Dostert (2002a), the interference scenario of PLC is complicated, because the noise consists of five different variations: coloured background noise, narrowband noise, periodic impulsive noise asynchronous or synchronous to the network frequency (50/60 Hz), and asynchronous impulsive noise.

In motor cable communication, the main noise source is the output stage of the inverter, which can be considered an aperiodic impulsive noise source regardless of the implementation of the switching method. The output voltage of an inverter basically consists of pulses or square waves with a variable frequency and duration (Chen et al., 1994). In modern industrial PWM

drives, the output voltage rise or fall times (du/dt) of IGBTs are in the range of 0.1−10 μs, and the switching frequencies vary between 2 and 20 kHz (Bartolucci and Finke, 2001). Each switching injects a surge wave, the frequency content of which may reach to several megahertz, into the motor power cable. In practice, an output filter can be used to slow the du/dt times, and consequently, the stress effects on the motor insulation materials, bearing currents, and shaft voltages are reduced (Chen and Lipo, 1998).

Impulsive noise characteristics in the broadband PLC are analyzed in (Zimmermann and Dostert, 2002a). The impulsive noise in an inverter-fed motor cable is an extreme case, because especially its amplitude differs from the noise existing in normal distribution networks. The amplitude of impulsive noise can be even twice the DC link voltage because of the result of the cable oscillation. The DC link voltage $U_{\text{DC link}}$ can be calculated based on the mains voltage $U_{\text{mains}}$ as follows:

$$U_{\text{DC link}} = \frac{3\sqrt{2}}{\pi} \cdot U_{\text{mains}} .$$

(2.24)

The noise current spectrum is illustrated in Publication II. A measured inverter output voltage waveform is illustrated in Fig. 2.26, which shows that the power spectral density (PSD) is at highest around the output and switching frequencies. The PSD of the noise starts to lower after the main cable oscillation frequency of 105 kHz, and the fall stops at 400 kHz. The peaks in the amplitude spectrum are mainly caused by the voltage rising edges. At megahertz frequencies, the PSD of the noise is at a reasonable level to reach the signal-to-noise ratio (SNR) required for communication with the transmission power of milliwatts. This makes it possible to use these frequencies for communication. The similar conclusion can also be made according to the results introduced in section 2.6 and in section 3.6. In the inverter-fed drives, the frequency band for communication has to be chosen carefully, because it is always a compromise between the PSD of the noise at the lower frequency band and the signal attenuation of a PVC-insulated motor power cable at the higher frequency band.
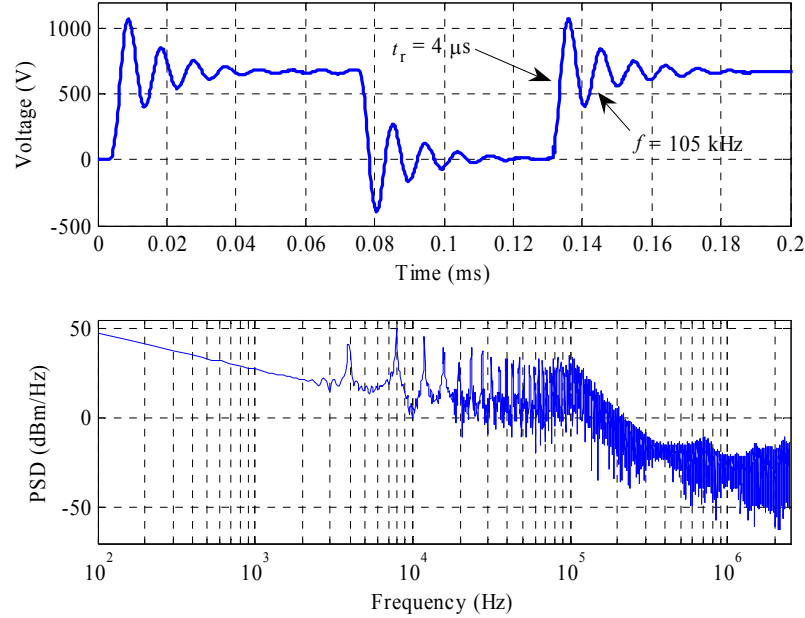
Fig. 2.26: Measured output voltage of an inverter between phase conductors (L1, L2) at the inverter end and its frequency content. The mains voltage is 500 V and the cable length 90 m. The switching of an inverter output stage generates steeply rising ($t_r = 4\ \mu s$) surge waves followed by the cable oscillation ($f = 105$ kHz). The energy content is at highest around the output and switching frequencies of an inverter, and also near the cable oscillation frequency. The noise includes frequency components up to several megahertz.

## 2.6  Theoretical information capacity

The information capacity analysis of a communication channel gives an estimate from the available bandwidth in an inverter-fed motor power cable. The information capacity of the channel depends on the signal-to-noise ratio at the receiver end and the available frequency band for the data transmission. According to the Hartley-Shannon law, an upper limit on the information capacity of a communication channel is:

$$C = B \log_2\left(1 + \frac{S}{N}\right),$$
(2.25)

where $C$ represents the information capacity of the channel (bps), $B$ the available bandwidth, and the symbols $S$ and $N$ the signal and noise power at the receiver end, respectively. The theory is not directly applicable to the analysis of a power line channel, because the signal-to-noise ratio is frequency dependent in an actual channel, and in the Hartley-Shannon law, the assumption is based on the AWGN channel, which is not true in PLC channels. However, the main idea is to obtain an indicative estimate of the channel information capacity.

The output voltage of the transmitter $|\mathbf{U}_{tx}(f)|$ can be presented by the output power of the transmitter $P_{tx}(f)$, and the input impedance of the communication channel at the transmitter end $\mathbf{Z}_{in,tx}(f)$:

$$|\mathbf{U}_{\mathrm{tx}}(f)| = \left| \sqrt{\frac{P_{\mathrm{tx}}(f)}{\cos\varphi(f)} \mathbf{Z}_{\mathrm{in,tx}}(f)} \right| , \qquad (2.26)$$

where $\cos\varphi(f)$ is the phase angle of the input impedance $\mathbf{Z}_{\mathrm{in,tx}}(f)$. The voltage of the received signal $|\mathbf{U}_{\mathrm{rx}}(f)|$ can be written as follows:

$$|\mathbf{U}_{\mathrm{rx}}(f)| = |\mathbf{H}(f)| \cdot |\mathbf{U}_{\mathrm{tx}}(f)| , \qquad (2.27)$$

where $|\mathbf{H}(f)|$ is the transfer function of the communication channel. The noise voltage at the receiver end $|\mathbf{U}_{\mathrm{n,rx}}(f)|$ is measured in the time-domain from the coupling interface at the receiver end, and it is then filtered by band-pass filters with 84 narrowband similarly as in HomePlug 1.0 explained in (Lee et al., 2003). The root mean square (RMS) value of the noise voltage can now be calculated individually for each sub-carrier. The information capacity of the power line channel can now be described according to the signal and noise voltages:

$$C = \int_{f_{\mathrm{l}}}^{f_{\mathrm{h}}} \log_2 \left[ 1 + \left( \frac{|\mathbf{U}_{\mathrm{rx}}(f)|}{|\mathbf{U}_{\mathrm{n,rx}}(f)|} \right)^2 \right] df , \qquad (2.28)$$

where $f_{\mathrm{h}}$, and $f_{\mathrm{l}}$ are the highest and lowest frequency of the applied band, respectively, and $df$ the bandwidth of the individual sub-carrier. The estimated channel capacity as a function of transmission power for the test drive in the frequency band of 4.49–20.7 MHz is presented in Fig. 2.27. The drive under test comprised an ABB 15 kW induction motor (4-pole), a 90-meter-long Pirelli MCCMK 3x35+16 motor cable, an ABB output filter, an ABB ACS400 frequency converter, and the developed coupling interfaces at the both cable ends. According to Fig. 2.27, the motor cable of a variable-speed drive provides a broadband communication channel for the frequency band used, even if the transmission power is in the range of milliwatts. The transmission power is distributed with a flat power spectrum even if the noise and channel characteristics are both frequency dependent. The power scale in Fig. 2.27 is proportional to the PSD of the HomePlug specification (section 3.4) as follows:

$$PSD = 10 \log_{10} \left( \frac{\dfrac{P_{\mathrm{tx,tot}}}{1\,\mathrm{mW}}}{f_{\mathrm{h}} - f_{\mathrm{l}}} \right) \leq -50\,\mathrm{dBm/Hz} , \qquad (2.29)$$

where $P_{\mathrm{tx,tot}}$ is the total transmission power. According to (2.29), the maximum transmission power of the HomePlug specification cannot be more than 160 mW for the frequency band to be used.
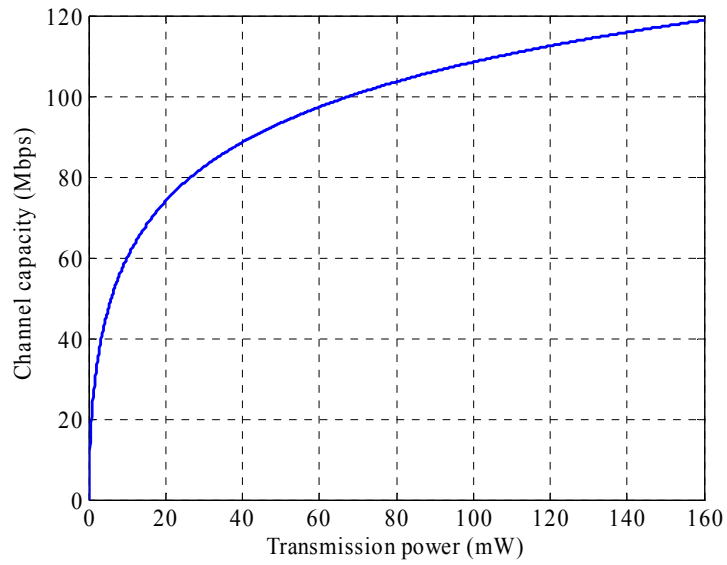
Fig. 2.27: Estimated channel capacity as a function of transmission power for the test drive in the frequency band of 4.49–20.7 MHz. The transmitter is at the motor end and the receiver at the inverter end. The drive under test comprised an ABB 15 kW induction motor (4-pole), a 90-meter-long Pirelli MCCMK 3x35+16 motor cable, an ABB output filter, an ABB ACS400 frequency converter, and the developed coupling interfaces at the both cable ends with signal coupling (L1, L2).

# 3 COMMUNICATION OVER MOTOR POWER CABLE

This chapter describes the methods applied to motor cable communication in this thesis. First, PLC regulations available at the moment in Europe are presented. Next, an effective multi-carrier method called orthogonal frequency division multiplexing (OFDM) is introduced. Some error-correcting methods are presented in brief. These methods are applied by HomePlug-certified products. HomePlug is an alliance that defines specifications for PLC. HomePlug itself and its two specifications are presented in more detail in section 3.4. The developed coupling interface that is generally applicable in LV inverter-fed motor cables is described, and its operation is verified by measurements. Finally, a test device is constructed, by which the practical data transmission tests are carried out. The test results are also illustrated and analyzed.

## 3.1 Available PLC regulations in Europe

There is only one valid standard in the European Union that concerns signalling on LV electrical installations intended for narrowband communication (kbps). The European standard EN 50065-1 (EN, 1991) was first published in 1991 by the European Committee for Electrotechnical Standardization (CENELEC), and it replaced all the other individual national standards in Europe. In addition, Germany has a national regulation NB30 (Hansen, 2002) that concerns signalling on power lines up to 30 MHz frequencies intended for broadband communication (Mbps).

In addition to these regulations, there are specifications, which are intended for manufacturers to support the co-operation of PLC products. The specifications are defined by Open PLC European Research Alliance (Opera, 2007), and HomePlug® Powerline Alliance (HomePlug, 2007), called DS2 and HomePlug, respectively. Furthermore, there is Consumer Electronics Powerline Communication Alliance (CEPCA, 2007) that develops and promotes managed coexistence of various PLC technologies. In this work, HomePlug standard compliant modems are used. The HomePlug spefications are described in more detail in section 3.4.

### 3.1.1 EN 50065-1

The European standard EN 50065-1 (Fig. 3.1) specifies the frequency bands allocated to the different applications, limits for the transmitter output voltage in the operating bands, and limits for conducted and radiated emissions. In addition, the methods for measurement are defined. The standard does not specify modulation methods or functional features. It reserves the frequency range from 3 kHz to 148.5 kHz (EN, 1991) that is called CENELEC frequency band. These frequencies differ considerably from other regulations, for example those applicable in the United States or in Japan, where a frequency range up to approximately 500 kHz is available (Dostert, 2001). In addition, signal injection between the neutral conductor and protective earth is admissible in these countries. In Fig. 3.1, the frequency range is divided into two parts, where frequencies below 95 kHz (A band) are reserved for use by electricity suppliers, while the frequencies between 95 and 148.5 kHz (B, C, and D bands) are meant for private use, mainly within buildings. A maximum signal level in general use within B, C, and D bands is 116 dBμV (0.63 V), but in an industrial environment it is allowed to be 134 dBμV (5 V). Similar values within A band may be 134 dBμV @ 9 kHz, and the values are lowered to 120 dBμV (1 V) @ 95 kHz, but with wide band modulation, the maximum level can be 134 dBμV within the whole range. The standard specifies a carrier sense multiple access (CSMA) protocol, which is well known from Ethernet, for the C band.
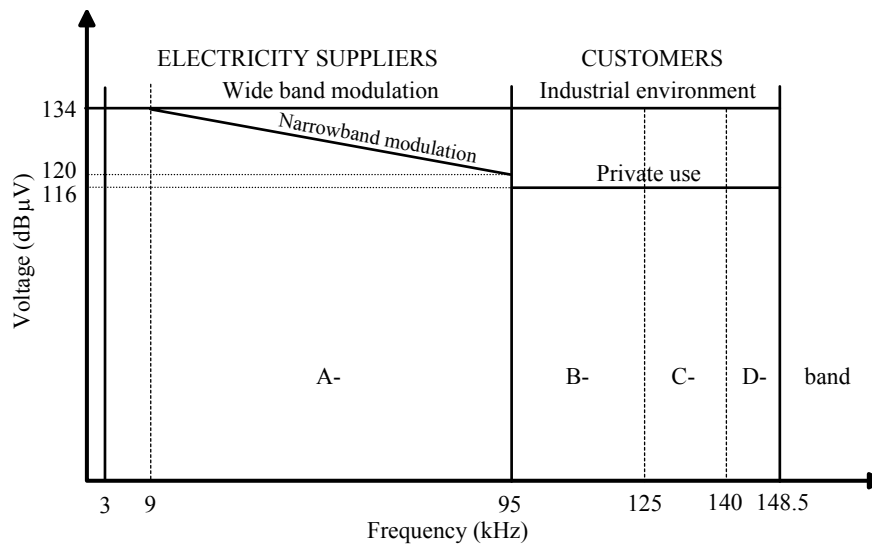
Fig. 3.1: Limits for the transmitter output voltage across the standard load in the operating frequency bands according to European CENELEC EN 50065-1 standard for signalling on LV electrical installations (EN, 1991).

## 3.1.2  IEEE P1901

Because the standardization is behind the available techniques, there is an ongoing project to develop a standard IEEE P1901 for high-speed (>100 Mbps at the PHY) communication devices via AC power lines (IEEE, 2007). It is a draft standard for broadband over power line (BPL) networks, which defines medium access control (MAC) and PHY specifications. The standard will use transmission frequencies below 100 MHz (Galli and Logvinov, 2008). It will be applicable to all classes of BPL devices, including BPL devices used for the first-/last-mile (<1500 m) connection as well as BPL devices used in buildings for local area networks (LANs) and other data distribution (<100 m).

## 3.2  Orthogonal frequency division multiplexing

OFDM (Bingham, 1990) is one of the most promising techniques for broadband communication over power lines. It is currently used in digital subscriber line (DSL) technologies, terrestrial digital video broadcasting (DVB-T) (EN, 2004), and IEEE's high-rate wireless local area network (WLAN) standards (IEEE 802.11b/g). The basic idea of OFDM is to divide the frequency band into multiple equally spaced narrowband and slow-bit stream sub-carriers, where data is transmitted in parallel. This reduces the impact of multipath effect compared with a single high-speed bit stream. Each sub-carrier can be handled individually and modulated with a conventional narrowband modulation method. The signal strength and interference, and thereby the signal-to-interference ratio (SIR), can differ between each channel (Steer, 2007). This can be compensated by using different bit rates and adjusting the power level in each sub-channel. Further, hostile sub-channels, where it is impossible to transmit data, can be ignored and the remaining transmission power can be freed for the available sub-channels. The main advantages of OFDM are its ability to cope with the effects of amplitude and delay distortion, and impulsive noise (Saltzberg, 1967). Also the impact of the multipath propagation is mitigated, because each sub-carrier has a relatively narrow bandwidth, or in time-domain, a long duration (Steer, 2007).

In OFDM, sub-carrier frequencies are located orthogonally (Fig. 3.2) to each other, which means that cross-talk or interference between the adjacent sub-channels is eliminated. The orthogonality allows high spectral efficiency, because sub-carriers are overlapping. According to Steer (2007), in an ideal case, other sub-carriers are zero at the peak of a single sub-carrier in OFDM. However, OFDM requires very accurate frequency synchronization between the transmitter and the receiver to avoid frequency deviation. This causes that the sub-carriers will no longer be orthogonal, which leads to the inter-carrier interference (ICI) effect, which means cross-talk between the sub-carriers.
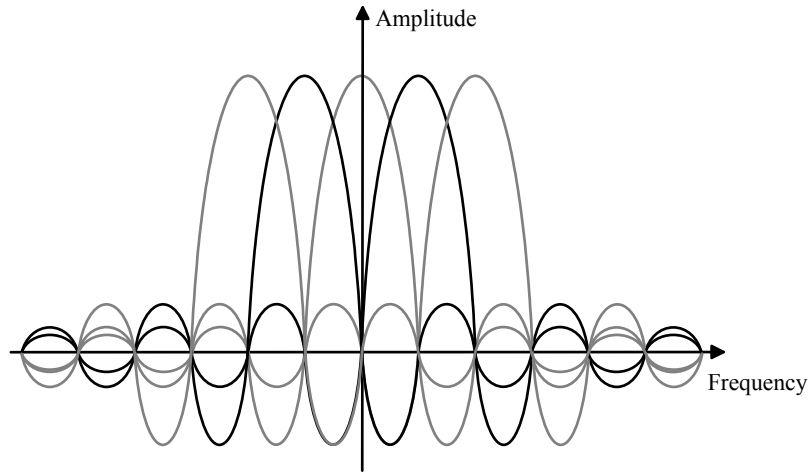


Fig. 3.2: OFDM spectrum showing orthogonality. The sub-carriers are ideally orthogonal; this is illustrated by the peak of a single sub-carrier, which is located at the zeros of the other sub-carriers.

Since low-symbol-rate modulation methods suffer less from inter-symbol interference (ISI) caused by the multipath propagation, it is favourable to transmit many low-rate streams instead of a single high-rate stream. Because the duration of a single symbol is relatively long, it is advisable to insert a guard interval between the OFDM symbols to eliminate the ISI effect. The guard interval eliminates the need for a pulse-shaping filter, and reduces the sensitivity to the time synchronization problem. In practice, the guard interval is implemented by a cyclic prefix (CP). The CP is formed from the last samples of the body of the OFDM symbol copied and appended as a preamble to form the complete OFDM symbol (Baig and Gohar, 2003).

OFDM can be implemented by using separate modulators for each sub-carrier. However, the orthogonality allows efficient modulator and demodulator implementation using inverse fast Fourier transform (IFFT) and fast Fourier transform (FFT) algorithms, respectively. The FFT is an algorithm for computing the discrete Fourier transform (DFT):

$$\mathbf{X}(k) = \sum_{n=0}^{N-1} \mathbf{x}(n) \mathrm{e}^{-\mathrm{j}2\pi kn/N} \quad k = 0, 1, 2, ..., N-1, \tag{3.1}$$

where $\mathbf{X}(k)$ are the coefficients of DFT for the sequence $\mathbf{x}(n)$ of length $N$. Correspondingly, the IFFT algorithm for computing the inverse DFT (IDFT) can be defined as follows:

$$\mathbf{x}(n) = \frac{1}{N} \sum_{k=0}^{N-1} \mathbf{X}(k) \mathrm{e}^{\mathrm{j}2\pi kn/N} \quad n = 0, 1, 2, ..., N-1, \tag{3.2}$$

where $\mathbf{x}(n)$ are the coefficients of IDFT for the sequence $\mathbf{X}(k)$ of length $N$. The FFT algorithm exploits symmetry and periodic properties of the phase factor (Proakis and Manolakis, 1996). Generally, the size $N$ is a power of 2, because this is vital for powerful FFT computation. Hence, the frequency band is also divided in the same way in OFDM. In practice, the separate modulators and demodulators are replaced by an IFFT and FFT, respectively. Nowadays, these can be implemented easily in a digital signal processor (DSP). The IFFT/FFT implementation of OFDM is called discrete multitone (DMT) (Steer, 2007). Here the sub-carriers share a common frequency band, and the frequency outputs of the IFFT of the data stream are the sub-carriers. According to Ma et al. (2005), OFDM can perform better than a single-carrier system in the channel interfered by an impulsive noise, because the DFT algorithm spreads the effect of an impulsive noise over multiple symbols, whereas it will affect only one symbol in a single-carrier system.

## 3.3  Forward error correction

Coding for error-detection, without correction, is simpler than error-correction coding (Carlson et al., 2002). The receiver can request a retransmission of information containing errors that cannot be corrected, if there is a bidirectional communication channel available between a source and destination. This error-control strategy is generally known as an automatic repeat request (ARQ). The forward error correction (FEC) is done by an error-correcting code. There are many different codes and techniques available; however, in this study, only the ones applied in the HomePlug technologies are considered.

### 3.3.1  Scrambling

Scrambling is a coding operation at the transmitter to reduce the length of long strings of like bits that might impair receiver synchronization. The synchronization is essential in digital communication. The scrambled sequence must be descrambled at the receiver to preserve overall bit sequence transparency. This can be done based on a scramble polynomial that must be known by both the transmitter and the receiver.

### 3.3.2  Interleaving

Impulse noise produced for example by switching transients causes errors in bursts that can corrupt several successive bits. These multiple errors cause problems with conventional codes and must be combated by special techniques. One solution is to spread out the transmitted codewords using a system of interleaving as illustrated in Fig. 3.3. Error correction bits enable the channel decoder to correct a certain number of altered bits. Hence, if a burst error occurs, and more than this number of bits is altered, the codeword cannot be correctly decoded. Interleaving spreads out the altered bits among several codewords, which can be decoded correctly by the decoder. Interleaving increases the latency, because the entire interleaved block must be received before the critical data can be deinterleaved. The length of latency depends on the implementation of the interleaving method.

| Error-free message: | a a a a b b b b c c c c d d d d e e e e f f f f g g g g |
| Transmission with a burst error: | a a a a b b b b c c c _ _ _ _ d e e e e f f f f g g g g |
| Interleaved: | a b c d e f g a b c d e f g a b c d e f g a b c d e f g |
| Transmission with a burst error: | a b c d e f g a b c d _ _ _ _ b c d e f g a b c d e f g |
| Deinterleaved with a burst error: | a a _ a b b b b c c c c d d d d e _ e e f _ f f g _ g g |

Fig. 3.3: Influence of interleaving on a message, the codeword length of which is 4, during a burst error. The interleaved message can be corrected by an FEC, which is only able to fix a single bit per a codeword.

### 3.3.3 Reed-Solomon codes

The Reed-Solomon (RS) codes were first presented by Reed and Solomon (1960). The RS codes belong to the block codes, and they are an important subclass of nonbinary Bose-Chaudhuri-Hocquenghem (BCH) codes (Haykin, 1994). Nowadays, RS codes are widely used in different applications, such as in compact disc (CD), digital versatile disc (DVD), satellite communication, DVB, and DSL technologies. The RS encoder differs from a binary encoder, because it operates on multiple bits rather than individual bits. The RS $(n, k)$ code is used to encode $m$-bit symbols into a code word consisting of

$$n = 2^m - 1 \tag{3.3}$$

symbols, where $m \geq 1$. Thus, the encoder expands the block of $k$ message symbols to $n$ symbols by adding

$$2e = n - k \tag{3.4}$$

redundant symbols. The RS code can correct up to $e$ errors and $2e$ erasures (the locations of the errors are known). Also any combination of errors and erasures as long as the inequality

$$2e_{\mathrm{err}} + e_{\mathrm{era}} \prec n - k \tag{3.5}$$

is satisfied, where $e_{\mathrm{err}}$ is the number of errors and $e_{\mathrm{era}}$ the number of erasures in the block. The properties of RS codes suit to applications where errors occur in bursts, because it does not matter how many bits in a symbol are corrupted; they are nevertheless counted as a single error. They are also commonly used in concatenated coding systems. A popular value for $m$ is 8, and the widely used RS code is (255, 223), which is able to correct up to 16 symbol errors per block. The RS codes can be shortened by changing the number of data symbols to zero at the encoder, not transmitting them, and re-inserting them at the decoder. An RS codeword is generated using a special polynomial, and hence all valid codewords are exactly divisible by the generator polynomial.

### 3.3.4 Convolution codes

Convolution codes are widely used in telecommunication. Convolutional codes have a structure that effectively extends over the entire transmitted bit stream, rather than being limited to codeword blocks (Carlson et al., 2002). A convolutional encoder, as its name indicates, performs the convolution of the input bit stream with the impulse responses of an encoder

$$y^{j}(n) = h^{j}(n) * x(n) = \sum_{k=0}^{\infty} h^{j}(k) x(n-k), \qquad (3.6)$$

which is true for causal linear time-invariant (LTI) systems, and where $x$ is the input sequence, $y^{j}$ the sequence from the output $j$, and $h^{j}$ the impulse response for the output $j$. A convolutional encoder has $n$ mod-2 summers, $k$ shift registers, and $m$ states. With these notations, the encoder produces an $(n, k, m)$ convolutional code. The code rate is

$$R_{\mathrm{c}} = k/n. \qquad (3.7)$$

The input bits have not been grouped into words. Each bit has an influence on the span of $n(m + 1)$ successive output bits, called a constraint length. To provide the extra bits needed for error control, a convolutional encoder has to generate output bits at a rate greater than the input bit rate $r_{\mathrm{b}}$. Hence, the number of mod-2 summers should be $n \geq 2$. A simple convolutional encoder with a code $(2, 1, 2)$ is illustrated in Fig. 3.4. The encoder in Fig. 3.4 generates $n = 2$ encoded bits

$$\begin{cases} x'_{j} = m_{j-2} \oplus m_{j-1} \oplus m_{j} \\ x''_{j} = m_{j-2} \oplus m_{j} \end{cases}, \qquad (3.8)$$

which are interleaved by the switch to produce the output bit stream

$$X = x'_{1} x''_{1} x'_{2} x''_{2} x'_{3} x''_{3} \cdots. \qquad (3.9)$$

Then, the output bit rate is $2r_{\mathrm{b}}$, the code rate $R_{\mathrm{c}} = 1/2$, and the constraint length 6.
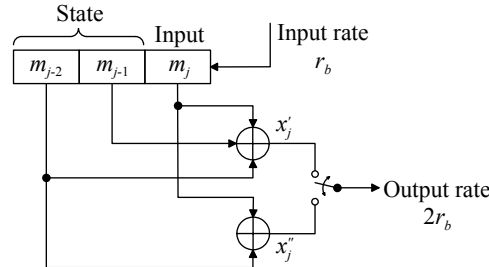


Fig. 3.4: Convolutional encoder for the code $(2, 1, 2)$.

Three variants of graphical representations have been devised for the study of convolutional encoding: the code tree, the code trellis, and the state diagram. The code trellis and the state diagram are depicted in Fig. 3.5 for the $(2, 1, 2)$ convolutional encoder. In the code trellis, the nodes on the left denote the four possible current states, while those on the right are the resulting next states. A solid line represents the state transition for $m_{j} = 0$, and a dashed line for $m_{j} = 1$. Each state transition is labelled with the resulting output bits $x'_{j} x''_{j}$. The state diagram representation can be obtained by combining the left and right sides of the code trellis.
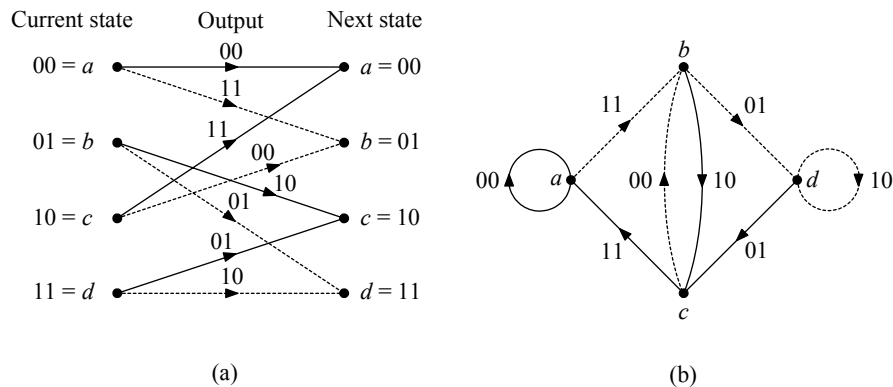
Fig. 3.5: Graphical representations for the $(2, 1, 2)$ convolutional encoder. (a) Code trellis. (b) State diagram. The solid line represents the state transition for the input bit 0, and the dashed line for the input bit 1.

According to Carlson et al. (2002), there are three generic methods for decoding convolutional codes; a maximum-likelihood decoding that is executed by the Viterbi algorithm, a feedback decoding, and sequential decoding. All of them have their special advantages. In this context, it is not necessary to go into detail about their operation, because they are described, for example, in (Carlson et al., 2002).

Instead, puncturing can be briefly discussed. Punctured convolutional codes are described, for example, in (Cain et al., 1979; Hagenauer, 1988). The main idea is that the code rate can be fixed via puncturing without changing the structure of neither the encoder nor the decoder. The basic idea of puncturing is to remove some bits after encoding. The encoded bits are punctured via the puncture vector, which is known by both the encoder and the decoder. Finally, the decoder is assigned to decide the state of the erasures according to the algorithm they execute. The bit stream is shorter after puncturing, and hence the empty places are replaced with $x$ according the puncture vector before the decoding process (Fig. 3.6). Therefore, the locations of errors made by puncturing are known.
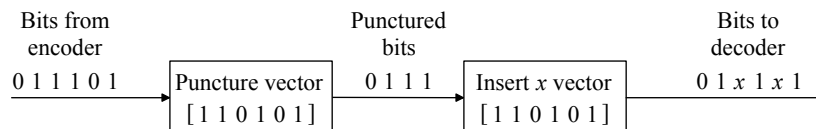


Fig. 3.6: Basic idea of a punctured code. The original code rate 1/2 is punctured to 3/4 (Bégin and Haccoun, 1989).

## 3.3.5 Turbo codes

Turbo codes are a relatively new class of convolutional codes, first introduced in 1993. Classically, concatenation has consisted of cascading a block code, for example the outer code is RS code, and a convolutional code (the inner code) in a serial structure (Berrou and Glavieux, 1996). Because of their structure, turbo codes are called parallel concatenated codes (PCC). A basic turbo encoder (rate 1/3) consists of two elementary recursive systematic convolutional (RSC) encoders concatenated in parallel through interleaving as illustrated in Fig. 3.7. Turbo codes have enabled channel capacities to nearly reach Shannon's limit. For example, the bit error ratio (BER) lower than $10^{-5}$ has been reached at the SNR of $E_b/N_0 = 0.7$ dB with the

simulation of turbo codes in (Berrou and Glavieux, 1996). This result is 0.7 dB from Shannon's limit. The main disadvantage of turbo codes with their relatively large codewords and iterative decoding process is their long latency (Carlson et al., 2002).
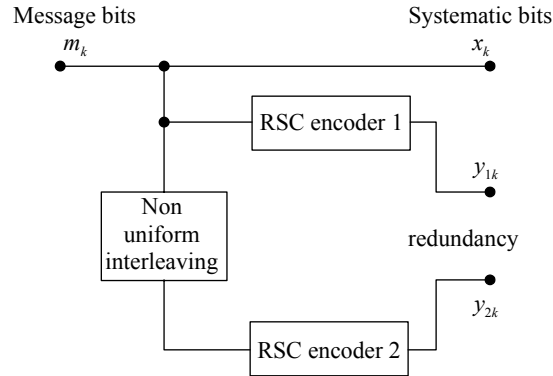


Fig. 3.7: Basic turbo encoder. Message bits $m_k$ are systematically transmitted as the symbol $x_k$ and the redundancies $y_{1k}$ and $y_{2k}$ produced by RSC encoders 1 and 2 may be completely transmitted with the code rate $R_c = 1/3$ or punctured for higher rates (Berrou and Glavieux, 1996).

## 3.4 HomePlug specifications

The HomePlug® Powerline Alliance was formed by thirteen industry-leading companies in March 2000 to guarantee co-operation of different PLC devices. The goal of the alliance was to create a way in which the same power outlets and electrical wires could be used to connect devices to each other and to the Internet. This was achieved by evaluating technologies and creating a specification. The first broadband power line communication specification HomePlug 1.0 was released in 2001. Since then, also HomePlug AV, HomePlug Access BPL, and HomePlug Command & Control specifications have been released (HomePlug, 2007).

HomePlug-certified products connect computers and other devices, which use Ethernet (IEEE 802.3), universal serial bus (USB), or WLAN technologies, to the power line (HomePlug, 2007). By Ethernet connection, the protocol forms an Ethernet link over the power line. HomePlug modems, which are connected to the same power line, act as an Ethernet repeater or switch. Normally, the bus inside the repeater/switch, which connects the Ethernet ports together, is decentralized to work by HomePlug protocol between HomePlug modems that are separated in the electric network. Thus, it encapsulates the Ethernet frames into its own protocol (Lee et al., 2003) and transmits them forward to the power line. Hence, HomePlug can be considered to work below the link layer in a transmission control protocol/Internet protocol (TCP/IP) 4-layer system (Stevens, 1994) according to Table 3.1. From the viewpoint of Ethernet devices, the HomePlug PLC modems are transparent. HomePlug technique offers a broadband communication channel over the power line, which can be encrypted. Only the modems that have a similar encryption key can understand each other. The security is implemented by a 56-bit data encryption standard (DES) and a 128-bit advanced encryption standard (AES) in HomePlug 1.0, and HomePlug AV, respectively. At present, the main competitor with HomePlug is WLAN. These two techniques are compared in (Lin et al., 2003; Lee et al., 2002). According to Lin et al. (2003), HomePlug offers a more reliable communication network than WLAN regardless of the size of the living area. HomePlug modems identify each other automatically because they are working in an ad-hoc mode. Hence, they require no base station for network controlling.

Table 3.1: Modified TCP/IP 4-layer system that includes HomePlug PLC protocol.

| Layer | Protocol |
|---|---|
| Application | FTP |
| Transport | TCP, UDP |
| Network | IP, ICMP, IGMP |
| Link | device driver, and interface card |
| PLC | HomePlug |

## 3.4.1 HomePlug 1.0

The HomePlug 1.0 specification defines the PLC protocol both in the PHY and MAC layers. It was taken into use in 2001 after extensive field tests in 500 houses located in a variety of geographical areas in the USA and Canada (HomePlug, 2003). Performance results were collected from more than 7000 electric paths in these houses.

The PHY is based on the available methods. The PHY uses adaptive OFDM with a CP in the band from approximately 4.49 to 20.7 MHz. The band from 0 to 25 MHz is divided into 128 evenly spaced sub-carriers, of which 84 (sub-carriers 23−106) fall within the band used in communication. In addition, eight of the sub-carriers are permanently masked to avoid amateur radio bands. The bandwidth of each sub-carrier is 195.3125 kHz. In order to avoid ISI, a CP of the last 172 samples from the IFFT interval of 256 samples is prepended to the IFFT interval to form a 428-sample OFDM symbol. Using a 50 MHz clock and eight samples for roll-off interval results in 8.4 µs per a single symbol, with 5.12 µs for the simple OFDM symbol and 3.28 µs for the CP. The PHY detects channel conditions using channel estimation for adaptation by avoiding poor sub-carriers and selecting an appropriate modulation method and coding rate for the remaining sub-carriers. The same modulation method and coding rate are used for all of the indicated sub-carriers. Turbo product codes are used for sensitive frame control data, and RS concatenated with convolutional codes are used for the payload. The RS code has code rates ranging from (39, 23) to (254, 238). The convolutional encoder has a constraint length of 7 and code rates of 1/2 or 3/4 via puncturing. Three variants of PSK modulation are used: BPSK, differential BPSK (DBPSK), and differential quadrature PSK (DQPSK). BPSK is always used for modulation of frame control symbols. The differential modulation methods are used for the payload (Table 3.2). The robust OFDM (ROBO) mode is used under noisy conditions. It always uses all carriers, and also a different interleaver than other modes. The bit rate is ¼ bit per carrier per symbol for ROBO modulation. The ROBO modulation is always employed to multicast or broadcast PHY frames (Lee et al., 2003).

Table 3.2: Maximum PHY throughputs for various modulation and FEC (HomePlug, 2004).

| | Modulation | FEC | PHY throughput (Mbps) |
|---|---|---|---|
| DQPSK 3/4 | DQPSK | 3/4 convolution and RS codes | 13.78 |
| DQPSK 1/2 | DQPSK | 1/2 convolution and RS codes | 9.19 |
| DBPSK 1/2 | DBPSK | 1/2 convolution and RS codes | 4.59 |
| ROBO | DBPSK | 1/2 convolution and RS codes, each bit is repeated four time | 1.02 |

Tone maps (TMs) are used by transmitter-receiver pairs to adapt to the varying channel conditions. The TM includes information about the usable sub-carriers, the modulation method, and the convolutional code rate to be used for the symbols sent between a single transmitter-receiver pair. TM is always used for the payload only, but it is ignored if the ROBO mode is employed either for unicast or multi-/broadcast. TMs are individual for every single transmitter-receiver pair. There are 139 distinct data rates available between 1 and 14.1 Mbps in PHY determined by a TM. The PHY frame format of HomePlug 1.0 is illustrated in Fig. 3.8. A preamble and frame control combination is used as delimiters that start and end long frames (Lee et al., 2003). The RIFS and EFG shown in Fig. 3.8 are abbreviations from response inter-frame space and end of frame gap, respectively.
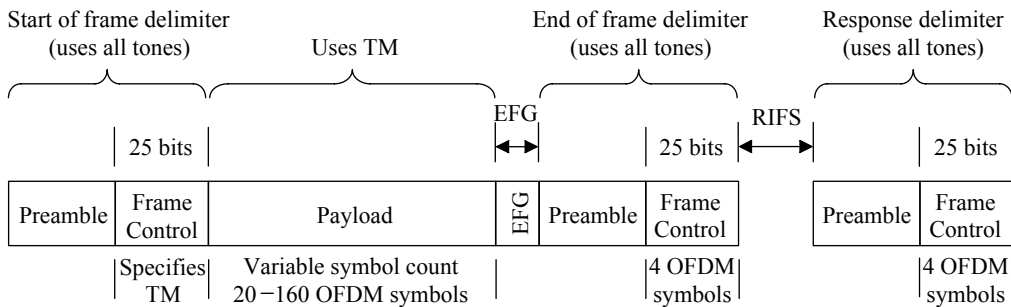


Fig. 3.8: HomePlug 1.0 PHY frame format (Lee et al., 2003).

The HomePlug 1.0 MAC layer uses channel access based on the carrier sense multiple access with collision avoidance (CSMA/CA) to transport data of 46−1500 bytes long from encapsulated IEEE 802.3 frames. HomePlug 1.0 exploits a contention based on a channel access protocol, and hence there is a priority resolution period (PRP), which includes two priority resolution signals (PRS). Stations contend using PRS0 and PRS1 to determine maximum priority traffic on the network. Therefore, four priority levels are supported: CA3 and CA2 for time sensitive, high priority traffic, and CA1 and CA0 for lower priority traffic. Fig. 3.9 shows the timing sequences for the transmission of frames on the medium. The space between the last and the incoming frames is a contention inter-frame space (CIFS).
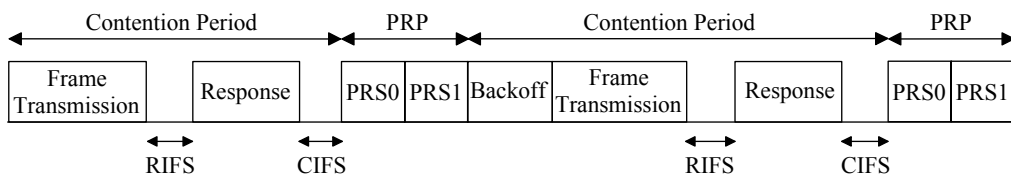


Fig. 3.9: Timing sequences on medium in HomePlug 1.0 (Jung et al., 2005).

The maximum throughputs at the various layers in HomePlug are depicted in Table 3.3. The throughput in the TCP/IP layer tells the practical data transmission rate. The transmission PSD is restricted to -50 dBm/Hz in HomePlug (Lee et al., 2003). This results in a total transmit power, injection losses excluded, of approximately 10 mW.

Table 3.3: Throughput at various layers in HomePlug 1.0 (HomePlug, 2004).

| Layer | Throughput (Mbps) |
|-------|-------------------|
| PHY | 13.78 |
| MAC | 8.2 |
| TCP/IP | 6.2 |

## 3.4.2 HomePlug AV

HomePlug AV was the second major standard released by the HomePlug Powerline Alliance (HomePlug, 2005). While HomePlug 1.0 was designed mainly to distribute broadband Internet access, the objective of HomePlug AV was to distribute audio/video content as well as data in homes (Afkhamie et al., 2005). HomePlug AV also defines the PHY and MAC layer. It provides approximately ten times throughput improvement over HomePlug 1.0, also noticing the quality of service (QoS) requirements.

The PHY uses windowed OFDM in the band from approximately 2 to 28 MHz. The long OFDM symbol includes 917 usable sub-carriers (amateur bands excluded), which is used in conjunction with a flexible guard interval. The band from 0 to 37.5 MHz is divided into 1536 evenly spaced sub-carriers with a 3072 point FFT resulting in an interval of 24.414 kHz for each sub-carrier. Depending on the regulations in different parts of the world, the transmit spectrum is adaptable. In the same way as in HomePlug 1.0, the existence of amateur radio bands causes some additional gaps in the frequency range used. The frequency notches are created in the transmission PSD by merely turning off sub-carriers. The PSD in HomePlug AV is also restricted to -50 dBm/Hz. HomePlug AV employs turbo codes with varying code rates, which provide robust performance within 0.5 dB of Shannon capacity. Coherent modulation methods are supported, which include BPSK, QPSK, and five quadrature amplitude modulation (QAM) methods such 8-QAM, 16-QAM, 64-QAM, 256-QAM, and 1024-QAM (that carries 10 bits of information per carrier per symbol). Several robust modes of operation are provided for the communication of network synchronization information for session setup, multicast, and broadcast modes. For example, a 10 Mbps broadcast mode can be employed on 99 % of all power line channels without exchanging channel information between a transmitter-receiver pair. HomePlug AV has channel estimation that supports variable bit-loading. This enables that each sub-carrier individually selects the modulation type according to the dominant SNR. The maximum throughput in PHY is 200 Mbps (Afkhamie et al., 2005; HPAV, 2005). According to the field test results described in (O'Mahony, 2006), the MAC throughput of HomePlug AV is restricted to about 120 Mbps. In practice, the maximum throughput in TCP/IP layer seems to be about 60 Mbps (Lin et al., 2006).

## 3.5 Coupling interface

In general, different coupling interfaces are developed and patented for PLC applications. Typically, PLC is applied in single-phase networks, in which the phase and neutral wires are used for signalling. The coupling is carried out by a capacitive coupling interface. The topology of a conventional coupling interface is illustrated in Fig. 3.10. The filtering of the mains voltage is based on the voltage partition between a coupling capacitor and the magnetizing inductance of a transformer. In the mains frequency, the impedance of a serially connected capacitor is dominating, while its impedance is low at the frequencies used for PLC. Similar coupling interfaces are applied for example in commercial HomePlug compliant modems.
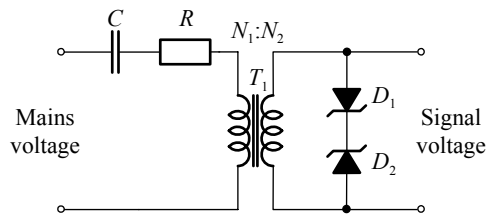
Fig. 3.10: Topology of a conventional coupling interface used for PLC in a single-phase electric network (Dostert, 2001).

In motor cable communication, the main purpose of a coupling interface is to separate the circuit of a motor cable and the circuit used in signalling from each other. The noise produced by an inverter has a high energy content that reaches up to the HF band. Hence, there is no point to completely attenuate the noise peaks caused by the inverter switching transients, because it would lead to an increased filter order, increased losses, complicated structure, and new resonant frequencies. Thus, it was decided to filter the noise to a certain level by a simple LC filter and then to clip the rest of the noise impulse to a level that is not harmful to a communication circuit anymore. The OFDM symbol can last long enough to be received correctly even if a short impulse noise occurs during the data transmission. Also FEC coding can correct single and burst errors. The OFDM technique in PLC is analyzed for example in (Ma et al., 2005; Babic et al., 2006).

There are two coupling methods available; capacitive and inductive. The main difference between these is that the capacitive interface is coupled in parallel and the inductive one in series with the mains network. The basic ideas of these are presented in (Bilal et al., 2004). The coupling method depends on the way the isolation from the mains voltage is carried out. Approximately below the frequency of 100 MHz, a conventional coupling capacitor seems to be a suitable alternative, while only at frequencies of hundreds of megahertz, a feed-through capacitor (Schubert, 2007), which could be a foil that surrounds the conductor, is applicable because of its very low capacitance value. The main difference between these two capacitive couplings is that the latter one can be connected without interrupting the mains voltage. Inductive coupling has to be fitted according to the line current to avoid saturation, and it is not suitable for the frequencies of hundreds of megahertz because of the collapse of magnetic properties, or for a low frequency band because of high cost. In MV (over 1 kV) applications, it seems to be feasible to use inductive coupling because of the size and cost of the coupling capacitor, the like of which is illustrated in Fig. 3.11.



Fig. 3.11: Coupling capacitor for the MV distribution network.

The topology of the proposed capacitive coupling interface is illustrated in Fig. 3.12. The developed coupling interface can be generally applied at both the transmitter and receiver ends with modern PLC techniques that use megahertz frequencies. It filters the output voltage of an inverter; both the output frequency and impulsive noise. It passes the frequencies used in communication with low attenuation at both the transmitter and the receiver ends. In addition, the coupling interface protects the PLC device from overvoltage peaks and realizes a galvanic isolation between the circuit of data transmission and the circuit of a motor cable. The coupling interface is coupled to a three-phase motor cable differentially between two phase conductors, such as (L1, L2), (L1, L3), or (L2, L3).
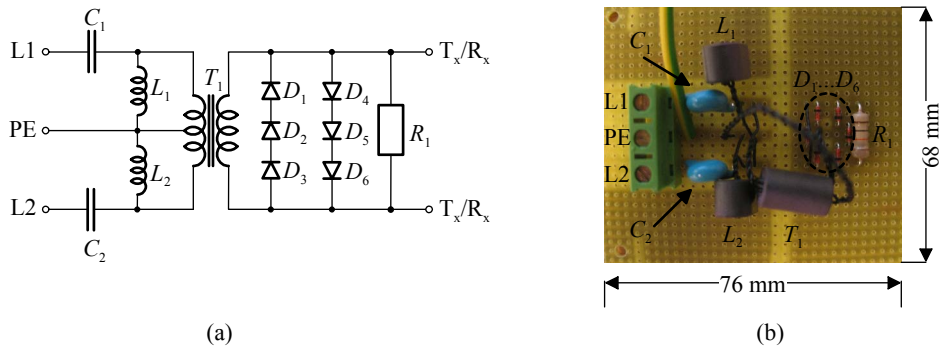


(a) (b)

Fig. 3.12: Developed capacitive coupling interface for a LV three-phase inverter-fed motor cable. (a) Schematic. (b) Photograph. The PLC signal is coupled differentially between two phase conductors. The electric parameters are as follows: $C_1 = C_2 = 680$ pF, $L_1 = L_2 = 0.8$ µH, the magnetizing inductance of the transformer ($T_1$) $L_m = 3.5$ µH, and $R_1 = 10$ kΩ. The diodes $D_1 \ldots D_6$ are small signal diodes and they act as a transient protection.

The capacitors provide the isolation from the output voltage of the inverter and operate together with inductors and the magnetizing inductance of the transformer as a high-pass filter. The galvanic isolation is carried out by the signal transformer. The middle point of the transformer and the other sides of the inductors are bound together and connected to the protective earth (PE). Hence, the signal can be injected differentially between two phases of a three-phase motor cable. The differential coupling does not produce a visible common-mode voltage component, which would be seen as a current in the PE wire or in other earth loops. This is shown in Publication VI.

### 3.5.1  Capacitive components

The component selection plays an important role in the coupling interface of motor cable communication. The maximum voltage rating of the capacitors has to be taken into account, because for example the voltage amplitudes can be even higher than 2 kV in an inverter-fed electric drive connected to a 690 V mains network because of the cable oscillation. Another task of the coupling capacitor is to pass the signal used in PLC with low losses. Hence, the dissipation factor and its frequency dependence have to be taken into account. Materials applicable to coupling capacitors are for example ceramic or plastic capacitors.

## 3.5.2  Inductive components

The transformer and the inductors can be built with double aperture ferrite cores, because they are suitable for HF applications. The behaviour of the magnetic material is described with complex permeability that is defined as follows:

$$\boldsymbol{\mu}(f) = \mu'(f) + j\mu''(f), \tag{3.10}$$

where $\mu'$ is the real and $\mu''$ the imaginary part of permeability. The real and imaginary parts of permeability define the ability of a material to produce magnetizing flux and its losses, respectively. In motor cable communication, the ferrite material has to be selected to minimize the imaginary part of the complex permeability at the selected frequencies. The magnetizing inductance of a transformer can be fixed by the number of winding turns. The ferrite material suitable for the coupling interface of motor cable communication is for example F10b manufactured by Neosid Pemetzrieder GmbH & Co. Its real and imaginary parts of relative permeability are illustrated in Fig. 3.13.
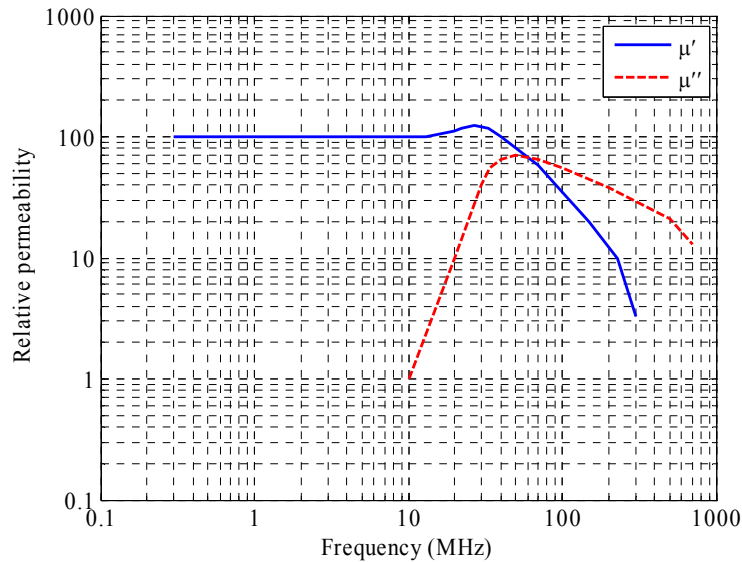


Fig. 3.13: Real and imaginary parts of relative permeability for the ferrite material F10b as a function of frequency applied in the developed coupling interface (Neosid, 2000).

The cross-section structure of a double aperture ferrite core and its dimensions are illustrated in Fig. 3.14. The dimensions of double aperture ferrites for the F10b material are presented in Table 3.4.
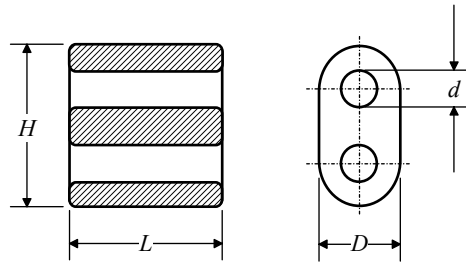
Fig. 3.14: Cross-section structure of a double aperture ferrite core and its dimensions.

Table 3.4: Dimensions of the applied double aperture ferrite cores fitted to the notes in Fig. 3.14.

| Mf. | Grade | Type | $D$ (mm) | $d$ (mm) | $L$ (mm) | $H$ (mm) |
|------|-------|------|------|------|------|------|
| Neosid | F10b | Ft 8 | 8.5 | 3.5 | 8.3 | 14.4 |
| Neosid | F10b | Ft 8a | 8.5 | 3.5 | 14.5 | 14.4 |

By using these ferrite cores with variable winding turns, different magnetizing inductances are built that can be applied in the coupling interface. The winding turn ratio is kept fixed in all cases. The magnetizing inductances are measured by an HP 4194A impedance analyzer with an HP 41941A impedance probe kit for the frequency band of 4−20 MHz applied by PLC. The measurement results are presented in Table 3.5.

Table 3.5: Measured magnetizing inductances for two different double aperture ferrite cores with variable winding turns for the frequency band of 4−20 MHz. The ferrite material is F10b manufactured by Neosid Pemetzrieder GmbH & Co. The variations used in the developed coupling interface are bolded.

| Type | Winding turns | Magnetizing inductance (µH) | Resistance (Ω) |
|------|------|------|------|
| Ft 8 | 1:1 | 0.3 | 0.4 |
| **Ft 8** | **2:2** | **0.8** | **0.9** |
| Ft 8 | 3:3 | 2.0 | 1.3 |
| Ft 8 | 4:4 | 3.6 | 9.4 |
| Ft 8 | 5:5 | 4.2 | 2.6 |
| Ft 8 | 6:6 | 6.3 | 3.4 |
| Ft 8a | 1:1 | 0.5 | 0.5 |
| Ft 8a | 2:2 | 1.6 | 0.9 |
| **Ft 8a** | **3:3** | **3.5** | **1.9** |
| Ft 8a | 4:4 | 6.2 | 1.2 |
| Ft 8a | 5:5 | 10.5 | 11.3 |
| Ft 8a | 6:6 | 13.7 | 28.5 |

### 3.5.3  Transient protection

The purpose of a transient protection is to block the overvoltage peaks passing the coupling interface to a data transmission device. Overvoltage protection is carried out by clipping the voltage peaks to a certain maximum level. A similar method but a digital version to clip the highest impulse noise peaks is applied in (Suraweera et al., 2003). In general, the transient protection is carried out by suppressor diodes. In this coupling interface, they would cause noticeable attenuation because of the large capacitance, approximately of the magnitude of nanofarads. According to Dostert (2001), a transient protection suitable for frequencies up to

about 30 MHz can be made by four Schottky diodes and by a bidirectional suppressor diode inserted diagonally into the bridge as illustrated in Fig. 3.15. By this arrangement, it is ensured that each of the four Schottky diodes always remains reverse-biased for all signal amplitudes to be transmitted. The diagonal voltage of the bridge remains almost unchanged and does not follow the HF signal because of the large capacitance of the suppressor diode. The Schottky diodes should be selected carefully, because their capacitance varies from one type to another.
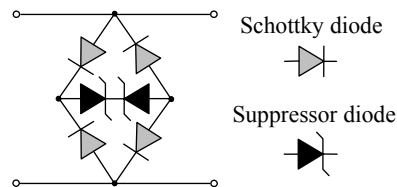


Fig. 3.15: Transient protection suitable for up to 30 MHz (Dostert, 2001).

In the developed coupling interface, the transient protection is implemented by small signal diodes (see Fig. 3.12). Diodes are divided into two parallel branches; one is forward biased and the other reverse biased. The protection causes a parallel capacitance of the magnitude of pikofarads. Three small signal diodes are connected in series to increase the forward voltage, which is about 0.7 V for each diode.

### 3.5.4  Experimental results for developed coupling interface

The values of the components in the coupling interface were defined according to the simulations, and the results were verified by measurements. The insertion and reception losses of the developed coupling interface were measured towards a purely resistive access impedance $\mathbf{Z}_{access}$ by a network analyzer Agilent 4395A with a S-parameter test set device Agilent 87511A as illustrated in Fig. 3.16. Both the output and input impedances of the network analyzer were 50 Ω, because the power losses were measured. In this case, the access impedance can be imagined to be a resistive electric network. In practice, the electric network consists also of inductive and capacitive components, and hence it cannot be purely resistive, as was shown in Chapter 2. The measurement setup for the losses is illustrated in Fig. 3.16.
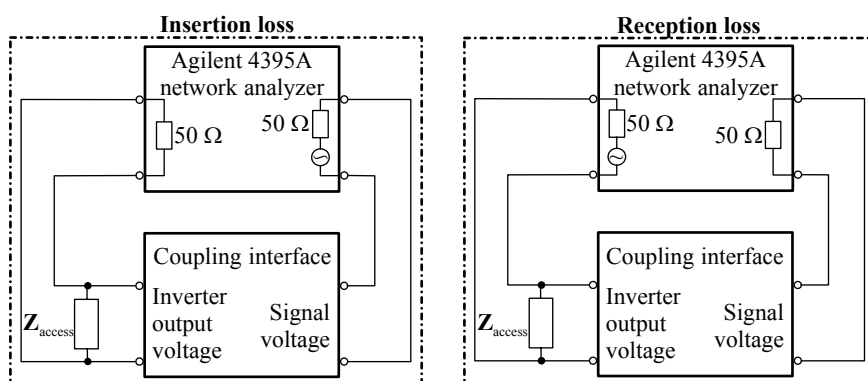


Fig. 3.16: Measurement setup for the insertion and reception losses with a network analyzer.

The measurement results are illustrated in Fig. 3.17, which shows that a small access impedance causes more losses than larger ones. However, this depends on the output impedance of the

transmitter and the coupling interface between the transmitter and the electric network. Now, the output impedance of a network analyzer is 50 Ω and the best result is obtained with the network access impedance of 47 Ω.

According to (2.15), an imperfect termination impedance of a communication channel causes signal reflection, and thereby more losses. However, a small access impedance is problematic for the capacitive coupling, because the coupling interface is connected to the power line in parallel. On the other hand, according to Janse and Ferreira (2005), the impedance levels can be matched by the winding turn ratio of a transformer. Janse and Ferreira (2008) show that the impedance transformation reduces losses in the CENELEC frequencies. The difference in losses between the transformation $N$:1:$N$ and the transparent 1:1:1 pairs is the larger, the smaller is the network access impedance. On the other hand, when using the maximum frequency of the CENELEC band, a transparent pair is the best choice among the transformation pairs regardless of the network access impedance. In motor cable communication, the applied frequencies are in the HF band, and hence it is reasonable to use a transparent pair in the coupling interfaces. According to Dostert (2001), typical access impedances in the CENELEC band are in the range of 0.2−2 Ω.

Impedance curves are divided into four different main types with typical characteristics in (Bausch et al., 2006). The access impedance increases as a function of frequency. The access impedance in motor cable communication measured from the coupling interface is illustrated in Fig. 3.18. The access impedance is now ranging between 20 and 700 Ω (mainly inductive) in the applicable HF band of 3−30 MHz, which is remarkably higher than the typical access impedance in the CENELEC band. However, the access impedance in this case is 0.9 Ω @ 100 kHz, which is of the same size as with the typical access impedances in normal LV electric networks. The access impedances can vary between different electric drives, but not in a single electric drive except between the switching states 1 and 2 as illustrated in Fig. 2.10 and Fig. 2.11. Hence, the channel characteristics are almost stabile apart from the noise characteristics.
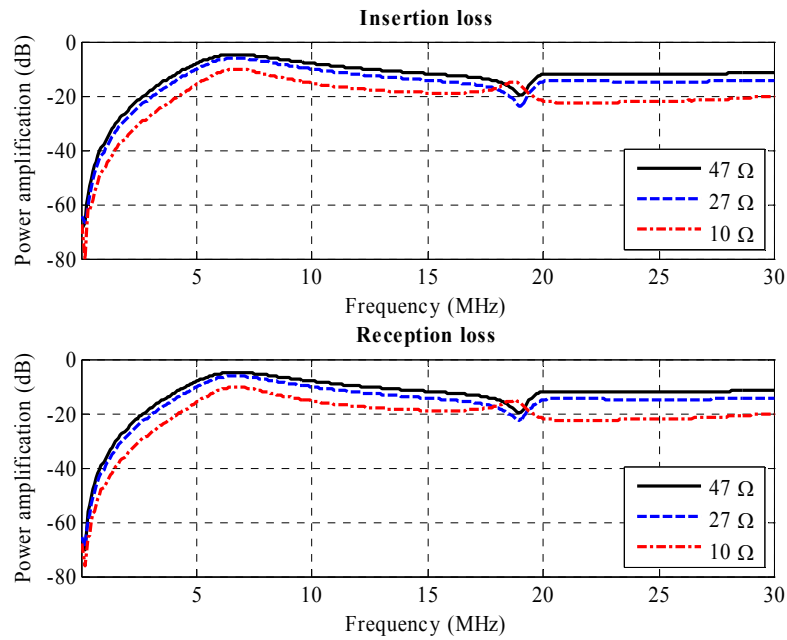
Fig. 3.17: Insertion and reception losses with different network access resistances for the frequency band of 100 kHz–30 MHz. Power amplification was measured with a 50 Ω output and input impedance of the network analyzer.
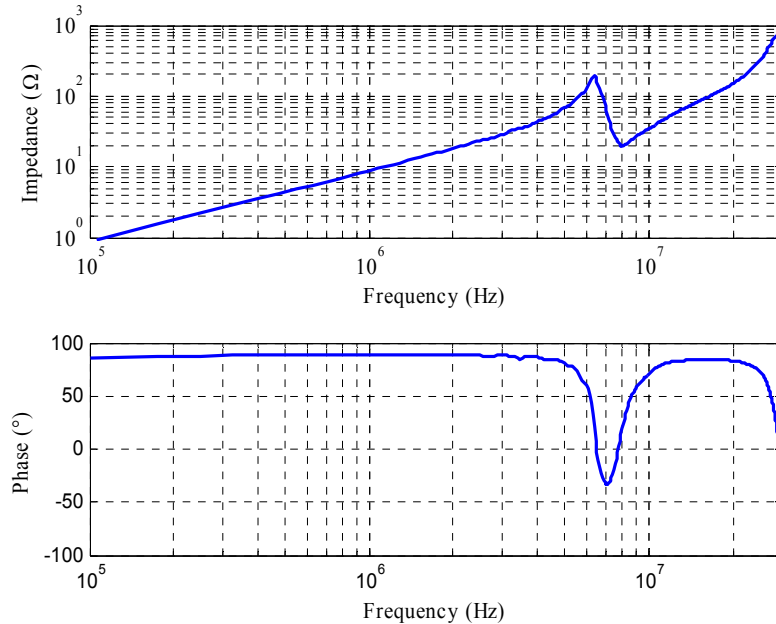


Fig. 3.18: Measured access impedance and its phase curves of an electric drive from the motor to the inverter in the frequency band of 100 kHz−30 MHz. The drive under test comprised an ABB 15 kW induction motor (4-pole), a 90-meter-long Pirelli MCCMK 3x35+16 motor cable, an ABB output filter, an ABB ACS400 frequency converter, and the developed coupling interfaces at the both cable ends.

The filtered noise measured from the signal connectors of the proposed coupling interface is illustrated in Fig. 3.19. The noise produced by the same inverter is presented in the time- and frequency-domain in Fig. 2.26. The noise pulse lasts about 6 μs, whereas 8.4 μs is reserved for a single OFDM symbol and for CP in HomePlug 1.0 (Lee et al., 2003). This means in practice that the symbol may get broken and has to be re-transmitted (if it cannot be corrected by FEC coding) if these occur simultaneously. On the other hand, the DFT algorithm spreads the power of an impulse noise over multiple symbols, and hence reduces its injurious effect, but reduces the SNR. However, if the switching frequency $f_{sw}$ and the duration of the data symbol $T_s$ and the noise $T_n$ are known, the number of corrupted symbols per second can be roughly estimated according to the worst case scenario if it is assumed that the whole symbols are corrupted in each switching state:

$$N_c = \left( \text{ceil}\left( \frac{T_n}{T_s} \right) + 1 \right) f_{sw} , \qquad (3.11)$$

where the function ceil($x$) rounds the elements of $x$ to the nearest integers towards infinity. The switching frequency affects linearly the number of corrupted symbols, which can be seen from (3.11). However, the HomePlug 1.0 protocol optimizes the data transmission for the dominant channel characteristics, and the FEC is able to correct the errors occurring during the data transmission. For example, the protocol can use simpler modulation methods and more powerful FEC coding to avoid losing any OFDM symbol during switching states. This leads to a lower bandwidth, but shorter jitter. In practice, no difference was noticed between the variable and fixed switching frequency as used in the direct torque control (DTC) and PWM, respectively.
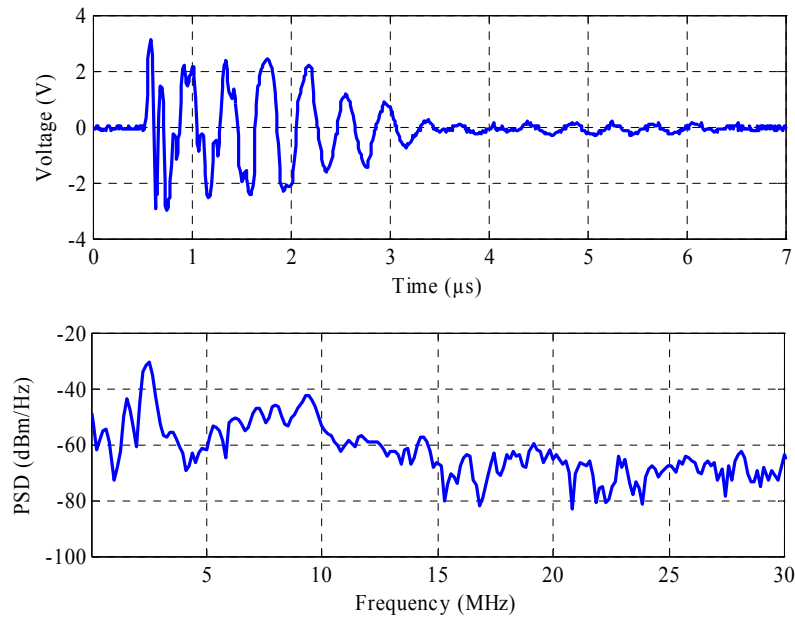


Fig. 3.19: Filtered noise signal in the time- and frequency-domain produced by the output stage of the inverter (Fig. 2.26). The frequency response approximation is computed by FFT. The coupling interface is coupled between two phase leads (L1, L2) at the inverter end.

## 3.6 Practical tests

The operation of the proposed data transmission method was verified by laboratory measurements. To this end, a test device was developed. A single test device includes a modified commercial HomePlug modem, the developed coupling interface, a battery, and a DC/DC converter. By using the battery as a power source, the HF signal path is restricted only to a motor power cable. The DC/DC converter is used to transform the battery voltage of 12 V suitable for the PLC modem that uses the voltage of ±5 V. The original coupling interface of the modem was removed and replaced by the developed one. The test device is illustrated in Fig. 3.20. In practice, the power delivery for the PLC modems should be implemented in a different way than with the batteries in motor cable communication. At the inverter end, the power supply is available. At the motor end, the implementation of the power supply is not that simple but it is feasible, because the motor is powered in any case. The total power consumption of a commercial HomePlug compliant modem is about 5 W. The necessary energy can be harvested from the magnetic field caused by the phase current. This kind of a current transformer is introduced and analyzed in (Ahola et al., 2008), which shows that the energy can also be harvested from the motor power cable even if it is supplied by an inverter. According to Ahola et al. (2008), 10 W output power can be produced when the primary RMS current is about 80 A.
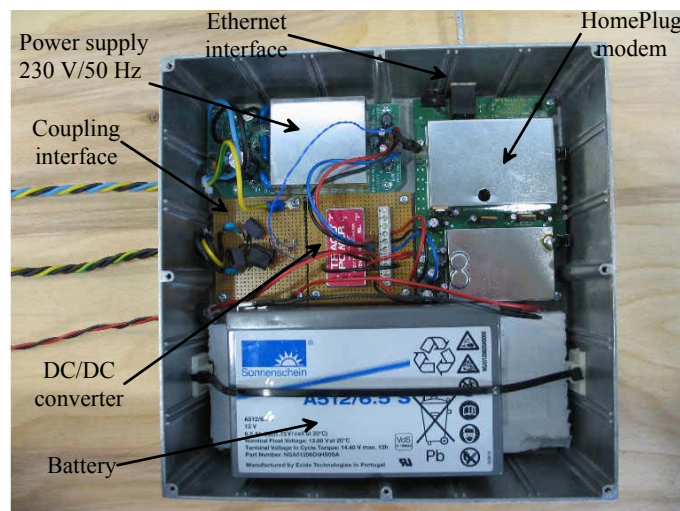


Fig. 3.20: Developed test device applicable to laboratory measurements. The original power source of the commercial modem is also included to the test device.

The current spectra, which include noise and signal spectra, measured from a phase conductor, are illustrated in Publications II, VI, and VII. According to these, HomePlug 1.0 compliant modems increase the peak current about 15−30 dB(μA) in the data transmission band they are using. The permanently masked amateur radio frequencies can be clearly seen in the band. In Publication VI, the HF signal propagation in the motor cable of an electric drive is studied. The developed test device operates as a HF signal source. This study shows that the frequency converter acts as a firewall for the HF communication signal if differential signal coupling is applied, and hence the communication signal is not recognized on the mains network side.

The throughput describes the bandwidth in a communication channel. It tells the number of bits that can be sent in a time unit. The throughput tests were carried out in the power electronics laboratory at Lappeenranta University of Technology. The throughput of PLC in the inverter-

fed motor power cable was tested by two laptops and file transmission protocol (FTP) software, which works above the TCP/IP layer. Modems were located at the both ends of the motor power cable according to Fig. 2.1, and they were connected to the laptops by RJ-45 cables (Ethernet). The configuration of the PLC test and the results are presented and analyzed in Publication II. In addition to this, some results are presented in (Ahola et al., 2005a; 2005b). The devices in the test drive were changed, such as the type of the frequency converter, the output filter, signal coupling, the communication direction, the length of the motor power cable, the motor, and the grounding method, to find out the affecting factors of PLC in motor cable communication. The throughput results illustrated in Publication VII in Fig. 8 include only the tests with signal coupling between two phases (L1, L2), while the results illustrated in Publication II in Fig. 6 include the tests both with signal couplings between (L1, PE) and (L1, L2).

The latency describes the delay between a transmitter and a receiver; in other words, how long does it take to receive the data packet after it is transmitted. The limits for latency can be defined according to the application. For example, on-line condition monitoring does not require strict latency or its jitter characteristics, whereas motor controlling does. These issues are discussed in more detail in Chapter 4. The latency characteristics are presented and analyzed in Publications I and II. In Publication II, the latency characteristics are studied by an Internet control message protocol (ICMP) ping software with a packet size of 32 bytes. The software measures the end-to-end latency and gives the minimum, maximum, and average latency as a result. In Publication I, the latency characteristics are studied by the constructed test equipment. This makes it easier to measure a larger number of statistic samples to compute the latency and its jitter than with the ICMP ping software. The latency of the proposed method is mainly caused by the processing time of the packet-based protocol. In motor cable communication, the communication channel does not include any branches, and hence the data transmission can be kept as a type of point-to-point, which includes only a single transmitter-receiver pair. Therefore, the jitter is mainly caused by the retransmitted packet of the ARQ mechanism because of the lost or corrupted packets that cannot be reconstructed by the FEC system.

# 4  APPLICATIONS

This chapter discusses the applications in which the proposed motor cable communication method can be applied. First, continuous on-line condition monitoring is discussed, focusing on its requirements, targets, and structure. Also other applications similar to condition monitoring are mentioned. The second main application addressed here is real-time motor control. The motor power cable is applied as a feedback channel instead of a signal cable. The requirements and restrictions are studied and analyzed with this setup. The method is also compared with the commercial drives, both the sensorless and direct feedback drives.

## 4.1  Continuous on-line condition monitoring

According to Lindh (2003), predictive condition monitoring refers to periodical or continuous evaluation of the healthiness of an apparatus. Periodic monitoring is carried out by human sensory observation, while continuous monitoring is based on measurements. Hence, continuous condition monitoring has several advantages over the periodic, as damages can be detected as soon as they appear, and trends can be formed automatically. Correspondingly, condition monitoring can be divided into off-line and on-line condition monitoring. Off-line monitoring is applied to an object that is not in the running state, while on-line monitoring is applied to a running object. According to the study by Albrecht et al. (1986), bearing damages represent 41 %, stator damages 37 %, and rotor damages 10 % of the total damages of electric motors. According to Ahola et al. (2005a), vibration measurement in bearing condition monitoring has proved its reliability in practical systems. However, continuous vibration condition monitoring requires a sensor, such as accelerometer, installed at the motor.

According to Ahola et al. (2005b), self-diagnostics has become a standard feature, because it provides additional value to the end users, services, and manufacturers. The benefits of the diagnostic system are considered to be higher than its costs, which has enabled the development and installation of these systems. Nowadays, several consumer products, such as modern cars, and personal computers, include self-diagnostics. Nevertheless, LV electric motors and generators are still sold without an on-line condition monitoring system. However, the amount of electric motors is vast in industry. The diagnostic information can mainly be used for planning future maintenance and replacement actions to avoid accidental production interruptions. The data produced by intelligent sensors at the motor have to be collected and managed in a centralized diagnostic system in a production-line-scale system as illustrated in Fig. 4.1. Hence, data transmission is also required from the motor to the condition monitoring system. For this purpose, the proposed method is applicable to avoid the large costs of additional cabling.

**Management level / Applications**
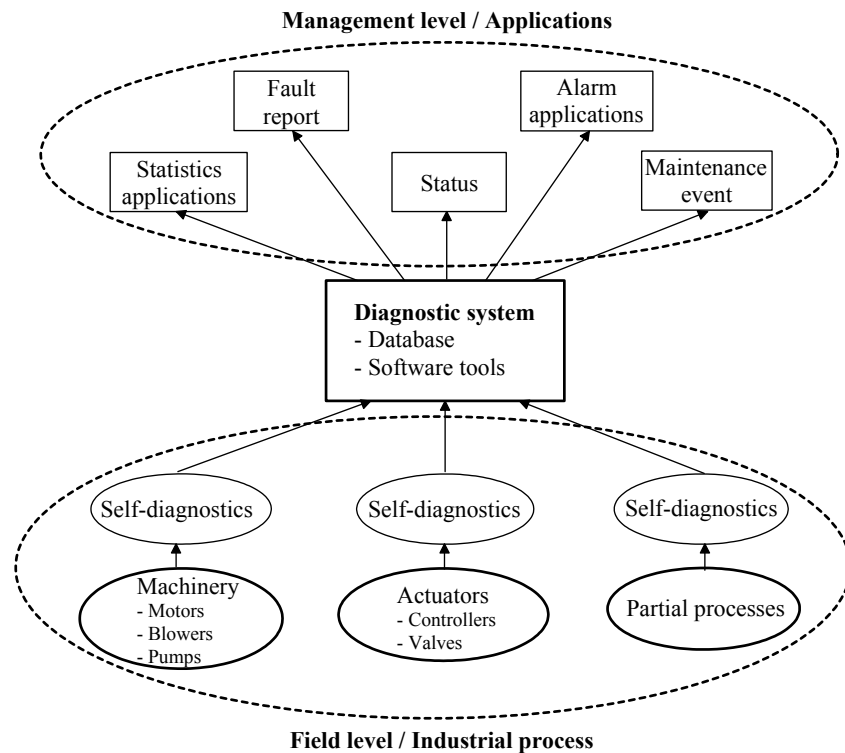


**Field level / Industrial process**

Fig. 4.1: Principle of a product-line-scale diagnostic system. The field level data is collected into the diagnostic system that generates information for maintenance purposes (Ahola et al., 2005b).

The possibilities of using the frequency converter in condition monitoring of an electric motor are studied in (Tiainen et al., 2006). Electric motors are not the only devices that can be monitored, but such are also for instance pumps, blowers, compressors, and other machines driven by a motor. In addition to condition monitoring, the operation efficiency of a pump can be observed (Ahonen et al., 2008). In this application, calculated estimates of a frequency converter, such as torque, rotation speed, power consumption, can be used, but the accuracy is then limited and it can be improved by external measurements from the pump (Ahonen et al., 2008). The application enables to optimize the operational efficiency of a pump, and hence saves its life cycle costs. The data transmission from the apparatus to the frequency converter has also an important role in this application.

Generally, a frequency converter requires motor parameters. Nowadays, these parameters are estimated through the identification run and user input data. All the required motor parameters, such as motor inductances, the stator resistance, and stator saturation effects, are estimated during the motor identification run, but only a few parameters, such as the stator resistance, can be estimated at standstill. Correspondingly, the user input data includes motor nominal voltage, current, frequency, speed, and power. The identification procedure is described in detail for permanent magnet synchronous machines (PMSMs) in (Luukko, 2000) and for induction machines in (Toliyat et al., 2003). There should be a communication medium via the power cable between the motor and the frequency converter to inquire the required motor parameters through the power line link from the electronics attached to the motor. The estimates of sensorless control methods can also be improved; for example, the inaccuracy of the motor

model can be reduced by transmitting the temperature of the stator through the motor power cable. This requires neither a wide bandwidth nor strict latency characteristics.

Applications have generally different data transmission requirements concerning bandwidth, latency, and jitter. Also the achievable data transmission distance can be an important factor. The required data transmission for a vibration measurement of induction motor bearing condition monitoring is estimated in (Tiainen et al., 2005). The vibration measurement that is used for envelope spectrum analysis produces about 500 kb of data, and hence the required average transmission rate for an interval of 4 hours leads to the rate of 40 bps (Tiainen et al., 2005). Other measurements, such as temperature or humidity, used in on-line condition monitoring produce less information than the vibration measurement. In general, the latency and jitter are not important parameters in the transmission of condition monitoring data.

The proposed data transmission method over the motor power cable offers a standard communication bus (Ethernet) for different kinds of information. According to Stevens (1994), Ethernet belongs to the link layer in the TCP/IP 4-layer system, and hence it can transmit different kinds of information encapsulated in several protocols, for example IP, user datagram protocol (UDP), TCP, hypertext transfer protocol (HTTP), and FTP, which all are above the link layer. The protocols are determined according to the requirements of different applications. The proposed method offers standard interface for different sensors, such as acceleration, pressure, acoustic emission (AE), temperature, and humidity, to be installed at the motors or other apparatuses. According to the practical tests, it is possible to transmit information produced by several sensors through the motor power cable without any problem, because the available bandwidth does not set any restrictions. In addition to information produced by the sensors, it is also possible to deliver multiple voice connections, or even video stream.

## 4.2  Feedback speed control

The proposed data transmission method forms an Ethernet link over the motor power cable. It encapsulates the Ethernet frames into its own protocol and transmits them forward. The latency of Ethernet is non-deterministic because of the carrier sense multiple access with collision detection (CSMA/CD) bus reservation mechanism. This causes problems in real-time applications, which require deterministic response, such as in control applications. According to Samaranayake et al. (2003), in applications that require a time delay less than 1 ms, Ethernet is not a practical solution. On the other hand, Ethernet for control automation technology (EtherCAT) can process 100 servo axes in 100 μs, because processing is performed at the hardware level (Jansen and Büttner, 2004). The utilization of real-time Ethernet (RTE) in industrial applications has been studied extensively, for instance in (Felser, 2001; 2005; Samaranayake and Alahakoon, 2002b; Decotignie, 2001). The utilization of Ethernet in distributed motion control is discussed in (Samaranayake et al., 2002a), in which the rotor feedback speed information of a brushless DC motor is delivered between the speed controller and the frequency converter by using a 10 Mbps Ethernet LAN and a frame size of 64 bytes.

The proposed method causes latency and jitter. These, in turn, cause problems with the feedback loop of a control application. The behaviour of the latency of the proposed method in the induction motor control is studied in Publication I. The proposed method is applied in the feedback speed control of an induction motor. The motor power cable is used for a feedback signal instead of an additional feedback signal cable. The laboratory test system is described in Publication I. The measurements are carried out and analyzed in Publications IV and V. In addition, real-time motor control is discussed in general in Publication VII.

A few important additional issues have to be mentioned concerning Publications I, IV, and V. In the introduced test system, the speed controller utilizes only the feedback rotation speed information in control, whereas the torque controller does not get this information from the induction motor. Hence, the torque control of an ACS800 frequency converter operates in the sensorless mode. Generally, the performance and stability of torque control methods depend on the estimation accuracy of the flux linkage of the motor. The available speed information is normally applied in flux estimation in addition to speed control. The main problem with the torque control without feedback speed information is its stability near the zero frequency. The applied estimation algorithms do not operate properly at low frequencies, and they can cause the torque controller to become unstable. Therefore, in the speed controller, the feedback speed information alone does not necessarily ensure the stability of an electric drive at low output frequencies.

The torque control method of the commercial drive used in the comparison tests was DTC. The drive was used both in the sensorless and speed feedback mode. All the control methods were parameterized so that they could be compared with each other. Identification run was carried out for the drive before the tests, which is essential especially with a sensorless control.

The controlled system was modelled by a control diagram in Publications IV and V. The feedback delay was depicted in the diagram as a transfer function $H(s)$ that can be represented according to Bade approximation as follows:

$$H(s) = \frac{1 - \dfrac{\tau}{2}s}{1 + \dfrac{\tau}{2}s}, \tag{4.1}$$

where $\tau$ is the delay in the feedback loop. The bandwidth of the system with different feedback delays was simulated. The bandwidth was defined according to the amplitudes of the actual and reference speeds. The delayed speed information received from the motor power cable was only used in speed control. In all the other cases, the actual speed of the motor was applied, and hence in Publications I, IV, and V, the given rotation speed corresponds to the actual speed.

# 5  CONCLUSION

This dissertation studies PLC in the motor power cable of variable-speed drives. Inverter-fed power lines differ completely from the normal electricity network, because switching components are used instead of transformers in power transformation. An inverter-fed power line contains voltage pulses or square waves with a variable frequency and duration, and hence it includes noise up to HF frequencies. In this dissertation, the HF frequency band is applied in PLC to avoid the most adverse effects of the noise generated by the inverter.

First, the long history of PLC is outlined. The fundamental principles of PLC are also presented. After the introductory chapter, the communication channel is presented in detail in the frequency band of 100 kHz−30 MHz. All the individual components including an electric motor, a power cable, an output filter, an inverter, and a coupling interface are modelled and parameterized as input impedance models in the frequency band, and for these, two-port models are formed. The two-port modelling method is feasible, because in motor cable communication, the channel topology is simple and similar in different cases. The channel model is verified by measurements. The noise characteristics are discussed. In this application, the noise is produced by an inverter, and therefore other sources are insignificant. A theoretical channel information capacity analysis is carried out. The analysis shows that an inverter-fed motor cable provides a broadband communication medium with the transmission power range of milliwatts in the estimated frequency band of 4.49−20.7 MHz.

Some PLC regulations available in Europe are described. Techniques applied in motor cable communication are addressed. An effective multi-carrier method called OFDM is presented, and its implementation is discussed. Forward error correction coding and some other advantageous methods are introduced. These include scrambling, interleaving, puncturing, RS codes, convolution codes, and turbo codes. Both HomePlug 1.0 and HomePlug AV specifications for PLC are presented. In this study, HomePlug 1.0 compliant products are applied. The developed and patented coupling interface for LV three-phase inverter-fed motor cables is discussed in detail. The coupling interface is designed to connect the PLC modem differentially between two phase conductors of a motor power cable. It filters the noise components produced by the inverter and passes the frequencies used in PLC at both the transmitter and receiver ends. The operation of the coupling interface is verified in the laboratory. A test device is also constructed for laboratory tests. Both the throughput and latency are measured with different electric drives.

The proposed data transmission method over an inverter-fed motor power cable provides a standard Ethernet-supported communication bus for different kinds of information. Different kinds of protocols can be applied in the upper layers because of the structure of the widely used TCP/IP 4-layer system. Potential applications, where the proposed method can be applied, are considered. Attention is also paid to the requirements and restrictions of communication. Two main applications, continuous on-line condition monitoring and real-time feedback speed control, are studied in detail, but also some other applications are mentioned in brief in this context. The proposed method is packet based, and it causes additional latency and jitter in communication. On-line condition monitoring requires neither strict latency characteristics nor wide bandwidth, whereas a real-time motor control requires especially strict latency characteristics. The latency affects the performance of the whole control system. The effect of latency on the control is studied and analyzed in more detail chiefly in Publications I, IV, V, and VII.

**Suggestions for future work**

During the dissertation work, the author has identified the following subjects, which should be studied further.

In this dissertation, the communication method was based on the HomePlug 1.0 specification, and commercial HomePlug 1.0 compliant modems were applied in the test system. To optimize the performance of the communication system for a specific application, such as a real-time control, it is worthwhile to develop the PLC modems for that purpose. For example in a control application, this way, it is possible to optimize essentially the latency, because there is no sense in transmitting the erroneous packet again if there is updated data available from the sensor. Similar frequency bands, modulation, and FEC methods as in the HomePlug protocol are still suitable for motor cable communication. The developed coupling interface can also be used as such without any modification.

The synchronization in inverter-fed motor cables would also be an interesting subject of study. Normally, the transmitter and the receiver are synchronized to the mains frequency of the electricity network. The output frequency of an inverter is also available in inverter-fed motor power cables among the other noise; however, the issue should be considered more thoroughly before making any conclusions.

A simple PHY simulation model of the HomePlug 1.0 protocol was already developed in Matlab$^®$ Simulink during the dissertation work. The simulation model could be developed further. A noise model for an inverter should be constructed in time-domain. By finalizing the PHY model of communication and by transforming the developed channel model into time-domain, it is possible to simulate the operation of the data transmission in an inverter-fed motor power cable. Consequently, different communication methods could be compared with each other in motor cable communication before implementing them. Different electric drives could also be compared with each other by simulations. The BER and throughput could be kept as comparison values.

The effects of the delayed feedback speed information on the accuracy of a torque controller are an interesting subject of study. In this thesis, the torque controller was used in sensorless mode, but the rotation speed information could also be applied in the estimation of the flux linkage of a motor. This should be studied further to find out the connection between the feedback delay and the accuracy of the estimation algorithms of a torque controller.

The market potential and other application areas of motor cable communication should be investigated. It would also be interesting to pilot a practical application in some test environment in industry. At present, there seems to be interest in motor cable communication among some equipment manufacturers and end users, but the potential products are still lacking.

# REFERENCES

Afkhamie, K. H., Katar, S., Yonge, L., and Newman, R. (2005), "An Overview of the Upcoming HomePlug AV Standard," in *Proc. of the 9th International Symposium on Power-Line Communications and Its Applications (ISPLC)*, Vancouver, Canada, April 2005, pp. 400−404.

Ahola, J. (2003), *Applicability of Power-Line Communications to Data Transfer of On-Line Condition Monitoring of Electrical Drives*, Doctoral dissertation, Lappeenranta University of Technology, Lappeenranta, Finland, 2003, 141 p.

Ahola, J., Toukonen, J., Kosonen, A., Lindh, T., and Särkimäki, V. (2005a), "Electric Motor Cable Communication Overcomes the Biggest Obstacle in On-line Condition Monitoring," in *Proc. of Condition Monitoring 2005 Conference (COMADIT)*, Cambridge, UK, July 2005, pp. 105−110.

Ahola, J., Toukonen, J., Kosonen, A., Lindh, T., and Tiainen, R. (2005b), "Ethernet to Electric Motor − via Mains Cable," in *Proc. of the 18th International Congress and Exhibition on Condition Monitoring and Diagnostic Engineering Management (COMADEM)*, Cranfield, UK, August/September 2005, pp. 525−534.

Ahola, J., Ahonen, T., Särkimäki, V., Kosonen, A., Tamminen, J., Tiainen, R., and Lindh, T. (2008), "Design Considerations for Current Transformer Based Energy Harvesting for Electronics Attached to Electric Motor," in *Proc. of 19th International Symposium on Power Electronics, Electrical Drives, Automation and Motion (SPEEDAM)*, Ischia, Italy, June 2008, pp. 901−905.

Ahonen, T., Tiainen, R., Viholainen, J., Ahola, J., and Kestilä, J. (2008), "Pump Operation Monitoring Applying Frequency Converter," in *Proc. of 19th International Symposium on Power Electronics, Electrical Drives, Automation and Motion (SPEEDAM)*, Ischia, Italy, June 2008, pp. 184−189.

Albrecht, P. F., Appiarius, J. C., McCoy, R. M., Owen, E. L., and Sharma, D. K. (1986), "Assessment of the Reliability of Motors in Utility Applications," *IEEE Transactions on Energy Conversion*, Vol. EC-1, No. 1, March 1986, pp. 39−46.

Babic, M., Bausch, J., Kistner, T., and Dostert, K. (2006), "Perfomance Analysis of Coded OFDM Systems at Statistically Representative PLC Channels," in *Proc. of the 10th IEEE International Symposium on Power-Line Communications and Its Applications (ISPLC)*, Orlando, Florida, USA, March 2006, pp. 104−109.

Baig, S., and Gohar, N. D. (2003), "A Discrete Multitone Transceiver at the Heart of the PHY Layer of an In-Home Power Line Communication Local Area Network," *IEEE Communications Magazine*, Vol. 41, No. 4, April 2003, pp. 48−53.

Banwell, T. C., and Galli, S. (2001), "A New Approach to the Modeling of the Transfer Function of the Power Line Channel," in *Proc. of the 5th International Symposium on Power-Line Communications and Its Applications (ISPLC)*, Malmö, Sweden, April 2001, pp. 319−324.

Bartolucci, E. J., and Finke, B. H. (2001), "Cable Design for PWM Variable-Speed AC Drives," *IEEE Transactions on Industry Applications*, Vol. 37, No. 2, March/April 2001, pp. 415−422.

Bausch, J., Kistner, T., Babic, M., and Dostert, K. (2006), "Characteristics of Indoor Power Line Channels in the Frequency Range 50 − 500 kHz," in *Proc. of the 10th IEEE International Symposium on Power-Line Communications and Its Applications (ISPLC)*, Orlando, Florida, USA, March 2006, pp. 86−91.

Bégin, G., and Haccoun, D. (1989), "High-Rate Punctured Convolutional Codes: Structure Properties and Construction Technique," *IEEE Transactions on Communications*, Vol. 37, No. 12, December 1989, pp. 1381−1385.

Berrou, C., and Glavieux, A. (1996), "Near Optimum Error Correcting Coding and Decoding: Turbo Codes," *IEEE Transactions on Communications*, Vol. 44, No. 10, October 1996, pp. 1261−1271.

Bilal, O., Liu, E., Gao, Y., and Korhonen, T. (2004), "Design of Broadband Coupling Circuits for Power-Line Communication," in *Proc. of the 8th IEEE International Symposium on Power-Line Communications and Its Applications (ISPLC)*, Zaragoza, Spain, March/April 2004, pp. 128−132.

Bingham, J. A. C. (1990), "Multicarrier Modulation for Data Transmission: An Idea Whose Time Has Come," *IEEE Communications Magazine*, Vol. 28, No. 5, May 1990, pp. 5−14.

Brooks, T. (2001), "Wireless Technology for Industrial Sensor and Control Networks," in *Proc. of the 1st ISA/IEEE Sensors for Industry Conference*, Rosemont, Illinois, USA, November 2001, pp. 73−77.

Brown, P. A. (1999), "Power Line Communications − Past Present and Future," in *Proc. of the 3rd IEEE International Symposium on Power-Line Communications and Its Applications (ISPLC)*, Lancaster, UK, March/April 1999, pp. 1−8.

Cain, J. B., Clark, G. C., and Geist, J. M. (1979), "Punctured Convolutional Codes of Rate $(n-1)/n$ and Simplified Maximum Likelihood Decoding," *IEEE Transactions on Information Theory*, Vol. IT-25, No. 1, January 1979, pp. 97−100.

Carlson, A. B., Crilly, P. B., and Rutledge, J. C. (2002), *Communication Systems: An Introduction to Signals and Noise in Electrical Communication*, McGraw-Hill, Boston, USA, 4th edition, 2002, 850 p.

CEPCA (2007), Consumer Electronics Powerline Communication Alliance, Available at http://www.cepca.org/home, Accessed on September 2007.

Chen, S., Zhong, E., and Lipo, T. A. (1994), "A New Approach to Motor Condition Monitoring in Induction Motor Drives," *IEEE Transactions on Industry Applications*, Vol. 30, No. 4, July/August 1994, pp. 905−911.

Chen, S., and Lipo, T. A. (1998), "Bearing Currents and Shaft Voltages of an Induction Motor Under Hard- and Soft-Switching Inverter Excitation," *IEEE Transactions on Industry Applications*, Vol. 34, No. 5, September/October 1998, pp. 1042−1048.

Coakley, N. G., and Kavanagh, R. C. (1999), "Real-Time Control of a Servosystem Using the Inverter-Fed Power Lines to Communicate Sensor Feedback," *IEEE Transactions on Industrial Electronics*, Vol. 46, No. 2, April 1999, pp. 360−369.

Decotignie, J. D. (2001), "A Perspective On Ethernet – TCP/IP as a Fieldbus," in *Proc. of the IFAC International Conference on Fieldbus Systems and Their Applications (FeT)*, Nancy, France, November 2001, pp. 138−143.

Dostert, K. (2001), *Powerline Communications*, Prentice-Hall, Upper Saddle River, New Jersey, USA, 2001, 338 p.

EN 50065-1 (1991), *Signalling on Low Voltage Electrical Installations in the Frequency Range 3 kHz to 148.5 kHz*, CENELEC, Brussels, Belgium, 1991.

EN 300 744 (2004), *Digital Video Broadcasting (DVB); Framing structure, channel coding and modulation for digital terrestrial television*, ETSI, Sophia Antipolis, France, 2004.

Echelon Corporation (2008), Available at http://www.echelon.com/, Accessed on April 2008.

EIA (2008), Electronic Industries Alliance, Available at http://www.eia.org/, Accessed on April 2008.

Esmailian, T., Kschischang, F. R., and Gulak, P. G. (2002), "An In-building Power Line Channel Simulator," in *Proc. of the 6$^{th}$ International Symposium on Power-Line Communications and Its Applications (ISPLC)*, Athens, Greece, March 2002, 5 p.

Fahie, J. J. (1883), "Edward Davy," *The Electrician*, July 1883, pp. 181−227.

Felser, M. (2001), "Ethernet TCP/IP in Automation: A Short Introduction to Real-Time Requirements," in *Proc. of the 8$^{th}$ IEEE International Conference on Emerging Technologies and Factory Automation*, Antibes-Juan les Pins, France, October 2001, pp. 501−504.

Felser, M. (2005), "Real-Time Ethernet—Industry Prospective," in *Proc. of the IEEE*, Vol. 93, No. 6, June 2005, pp. 1118−1129.

Galli, S., and Logvinov, O. (2008), "Recent Developments in the Standardization of Power Line Communications within the IEEE," *IEEE Communications Magazine*, Vol. 46, No. 7, July 2008, pp. 64−71.

Götz, M., Rapp, M., and Dostert, K. (2004), "Power Line Channel Characteristics and Their Effect on Communication System Design," *IEEE Communications Magazine*, Vol. 42, No. 4, April 2004, pp. 78−86.

Hagenauer, J. (1988), "Rate-Compatible Punctured Convolutional Codes (RCPC Codes) and their Applications," *IEEE Transactions on Communications*, Vol. 36, No. 4, April 1988, pp. 389−400.

Hansen, D. (2002), "Update on Power Line Telecommunication (PLT) Activities in Europe," in *Proc. of the 2002 IEEE International Symposium on Electromagnetic Compatibility*, Vol. 1, Minneapolis, Minnesota, USA, August 2002, pp. 17−22.

Haykin, S. (1994), *Communication Systems*, John Wiley & Sons, Inc., New York, USA, 3$^{rd}$ edition, 1994, 872 p.

HomePlug Powerline Alliance (2003), HomePlug Technology Field Test Results: A White Paper, 2003, 6 p.

HomePlug Powerline Alliance (2004), HomePlug 1.0 Technical White Paper, September 2004, 13 p.

HomePlug Powerline Alliance (2005), HomePlug AV White Paper, 2005, 11 p.

HomePlug Powerline Alliance (2007), Available at http://www.homeplug.org/home, Accessed on September 2007.

Hrasnica, H., Haidine, A., and Lehnert, R. (2004), *Broadband Powerline Communications Networks: Network Design*, John Wiley & Sons Ltd, Chichester, England, 275 p.

IEEE P1901 Draft Standard for Broadband over Power Line Networks: Medium Access Control and Physical Layer Specifications (2007), Available at http://standards.ieee.org/, Accessed on September 2007.

INSTEON (2008), The Details, Smarthome Technology, Aug. 2005, 64 p., Available at http://www.insteon.net/, Accessed on April 2008.

Janse van Rensburg, P. A., and Ferreira, H. C. (2005), "Design of a Bidirectional Impedance-Adapting Transformer Coupling Circuit for Low-Voltage Power-Line Communications," *IEEE Transactions on Power Delivery*, Vol. 20, No. 1, January 2005, pp. 64−70.

Janse van Rensburg, P. A., and Ferreira, H. C. (2008), "Coupler Winding Ratio Selection for Effective Narrowband Power-Line Communications," *IEEE Transactions on Power Delivery*, Vol. 23, No. 1, January 2008, pp. 140−149.

Jansen, D., and Büttner, H. (2004), "Real-Time Ethernet the EtherCAT Solution," *IEE Computing & Control Engineering Journal*, Vol. 15, No. 1, February/March 2004, pp. 16−21.

Jung, M.-H., Chung, M. Y., and Lee, T.-J. (2005), "MAC Throughput Analysis of HomePlug 1.0," *IEEE Communications Letters*, Vol. 9, No. 2, February 2005, pp. 184−186.

Konaté, C., Kosonen, A., Ahola, J., Machmoum, M., and Diouris, J. F. (2008), "Power Line Channel Modelling for Industrial Application," in *Proc. of the 12$^{th}$ IEEE International Symposium on Power-Line Communications and Its Applications (ISPLC)*, Jeju Island, Korea, April 2008, pp. 76−81.

Lee, M. K., Latchman, H. A., Newman, R. E., Katar, S., and Yonge, L. (2002), "Field Performance Comparison of IEEE 802.11b and HomePlug 1.0," in *Proc. of the 27th Annual IEEE Conference on Local Computer Networks (LCN)*, Tampa, Florida, USA, November 2002, pp. 598−599.

Lee, M. K., Newman, R. E., Latchman, H. A., Katar, S., and Yonge, L. (2003), "HomePlug 1.0 Powerline Communication LANs – Protocol Description and Performance Results," *International Journal of Communication Systems*, Vol. 16, No. 5, May 2003, pp. 447−473.

Lin, Y., Latchman, H. A., Newman, R. E., and Katar, S. (2003), "A Comparative Performance Study of Wireless and Power Line Networks," *IEEE Communications Magazine*, Vol. 41, No. 4, April 2003, pp. 54−63.

Lin, C.-K., Chu, H.-W., Yeh, S.-C., Lu, M.-T., Yao, J., and Chen, H. (2006), "Robust Video Streaming over Power Lines," in *Proc. of the 10th IEEE International Symposium on Power-Line Communications and Its Applications (ISPLC)*, Orlando, Florida, USA, March 2006, pp. 196−201.

Lindh, T. (2003), *On the Condition Monitoring of Induction Machines*, Doctoral dissertation, Lappeenranta University of Technology, Lappeenranta, Finland, 2003, 146 p.

Liu, C.-H., Wade, E., and Asada, H. H. (2001), "Reduced-Cable Smart Motors Using DC Power Line Communication," in *Proc. of the 2001 IEEE International Conference on Robotics & Automation*, Seoul, Korea, May 2001, pp. 3831−3838.

Luukko, J. (2000), *Direct Torque Control of Permanent Magnet Synchronous Machines – Analysis and Implementation*, Doctoral dissertation, Lappeenranta University of Technology, Lappeenranta, Finland, 2000, 172 p.

Ma, Y. H., So, P. L., and Gunawan, E. (2005), "Performance Analysis of OFDM Systems for Broadband Power Line Communications Under Impulsive Noise and Multipath Effects," *IEEE Transactions on Power Delivery*, Vol. 20, No. 2, April 2005, pp. 674−682.

Majumder, A., and Caffery, J. Jr. (2004), "Power Line Communications," *IEEE Potentials*, Vol. 23, No. 4, October/November 2004, pp. 4−8.

Mirafzal, B., Skibinski, G. L., Tallam, R. M., Schlegel, D. W., and Lukaszewski, R. A. (2007), "Universal Induction Motor Model With Low-to-High Frequency-Response Characteristics," *IEEE Transactions on Industry Applications*, Vol. 43, No. 5, September/October 2007, pp. 1233−1246.

Neosid Pemetzrieder GmbH & Co. (2000), Soft Ferrite Components 1, 2000, 34 p., Available at http://www.neosid.de/, Accessed on March 2008.

O'Mahony, B. (2006), "Field Testing of High-Speed Power Line Communications in North American Homes," in *Proc. of the 10th IEEE International Symposium on Power-Line Communications and Its Applications (ISPLC)*, Orlando, Florida, USA, March 2006, pp. 155−159.

Opera (2007), Open PLC European Research Alliance, Available at http://www.ist-opera.org/, Accessed on September 2007.

Papaleonidopoulos, I. C., Karagiannopoulos, C. G., Theodorou, N. J., and Capsalis, C. N. (2005), "Theoretical Transmission-Line Study of Symmetrical Indoor Triple-Pole Cables for Single-Phase HF Signalling," *IEEE Transactions on Power Delivery*, Vol. 20, No. 2, April 2005, pp. 646−654.

Paul, C. R. (1994), *Analysis of Multiconductor Transmission Lines*, John Wiley & Sons, Inc., New York, USA, 1994, 559 p.

Phillips, H. (1999), "Modelling of Power-Line Communication Channels," in *Proc. of the 3$^{rd}$ International Symposium on Power-Line Communications and Its Applications (ISPLC)*, Lancaster, UK, March/April 1999, pp. 14−21.

Proakis, J. G., and Manolakis, D. G. (1996), *Digital Signal Processing: Principles, Algorithms, and Applications*, Prentice-Hall, Upper Saddle River, New Jersey, USA, 1996, 968 p.

Reed, I. S., and Solomon, G. (1960), "Polynomial Codes over Certain Finite Fields," *Journal of the Society for Industrial and Applied Mathematics*, Vol. 8, No. 2, June 1960, pp. 300−304.

Routin, J., and Brown, C. E. L. (1897), "Power Line Signalling Electricity Meters," UK Patent Office, British Patent No. 24833, 1897.

Samaranayake, L., Leksell, M., and Alahakoon, S. (2002a), "Real-Time Speed Control of a Brushless DC Motor via Ethernet," in *Proc. of Nordic Workshop on Power and Industrial Electronics (NORPIE)*, Stockholm, Sweden, August 2002, 6 p., CD-ROM.

Samaranayake, L., and Alahakoon, S. (2002b), "Closed − loop Speed Control of a Brushless DC Motor via Ethernet," in *Proc. of the 9$^{th}$ Annual Technical Conference of IEEE*, Colombo, Sri Lanka, September 2002, 8 p.

Samaranayake, L., Alahakoon, S., and Walgama, K. (2003), "Speed Controller Strategies for Distributed Motion Control via Ethernet," in *Proc. of the 18$^{th}$ IEEE International Symposium on Intelligent Control (ISIC)*, Houston, USA, October 2003, pp. 322−327.

Saltzberg, B. R. (1967), "Performance of an Efficient Parallel Data Transmission System," *IEEE Transactions on Communication Technology*, Vol. 15, No. 6, December 1967, pp. 805−811.

Sarén, H. (2005), *Analysis of the Voltage Source Inverter with Small DC-link Capacitor*, Doctoral dissertation, Lappeenranta University of Technology, Lappeenranta, Finland, 2005, 143 p.

Schubert, F. M. (2007), *Feedback Data Communications on and Modeling of Power Lines for Pulse-Width Modulated Brushless DC Motors*, Diploma thesis, Massachusetts Institute of Technology, Cambridge, UK, 2007, 103 p.

Sheng, K., Williams, B. W., and Finney, S. J. (2000), "A Review of IGBT Models," *IEEE Transactions on Power Electronics*, Vol. 15, No. 6, November 2000, pp. 1250−1266.

Silventoinen, P. (2001), *Electromagnetic Compatibility and EMC-Measurements in DC-Voltage Link Converters*, Doctoral dissertation, Lappeenranta University of Technology, Lappeenranta, Finland, 2001, 115 p.

Steer, M. (2007), "Beyond 3G," *IEEE Microwave Magazine*, Vol. 8, No. 1, February 2007, pp. 76−82.

Stevens, W. R. (1994), *TCP/IP Illustrated, Volume 1: The Protocols*, Addison-Wesley publishing company, Massachusetts, USA, 1994, 576 p.

Suraweera, H. A., Chai, C., Shentu, J., and Armstrong, J. (2003), "Analysis of Impulse Noise Mitigation Techniques for Digital Television Systems," in *Proc. of the 8th International OFDM Workshop*, Hamburg, Germany, September 2003, pp. 172−176.

Thoradson, C. (1905), "Meters," US Patent Office, US Patent Nos. 784712 and 784713, 1905.

Tiainen, R., Särkimäki, V., Lindh, T., and Ahola, J. (2005), "Estimation of the Data Transfer Requirements of Vibration and Temperature Measurements in Induction Motor Condition Monitoring," in *Proc. of the 11th European Conference on Power Electronics and Applications (EPE)*, Dresden, Germany, September 2005, 10 p., CD-ROM.

Tiainen, R., Särkimäki, V., Ahola, J., and Lindh, T. (2006), "Utilization Possibilities of Frequency Converter in Electric Motor Diagnostics," in *Proc. of 18th International Symposium on Power Electronics, Electrical Drives, Automation and Motion (SPEEDAM)*, Taormina (Sicily), Italy, May 2006, pp. 1269−1274.

Toliyat, H. A., Levi, E., and Raina, M. (2003), "A Review of RFO Induction Motor Parameter Estimation Techniques," *IEEE Transactions on Energy Conversion*, Vol. 18, No. 2, June 2003, pp. 271−283.

Wade, E., and Asada, H. H. (2002), "One-Wire Smart Motors Communicating over the DC Power Bus-Line with Application to Endless Rotary Joints," in *Proc. of the 2002 IEEE International Conference on Robotics & Automation*, Washington, DC, USA, May 2002, pp. 2369−2374.

Wade, E., and Asada, H. H. (2003), "Reduced Cable Smart Motors Communicating over the DC Power Bus-Line for High Degree of Freedom Systems," in *Proc. of the 2003 IEEE/RSJ International Conference on Intelligent Robots and Systems*, Las Vegas, Nevada, USA, October 2003, pp. 1987−1991.

X10 (2008), Available at http://www.x10.com/homepage.htm, Accessed on April 2008.

Zimmermann, M., and Dostert, K. (2002a), "Analysis and Modeling of Impulsive Noise in Broad-Band Powerline Communications," *IEEE Transactions on Electromagnetic Compatibility*, Vol. 44, No. 1, February 2002, pp. 249−258.

Zimmermann, M., and Dostert, K. (2002b), "A Multipath Model for the Powerline Channel," *IEEE Transactions on Communications*, Vol. 50, No. 4, April 2002, pp. 553−559.

# Publication I

A. KOSONEN, M. JOKINEN, V. SÄRKIMÄKI, J. AHOLA, AND M. NIEMELÄ

**Motor Feedback Speed Control by Utilizing the Motor Feeder Cable as a Communication Channel**

# Motor Feedback Speed Control by Utilizing the Motor Feeder Cable as a Communication Channel

A. Kosonen*, M. Jokinen*, V. Särkimäki*, J. Ahola*, and M. Niemelä*

* Department of Electrical Engineering, Lappeenranta University of Technology, P.O. Box 20, 53851 Lappeenranta
(*Finland*)

*Abstract*--A feedback loop is used in the motor speed control in order to transmit the measured motor rotational speed information to the controller. The implementation of the feedback loop requires cabling between the motor and the frequency converter both for signalling and powering. However, the motor power cables could be also used for data transmission. The possibility of using the same motor feeder cable for supplying power to the motor and for transferring the motor rotational speed information to the controller is researched in this article. The data transmission utilizes a PLC (Power Line Communication) method that forms an Ethernet connection over the motor feeder cable.

*Index Terms*--power line communication, Ethernet, feedback control, rotational speed, HomePlug.

## I. INTRODUCTION

In electrical drives, motor rotational speed and the rotor angle are typical measurements that are used as a feedback information to a controller. The vector control methods, such as, DTC (Direct Torque Control) [1] do not necessarily need rotational speed as a feedback information. However, in demanding applications, especially, at low rotational speeds, also these control methods require measured rotor speed or angle as a feedback information. The main problem in the sensorless induction motor control methods is an error of static rotational speed. This problem is caused by estimation errors in the motor model parameters of the speed estimator.

The feedback loop generally requires a data transmission link from the motor to the controller. In practice, this means extra cabling. It is also possible to use the same cables for the data transmission and for supplying power to the motor [2]. According to [2], the main purpose of the data transmission in the motor feeder cable from the motor to the frequency converter is the need of on-line condition monitoring.

In on-line condition monitoring the measured data from a motor, a pump, a blower, etc. is transmitted forward to the upper data system level, where the data can be analyzed by expert systems. The data transmission requirements of the induction motor on-line condition monitoring for vibration and temperature measurements do not require wide bandwidth [3] compared to the whole

data transfer capacity of the used PLC (Power Line Communication) method [2]. Hence, it is possible to use this additional data transfer capacity, e.g. for forming the motor rotational speed feedback loop.

According to [4], the data transmission requirements of the motor control are generally stricter than those of the motor diagnostics. The maximum latency of the data transmission should be taken into consideration in the motor control design. A principle of the motor feedback speed control, which utilizes the motor feeder cable as a communication channel is illustrated in Fig. 1.
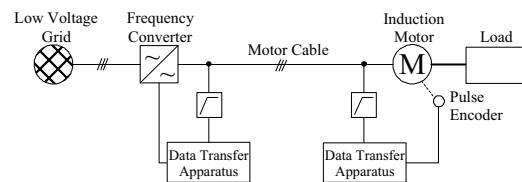


Fig. 1. A principle of the motor feedback speed control that utilizes the motor feeder cable as a communication channel. An Ethernet connection can be created over the motor feeder cable by using the PLC modems, which are included in the data transfer apparatus.

The PLC method, used in this application, forms an Ethernet connection over the motor feeder cable. The PLC method encapsulates the Ethernet frames (IEEE 802.3) into its own protocol [5]. Then the motor cable looks like an Ethernet connection in the viewpoint of Ethernet devices. The latency of the method as a function of the data transfer rate has been considered in [2], [4], [6].

The latency of Ethernet is non-deterministic due to the CSMA/CD (Carrier Sense Multiple Access with Collision Detection) bus reservation mechanism. This can cause problems in real-time applications, which require deterministic response, e.g. in control applications. According to [7], in applications, which demand time delay less than 1 ms, Ethernet is not a practical solution. The utilization of Ethernet in industrial applications has been researched e.g. in [8] - [10].

The utilization of Ethernet in the distributed motion control is researched in [11], where the rotor feedback speed information of a brushless DC-motor is delivered

between the speed controller and the frequency converter by using a 10 Mb/s Ethernet LAN (Low Area Network) and frame size of 64 bytes. First, the rotor speed is computed in the local current controller and then it is transferred to the speed controller via Ethernet/IP Network (Internet Protocol). Next, the speed controller computes the torque reference (reference current signal $i^{*}_{q}$) and sends it via Ethernet/IP network back to the local current controller, which controls the brushless DC-motor.

The application described in [11] differs from the application presented in this article. In this application, the rotational speed signal is transferred through the motor cable, whereas in [11], separated Ethernet cabling is utilized. The speed controller gives the torque reference directly to the frequency converter, whereas in [11], separated Ethernet cabling is utilized again. The direct connection between the speed controller and the frequency converter is reasoned, because the controller is generally implemented in the frequency converter or nearby it.

The structure of this article is following. The control system and the data transmission implementation are presented in section II. In section III, the laboratory experiments are carried out and based on them; performance of the introduced motor feedback speed control method is evaluated. The test results are analyzed in section IV. A summary of the introduced speed control method and its test results are introduced in section V.

## II. A DESCRIPTION OF THE TEST EQUIPMENT

An induction motor ABB M2AA160L4 is used as an adjustable motor. A load generator, which is a DC motor ABB DMP 160-4M, is connected directly to the shaft of the induction motor. The DC motor was chosen for this task for the sake of easy controllability. The main electrical and mechanical parameters of the motors used in the laboratory tests are introduced in Table I, where $P_{n}$ is nominal power, $V_{n}$ nominal voltage, $I_{n}$ nominal current, $T_{n}$ nominal torque, $n_{n}$ nominal rotational speed, and $J$ moment of inertia.

TABLE I
THE MAIN ELECTRICAL AND MECHANICAL PARAMETERS OF MOTORS
USED IN THE TEST EQUIPMENT

| Motor | $P_{n}$ (kW) | $V_{n}$ (V) | $I_{n}$ (A) | $T_{n}$ (Nm) | $n_{n}$ (rpm) | $J$ (kgm$^{2}$) |
|---|---|---|---|---|---|---|
| Induction | 15 | 400 | 28.5 | 98 | 1455 | 0.102 |
| DC | 75.5 | 410 | 200 | 240 | 3000 | 0.25 |

In the test configuration, the induction motor is supplied with the ABB ACS800 frequency converter. The frequency converter is equipped with an output filter. Rotational speed of a rotor of the induction motor is measured with a Leine&Linde pulse encoder, which resolution is 4096 ppr (pulse per revolution). The motor cable between the motor and the frequency converter is

MCCMK 3x35+16 (90 m). A dSPACE DS1103 PPC equipment is used as a speed controller. The similar HomePlug standard compliant PLC modems, as in [2], [4], and [6], but newer ones are used for motor cable communications. The PLC modems are connected differentially to the motor cable between two phases. Rotational speed has to be converted to a suitable data format, which could be sent via Ethernet. This is carried out by using embedded PICDEM.net Ethernet demonstration kits.

### A. Operation of the Test Equipment

The laboratory experiment was constructed at the power electronics laboratory at Lappeenranta University of Technology. A diagram of the laboratory equipment is illustrated in Fig. 2.
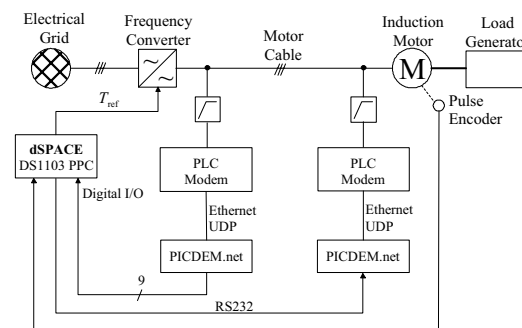


Fig. 2. A diagram of the laboratory equipment. An Ethernet connection can be created over the motor feeder cable by using the HomePlug standard compliant PLC modems.

A low voltage electrical grid (400 V, 50 Hz) supplies power to the frequency converter, which supplies, in turn, power to the induction motor. The induction motor is connected to the frequency converter with a 90 m long motor cable.

Rotational speed of the induction motor is measured with the pulse encoder. Pulse shaped data given by the encoder is transmitted directly to the dSPACE equipment. The number of pulses does not limit the performance of the control system, because pulses are not transmitted via the motor cable. In this case, dSPACE computes rotational speed of the induction motor according to received pulse shaped data. The sampling time of rotational speed is similar all the time despite of data given by the pulse encoder.

Computed rotational speed is sent to an embedded Ethernet board via the serial communication interface in the digital format. The serial communication data transmission speed is 38400 b/s. The embedded Ethernet board at the motor encapsulates the digital rotational speed data into a UDP (User Datagram Protocol) packet. From the embedded Ethernet board the UDP packet is transmitted via an Ethernet cable to a motor cable communication device (a PLC modem), which is based on the HomePlug standard technology. The HomePlug device, in turn, encapsulates the data packet into its own protocol and transmits it forward from the motor side

through the motor cable to the frequency converter. Another HomePlug PLC modem is installed in the frequency converter side to receive the data packets from the motor cable. In the receiver side the operations are contrary to those in the transmission side, on the difference that digital rotational speed is transmitted from the embedded Ethernet board to the digital I/O of the dSPACE equipment with the parallel data format.

Rotational speed of the induction motor is used as a feedback information for the speed controller that is implemented to the dSPACE equipment. The frequency converter is controlled by the torque reference, which is computed in the dSPACE equipment.

### B. Embedded Ethernet Boards

One Microchip's PICDEM.net Ethernet demo board is used to encapsulate data from the dSPACE equipment into UDP packets that are transmitted to the PLC modem. In the other end, the second PICDEM.net board receives the UDP packets and transfers data to the dSPACE equipment. The demo boards and connections are shown in Fig. 3.
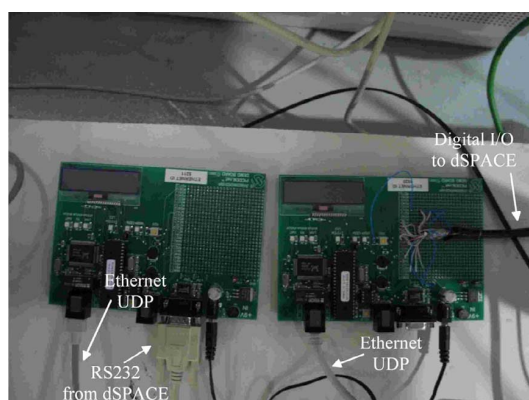


Fig. 3. The PICDEM.net Embedded Ethernet Boards.

Microchip's PICDEM.net demo boards include an 8-bit PIC18-series microcontroller and Realtek's RTL8019AS Ethernet driver circuit. The boards execute Microchip's TCP/IP (Transmission Control Protocol / Internet Protocol) stack and a special application program [12]. The stack implements both TCP and UDP protocols, which can be used by user applications. The UDP protocol was chosen, because the transmission rate is more important than detecting occasional errors in communication. On the other hand, the HomePlug modems correct the errors in PLC data transmission.

Rotational speed of the induction motor is a 16-bit value. It is computed in the dSPACE equipment and transferred to the PICDEM.net board at the motor. A single measurement is then encapsulated into the UDP packet, which is transmitted to the PLC modem. UDP packets can be processed much faster on demo boards than TCP packets. At the other end of the power cable, the UDP packets are received from the PLC modem. Single measurement is then transferred to the dSPACE

equipment in two 8-bit packets by using a parallel connection. The microcontroller puts the first byte to the parallel line and uses an additional interrupt signal to notify the dSPACE equipment that the data can be read. The second byte is transferred similar to the first one.

### C. dSPACE Equipment

The dSPACE equipment (DS1003) is based on the Texas Instruments TMS320F240 processor. The dSPACE system is used for computation of rotational speed, implementation of the speed controller that gives the reference torque to the frequency converter, and circulation of rotational speed via the motor cable. The utilized dSPACE equipment mainly restricted the final implementation of the whole system.

Rotational speed is formed in accuracy of 16-bits. The resolution of rotational speed gives in accuracy of 0.1 rpm in the rotational speed range of -3276.8 – 3276.8 rpm. The rotational speed information has to be divided into two 8-bit data packets because both the serial and the parallel data communications use the packet size of 8-bits. Receiving via a digital I/O demanded work. Data communication implementation by using the digital I/O is carried out by an interrupt routine, because the digital I/O pins reading has to be done asynchronously, because of the fluctuation of the latency.

The latency of the data transmission method is not fixed due to lost and corrupted packets that cannot be reconstructed. These packets are sent again by ARQ (Automatic Repeat reQuest) mechanism implemented in HomePlug [5]. Corrupted data packets can be detected with CRC (Cyclic Redundancy Check) and they can be reconstructed, if possible, with FEC (Forward Error Control). Both of these techniques are implemented in HomePlug [5].

A conventional PI (Integrator with a Proportional gain) controller was used as a speed controller. Computation time $h_c$ was chosen to 2 ms. In generally, computation time $h_c$ is assumed to be longer than the delay of the feedback loop $\tau$ ($\tau < h_c$) caused by the system itself [13]. With this assumption transfer functions can simply be discretized. In this application, this delay is longer than the computation time.

### D. Analyzing the Test Arrangement

It is possible to compare the influences of two different routes of the feedback loop to the operation of the speed controller with the earlier described equipment. In this arrangement, it is easy to choose either the direct or the motor cable feedback loop signal, because the direct feedback signal is brought to the controller (dSPACE) anyway. The feedback loop signal is utilized in the speed controller. It is also possible to research the latency and its fluctuation caused by the data communication method used in the feedback loop. The latency has effect on the tuning parameters of the PI speed controller. The constructed test equipment is illustrated in Fig. 4.
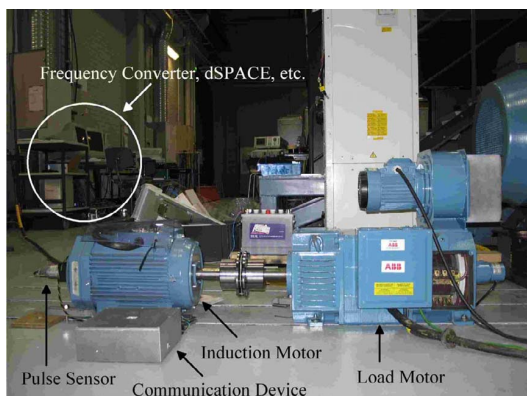
Fig. 4. The test equipment constructed at the power electronics laboratory at Lappeenranta University of Technology.

### III. LABORATORY MEASUREMENTS

The transmission latency and its variation are critical part in the introduced control system, because they affect directly the speed controller tuning. The parameters of the speed controller, in turn, have direct effect on the performance of the whole system.

The latency of the feedback loop was researched using the test setup. The resolution of 100 μs was considered to be enough in the measurement. The latency consists of following components

$$\tau = \frac{h_s}{2} + \tau_{RS232} + \tau_{UDP} + \tau_{PLC} , \qquad (1)$$

where $h_s$ is the sampling time of the rotational speed signal received from the pulse encoder, $\tau_{RS232}$ is the latency caused by the serial communication, $\tau_{UDP}$ is the latency caused by forming UDP packet in the embedded Ethernet boards, and $\tau_{PLC}$ is the data transfer latency caused by the PLC modems used in the motor cable communication. All the other latencies can be considered to be constant all the test time except the latency caused by the PLC modems. The latency component, which is half of the sampling time $h_s$, is caused from the fact that the data should be transmitted in 8-bit data packets through the serial interface. The first 8-bit component is transmitted with time instant zero and the second one with time instant $h_s/2$. In this case, the latency of the serial communication is as follows

$$\tau_{RS232} = \frac{8\,b}{38400\,\dfrac{b}{s}} = 0.21\,\text{ms} , \qquad (2)$$

because the latency caused by transmitting the first 8-bits is simultaneous with the latency caused by sampling ($h_s/2$). The latency can be determined by transmitting increasing 16-bit values through the feedback loop and measuring the time difference between the transmitted and the received values.

### A. Statistical Methods for the Latency Measurements

A histogram can be used to illustrate the behaviour of the latency and its variation. In addition, sample statistics tells detailed information about the latency behaviour.

The sample mean of a data set $\bar{x}$ is simply the arithmetic average of the data observation. It can be calculated according to

$$\bar{x} = \frac{1}{n} \sum_{i=1}^{n} x_i , \qquad (3)$$

where $x_i$ are the data observations and $n$ is the number of the observations. The sample variance $s^2$ describes the variance of an unknown distribution of the observations in the data set [14]. It can be written

$$s^2 = \frac{1}{n-1} \sum_{i=1}^{n} (x_i - \bar{x})^2 . \qquad (4)$$

The sample standard deviation $s$ does not commit on the form of a distribution of the data set. Standard deviation can be described as follows

$$s = \sqrt{\frac{1}{n-1} \sum_{i=1}^{n} (x_i - \bar{x})^2} . \qquad (5)$$

The parameters, denoted as $\tau_{min}$ and $\tau_{max}$, are the minimum and the maximum values of the data set, respectively. The sample median is $Md$. The sample mode $Mo$ denotes to the data value that contains the largest number of data observations. It can also be thought as the value that has the highest probability.

### B. The Test Results

First, the embedded Ethernet boards were connected together with a cross-connected Ethernet cable. Then the latency caused by generating and unpacking UDP packets and transferring the data to the dSPACE equipment was possible to measure. The sampling time for the 16-bit rotational speed information was 2 ms, which is same as the computation time in the used controller. The latency of the feedback loop without the PLC modems is illustrated in Fig. 5.

It can be seen from Fig. 5 that the latency gets the values 3.9 ms and 4.0 ms with the 100 μs measurement accuracy. The average latency ($\bar{x}$) with this arrangement settles down to slightly over 3.9 ms.
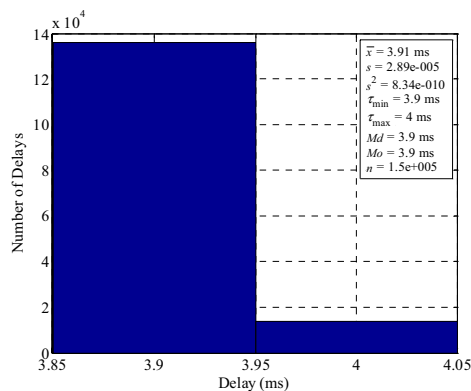
Fig. 5. A histogram of the latency caused by generating and unpacking UDP packets and transferring the data to the dSPACE equipment. The embedded Ethernet boards are connected together with a cross-connected Ethernet cable. The measurement resolution was 100 µs.

The latency of the whole feedback loop (Fig. 2) is illustrated in Fig. 6. The measurements were carried out when the induction motor was driven with a constant speed of 695 rpm by the frequency converter. The equipment was similar to the one described in section II.
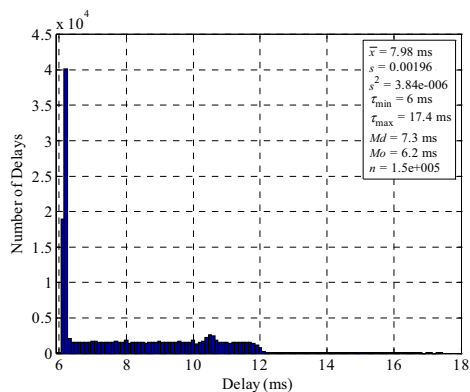


Fig. 6. A histogram of the latency caused by the whole feedback loop showed in Fig.2. The frequency converter drives the induction motor at the same time with a constant speed of 695 rpm. The measurement resolution was 100 µs.

According to Fig. 6, the latency and its variation increases compared to the case illustrated in Fig. 5. The latency is weighted to 6 ms, but the average value settles down to slightly under 8 ms, because of the variation of the latency. The latencies over 12 ms are relatively rare, for example, the probability of latencies over 12.3 ms in the feedback loop is less than 0.2 %. This means that if the rotational speed information is updated in every 2 ms, over 12.3 ms latencies occur on average less than one per second.

It can be ensured with the measurements that rotational speed of the induction motor does have no effect on the communication latencies. This is because the noise level does not fundamentally rise according to rotational speed. The rate of the frequency converter's output stage switching affects to the noise level in the motor cable. In several frequency converters, the rate of switching is variable. Even if the data transfer rate is getting lower, it does not have direct influence on the latencies, if the communication channel is good enough, as in this case.

The effect of the output filter for the motor cable communications was also researched. The same test setup as described earlier was used in the measurements on the difference that the output filter was removed. The test results illustrated in Fig. 7 are comparable with ones illustrated in Fig. 6, because all other test equipment and arrangement was identical on the difference with the sampling time. According to Fig. 7, the latency and, especially, its variation are increased compared to the case illustrated in Fig. 6.
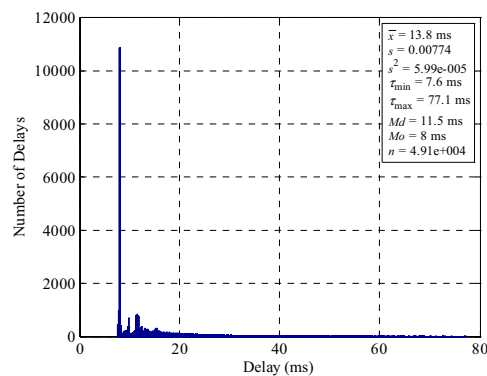


Fig. 7. A histogram of the latency caused by the whole feedback loop showed in Fig.2. The frequency converter drives the induction motor at the same time with a constant speed of 695 rpm. An output filter is not in use. The measurement resolution was 100 µs.

The growth of the minimum latency can be explained with the fact that the used sampling time was 6 ms. This increases minimum latency about 2 ms compared to the earlier cases. The growth of the latency variation is caused by the increased packet losses or corrupts. The quality of the communication channel affects directly on the bandwidth and the latency if the channel is heavy noisy, as in Fig. 7. The output filter raises the impedance level on the frequency converter side and also filters the noise produced by the frequency converter. The differences between these two cases (with an output filter and no output filter) are remarkable and that's why this should be taken into consideration, especially, in the control application.

An operation of the speed control method is illustrated in Fig. 8. The operation ensures that different feedback loops have no significant difference between each other according to this step response test. The test setup is similar to the case illustrated in Fig. 2. The frequency converter was equipped with an output filter.
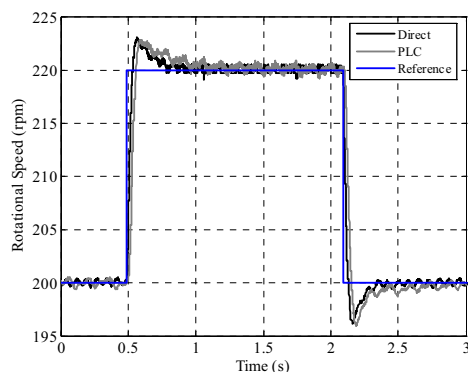
S36 - 21

Fig. 8. The speed control with a direct feedback vs. the speed control with a feedback implemented through a motor cable.

## IV. ANALYSIS OF TEST RESULTS

The latency in the feedback channel has direct effect on the control, its rapidity and tuning parameters. Generally, the applicability of this speed control method is directly dependent on the mechanical time constant of a motor or a system. However, the suitability of the described method depends mainly on the application and its requirements.

According to the test results, the frequency converter should be equipped with an output filter in order to minimize the latency fluctuation. Because the delay is longer than the computation time in this application, the mathematical processing of the model will become complicated. At this point, it is very clear that this control method is not appropriate in applications, which are time critical.

The connection between the latency in the feedback loop and the time constant of the motor should be researched carefully. Extensive performance tests should be also carried out.

## V. CONCLUSIONS

The speed control method with feedback that utilizes a motor cable as a feedback channel was introduced in this article. The latency and its fluctuation in the feedback channel produced by this method were researched. The PLC method can be thought to be Ethernet based, because it encapsulates the Ethernet frames to its own protocol.

Advantages of the output filter of the frequency converter were proved, especially, in the control applications. The operation of the speed control method was also illustrated. The results of the introduced speed control method were promising. However, more performance tests should be carried out in order to map the possibilities of the method in practical applications.

## ACKNOWLEDGMENT

## REFERENCES

[1] Isao Takahashi and Toshihiko Noguchi, "A New Quick-Response and High-Efficiency Control Strategy of an Induction Motor," *IEEE Transactions on Industry Applications*, vol. 22, no. 5, September/October 1986.

[2] J. Ahola, J. Toukonen, A. Kosonen, T. Lindh, and V. Särkimäki, "Electric Motor Cable Communication Overcomes the Biggest Obstacle in On-line Condition Monitoring," in *Proceedings of Condition Monitoring 2005 Conference*, COMADIT, 18th - 21st July 2005, King's College, Cambridge, UK.

[3] R. Tiainen, V. Särkimäki, T. Lindh and J. Ahola, "Estimation of the Data Transfer Requirements of Vibration and Temperature Measurements in Induction Motor Condition Monitoring," in *Proceedings of European Conference on Power Electronics and Applications*, 12-15.9.2005, Dresden, Germany.

[4] J. Ahola, J. Toukonen, A. Kosonen, T. Lindh and R. Tiainen, "Ethernet to Electric Motor – via Mains Cable," in *Proceedings of the 18th International Congress and Exhibition on Condition Monitoring and Diagnostic Engineering Management*, COMADEM, 31st August – 2nd September 2005, Cranfield University, UK.

[5] M. K. Lee, R. E. Newman, H. A. Latchman, S. Katar, and L. Yonge, "HomePlug 1.0 Powerline Communication LANs – Protocol Description and Performance Results, version 5.4," *International Journal of Communication Systems*, 2000; **00**:1-6

[6] J. Ahola, A. Kosonen, J. Toukonen, and T. Lindh, "A New Approach to Data Transmission between an Electric Motor and an Inverter," to be published in *Proceedings of International Symposium on Power Electronics, Electrical Drives, Automation and Motion*, SPEEDAM 2006, Taormina (Sicily), Italy, 23rd – 26th May 2006.

[7] L. Samaranayake, S. Alahakoon and K. Walgama, "Speed Controller Strategies for Distributed Motion Control via Ethernet," in *Proceedings of the 18th IEEE International Symposium on Intelligent Control*, ISIC03, Houston, USA, October 2003, pp. 322-327.

[8] Max Felser, "Ethernet TCP/IP in Automation a Short Introduction to Real-Time Requirements," in *Proceedings of the 8th IEEE International Conference on Emerging Technologies and Factory Automation*, Antibes-Juan les Pins, France, 15th – 18th October 2001.

[9] L. Samaranayake and S. Alahakoon, "Closed – loop Speed Control of a Brushless DC Motor via Ethernet," in *Proceedings of the 9th Annual Technical Conference of IEEE*, Sri Lanka Centre, Colombo, Sri Lanka, September 2002.

[10] J. D. Decotignie, "A Perspective On Ethernet – TCP/IP as a Fieldbus," in *Proceedings of the Proc. IFAC Int. Conf. Fieldbus Systems and their Applications*, FeT 2001, Nancy, France, 15th – 16th November 2001, pp. 138-143.

[11] L. Samaranayake, M. Leksell and S. Alahakoon, "Real-Time Speed Control of a Brushless DC Motor via Ethernet," in *Proceedings of Nordic Workshop on Power and Industrial Electronics*, 12-14 August, Stockholm, Sweden, 2002.

[12] Microchip, AN833 – Microchip TCP/IP Stack Application Note. www.microchip.com

[13] Karl J. Åström, and Björn Wittenmark, *Computer-Controlled Systems Theory and Design*, Prentice Hall 1997, Inc., Third edition, ISBN 0-13-314899-8

[14] Anthony J. Hayter, *Probability and Statistics for Engineers and Scientists*, Duxbury Thomson Learning 2002, USA, Second Edition, ISBN 0-534-38669-5

# Publication II

J. AHOLA, A. KOSONEN, J. TOUKONEN, AND T. LINDH

**A New Approach to Data Transmission between an Electric Motor and an Inverter**

*in Proceedings of 18$^{th}$ International Symposium on Power Electronics, Electrical Drives, Automation and Motion (SPEEDAM), Taormina (Sicily), Italy, May 2006, pp. 126−130.*

# A New Approach to Data Transmission between an Electric Motor and an Inverter

J. Ahola*, A. Kosonen*, J. Toukonen**, and T. Lindh*

\* Department of Electrical Engineering, Lappeenranta University of Technology, P.O. Box 20, 53851 Lappeenranta, (*Finland*)
\*\* ABB, Corporate Research Center in Finland, P.O. Box 608, 65101 Vaasa, (*Finland*)

*Abstract*-- **In electrical drives data transmission between a motor and an inverter is required due to sensors, installed at the motor, that are used in the motor diagnostics or controlling. Generally, the data transmission is carried out using additionally installed cabling, such as, twisted pairs. In this article a new method is proposed that provides an Ethernet based communication link between the electric motor and the inverter. The method uses a motor feeder cable as a media and power line communications (PLC) as a communication method. Laboratory measurements with the method are carried out and the results of the measurements are analyzed.**

*Index Terms*— **Power line communications, Condition monitoring, Electrical drives, Ethernet, Field bus, HomePlug**

## I. Introduction

The on-line self diagnostics is becoming as a standard feature in consumer electronics, as well as in industrial power electronics products. According to [1], the reliable on-line diagnostics of an electric motor condition requires sensors that are installed at the motor. Correspondingly, several applications of electrical drives are based on the measurements of motor rotor speed or angle. Data transmission between a motor and an inverter is required in both cases. Traditionally separate cabling is used that provides the supply power to the sensors, as well as the required amount of twisted pairs for signaling purposes. However, the installation of additional cabling always increases costs. In this paper, a new method is presented that allows one to use the motor feeder cable also in data transmission between the motor and the inverter (Fig. 1).

The idea of using the motor feeder cable as a communication channel for the electric motor condition monitoring was first proposed in [2] and further researched in [3]-[5]. Correspondingly, an approach using DC power bus for controlling servo motors was presented in [6]. In this article, a method is described that provides a broadband communication link between the electric motor and the inverter. Laboratory experiments with the method are carried out. The results of the experiments are analyzed.
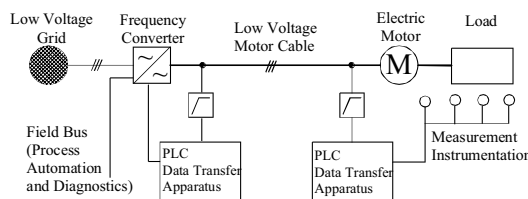
Fig. 1. A data transmission concept between an electric motor and an inverter that is based on power line communications.

The paper is organized as follows. In Section II, the characteristics of a motor feeder cable as a communication channel are described. The equipment used in the laboratory tests is presented in Section III. The Section IV describes the tests carried out. The test results are analyzed in Section V. The paper finishes with a concluding discussion in Section VI.

## II. Characteristics of Communication Channel

The proposed data transmission concept is illustrated in Fig. 1. It can be described with a general communication channel model in Fig. 2. The model consists of two parts: a channel model and a noise or interference model. In the communication channel model, the received signal $y(t)$ is given by

$$y(t) = x(t) * h(t) + n(t), \qquad (1)$$

where $x(t)$ is the signal injected to the channel by the transmitter, $h(t)$ is the impulse response of the channel and $n(t)$ is the noise signal at the receiver.

### A. Communication Channel

In this application, the motor cable forms the media. The cable is terminated at both cable ends. At the frequency converter end, the termination is either an output filter or an output stage of the inverter. Correspondingly, at the other end, the cable is terminated by the electric motor. The PLC modems are coupled to the motor cable, using coupling interfaces at both cable ends. The coupling interfaces are a part of the communications channel. Hence, their effect on the channel characteristics has to be taken into account.

Three-phase motor cables used in variable speed drives are, in general, symmetric and shielded. The cable structure allows several coupling configurations, such as,

phase-to-phase, phase-to-phases, and phase-to-protective earth. The main cable parameters affecting power line communications are characteristic impedance $Z_0$, attenuation coefficient $\alpha(f)$, and cable length $L$. In this application, the cable attenuation is primarily caused by PVC (Polyvinyl Chloride) insulation, which is both frequency and temperature dependent [3]. According to [3], the characteristic impedance of the motor cable depends on the coupling, insulation materials, the cable cross-sectional structure, and frequency. With feeder cable used in variable speed drives impedance values $Z_0 = 5...50\,\Omega$ are typical [3]. Typical low voltage power cable lengths are correspondingly less than 100 meters.
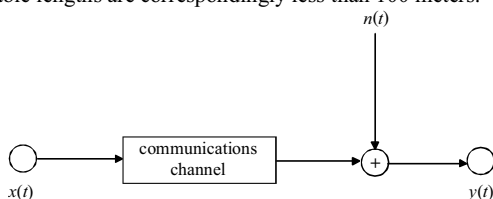


Fig. 2. A general communication channel model. The signal is injected into a system by a transmitter. It is first manipulated by a channel model. The noise is added to the signal at a receiver

The motor, the inverter, and the coupling interfaces can be considered as cable termination impedances. The frequency behavior of an electric motor input impedance is presented e.g. in publications [3], [7]. The coupling interface isolates the PLC modem from the mains voltage, but passes through the frequency band used in communications. Practically, the motor cable is mismatched at the both cable ends, which cause signal reflections and multi-path signal propagation. The reflection coefficient $\overline{\Gamma}_R$ at the interface of two impedances can be written

$$\overline{\Gamma}_R = \frac{\overline{Z}_L - Z_0}{\overline{Z}_L + Z_0} , \qquad (2)$$

where $\overline{Z}_L$ is a load impedance. In the research of PWM drives this phenomena is called cable oscillations, which is researched e.g. in [8]-[10].

Generally, PLC channel frequency characteristics are modeled by using an echo model [11], [12] which parameters are obtained from measurements of the complex channel transfer function. The echo model proposed in [12] represents the superposition of the signal from $N$ different paths. Each path is individually characterized by a weighting factor $g_i$ and length $d_i$. The frequency dependent attenuation is modeled by the parameters $a_0$, $a_1$ and $k$. The transfer function

$$\overline{H}(f) = \sum_{i=1}^{N} g_i \cdot e^{-\left(a_0 + a_1 f^k\right)d_i \cdot e^{-j2\pi f \frac{d_i}{v_p}}} \qquad (3)$$

describes the channel attenuation as a function of frequency. The parameter $v_p$ is the propagation speed of an electromagnetic wave in the cable, which is with PVC insulated cables about $0.5...0.6 c_0$ [3]. In this application, the channel structure is simple and the typical frequency characteristics of components, such as, motors and cables are known. Hence, it is convenient to model the channel attenuation by using two-port network models and transmission line equations for cabling. The usage of this method for PLC channels is presented in [13], [14].

### B. Noise Characteristics

The channel transmission characteristics are not sufficient for modeling or planning communication systems. The interference scenario is also important. In the proposed application this is obvious. Despite of feasible transmission characteristics at low frequencies, the band can not utilized for communication purposes due to interference produced by the inverter. The power lines do not represent additive white Gaussian noise (AWGN) channels. According to [15], the interference scenario is rather complicated consisting of colored broadband noise, narrowband interference and different types of impulsive disturbance. Based on [16], the interference scenario can be separated into five classes, colored background noise, narrowband noise, periodic impulsive noise that is synchronous or asynchronous to the mains frequency (50/60 Hz), and asynchronous aperiodic impulsive noise.

In this application the main noise source is the output stage of the inverter. It can be considered as impulsive noise that is asynchronous to the mains frequency. The switching of insulated gate bipolar transistors (IGBT) generates surge waves into the motor cable. The surge waves propagate and reflect in the cable attenuating exponentially. According to [17], with modern PWM (pulse width modulation) inverters the voltage rise and fall times are in the range of 0.1-10 µs. Correspondingly, the switching frequency, in general, varies in the range of 2-20 kHz. A noise current spectrum measured from a single phase from the inverter output with a current probe is illustrated in Fig. 5. In the measurement, the inverter output was equipped with a du/dt filter.

According to Fig. 5, the inverter produces high noise current amplitudes at the frequency range of several MHz and the noise current level stabilizes at the frequency of 6 MHz to 40-50 dB(µA). Due to the noise generated by the inverter, frequencies higher than 6 MHz should be used for power line communications. The higher the carrier frequency is, the less, in general, the noise power produced by the inverter. On the other hand, the signal attenuation in the cabling is increased as a function of frequency. It determines the upper frequency limit. These factors together define a practical frequency band to PLC.
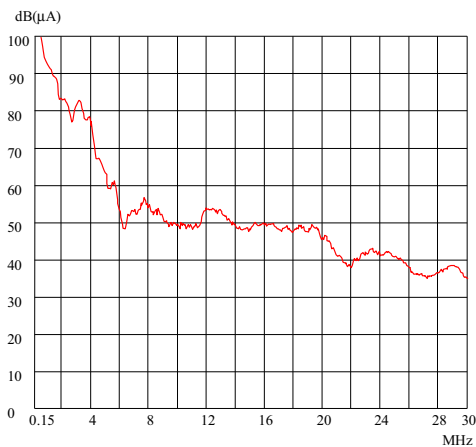
dB(μA)



Fig. 3. A noise current spectrum measured from a single phase from a du/dt filter output with an EMI test receiver (Rohde & Schwartz EHSHS 30) and a current probe (Rohde & Schwartz EZ-17). The measurement parameters were: frequency band 150 kHz - 30 MHz, stepping 10 kHz, IF BW = 10 kHz, sample time 20 ms, peak detect.

## III. TEST ENVIRONMENT

A test environment was constructed at the power electronics laboratory at Lappeenranta University of Technology. A diagram of the test environment is illustrated in Fig. 4. The electrical drive consists of an inverter, an output filter (was not connected in all tests), a low voltage power cable and an electric motor. The PLC modems were connected to the motor terminals and the output filter terminals or directly to the inverter output terminals.

Both modems (Fig. 4) were HomePlug 1.0 compliant. They were supplied from batteries in order to ensure that there are no other routes for the communication signal than the low voltage motor cable. Laptop computers were connected to the Ethernet ports of the modems with RJ-45 cables. One laptop computer was configured as a FTP (File Transfer Protocol) server and the other as a client. The standard modem coupling interfaces are designed to be used in the mains network. They do not protect the modems from the surge waves generated by the inverter output stage switching. Hence, a new coupling interface was developed for the modems.
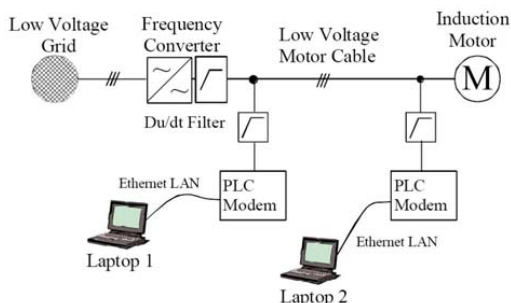


Fig. 4. A diagram of the test environment used in power line communication tests.

## A. HomePlug 1.0

The HomePlug 1.0 is a PLC standard developed by the HomePlug alliance [18]. It provides a connection between Ethernet devices over power lines encapsulating the Ethernet frames (IEEE 802.3). The HomePlug 1.0 standard defines both the physical layer (PHY) and the media access control (MAC) protocol. The PHY layer uses frequency band from 4.49 to 20.7 MHz and OFDM (Orthogonal Frequency Division Multiplexing) in data transmission. The band is divided into 84 carrier frequencies. However, according to [18], eight of the subcarriers within the usable band are permanently masked to avoid interference to amateur radio. Each carrier frequency is modulated separately. The modems periodically adjust their data rate according to the quality of the communication channel by selecting used carrier frequencies, modulation techniques and forward error correction (FEC). The data rate of MAC layer can vary from 0.7 to 8.08 Mb/s. The maximum MAC layer throughput (8.08 Mb/s) approximately corresponds the data rate of 6 Mb/s at the TCP/IP layer.

## IV. LABORATORY MEASUREMENTS

The test setup used in laboratory measurements is illustrated in Fig. 4. First, noise current spectrum measurements were carried out connecting the current sensor to a single phase conductor. The modem's coupling interface was coupled between two phases. The results are illustrated in Fig. 5.
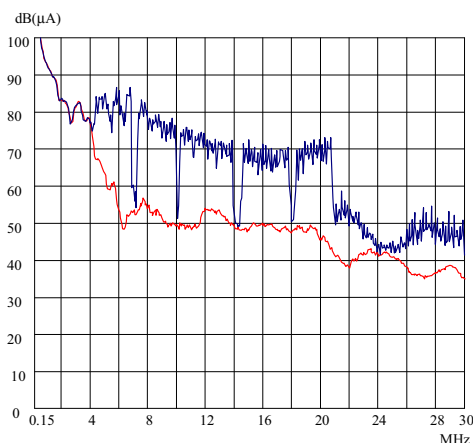
dB(μA)



Fig. 5. Noise current spectrums measured from a single phase from a du/dt filter output with EMI test receiver (Rohde & Schwartz EHSHS 30) and a current probe (Rohde & Schwartz EZ-17). The measurement parameters were: frequency band 150 kHz - 30 MHz, stepping 10 kHz, IF BW = 10 kHz, sample time 20 ms, peak detect. In the lower curve the data transmission was not active. In the upper curve, the data transmission was active.

According to Fig. 5, the modems seem to use the whole frequency band available (4.49-20.7 MHz) in data transmission. The data transmission increases the peak current values at the whole data transmission band with about 20 dB. However, due to the peak value

measurement method it is impossible to accurately estimate RMS (Root-Mean-Square) current spectrums.

Next, data transmission between an electric motor and an inverter was tested. Both data transmission rate and latency were measured. A file transfer with FTP software was used for data transmission rate measurements and ICMP (Internet Control Message Protocol) ping software with packet size of 32 bytes for latency tests. The latency and its statistical characteristics are important, especially, in controlling applications. According to [19], the applied HomePlug 1.0 method fulfills easily the minimum data transmission rate requirements of electric motor condition monitoring. However, the achieved data transmission rate represents the quality of the communication channel. The modems continuously adapt to the channel by selecting frequency bands, modulations and error correction methods used for the communications. Hence, the data transmission rate can be applied in order to determine which factors affect the performance of the data transmission method.

The test environment was varied during the measurements by changing its characteristics one in time, such as, cable length, an output filter/no an output filter, motor size, signal coupling, grounding of the motor and the data transmission direction. It is obvious that the cable length affects the data transmission rate. The maximum cable length used in the measurements was 200 meters, which is also the maximum range of operation commonly promised to HomePlug 1.0 compliant devices.

## V. ANALYSIS

The modems with the developed coupling interface were able to form a data link between an inverter and an electric motor almost in every test carried out. The formation of a data link failed only in four tests. They were carried out with a 200 m cable and using a signal coupling phase-to-protective earth. The results of the data transmission rate measurements are illustrated in Fig. 6. The maximum achievable FTP data rate is less than 6 Mb/s. According to the Fig. 6, the FTP throughput was more than 2.8 Mb/s in 50% of tested links and more than 1 Mb/s in 70% of tested links. The results of data transmission delay measurements are illustrated in Fig. 7. The average end-to-end data transmission delay remained below 10 ms even when the data transmission rate was below 1 Mb/s. Probably, some packets were lost or corrupted and thus retransmitted by the ARQ (Automatic Repeat Request) mechanism of the HomePlug. It increased maximum delays to 30-50 ms. However, the minimum delay was still 2 ms in all tested data transmission links.

The main factors that affect the data transmission rate are presented in Table I. The cable length and the du/dt filter are the most significant. The data transmission direction and signal coupling has also effect on the data transmission rate. All factors presented in Table I affect the SNR (Signal-to-Noise Ratio). Finally, the achieved data transmission rate depends on the SNR at the receiver.
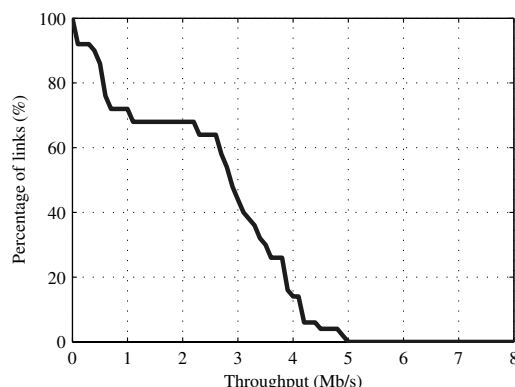


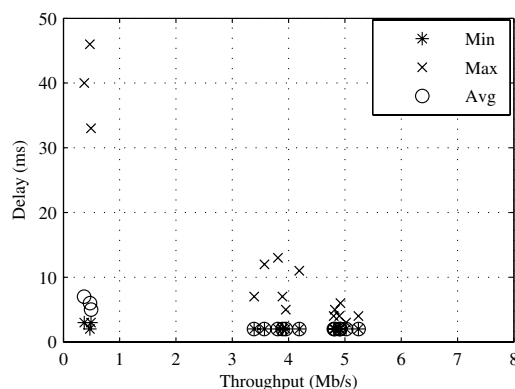Fig. 6. Percentage of links vs. throughput. The number of tested links was 50.



Fig. 7. Minimum, maximum and average delay vs. throughput. The number of links in the tests was 15. The measurements were carried out with a ping software. In each tested link, the number of messages was 100 and data packet size was 32 bytes.

TABLE I
THE DEPENDENCY OF DATA TRANSMISSION RATE ON THE TEST ENVIRONMENT CHARACTERISTICS

| Parameter | Effect | Comments |
|---|---|---|
| Cable length | +++ | Increasing cable length decreases data transmission rate with long cables (~200 m) |
| Du/dt filter / no filter | +++ | Filter decreases noise power and increases impedance level. The data transmission rate with output filter is higher than without filter. |
| Data transmission direction | ++ | Data transmission rate from the inverter to the motor is greater than to the opposite direction |
| Signal coupling | + | Phase-to-phase coupling gives higher data transmission rate than phase-to-protective earth coupling |
| Cable grounding | no effect | The grounding of motor at both ends did not affect data transmission rate |

## VI. CONCLUSIONS

The condition monitoring of electric motors requires communication between a motor and an inverter or a motor controller. The power line communication is an alternative for this purpose. In this article the PLC based method for motor cable communications was proposed and described. The method allows one to use the motor feeder cable in data transmission between the motor and the inverter. Laboratory measurements with the method were carried out and the results were analyzed. According to the tests, the method is promising, at least, to be used in the data transfer required by electric motor condition monitoring. However, more research work is still required.

## ACKNOWLEDGMENT

## REFERENCES

[1] T. Lindh, On the Condition Monitoring of Induction Machines, Doctoral Dissertation, Lappeenranta University of Technology, Finland, 2003, ISBN 951-764-841-3.

[2] Shaotang Chen, Erkuan Zhong, Thomas A. Lipo, "A New Approach to Motor Condition Monitoring in Induction Motor Drives", in the IEEE Transactions on Industry Applications, vol. 30, no. 4, July / August 1994.

[3] J. Ahola, Applicability of Power-line Communications to Data Transfer of On-line Condition Monitoring of Electrical Drives, Doctoral Dissertation, Lappeenranta University of Technology, Finland, 2003, ISBN 951-764-783-2.

[4] J. Ahola, J. Toukonen, A. Kosonen, T. Lindh, and V. Särkimäki, "Electric Motor Cable Communication Overcomes the Biggest Obstacle in On-line Condition Monitoring", in the Proceedings of Condition Monitoring 2005 Conference, 18th - 21st July, 2005, King's College, Cambridge, U.K.

[5] J. Ahola, J. Toukonen, A. Kosonen, T. Lindh, and R. Tiainen, "Ethernet to Electric Motor – via Mains Cable", in the Proceedings of COMADEM 2005, Cranfield, 31.8-2.9, 2005, U.K.

[6] Eric Wade, Harry Asada, "One-Wire Smart Motors Communicating over the DC Power Bus-Line with Application to Endless Rotary Joints", in the Proceedings of the 2002 IEEE International Conference on Robotics & Automation, May 2002, Washington DC, USA.

[7] D. Schlegel, G. Wrate, R. Kerkman, G. Skiblinski, "Resonant Tank Motor Model for Voltage Reflection Simulations with PWM Drives", in the Proceedings of the IEEE International Electrical Machines and Drives Conference, May 1999, Seattle, USA, pp. 463-465.

[8] S. Evon, D. Kempkes, L. Saunders, G. Skiblinski, "Riding the Reflected Wave – IGBT Drive Technology Demands New Motor and Cable Consideration", in the Proceedings IEEE PCIC, September 1996, pp. 75-84.

[9] R. J. Kerkman, D. Leggate, G. L. Skibinski, "Interaction of Drive Modulation and Cable Parameters on AC Motor Transients", IEEE Trans. on Ind. Appl., vol 3., no 3, May/June 1997, pp. 722-731.

[10] E. Zhong, T. A. Lipo, S. Rossiter, "Transient Modeling and Analysis of Motor Terminal Voltage on PWM Inverter-Fed AC Motor Drives", Record of the 33rd Annual IEEE Industry Applications Conference, vol. 1, St. Louis, USA, 12-15 Oct. 1998, pp. 773-780.

[11] H. Philipps, "Modeling of Powerline Communication Channels" in the Proceedings of 3rd International Symposium on Power-Line Communications and its Applications, Lancaster, UK, 1999, pp. 14-21.

[12] M. Zimmermann and K. Dostert, "A Multipath Model for the Power Line Channel", in the IEEE Transactions on Communications, vol. 50, no. 4, April 2002, pp. 553-559.

[13] T. Banwell, S. Galli, "A New Approach to the Modeling of the Transfer Function of the Power Line Channel, ISPLC 2002, Athens, Greece, March 27-29th , 2002.

[14] T. Esmailian, F. Kschischang, P. Gulak, "An In-building Power Line Channel Simulator, ISPLC 2002, Athens, Greece, March 27-29th, 2002.

[15] M. Götz, M. Rapp, K. Dostert, "Power Line Channel Characteristics and Their Effect on Communication System Design", in the IEEE Communications Magazine, April 2004.

[16] M. Zimmermann and K. Dostert, "Analysis and Modeling of Impulsive Noise in Broadband Power Line Communications", in the IEEE Transactions of Electromagnetic Compatibility, vol. 44, no. 1, February 2002, pp. 249-258.

[17] E. Bartolucci, B. Finke, "Cable Design for PWM Variable Speed AC Drives, in the IEEE Transactions on Industry Applications, vol. 37, no. 2, March/April 2001.

[18] M. Lee, R. Newman, H. Latchman, S. Katar, and L. Yonge, "HomePlug 1.0 power line communication LANs-protocol description and performance results, in the International Journal of Communication Systems, no. 16, 2003.

[19] R. Tiainen, V. Särkimäki, T. Lindh, and J. Ahola, "Estimation of the Data Transfer Requirements of Vibration and Temperature Measurements in Induction Motor Condition Monitoring", in the Proceedings of European Conference on Power Electronics and Applications, 12-15.9.2005, Dresden, Germany.

# Publication III

A. KOSONEN, J. AHOLA, AND M. JOKINEN

**Modelling the RF Signal Propagation in the Motor Feeder Cable**

# Modelling the RF Signal Propagation in the Motor Feeder Cable

A. Kosonen, J. Ahola, and M. Jokinen

Department of Electrical Engineering
Lappeenranta University of Technology
P.O. Box 20, 53851 Lappeenranta
FINLAND

Antti Kosonen; tel: +358 5 621 6765; fax: +358 5 621 6799; email: antti.kosonen@lut.fi

*Abstract*— **The motivation for this work was the possibility of utilizing the motor feeder cable as a communication channel in the inverter driven electrical drives. The simulation of the data transmission and electromagnetic interference in the motor cable claims a model. The newest power line transmission methods utilize the frequency band up to 30 MHz. In this article, modelling RF (Radio Frequency) signal propagation in the motor feeder cable is discussed. The RF signal propagation is modelled in the inverter driven electrical drives. The simulation is concerned the frequency band 100 kHz – 30 MHz. The effect of each component is taken into account with a model or a measurement. The simulation model takes into consideration the frequency depending damping of the channel and the effect of the coupling interfaces and impedance mismatching. The laboratory experiments are carried out for proving the applicability of the proposed method. The channel model is a tool in developing the coupling interfaces to the power line modems. It also helps to estimate the data transfer rates and limitation in the motor cable.**

*Index Terms*— **electrical drive, data transmission, simulation model, motor feeder cable**

## I. Introduction

NOWADAYS, it is very general to use the low voltage power line for the data transmission. This means that the same cables are used for the data transmission as well as for the power transmission. The newest power line data transmission methods, such as OFDM (Orthogonal Frequency Division Multiplexing) with FEC (Forward Error Control), have made a reliable broadband communication over the power lines possible. These methods utilize frequency band up to 30 MHz for the data transmission.

The power line channel can be thought as a multi path communication channel [1]. The impedance mismatching and branching cause this effect. The signal can propagate through many different routes to the end point. An electrical drive can also be thought in the same way. Power line channel models are required for the simulation of power line communication.

The channel model consists of the part that describes the signal attenuation including the multi path propagation and the part that describes the noise at the receiver.

Modelling the high frequency characteristics of low voltage industrial distribution network has been concerned in [2]. Statistical channel models for normal low voltage power line have been presented in [3]. They are based on the measurements from typical European three-phase underground distribution grids using PVC (Polyvinyl Chloride) isolated cables [3].

Modelling RF signal propagation in electrical drives in the motor feeder cable is presented in this article. The structure of this article is following. The test environment is described in section II. A simulation model is formed in section III and the simulation results are verified with laboratory measurements in section IV. The summary of modelling is presented in conclusion section.

## II. Test Environment

A test environment was constructed for the communication channel amplitude response measurements in the power electronics laboratory at Lappeenranta University of Technology. The test environment is illustrated in Fig. 1. In order to form a simulation model the effect of a motor,
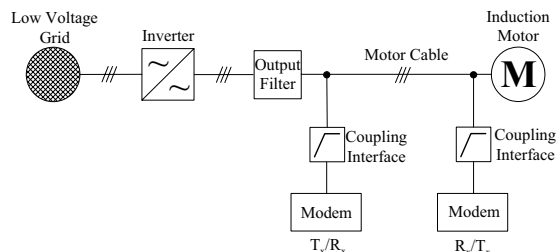


Fig. 1. The test environment. Both modems can be used as a transmitter or a receiver. The length of the communication channel depends on the length of the motor cable.

coupling interfaces, a motor cable, an output filter, and an inverter should be taken into account. Three-phase system is used in all test environments. The motor cables used in tests have four wires and are the type of MCCMK. The simulation is based on two-port modelling. This is not a problem according to [4] because mostly shielded and symmetrical low voltage power cables are installed as low voltage motor cables nowadays. The theoretical justification of applying two-port modelling of transmission lines in the case of symmetric cables is presented in [5].

If an output filter, such as a du/dt filter, is connected to an inverter, the impedance of the inverter can be ignored from the simulations. In the frequency band 100 kHz – 30 MHz the output filter can be considered to be a serially connected high impedance load. If there is no output filter connected then the inverter input impedance should be taken into account. This is quite problematic, because in an active mode the inverter input impedance depends on the switching state of the output stage semiconductors.

### III. SIMULATION MODEL

The purposes of modelling are the simulation of data transmission and electromagnetic interference. It also helps on developing the coupling interfaces and on finding the boundary terms of data transmission, for example, where the data transmission works and where does not. The model can also be utilized in researching power line communication, electromagnetic interference and cable oscillations. The simulation model should take into consideration the frequency depending damping of the channel and the effect of the coupling interfaces and impedance mismatching. There are several methods that can be used to model the power line communication channel. According to [4], only two of them are mostly used. The first one applies the methods used for the modelling of radio channels. These are presented e.g. in [6] and [7]. The second one applies the methods used to model electricity distribution networks. These are presented e.g. in [8] and [9]. In this article, the latter method was chosen, because the topology of the test environment is known and most of the high frequency characteristics of the individual network components were modelled and measured earlier in [4].

In the proposed method the transmission or chain parameter matrices are used for modelling the transfer function of a communication channel. The analysis is applicable for TEM (Transverse Electromagnetic) waves. TEM wave has only transversal electric and magnetic fields, and longitudinal fields do not exist. Because of the resistive losses there is also a small longitudinal electric field component in a motor cable. However, this does not prevent applying the analysis for the modelling of a communication channel. The relation between input voltage and current, and output voltage and current can be described as follows

$$\begin{bmatrix} \mathbf{V}_1 \\ \mathbf{I}_1 \end{bmatrix} = \begin{bmatrix} \mathbf{A} & \mathbf{B} \\ \mathbf{C} & \mathbf{D} \end{bmatrix} \begin{bmatrix} \mathbf{V}_2 \\ \mathbf{I}_2 \end{bmatrix}, \tag{1}$$

where $\mathbf{A}$, $\mathbf{B}$, $\mathbf{C}$ and $\mathbf{D}$ are frequency dependent coefficient matrices. Equation (1) can also be illustrated in Fig. 2.

The frequency dependent input impedance of the two-port network can be described as follows

$$\mathbf{Z}_{in} = \frac{\mathbf{A}\mathbf{Z}_L + \mathbf{B}}{\mathbf{C}\mathbf{Z}_L + \mathbf{D}}. \tag{2}$$

For the transfer function of the channel can be written as follows

$$\mathbf{H} = \frac{\mathbf{V}_2}{\mathbf{V}_S} = \frac{\mathbf{Z}_L}{\mathbf{A}\mathbf{Z}_L + \mathbf{B} + \mathbf{C}\mathbf{Z}_L\mathbf{Z}_S + \mathbf{D}\mathbf{Z}_S}. \tag{3}$$

The coefficients of the transmission matrix are dependent on the type of a load impedance. The transmission matrix of the cable of the communication channel can be written

$$\begin{bmatrix} \mathbf{A} & \mathbf{B} \\ \mathbf{C} & \mathbf{D} \end{bmatrix} = \begin{bmatrix} \cosh(\gamma L) & \mathbf{Z}_0 \sinh(\gamma L) \\ \dfrac{1}{\mathbf{Z}_0} \sinh(\gamma L) & \cosh(\gamma L) \end{bmatrix}, \tag{4}$$

where $L$ is the length of the cable and $\boldsymbol{\gamma}$ is propagation constant, which can be calculated according to (5)

$$\boldsymbol{\gamma} = \sqrt{(r + j\omega l)(g + j\omega c)} = \alpha + j\beta, \tag{5}$$

where $c$ is a distributed capacitance, $g$ is a distributed conductance, $l$ is a distributed inductance, and $r$ is a distributed resistance. $\alpha$ is an attenuation coefficient and $\beta$ is a propagation coefficient.

The transmission matrix for serially connected impedance $\mathbf{Z}_S$ can be calculated as follows

$$\begin{bmatrix} \mathbf{A} & \mathbf{B} \\ \mathbf{C} & \mathbf{D} \end{bmatrix} = \begin{bmatrix} 1 & \mathbf{Z}_S \\ 0 & 1 \end{bmatrix}, \tag{6}$$
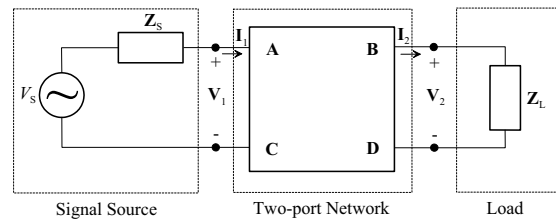


Fig. 2. Two-port network connected to a signal source and a load impedance. The signal source consists of a voltage source and a serially connected internal impedance.
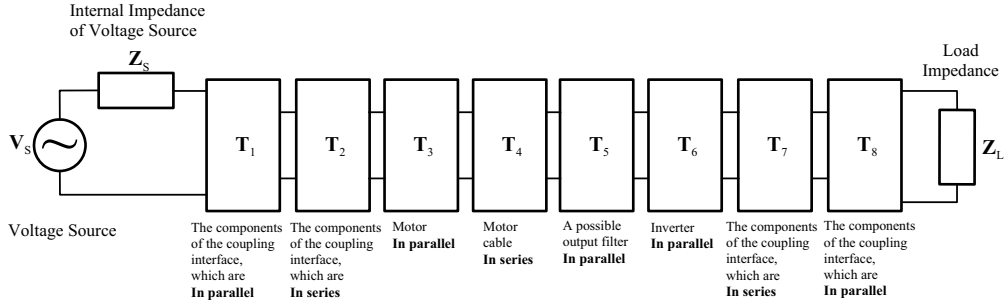
Fig. 3. The transmission matrix based on the channel model for the test environment. The model describes the communication channel illustrated in Fig. 1, when the transmitter is in the motor side and the receiver is in the inverter side.

and for parallel connected impedance $\mathbf{Z}_P$ can be written as follows

$$\begin{bmatrix} \mathbf{A} & \mathbf{B} \\ \mathbf{C} & \mathbf{D} \end{bmatrix} = \begin{bmatrix} 1 & 0 \\ 1/\mathbf{Z}_P & 1 \end{bmatrix}. \tag{7}$$

The communication channel from a source to a load may consist of several network sections that have different cabling and loads. Each section has to be described as its own transmission matrix. These sections are serially connected with each others. The transmission matrix $\mathbf{T}$ from a source to a load can be described by chain rule

$$\mathbf{T} = \prod_{i=1}^{n} \mathbf{T}_i, \tag{8}$$

where $n$ is the number of network sections. The channel model from the motor side to the inverter side for the test environment (Fig. 1) by using the transmission matrix (8) is illustrated in Fig. 3.

The components in the simulation model are based on modelling or measurements. All the components can be connected to each other by applying the chain rule because the sections are serially connected [4]. It is important to notice that both serial and parallel parts should be considered separately.

## IV. LABORATORY MEASUREMENTS

The voltage amplification for the frequency band 100 kHz – 30 MHz was measured for different test environments. Frequency stepping size of 100 kHz was used for the frequency band 100 kHz – 3 MHz and 200 kHz for the frequency band 3 – 30 MHz. A motor, cable length, an output filter, and an inverter were varied during the measurements. The measurements were carried out by supplying signal with the signal generator. The peak-to-peak voltages were measured from both ends with the oscilloscopes. Signal couplings (L1, PE) and (L1, L2, PE) were used in the measurements. The measurements were carried out with the

designed power line coupling interfaces and without them. The measurements were also carried out from the motor to the inverter and vice versa. The measurement arrangement is illustrated in Fig. 4.

The voltage was measured over the 10 kΩ load resistance. The magnitude of the load resistance affects on the amplification of the communication channel. In this article, the 10 kΩ load resistance was used in voltage measurements, because also the power line modems receive the signal over this same load. The magnitude of voltage amplification depends completely on the way of the measurement principle and the coupling interfaces. This should always be taken into account when the results are analyzed. The way of voltage measurement is illustrated in Fig. 5.
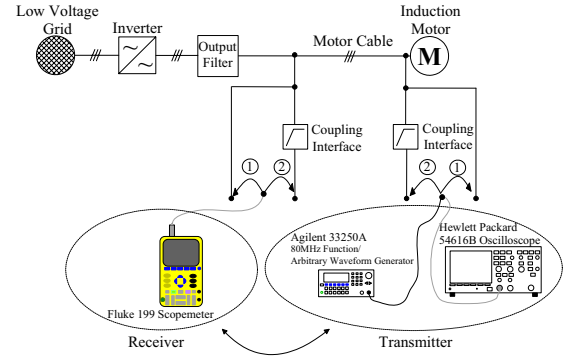


Fig. 4. The measurement arrangement. The voltage amplification was measured both with the coupling interfaces and without them, and in addition from the motor side to the inverter side and vice versa.
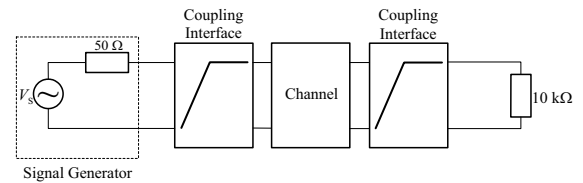


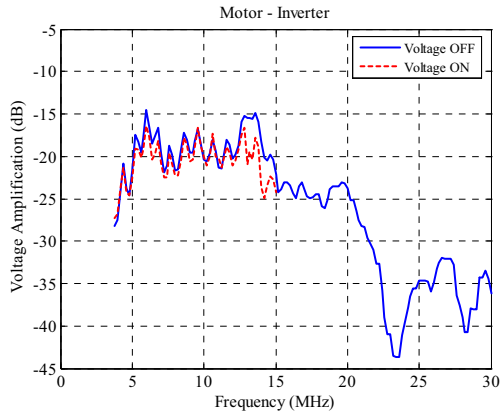Fig. 5. The method used in the measurements of voltage amplification.

Fig. 6. The voltage amplification of the communication channel from the motor to the inverter with the mains voltage switched on and off. The measurements with the mains voltage were carried out only up to 15 MHz due to the limitations of signal generator.
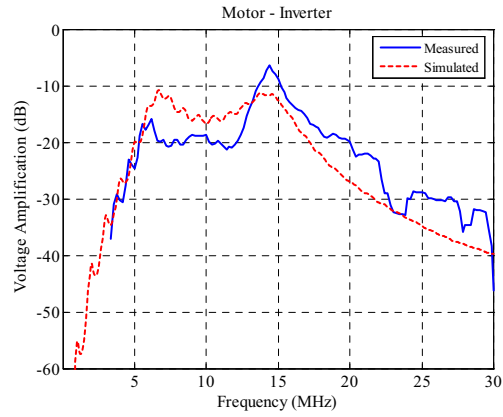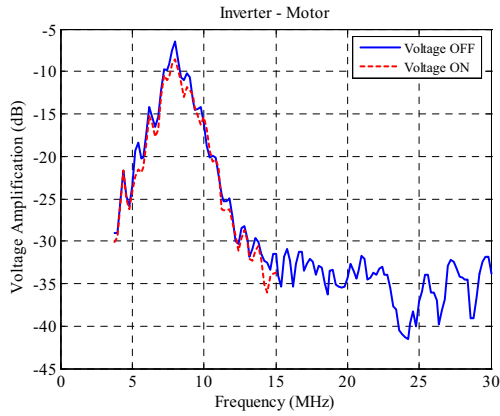


Fig. 8. Measured and simulated voltage amplification from the motor to the inverter. There were used an inverter ACS400, an output filter, a motor Invensys T-01F160L4/01 (15 kW), a motor cable Pirelli MCCMK 3x35+16 (90 m), and coupling (L3, PE) as a test equipment.



Fig. 7. The voltage amplification of the communication channel from the inverter to the motor with the mains voltage switched on and off. The measurements with the mains voltage were carried out only up to 15 MHz due to the limitations of signal generator.
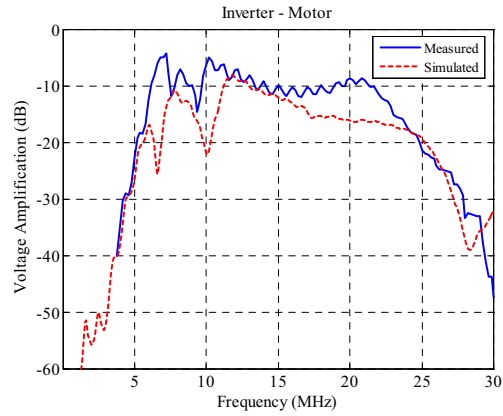


Fig. 9. Measured and simulated voltage amplification from the inverter to the motor. There were used an inverter Vacon, an output filter, a motor ABB M3BP315MLA4B3 (200 kW), a motor cable Pirelli MCCMK 3x35+16 (90 m), and coupling (L1, L2, PE) as a test equipment.

### A. The Effect of Mains Voltage to the Voltage Measurement Principles

All the voltage amplification measurements were carried out without the mains voltage. This is based on the assumption that the mains voltage does not affect the measurement results in this case. In order to verify the assumption, some of measurements were performed with the mains voltage switched on. The results are illustrated in Figs. 6 and 7. The test environment setup was: an inverter ABB ACS400, an output filter, a motor Invensys T-01F160L4/01 (15 kW), a motor cable Pirelli MCCMK 3x35+16 (90 m), and developed coupling interfaces (L1, L2, PE). The measurements with the mains voltage were carried out only up to 15 MHz due to the limitations of signal generator. Otherwise the measurements were carried out for the

frequency band 3.8 – 30 MHz. According to Figs. 6 and 7, there is no significant difference between amplification measurements with the mains voltage switched on or off. The result is logical, because the signal frequencies do not participate to yielding on mechanical power in the motor.

### B. The Comparison of Simulation and Measurement Results

A simulation model was built for the test environment. Simulated voltage amplification results were compared to the measured ones. Two comparisons are illustrated in Figs. 8 and 9. The measurements are for the frequency band 3.8 – 30 MHz (resolution 200 kHz) and simulations are for the frequency band 100 kHz – 30 MHz (resolution 74.750 kHz). According to Figs. 8 and 9, visible correlation can be seen between the simulations and the measurements. The success of simulation depends on the accuracy of the components

models. Generally, they are more or less simplified.

The channel causes signal attenuation that is frequency dependent. The biggest reason for attenuation is the coupling interfaces. The biggest loss is the insertion loss that happens when a transmitter injects the signal to the motor cable, which impedance is generally quite low compared to the impedance of the coupling interface of the transmitter. The coupling interface was developed to filter the noise generated by an inverter. According to [1] and [10], the insulation material (PVC) of the motor cable causes mainly dielectric losses in the simulated frequency band 100 kHz – 30 MHz. According to (4) and (5), losses depend mainly on the frequency, the length of the motor cable, and the characteristic impedance of the cable. In addition, multi path signal propagation, that is caused by impedance mismatching, cause notches and peaks to the frequency response of the channel. The loads can be considered as termination impedances [2]. A motor, an output filter, and a coupling interface act as loads in the viewpoint of communication signal in used test environment. These impedances are frequency dependent because they include inductive and capacitive components.

## V. CONCLUSION

The simulation of RF signal propagation in the motor feeder cable needs a channel model. In this article the method for modelling the RF signal propagation in the motor feeder cable in the inverter driven electrical drives was proposed and simulated. Each component was taken into account with a model or a measurement. The simulation was carried out for the frequency band 100 kHz – 30 MHz, because the current power line data transmission methods utilize frequency band up to 30 MHz. The applicability of the modelling method was ensured in the laboratory environment by measuring the voltage amplification of different communication channels. The measurements were carried out without any mains voltage switched on. But it was showed in this article that it has no effect on the measurements, at least, there is used an output filter on the inverter output stage. The simulated and measured voltage amplifications correlated with each other. These results ensured that the method is applicable for modelling the RF signal propagation in the inverter driven motor feeder cable.

## REFERENCES

[1] Klaus Dostert, *Power Line Communications*, Prentice-Hall International 2001, Inc.: Upper Saddle River, NJ 07458. ISBN 0-13-029342-3

[2] J. Ahola, T. Lindh, V. Särkimäki and R. Tiainen, "Modeling the High Frequency Characteristics of Industrial Low Voltage Distribution Network," in *Proceedings of Nordic Workshop on Power and Industrial Electronics*, NORPIE, Trondheim Norway 14th – 16th June 2004.

[3] Matthias Götz, Manuel Rapp and Klaus Dostert, "Power Line Channel Characteristics and Their Effect on Communication System Design," *IEEE Communications Magazine*, Vol. 42, No. 4, April 2004.

[4] Jero Ahola, *Applicability of Power-Line Communications to Data Transfer of On-Line Condition Monitoring of Electrical Drives*, Dissertation, Lappeenranta University of Technology, 2003. ISBN 951-764-783-2

[5] Ioannis C. Papaleonidopoulos, Constantinos G. Karagiannopoulos, Nickolas J. Theodorou and Christos N. Capsalis, "Theoretical Transmission-Line Study of Symmetrical Indoor Triple-Pole Cables for Single-Phase HF Signalling," *IEEE Transactions on Power Delivery*, Vol. 20, No. 2, April 2005.

[6] Manfred Zimmermann and Klaus Dostert, "A Multi-Path Signal Propagation Model for the Power Line Channel in the High Frequency Range," in *Proceedings of the 3rd International Symposium on Power-Line Communications and It's Applications*, ISPLC 1999, Lancaster UK 30th May – 1st June 1999, pp. 45-51.

[7] Holger Phillips, "Modelling of Power-line Communication Channels," in *Proceedings of the 3rd International Symposium on Power-Line Communications and It's Applications*, ISPLC 1999, Lancaster UK 30th May – 1st June 1999, pp. 14-21.

[8] T. C. Banwell and S. Galli, "A New Approach to the Modelling of the Transfer Function of The Power Line Channel," in *Proceedings of the 5th International Symposium on Power-Line Communications and It's Applications*, ISPLC 2001, Lund University, Malmö, Sweden, 4th – 6th April 2001, pp. 319-324.

[9] T. Esmailian, F. R. Kschischang and P. G. Gulak, "An In-building Power Line Channel Simulator," in *Proceedings of the 6th International Symposium on Power-Line Communications and It's Applications*, ISPLC 2002, Athens, Greece, 27th – 29th March 2002.

[10] Jero Ahola, Tuomo Lindh and Jarmo Partanen, "Determination of Properties of Low Voltage Power Cables at Frequency Band 100 kHz – 30 MHz," in *Proceedings of the International Conference on Electrical Machines,* ICEM 2002, Bruges, Belgium, 26th – 28th August 2002.

# Publication IV

A. KOSONEN, M. JOKINEN, J. AHOLA, AND M. NIEMELÄ

**Real-Time Induction Motor Speed Control with a Feedback Utilizing Power Line Communications and Motor Feeder Cable in Data Transmission**

# Real-Time Induction Motor Speed Control with a Feedback Utilizing Power Line Communications and a Motor Feeder Cable in Data Transmission

Antti Kosonen, Markku Jokinen, Jero Ahola, and Markku Niemelä
Department of Electrical Engineering
Lappeenranta University of Technology
P.O. Box 20, 53851 Lappeenranta
FINLAND
*antti.kosonen@lut.fi*

*Abstract –* **In a motor speed control, a feedback loop is used to transfer the measured motor rotational speed information to the controller. The implementation of the feedback loop requires cabling between the motor and the frequency converter both for signalling and powering. However, the motor feeder cable could be used as a medium for data transmission. A feedback loop that utilizes a motor cable as a communication channel is researched in this article. The method is applied in this application for the first time. The data transmission utilizes a standardized PLC (Power Line Communications) method that forms an Ethernet connection over the motor feeder cable. The applied method generates an additional latency to the feedback loop and hence, sets some limits to the performance of a speed controller. In this article, the performance of the method is researched and analyzed with simulations and laboratory experiments.**

## I. INTRODUCTION

In electrical drives, motor rotational speed and the rotor angle are typical measurement values that are used as a feedback information to a controller. The vector control methods, such as, DTC (Direct Torque Control) [1] do not necessarily require rotational speed signal as a feedback information from a motor. However, in demanding control applications, especially, at low rotational speeds, these control methods also require measured rotor speed or angle as a feedback information. The main problem in the sensorless induction motor control methods is the error of static rotational speed. This problem is caused by errors in the motor model parameters of the speed estimator.

Generally, the sensorless control methods are based on various control algorithms that eliminate the need of the speed sensor. The articles that introduce these algorithms are collected extensively in [2]. According to [3], sensorless vector control methods are mainly based on speed estimation methods, such as, slip calculation, model reference adaptive system (MRAS), and etc. The MRAS method is proposed in [4]. In the DTC method, a motor model is used to reform the errors of a voltage model and to prevent the voltage model to drift from the origin.

The feedback loop generally requires a wired connection from the motor to the controller. In practice, this means some extra cabling. It is also possible to use the same cables for data transmission and for supplying power to the motor. According to [5], the main application of PLC (Power Line Communications) between the motor and the frequency converter is the need of on-line condition monitoring. However, it is also possible to use the same data transmission channel for transferring the feedback information to the controller.

According to [6], the data transmission requirements of the motor control are generally stricter than those of the motor diagnostics due to latency requirements.

There are only a few previously presented control applications related to the feedback signal transmission via power cables. Articles [7] and [8] concentrate on the servo systems and the DC bus line are utilized for data communications. According to [7], the noise level and signal attenuation are much lower in the DC bus line than in the traditional 50 Hz / 60 Hz mains network. According to [9], the motor cable is much more hazardous environment than the traditional AC mains network in the viewpoint of power line communications, because the frequency converter output voltage basically consists of pulses or square waves with variable frequency and duration. The mains network is also supplied by a transformer or a generator, while the output of a PWM (Pulse Width Modulation) inverter-fed power line is supplied by transistors or switching components, which results in different impedance characteristics [9]. The characteristics of the motor cable as a communication channel are also presented in [10]. The article [11] was earlier concerned with the method introduced herein, but this article analyzes its performance.

The structure of this article is following. The PLC modems and the speed controller tuning are described in section II. The applied performance tests are introduced in section III. In section IV, simulations of the latency effect on the control system performance are presented. The performance tests are included in section V. The test results are analyzed in section VI. The summary of the introduced speed control method in real-time application is formed in conclusion section.

## II. SPEED CONTROL SYSTEM

The control system and the necessary equipment are described detailed in [11]. The diagram of a test equipment is illustrated in Fig. 1. First, the dSPACE computes a 16-bit rotational speed information according to the received data given by the pulse encoder. Next, the speed information is sent to the motor cable. Then the feedback speed controller (the dSPACE equipment) gives a torque reference to the frequency converter according to the received feedback information from the motor cable.

### A. Ethernet in Control Applications

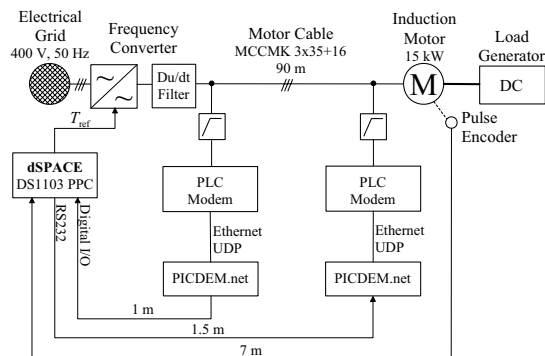The PLC method used in this application forms an

Fig. 1. The diagram of the laboratory test equipment that was constructed at the power electronics laboratory at Lappeenranta University of Technology.

Ethernet connection over the motor feeder cable. The PLC method encapsulates the Ethernet frames (IEEE 802.3) into its own protocol [12] and transmits these to the motor cable.

The latency of Ethernet is non-deterministic due to the CSMA/CD (Carrier Sense Multiple Access with Collision Detection) bus reservation mechanism. This can cause problems in real-time applications, which require deterministic response, such as, control applications. According to [13], in applications, which demand time delay less than 1 ms, Ethernet is not a practical solution. The utilization of Ethernet in industrial applications has been researched e.g. in [14] – [16].

The utilization of Ethernet in distributed motion control is researched in [17], where the rotor feedback speed information of a brushless DC-motor is delivered between the speed controller and the frequency converter by using a 10 Mb/s Ethernet LAN (Low Area Network) and frame size 64 bytes.

*B. The Utilized Power Line Communication Method*

The PLC modems used in this application are Ethernet based. In the viewpoint of Ethernet devices, the PLC modems are transparent. The PLC modems are based on the industrial HomePlug standard [18]. Two different HomePlug standard compliant PLC modems are used in the tests. The first one utilizes the HomePlug 1.0 standard, which was published at first. The second one utilizes newer HomePlug 1.0 with Turbo standard. The main difference between these two standards is that the latter one utilizes QAM (Quadrature Amplitude Modulation) 256/64/16 methods in data transmission [19]. This provides higher bandwidth with the newer standard modems than with the older ones that utilize DQPSK (Differential Quadrature Phase Shift Keying).

At the beginning, the latency of the feedback loop was researched with two different PLC modems. The extensive test results are presented in [11] for the newer modems. The main results are presented in Table I. The modulation methods of inverters have no direct influence on data transfer latencies in the motor feeder cable data transmission. The latency is shorter with the newer modems because they have probably quicker UDP (User Datagram Protocol) packets encapsula-

| HomePlug Standard | Sampling Time (ms) | Latency Avg. (ms) | Latency (ms) | Samples |
|---|---|---|---|---|
| HomePlug 1.0 with Turbo | 2 | 8.0 | 6.0 – 17.4 | 150000 |
| HomePlug 1.0 | 18 | 26.3 | 14.8 - 139 | 5050 |

tion than the older ones. Every UDP packet consists of a 16-bit rotational speed information. Hence, it is not possible to transmit quicker than it takes to encapsulate a UDP packet. The sampling time of the rotational speed $h_s$ was adjusted longer for the older HomePlug modems than for the new ones, which had sampling time of 2 ms. Sampling times were chosen as short as possible in both cases. The sampling time increases the latency about by half of its magnitude as mentioned in [11].

*C. Tuning the PI Speed Controller*

The PI (Integrator with a Proportional gain) speed controller had to be tuned individually in every test, because the latency depended on the configuration of the feedback loop. The speed controllers were tuned experimentally to fulfill the same requirements (the same magnitude of the output) in order that the results would be comparable with each other. The computation time $h_c$ for the controller was 2 ms in every test. $h_c$ is typically 0.5 – 1 ms in commercial solutions.

The 15 kW motor was driven at a constant speed reference of 200 rpm. Then it was supplied with an additional speed reference of 20 rpm as illustrated in Fig. 2. The controller was allowed 15 % overshooting from the transition step of the reference value and it was tuned as fast as possible. The PI speed controller parameters for different cases are showed in Table II. The note *Direct* in the column "Feedback Loop" means that the direct pulse sensor information is used as a feedback information for the controller. The notes *HP 1.0 with Turbo* and *HP 1.0* mean that the motor cable is used as a
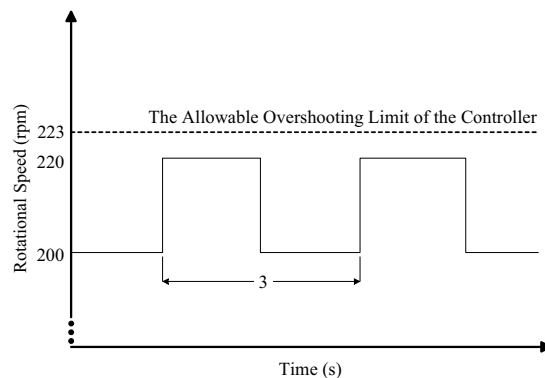


Fig. 2. The speed reference of the step response test for tuning the PI speed controller.

TABLE II
SELECTED PI SPEED CONTROLLER PARAMETERS ACCORDING TO
EXPERIMENTALLY TUNING

| Feedback Loop | Controller | $K_P$ | $K_I$ | Latency Avg. |
|---|---|---|---|---|
| Direct | dSPACE | 15.7 | 7.5 | 0 ms |
| HP 1.0 with Turbo | dSPACE | 11.0 | 3.0 | 8.0 ms |
| HP 1.0 | dSPACE | 4.8 | 0.6 | 26.3 ms |

feedback loop with HomePlug 1.0 with Turbo and HomePlug 1.0 PLC modems, respectively.

## III. PERFORMANCE TESTS

The performance of feedback loops was simulated and measured in tests. The tests were carried out by using the simulated (Table III) and experimentally tuned (Table II) parameters for feedback loop configurations. The applied tests were: a step response test, a ramp test and a loading test.

### A. Step Response Test

The results of the step response test ensure that the controllers are tuned to be comparable. This means that the maximum overshooting from the reference value should be identical.

### B. Ramp Test

One of the most important performance measurements in industrial process drives is tracking capability of the reference signal. Thereby, it is interesting to research the influence of the feedback latency on tracking capability of control. In the test, rotational speed of the motor was accelerated from the zero speed to the nominal speed of the induction motor (1455 rpm) in time of 0.8 s.

### C. Loading Test

The changes in the loading condition are very typical phenomena in the industrial process drives. The loading condition can change, for instance, linearly or step-visely. The step-vise change reveals the control's incompleteness or its weakness. The step-vise loading change is also used in these tests. The motor is driven at a constant speed of 750 rpm that is about half of its nominal value. In a random time instant a 58 % (of the motor nominal torque value) loading change is caused. This kind of change ensures that, for example, the current limit is not exceeded.

## IV. SIMULATION

A controlled system can be modelled based on a control diagram presentation as illustrated in Fig. 3, where $r$ is a reference signal, $y$ is an output signal, $d$ is a process disturbance, $\xi$ is the noise of a measurement, $e$ is an error signal
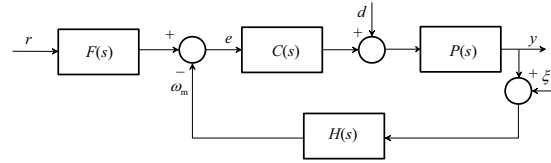


Fig. 3. The block diagram presentation that can illustrate a controlled process.

and $\omega_m$ is a measured rotational speed signal. The transfer functions $F(s)$, $C(s)$, $P(s)$, and $H(s)$ are for a pre-filter, a controller, a process, and a feedback loop, respectively.

If the process is a PI speed controlled motor and if current control is assumed to be ideal and the rotational speed information is transmitted via the motor cable from the motor to the frequency converter, the next few equations can be formed. Because the PI speed controller does not use pre-filtering, the transfer function of the pre-filter $F(s) = 1$. The motor can be modelled according to its mass of inertia

$$P(s) = \frac{K_T}{Js}, \tag{1}$$

where $K_T$ is the gain of torque (Nm/A) and $J$ is the mass of inertia of the motor (kgm$^2$). The transfer function of the PI speed controller can be described as follows

$$C(s) = K_P\left(1 + \frac{K_I}{s}\right), \tag{2}$$

where $K_P$ is the proportional gain of the controller, and $K_I$ is the gain of the integrator, which has also inverse proportionate to the integration time of the controller.

Parameters of the speed controller, the bandwidth of the system and the integrated absolute error (IAE) for the speed measurement in the case of the load disturbance with different feedback latencies are collected in Table III. The latencies are chosen based on the measured ones. Integrated absolute errors were calculated according to [20]

$$IAE = \int_0^\infty |e(t)| dt, \tag{3}$$

where $e(t)$ is the error between the measured speed and the reference value. The time range, which was used to calculate

TABLE III
SIMULATED PI SPEED CONTROLLER PARAMETERS, BANDWIDTH AND IAE
FOR DIFFERENT LATENCIES IN THE FEEDBACK LOOP

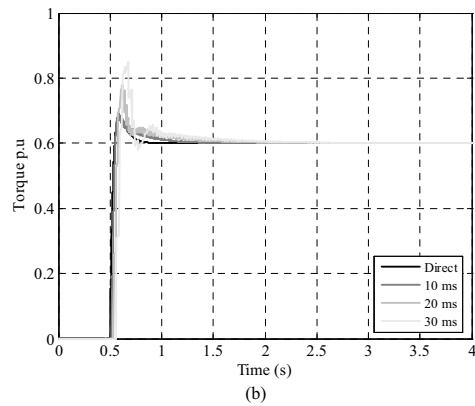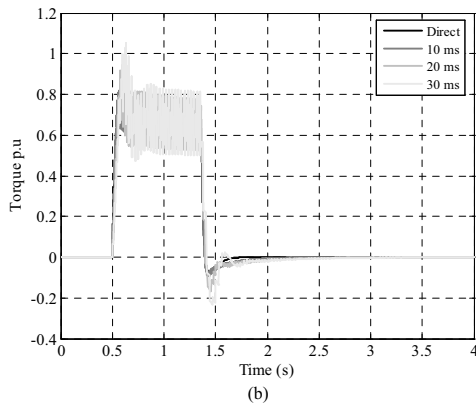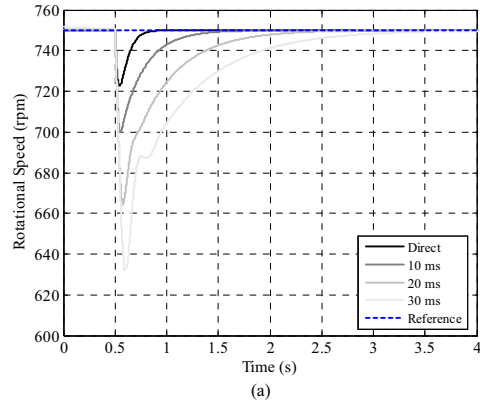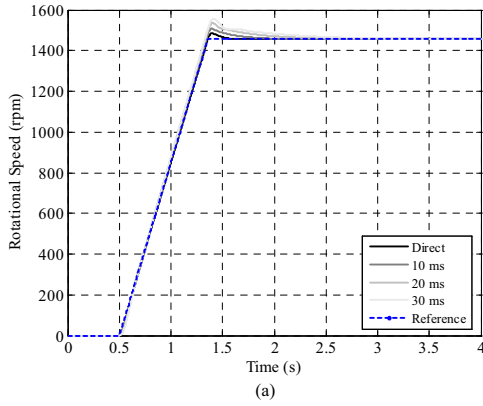| Latency Avg. | $K_P$ | $K_I$ | Bandwidth | IAE |
|---|---|---|---|---|
| 0 ms | 15.7 | 10.0 | 57 rad/s | 8.2 |
| 10 ms | 11.0 | 3.8 | 69 rad/s | 28.0 |
| 20 ms | 7.5 | 2.2 | 51 rad/s | 60.6 |
| 30 ms | 6.0 | 1.5 | 40 rad/s | 99.2 |

Fig. 4. The simulated ramp test. (a) The behaviour of rotational speed as a function of time. (b) The torque reference given by the controller during the test.

Fig. 5. The simulated loading test. (a) The behaviour of rotational speed as a function of time. (b) The torque reference given by the controller during the test.

the value of IAE was from zero to four second and the used sampling time of the speed measurement was 100 μs.

The bandwidth of the system was evaluated with a simulation model. The frequency of the speed reference signal was increased to the value until the amplitude of the measured speed was decreased 3 dB compared to the amplitude of the reference speed.

The simulated ramp test results are illustrated in Figs. 4 (a) and (b).

The simulated loading test results are illustrated in Figs. 5 (a) and (b).

## V. MEASUREMENTS

The simulated results were verified with measurements. Similar tests as introduced in section III were performed for configurations introduced in Table II. The laboratory equipment was similar to one illustrated in Fig. 1.

The step response results retrieved from tests are illustrated in Figs. 6 (a) and (b).

The ramp results retrieved from tests are illustrated in Figs.

7 (a) and (b).

The loading results retrieved from tests are illustrated in Figs. 8 (a) and (b).

## VI. ANALYSIS OF TEST RESULTS

There is visible correlation between simulation and measurement results. The small differences come from the fact that the measurement noise of the speed signal or the friction disturbances was not taken into consideration in the simulation model. Hence, the simulation results may create too optimistic image from the behaviour of the control system.

According to Figs. 4 – 8, the latency of the feedback loop deteriorates the performance of the control system. The mechanical time constant of a motor or a system should be essentially longer than the latency of the feedback loop ($\tau_M \gg \tau$). The bandwidth of the system was not completely clear because in this case, 10 ms delay in the feedback loop improved the reached bandwidth of the control system. However, the bandwidth of a system depends mainly on the parameters of a controller, the latency of a feedback loop, and
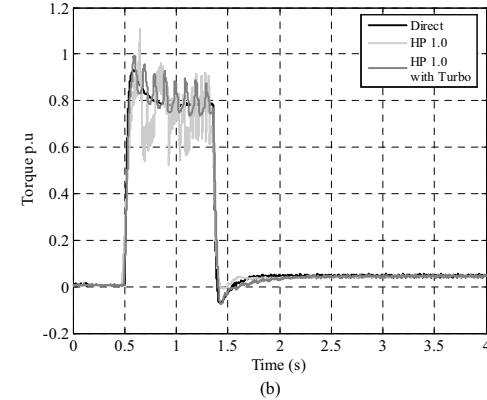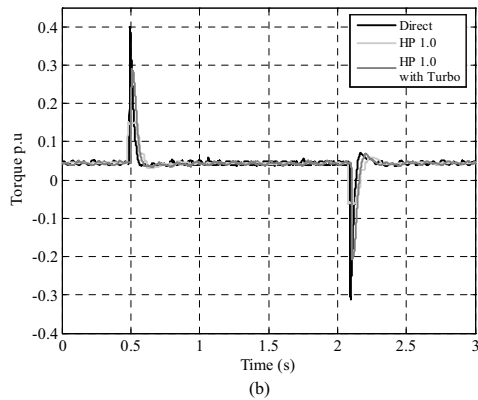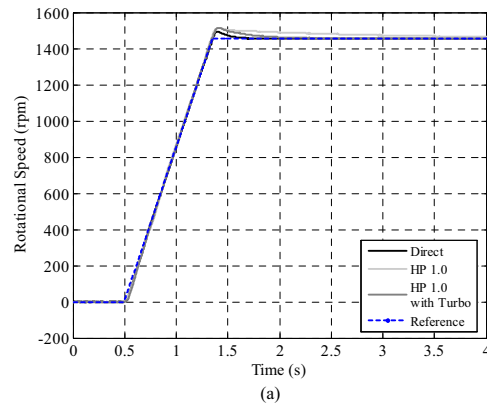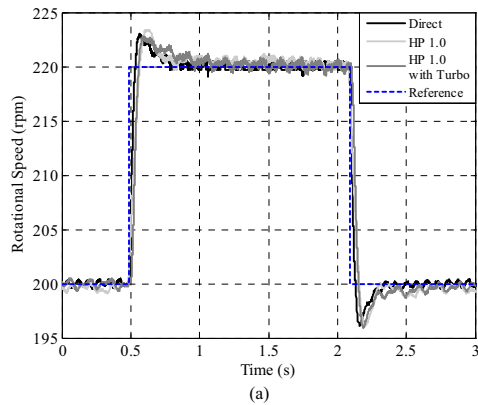
Fig. 6. The step response test. (a) The behaviour of rotational speed as a function of time. (b) The torque reference given by the controller during the test.



Fig. 7. The ramp test. (a) The behaviour of rotational speed as a function of time. (b) The torque reference given by the controller during the test.

the mechanical time constant of a system.

As the results display, the latency of the feedback signal increases the value of IAE significantly compared to the case where no latency occurs. Hence, the latency of the feedback signal can be problematic in processes where dynamic load regulation performance is demanded. However, the feedback loop implemented with HomePlug 1.0 with Turbo standard modems has only slightly differences in its performance compared to the direct feedback implementation. The result is very promising because only a conventional PI controller is used in every configuration. The performance is possible to improve with different control strategies.

According to the ramp tests, the torque reference signal tries to oscillate during the acceleration with the feedback loops that include latency. However, this could be prevented, in future, with some kind of delay compensator in the control system.

## VII. CONCLUSION

The speed control method with a feedback utilizing power line communications in motor cable data transmission for transmitting feedback information was applied for the first time in this article. The modems used in PLC encapsulate the Ethernet frames to their own protocol.

The performance of the method was tested with simulations and they were verified with the measurements. The tests pointed out that the latency in the feedback loop affects directly the selection of the parameters of a controller. The control system implemented with HomePlug 1.0 with Turbo standard modems was competitive compared to the normal direct feedback implementation. However, competitiveness of the method depends mainly on the mechanical time constant of a motor or a system.

Measurements proved that the motor feeder cable could be used as a speed feedback communication channel in the place of a pulse encoder cable. In future, comparisons with commercial products, like sensorless control methods, would be very interesting.
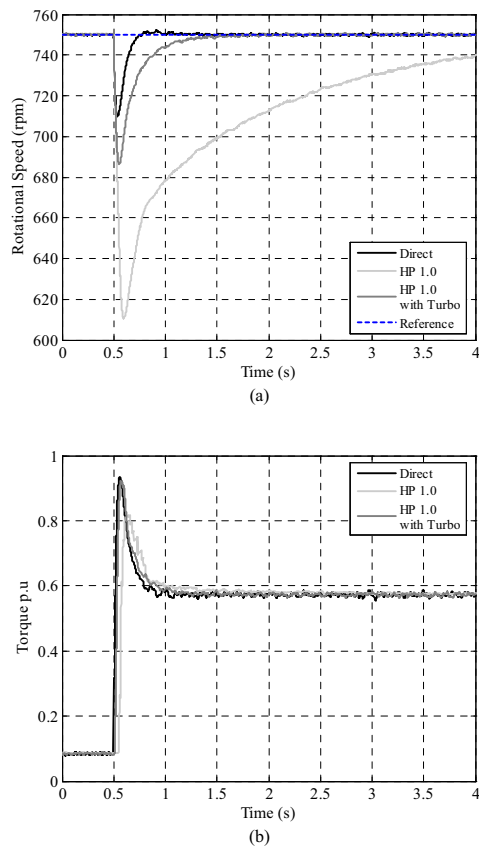
## VIII. ACKNOWLEDGMENT

Fig. 8. The loading test. (a) The behaviour of rotational speed as a function of time. (b) The torque reference given by the controller during the test. The load generator causes a static initial load.

## IX. REFERENCES

[l]   Isao Takahashi and Toshihiko Noguchi, "A New Quick-Response and High-Efficiency Control Strategy of an Induction Motor," *IEEE Transactions on Industry Applications*, vol. 22, no. 5, Sep./Oct. 1986, pp. 820-827.

[2]   Young Ahn Kwon, and Sung Hwan Kim, "A New Scheme for Speed-Sensorless Control of Induction Motor," *IEEE Transactions on Industrial Electronics*, vol. 51, no. 3, Jun. 2004, pp. 545-550.

[3]   Bimal K. Bose, *Modern Power Electronics and AC Drives*, Prentice Hall 2002, Inc., ISBN 0-13-016743-6

[4]   Colin Schauder, "Adaptive Speed Identification for Vector Control of Induction Motors without Rotational Transducers," *IEEE Transactions on Industry Applications*, vol. 28, no. 5, Sep./Oct. 1992, pp. 1054-1061.

[5]   J. Ahola, J. Toukonen, A. Kosonen, T. Lindh, and V. Särkimäki, "Electric Motor Cable Communication Overcomes the Biggest Obstacle in On-line Condition Monitoring," in *Proceedings of Condition Monitoring 2005 Conference (COMADIT)*, Cambridge, UK, Jul. 2005, pp. 105-110.

[6]   J. Ahola, J. Toukonen, A. Kosonen, T. Lindh and R. Tiainen, "Ethernet to Electric Motor – via Mains Cable," in *Proceed-

ings of the 18th International Congress and Exhibition on Condition Monitoring and Diagnostic Engineering Management (COMADEM)*, Cranfield, UK, Aug./Sep. 2005, pp. 525-534.

[7]   Eric Wade, and H. Harry Asada, "One-Wire Smart Motors Communicating over the DC Power Bus-Line with Application to Endless Rotary Joints," in *Proceedings of the 2002 IEEE International Conference on Robotics & Automation*, Washington, DC, USA, May 2002, pp. 2369-2374.

[8]   Eric Wade, and H. Harry Asada, "Reduced Cable Smart Motors Communicating over the DC Power Bus-Line for High Degree of Freedom Systems," in *Proceedings of the 2003 IEEE/RSJ International Conference on Intelligent Robots and Systems*, Las Vegas, Nevada, USA, Oct. 2003, pp. 1987-1991.

[9]   Shaotang Chen, Erkuan Zhong and Thomas A. Lipo, "A New Approach to Motor Condition Monitoring in Induction Motor Drives," *IEEE Transactions on Industry Applications*, vol. 30, no. 4, Jul./Aug. 1994, pp. 905-911.

[10]  J. Ahola, A. Kosonen, J. Toukonen, and T. Lindh, "A New Approach to Data Transmission between an Electric Motor and an Inverter," in *Proceedings of International Symposium on Power Electronics, Electrical Drives, Automation and Motion (SPEEDAM)*, Taormina (Sicily), Italy, May 2006, pp. 126-130.

[11]  A. Kosonen, M. Jokinen, V. Särkimäki, J. Ahola, and M. Niemelä, "Motor Feedback Speed Control by Utilizing the Motor Feeder Cable as a Communication Channel," in *Proceedings of International Symposium on Power Electronics, Electrical Drives, Automation and Motion (SPEEDAM)*, Taormina (Sicily), Italy, May 2006, pp. 131-136.

[12]  M. K. Lee, R. E. Newman, H. A. Latchman, S. Katar, and L. Yonge, "HomePlug 1.0 Powerline Communication LANs – Protocol Description and Performance Results, version 5.4," *International Journal of Communication Systems*, 2000; 00:1-6, pp. 1-25.

[13]  Lilantha Samaranayake, Sanath Alahakoon, and Keerthi Walgama, "Speed Controller Strategies for Distributed Motion Control via Ethernet," in *Proceedings of the 18th IEEE International Symposium on Intelligent Control (ISIC03)*, Houston, USA, Oct. 2003, pp. 322-327.

[14]  Max Felser, "Ethernet TCP/IP in Automation a Short Introduction to Real-Time Requirements," in *Proceedings of the 8th IEEE International Conference on Emerging Technologies and Factory Automation*, Antibes-Juan les Pins, France, Oct. 2001, pp. 501-504.

[15]  L. Samaranayake and S. Alahakoon, "Closed – loop Speed Control of a Brushless DC Motor via Ethernet," in *Proceedings of the 9th Annual Technical Conference of IEEE*, Colombo, Sri Lanka, Sep. 2002, 8 pages.

[16]  J. D. Decotignie, "A Perspective On Ethernet – TCP/IP as a Fieldbus," in *Proceedings of the IFAC Int. Conf. Fieldbus Systems and their Applications (FeT)*, Nancy, France, Nov. 2001, pp. 138-143.

[17]  Lilantha Samaranayake, Mats Leksell, and Sanath Alahakoon, "Real-Time Speed Control of a Brushless DC Motor via Ethernet," in *Proceedings of Nordic Workshop on Power and Industrial Electronics (NORPIE)*, Stockholm, Sweden, Aug. 2002, 6 pages, CD-ROM.

[18]  HomePlug Powerline Alliance, www.homeplug.org.

[19]  Product Overview, Intellon HomePlug® Family of Products, 2005. www.intellon.com.

[20]  Åström K., Hägglund T., *PID Controllers: Theory, Design, and Tuning*, 2nd edition, 1995, ISBN 1-55617-516-7.

# Publication V

A. Kosonen, M. Jokinen, J. Ahola, and M. Niemelä

**Performance Analysis of Induction Motor Speed Control Method that Utilizes Power Line Communication**

# Performance Analysis of Induction Motor Speed Control Method that Utilizes Power Line Communication

A. Kosonen, M. Jokinen, J. Ahola, M. Niemelä

**Abstract** – *In motor control, a feedback loop is used to transfer the measured motor rotor speed or angle information to a controller. The implementation of the feedback loop between a motor and a frequency converter requires instrumentation cabling. However, the motor power feeder cable could be used as a medium for data transmission. The data transmission utilizes a standardized PLC (Power Line Communication) method that forms an Ethernet connection over the motor feeder cable. The adopted method is packet based, and hence generates latency, which may vary due to packet retransmissions. In this article, the performance of the method is studied and analyzed with simulations and laboratory experiments. In addition, comparison measurements with a commercial drive are also carried out. The commercial drive is used both as speed feedback and sensorless mode. The performance of the applied method is compared, in particular, with a sensorless method. **Copyright © 2006 Praise Worthy Prize S.r.l. - All rights reserved.***

*Keywords: Power Line Communication, Electrical Drive, Ethernet, Feedback Speed Control, Rotation Speed, HomePlug, Motor Feeder Cable, Latency*

## Nomenclature

Roman letters:

| | |
|---|---|
| $d$ | process disturbance |
| $e$ | error signal |
| $e(t)$ | error between actual and reference speed |
| $e_{\%max}$ | percentual value of maximum speed error |
| $h_c$ | computation interval |
| $\mathbf{i}_s$ | stator current vector |
| $J$ | mass of inertia |
| $K_I$ | integral gain of speed controller |
| $K_P$ | proportional gain of speed controller |
| $K_T$ | torque constant |
| $r$ | reference signal |
| $\hat{r}_s$ | stator resistance estimate |
| $t$ | time |
| $T_{ref}$ | torque reference |
| $t_{s90\%}$ | settling time |
| $\mathbf{u}_s$ | stator voltage vector |
| $y$ | output signal |

Greek letters:

| | |
|---|---|
| $\tau$ | latency of feedback loop |
| $\tau_M$ | mechanical time constant |
| $\omega_m$ | measured rotation speed |
| $\xi$ | measurement noise |

| | |
|---|---|
| $\hat{\boldsymbol{\psi}}_s$ | stator flux estimate |

Acronyms:

| | |
|---|---|
| ARQ | Automatic Repeat reQuest |
| CSMA/CD | Carrier Sense Multiple Access with Collision Detection |
| DQPSK | Differential Quadrature Phase Shift Keying |
| DTC | Direct Torque Control |
| EtherCAT | Ethernet for Control Automation Technology |
| IAE | Integrated Absolute Error |
| LAN | Local Area Network |
| MRAS | Model Reference Adaptive System |
| PI | Proportional Integral |
| PLC | Power Line Communication |
| QAM | Quadrature Amplitude Modulation |
| UDP | User Datagram Protocol |

## I. Introduction

In electrical drives, the motor rotation speed or the rotor angle are typical measurements provided as feedback information to a motor controller. The vector control methods, such as DTC (Direct Torque Control) [1] or current vector control [2], do not necessarily require measurements from the rotor as feedback information.

However, in demanding control applications, especially at low rotation speeds, also feedback

*A. Kosonen, M. Jokinen, J. Ahola, M. Niemelä*

information is required. According to [3], the main problems with sensorless induction motor control methods are the static error of the rotation speed, and a weakness of performance around the zero speed state. These problems are mainly caused by errors in the induction motor model parameters of a speed estimator.

Generally, the feedback loop from the motor to the controller requires a wired connection. On the other hand, the power cable between an induction motor and a frequency converter could be utilized as a communication channel. In this work, this is referred to as motor cable communication. A single-direction motor cable communication method between a frequency converter and an induction motor was first introduced in [4], and a two-way broadband method in [5].

The bi-directional broadband motor cable communication method is studied in [5]−[7]. The characteristics of the motor cable as a communication channel are analyzed in [7]. In literature, only a few control applications have been presented so far related to the feedback signal transmission via power cables. The articles [8]−[10] concentrate on the servo systems, in which the DC distribution bus line are utilized for data communication.

The method introduced herein has previously been studied also in [11] and [12]. The article [11] concentrated mainly on latencies produced by the applied method and on the construction of the control system implementation.

The study introduced in this paper is an extended version of the article [12]. The performed comparison test of a commercial drive and different simulations is included in this work in addition to material presented in [12]. The purpose of the tests is to compare the performance of the applied method with a sensorless control method.

The study is carried out with several performance tests, simulations, and comparison tests. The results obtained with the applied method are compared to similar ones carried out by a control system with direct feedback, which is the ideal case, and by a commercial drive with sensorless and direct feedback mode. The main advantage of the applied control method is that no extra cables in addition to the power supply cable are needed. In addition, the applied control method may perform better than sensorless control methods.

The structure of this article is following. Sensorless induction motor control methods, their main problems, and their performance are briefly described in section II. The control system is described in section III. The applied performance tests are introduced in section IV. In section V, simulations of the performance of the used control system are presented. The laboratory experiments are included in section VI. The test results are analyzed in section VII.

The main contributions of the study are summarized in the conclusion section.

## II. Sensorless Control

Nowadays, sensorless motor control is perhaps the most rapidly expanding motor control method in industrial applications due to its low costs compared to achievable performance. Generally, the drive system reliability can be improved by removing the speed sensor. At the same time, the total cost of the system decreases, because there is no need for a pulse sensor or any additional cabling from the sensor to the controller. Sensorless control is also suitable for hostile environments, where extra cables, except the motor power cable, are difficult and expensive to install. The main disadvantages of the sensorless induction motor control methods are a steady-state error and a weakness of performance around the zero speed state. Also these methods require a good knowledge of the parameters of the controlled motors. There are two main implementation methods for sensorless induction motor control: a fundamental motor model-based and an injection-method-based.

The fundamental model of an induction motor is mostly utilized in the sensorless control algorithms of commercial frequency converters. Several methods based on the fundamental model are analyzed in [3]. These can be categorized in two classes; open-loop structures, such as a stator model, or closed-loop observers. The open-loop structure estimates the stator flux as follows:

$$\hat{\boldsymbol{\psi}}_s = \int (\mathbf{u}_s - \hat{r}_s \mathbf{i_s}) d\tau \qquad (1)$$

where $\mathbf{u}_s$ is the stator voltage vector, $\hat{r}_s$ the stator resistance estimate, and $\boldsymbol{i}_s$ the stator current vector. On the other hand, the estimated stator flux accuracy is proportional to the accuracy of the induction motor speed. The stator resistance depends on the temperature of stator windings.

Closed-loop observers apply a rotor model in addition to a stator model to improve the robustness and dynamics of the system. A solution of a closed-loop observer is a model reference adaptive system (MRAS), which is studied in [13]. The accuracy of the closed-loop speed estimator depends on the error of the estimated rotor time constant $\tau_r$, which in turn depends on the accuracy of the induction motor reference model.

Typically, in commercial sensorless high performance control of frequency converters, a closed-loop observer solution is used to estimate the rotation speed of the controlled motor. The accuracy of the applied method is also a function of the precision of the motor drive initialization. For example, the rotor time constant $\tau_r$ can be estimated with the identification algorithm of motor parameters. The performance of available commercial sensorless drives is studied in [14]. The summary of the results is gathered in Table I, and it is complemented with the similar information of a

*A. Kosonen, M. Jokinen, J. Ahola, M. Niemelä*

closed-loop speed controller. Additional information is gathered from the manuals of the high performance drives of the most important manufacturers.

TABLE I
ACCURACY OF OPEN-LOOP AND CLOSED-LOOP SPEED CONTROL OF COMMERCIAL DRIVES

| Accuracy | Open-Loop | Closed-Loop |
|---|---|---|
| Static Speed | 0.3–1 % | 0.01–0.02 % |
| Dynamic Speed | 0.3–1 %s | 0.1–0.4 %s |

## III. Speed Control System

The control system and the necessary peripheral devices are described in detail in [11]. The diagram of the test system is illustrated in Fig. 1. The dSPACE equipment is used as a speed controller. First, the dSPACE equipment computes the 16-bit induction motor rotation speed information according to the received data given by the pulse encoder. Next, the speed information is sent through a 90-meter long motor cable by a motor cable communication method. Finally, the feedback speed controller gives a torque reference to the frequency converter according to the received feedback information from the motor cable. The frequency converter operates in the torque control mode in the test arrangement. The feedback latency and its components are studied in detail in [11].
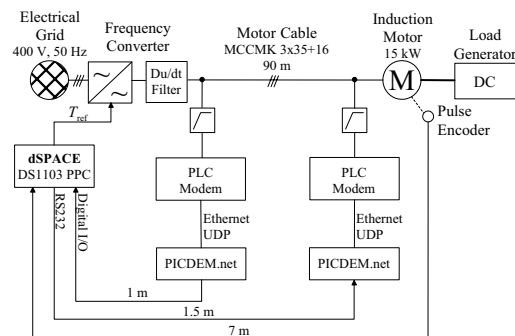


Fig. 1. Diagram of the test equipment constructed at the power electronics laboratory at Lappeenranta University of Technology

### III.1. Applied Power Line Communication Method

The adopted PLC method utilized in this application forms an Ethernet link over the motor feeder cable. The PLC method encapsulates the Ethernet frames (IEEE 802.3) into its own protocol [15] and transmits them to the motor cable.

From the viewpoint of Ethernet devices, the PLC modems are transparent. The PLC modems are based on the industrial HomePlug 1.0 standard [16]. HomePlug 1.0 with Turbo standard modems are applied in the tests. This is a more recent standard than the basic

HomePlug 1.0 standard. The main difference between these two standards is that the latter utilizes QAM (Quadrature Amplitude Modulation) 256/64/16 methods in data transmission [17]. This provides a higher bandwidth with the newer standard modems than with the older ones that apply DQPSK (Differential Quadrature Phase Shift Keying).

At the beginning, the latency of the feedback loop was measured. The sampling time was 2 ms. The latency varied between 6.0–17.4 ms and the average value settled down to 8.0 ms. According to [11], the latency is not necessarily fixed due to lost or corrupted packets. Packets that are lost or they cannot be reconstructed are sent again by the ARQ (Automatic Repeat reQuest) mechanism that is implemented in HomePlug 1.0 standard [15].

### III.2. Ethernet in Control Applications

The latency of Ethernet is non-deterministic due to the CSMA/CD (Carrier Sense Multiple Access with Collision Detection) bus reservation mechanism. This causes problems in real-time applications, which require deterministic response, such as in control applications. According to [18], in applications that require a time delay less than 1 ms, Ethernet is not a practical solution. However, EtherCAT (Ethernet for Control Automation Technology) can process 100 servo axes in 100 μs, because processing is performed on hardware level [19]. The utilization of Ethernet in industrial applications has been studied for example in [20]–[22].

The utilization of Ethernet in distributed motion control is studied in [23], in which the rotor feedback speed information of a brushless DC motor is delivered between the speed controller and the frequency converter by using a 10 Mb/s Ethernet LAN (Local Area Network) and frame size 64 bytes.

### III.3. Tuning PI Speed Controller

The PI (Proportional Integral) speed controller had to be tuned individually in every test, because of different feedback configurations. The speed controllers were tuned experimentally to fulfil the same requirements (the same magnitude of the output) in order for the results to be comparable with each other. The computation interval $h_c$ for the controller was 2 ms in every test. $h_c$ is typically 0.5–1 ms in commercial solutions.

The 15 kW motor was driven at a constant speed reference of 200 rpm. Next, it was supplied with an additional speed reference of 20 rpm as illustrated in Fig. 2. The controller was allowed 15 % overshooting from the transition step of the reference value and it was tuned as fast as possible. The PI speed controller parameters for different cases are shown in Table II. The term *Direct* in the column "Feedback Loop" indicates that the direct pulse sensor information is used

as feedback information for the controller. The term *Motor Cable* indicates that the motor cable is used as a feedback loop. The term *Sensorless* implies that no feedback signal is used.
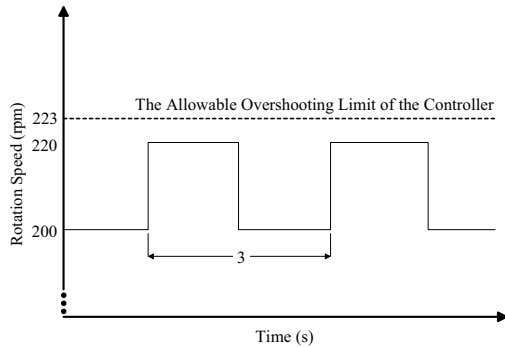


Fig. 2. Speed reference of the step response test for tuning the PI speed controller

TABLE II
SELECTED PI SPEED CONTROLLER PARAMETERS ACCORDING TO
EXPERIMENTALLY TUNING

| Feedback Loop | Controller | $K_P$ | $K_I$ | Latency Avg. |
|---|---|---|---|---|
| Direct | dSPACE | 15.7 | 7.5 | – |
| Direct | Commercial Drive | 15.7 | 7.5 | – |
| Sensorless | Commercial Drive | 9.8 | 4.4 | – |
| Motor Cable | dSPACE | 11.0 | 3.0 | 8.0 ms |

## IV. Performance Tests

The performance of different feedback loop configurations was simulated and measured with several tests. Simulations were only carried out for a control system with a feedback loop. The experimentally tuned parameters presented in Table II were used in the tests. The applied tests were: a step response test, a ramp test, and a loading test.

### IV.1. Step Response Test

The results of the step response test ensure that the controllers are tuned to be comparable. This means that the maximum overshooting from the reference value should be identical (see Fig. 2).

### IV.2. Ramp Test

One of the most important performance measurements in industrial process drives is the tracking capability of the reference signal. Therefore it is relevant to study the influence of the feedback latency on the tracking capability of control. In the test, the rotation speed of the rotor was accelerated from zero

speed to the nominal speed of the induction motor (1455 rpm) in about 0.8 s.

### IV.3. Loading Test

The changes in the loading condition are very typical phenomena in the industrial process drives. The loading condition can change, for instance, linearly or stepwise. The stepwise change reveals the control's incompleteness or its weakness. Also the stepwise loading change is used in the tests. The motor is driven at a constant speed of 750 rpm that is about a half of its nominal value. In a random time instant a 58 % (of the motor nominal torque value) loading change is caused. This kind of change ensures that for example the current limit is not exceeded.

## V. Simulation

A controlled system can be modelled based on a control diagram presentation as illustrated in Fig. 3, where *r* is a reference signal, *y* an output signal, *d* a process disturbance, *ξ* the noise of a measurement, *e* an error signal, and $\omega_m$ a measured rotation speed signal. The transfer functions *F(s)*, *C(s)*, *P(s)*, and *H(s)* are for a pre-filter, controller, process, and feedback loop, respectively.
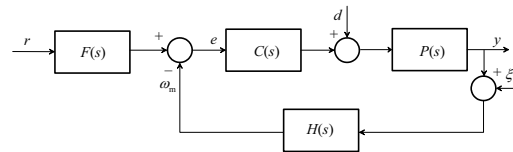


Fig. 3. Block diagram presentation to illustrate a controlled process

If the process is a PI speed-controlled motor and the current control is assumed to be ideal, and the rotation speed information is transmitted via the power cable from the motor to the frequency converter, the next few equations can be formed. Because the PI speed controller does not use pre-filtering, the transfer function of the pre-filter *F(s)* = 1. The motor can be modelled according to its mass of inertia:
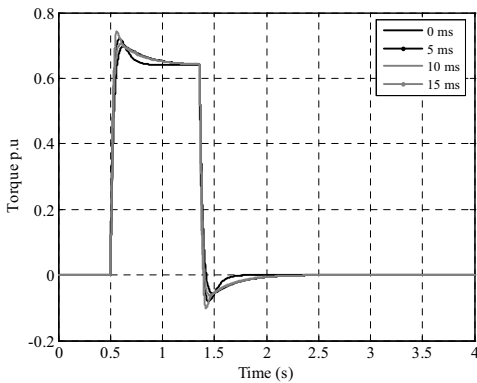
$$P(s) = \frac{K_T}{Js} \qquad (2)$$

where $K_T$ is the torque constant of the motor (Nm/A), and *J* is the mass of inertia of the motor (kgm$^2$). The transfer function of the PI speed controller can be described as follows:

$$C(s) = K_P\left(1 + \frac{K_I}{s}\right) \qquad (3)$$
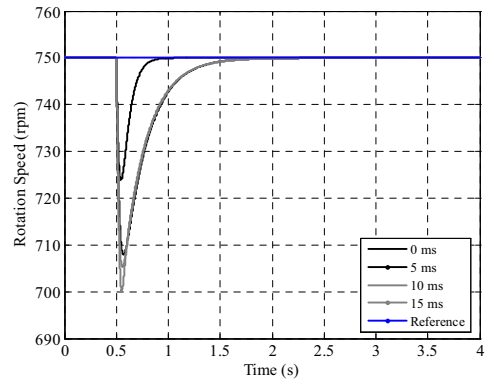
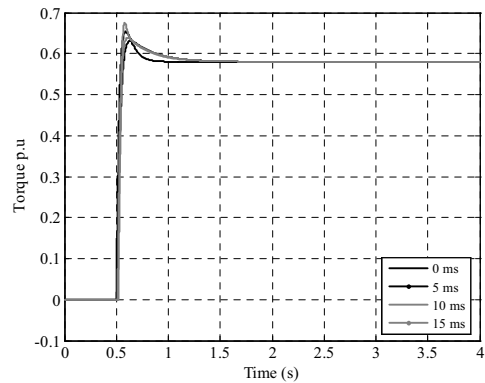*A. Kosonen, M. Jokinen, J. Ahola, M. Niemelä*
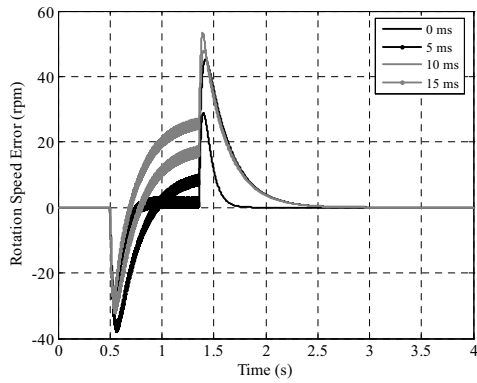


(a)



(b)

Fig. 4. Simulated ramp test. (a) Behaviour of rotation speed error as a function of time. (b) Torque reference given by the controller during the test



(a)



(b)

Fig. 5. Simulated loading test. (a) Behaviour of rotation speed as a function of time. (b) Torque reference given by the controller during the test

where $K_P$ is the proportional gain of the controller, and $K_I$ is the gain of the integrator, which has also inverse proportionate to the integration time of the controller.

The bandwidth of the system, the phase shift, the integrated absolute error (IAE), and a value of %s are gathered in Table III. The values of IAE and %s are for the speed measurement in the case of the load disturbance with different feedback latencies. The latencies are chosen based on the measured ones.

TABLE III
SIMULATED BANDWIDTH, PHASE SHIFT, IAE, AND %S FOR DIFFERENT LATENCIES IN FEEDBACK LOOP

| Latency Avg. | Bandwidth | Phase Shift | IAE (rpm·s) | %s |
|---|---|---|---|---|
| 0 ms | 58 rad/s | 60º | 2.1 | 0.22 |
| 5 ms | 45 rad/s | 57º | 9.8 | 0.90 |
| 10 ms | 59 rad/s | 62º | 9.7 | 0.94 |
| 15 ms | 73 rad/s | 78º | 9.7 | 0.99 |

The bandwidth of the system was evaluated with a simulation model. The frequency of the speed reference signal was increased to a value at which the amplitude of the measured speed was decreased by 3 dB compared to the amplitude of the reference speed. The phase shift is given at this frequency for each case.

The integrated absolute errors were calculated according to [24]:

$$IAE = \int_0^\infty \left| e(t) \right| dt \qquad (4)$$

where $e(t)$ is the error between the actual speed and the reference value. The time range used to calculate the value of IAE was from zero to two seconds, and the used sampling time of the speed measurement was 100 μs.

The values of %s were calculated based on the area of a triangle as follows:

$$\%s = \frac{e_{\%\max} \cdot t_{s90\%}}{2} \qquad (5)$$

where $e_{\%\max}$ is the percentual value of the maximum rotation speed error from the nominal speed of the induction motor (1455 rpm) after the load impact, and $t_{s90\%}$ is the settling time required to return to the 90 % value of the magnitude of the rotation speed drop.

The parameters of the PI controller were tuned with the simulation model according to section III.3. The PI parameters used for the delay of 0 ms were $K_P = 15.7$ and $K_I = 10.0$, and for delays of 5 ms, 10 ms, and 15 ms were $K_P = 11.0$ and $K_I = 3.8$.

The simulated ramp results obtained from the tests are illustrated in Fig. 4.

The simulated loading results obtained from the tests are illustrated in Fig. 5.

## VI.  Laboratory Experiments

### VI.1.  Measurements

The simulated results were verified with measurements. Similar tests as introduced in section IV were performed with the applied control method and with a control system with a direct feedback loop. The laboratory equipment is illustrated in Fig. 6.
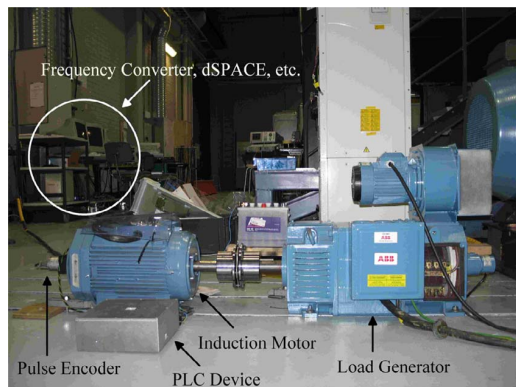


Fig. 6. Test equipment constructed at the laboratory

The step response results obtained from the tests are illustrated in Fig. 7.

The ramp results obtained from the tests are illustrated in Fig. 8.

The loading results obtained from the tests are illustrated in Fig. 9.

### VI.2.  Comparison Tests with Commercial Drive

The tests were carried out for investigating the competitiveness of the applied control method compared to the commercial solution, especially to a sensorless control method.

The comparison tests were carried out for a commercial frequency converter by utilizing its own control system. The controller was used both in a feedback and sensorless modes. The pulse encoder was similar as in the previous test. Naturally, the pulse encoder was not required with the sensorless system. Similar performance tests as introduced in section IV were carried out for the commercial drive. The results were compared with the ones performed for the applied feedback speed control method implemented with the HomePlug 1.0 with Turbo standard PLC modems.

The step response results obtained from the tests are illustrated in Fig. 10.

The ramp results obtained from the tests are illustrated in Fig. 11.

The loading results obtained from the tests are illustrated in Fig. 12.

## VII.  Analysis of Results

### VII.1.  Simulation and Measurement

The simulation model does not exactly correspond to the real system, because the model uses only the mass of inertia of the motors. Hence, the selected torque values could differ from each other in the simulation and in the measurement. The purpose of the simulation was to study the influence of latency in the feedback loop on the behaviour of the whole system.

According to the simulated ramp and loading tests illustrated in Figs. 4 and 5, respectively, the behaviour of the rotation speed is almost identical in all three delayed cases. The overshoot in Fig. 4 is 29 rpm, 45 rpm, 48 rpm, and 54 rpm for the delays 0 ms, 5 ms, 10 ms, and 15 ms, respectively. The maximum rotation speed error in Fig. 6 is 26 rpm, 42 rpm, 45 rpm, and 50 rpm for the delays 0 ms, 5 ms, 10 ms, and 15 ms, respectively. The settling time is similar in three cases despite the magnitude of delays because all the control systems with delayed feedback signal have same PI parameters. In this case, it is possible to use same PI parameters for all four cases without any risk that the system could start to oscillate heavily or even fall into an unstable state. Nevertheless with longer latencies, unaccepted behaviour may occur, if the parameters of the controller are not re-verified to correspond to the increased latency.

The bandwidth of a system depends mainly on the parameters of the controller, the feedback latency, and the mechanical time constant of the system. When the latency increases and controller parameters remain constant, the bandwidth also increases. This phenomenon is a consequence of the fact that the feedback latency increases the gain of the resonant frequency of the system, which shifts at the same time
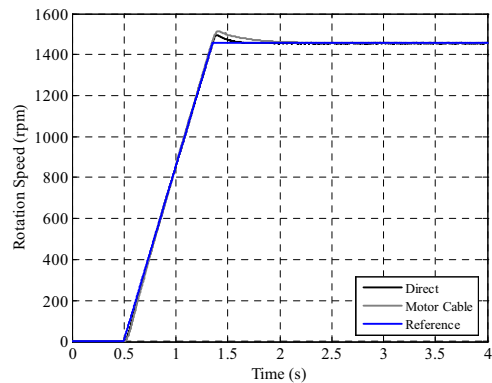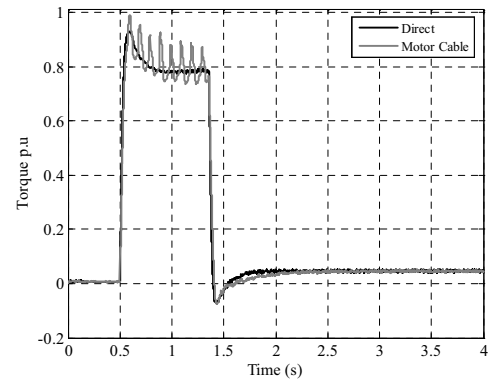
*A. Kosonen, M. Jokinen, J. Ahola, M. Niemelä*
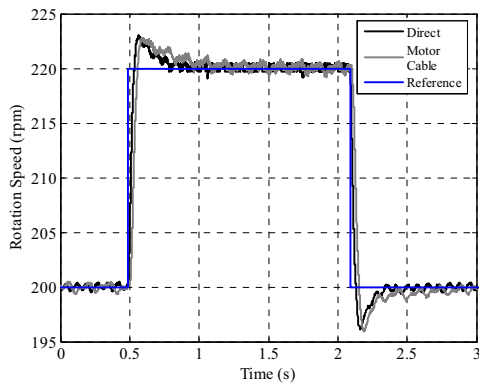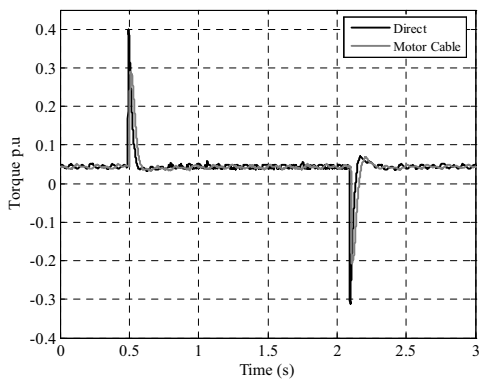
Fig. 7. Step response test. (a) Behaviour of rotation speed as a function of time. (b) Torque reference given by the controller during the test



Fig. 8. Ramp test. (a) Behaviour of rotation speed as a function of time. (b) Torque reference given by the controller during the test

the −3 dB limit to higher frequencies. This additional gain of the resonant frequency produces also larger overshoot for the reference changes. The latency adds a pole and a zero to the transfer function.

According to the ramp test illustrated in Fig. 8, the torque reference signal tries to oscillate during the acceleration due to the feedback latency. However, this could be prevented with some kind of delay compensator in the control system.

According to Figs. 4, 5, and 7–9, the latency of the feedback loop slightly deteriorates the performance of the control system. The mechanical time constant of a motor or a system should be essentially longer than the latency of the feedback loop ($\tau_M \gg \tau$) as in this case. The latency of the feedback signal can be problematic in processes where dynamic load regulation performance is required. However, the results are very promising, because only a conventional PI controller was used in each configuration. The performance of the applied control method could be improved by changing the parameters of the PI controller, or by utilizing

modern and sophisticated control methods, such as predictors and compensators.

It is possible to add a time stamp to the packet of rotation speed in order to analyze the feedback delay in real-time.

The delay information can be used to estimate the actual rotation speed, which can be sampled faster and in a fixed interval.

This can be applied in delay compensator methods, such as Smith predictor. The identification of the feedback delay is useful in industrial system initialization.

The motor cable communication method can also be utilized to improve the performance of the sensorless control methods; for example, the inaccuracy of the motor model can be reduced by transmitting the temperature of the stator through the motor cable. This does not require a wide bandwidth or strict latency characteristics.

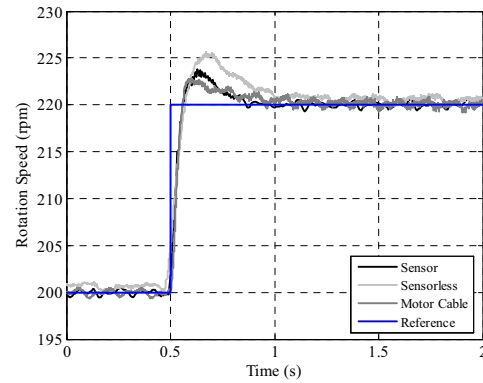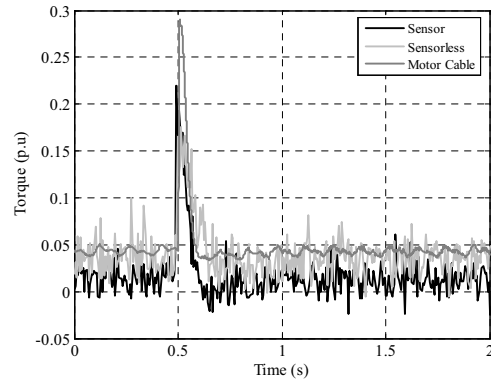*A. Kosonen, M. Jokinen, J. Ahola, M. Niemelä*
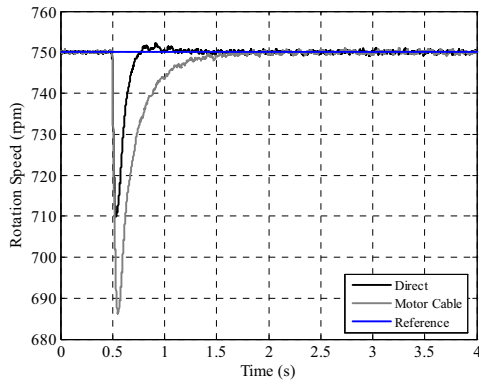


(a)
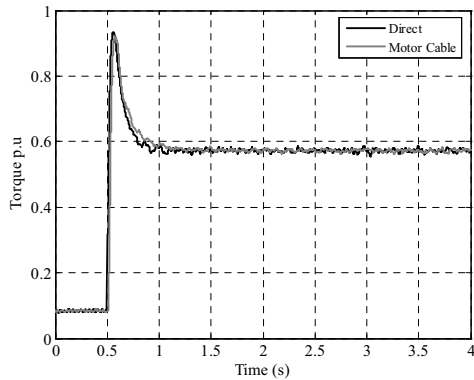


(b)

Fig. 9. Loading test. (a) Behaviour of rotation speed as a function of time. (b) Torque reference given by the controller during the test. The load generator causes a static initial load



(a)



(b)

Fig. 10. Step response test with a commercial drive. (a) Behaviour of rotation speed as a function of time. (b) Torque reference given by the controller during the test

### VII.2.  Comparison Tests

The step response test showed that it is difficult to tune the sensorless control system to meet the restrictions described in section III.3. The same PI parameters (Table II) were given for the commercial drive with feedback as in the similar case implemented with the dSPACE equipment. It can be seen from Fig. 10 that only the control system implemented with the motor cable feedback loop meets the given restrictions. The overshoots in the step response test are 3 rpm, 4 rpm, and 5.5 rpm for the motor cable feedback loop and for commercial drive with and without feedback, respectively. In the case like this, it could be possible to increase the gains with a controller implemented with a motor cable feedback loop and to allow a bigger overshoot similarly as in the other cases; however, this was not done in this study.

In the ramp test (Fig. 11), the overshoot is larger with the sensorless control system than with the other

methods. The settling time of the control system implemented with the motor cable feedback loop is the longest among these three cases due to the smallest gains of the PI controller. The overshoot in the ramp test is 61 rpm, 53 rpm, and 97 rpm for the motor cable feedback loop and for the commercial drive with and without feedback, respectively.

The loading test illustrated in Fig. 12 reveals unquestionably the weakness of the sensorless control system. Before the load impact, there is no visible steady state error of rotation speed with sensorless control. After the load impact, the steady state error is 3.5 rpm, which is significant.

The most important results obtained from the loading test both with the dSPACE equipment and with the commercial drive are gathered in Table IV. The values of IAE and %s were calculated according to (4) and (5), respectively. The time range for the IAE calculation was 0−2 s, and the sampling time of the measurement was 100 µs for all other cases except for commercial drive with feedback, for which the sampling time was

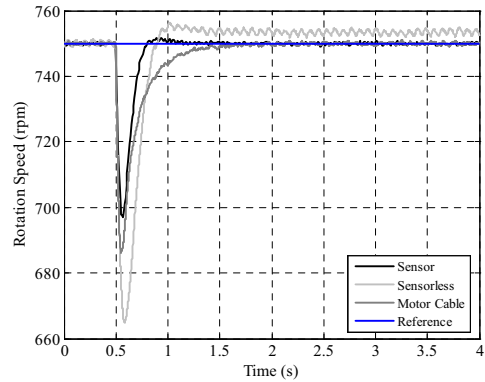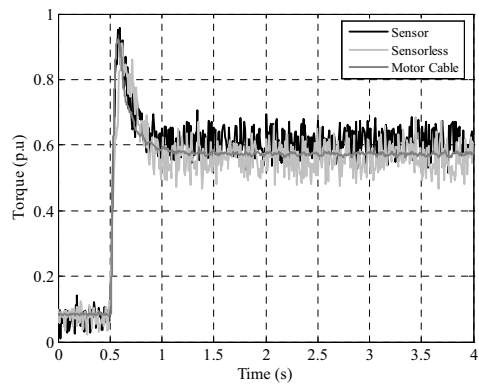*A. Kosonen, M. Jokinen, J. Ahola, M. Niemelä*
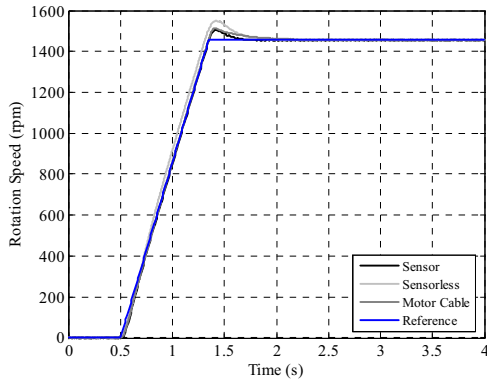


(a)
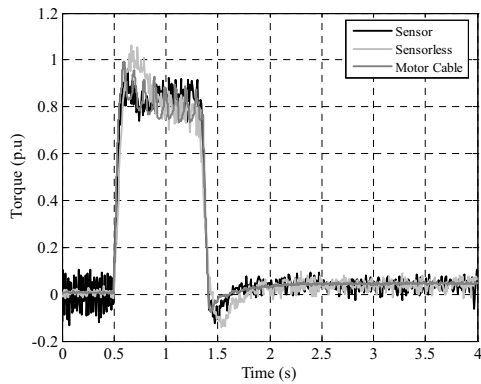


(b)

Fig. 11. Ramp test with a commercial drive. (a) Behaviour of rotation speed as a function of time. (b) Torque reference given by the controller during the test



(a)



(b)

Fig. 12. Loading test with a commercial drive. (a) Behaviour of rotation speed as a function of time. (b) Torque reference given by the controller during the test. The load generator causes a static initial load

8 ms.

The allowable deviation band was ±1.5 rpm, which was defined to be ±0.1 % of the induction motor synchronous speed (1500 rpm). Thus, the settling time could be calculated based on the time required by the average curve of rotation speed to return inside the band after the load impact.

TABLE IV
ANALYSIS OF LOADING TEST RESULTS

| Feedback Loop | Maximum Error | Settling Time | IAE (rpm·s) | %s |
|---|---|---|---|---|
| Direct | 40 rpm | 0.23 s | 4.8 | 0.27 |
| Sensor | 53 rpm | 0.27 s | 7.8 | 0.43 |
| Motor Cable | 64 rpm | 0.85 s | 13.9 | 1.11 |
| Sensorless | 85 rpm | – | 20.8 | 0.96 |

According to Table IV, it was impossible to define the settling time for the sensorless control, because the allowable deviation band was ±1.5 rpm, but the steady state error was 3.5 rpm. The steady state error increases also the IAE value. The valid PI parameters have visible influence on the settling time, and hence the sensorless control method achieves smaller %s value than the applied control method due to definition of %s.

## VIII. Conclusion

In this article, the performance of the speed control method with a feedback utilizing power line communication and motor cable in data transmission is studied and analyzed. In particular, the method is compared to a commercial solution that applies both a sensorless and speed feedback method. The applied method does not require a pulse encoder cable, because feedback information is transmitted through the motor power cable in real-time. Instrumentation cables may reduce the reliability of the electrical drive and on the other hand, they are typically expensive to install.

*A. Kosonen, M. Jokinen, J. Ahola, M. Niemelä*

The motor cable communication method can be considered to be Ethernet based because it encapsulates Ethernet frames into their own protocol. The packet based data transmission causes additional latency to the feedback loop. This latency varies due to possible packet retransmissions.

The study concentrates mainly on the comparison of the performance of the applied method and the commercial solution. The main interest in the analysis is in the performance of a sensorless method compared to the one performed with the applied method. In the tests, the dSPACE equipment and a commercial frequency converter is used as a controller.

Measurements show that the motor feeder cable could be used as a speed feedback communication channel instead of a pulse encoder cable. The method applied here is competitive in performance even if it was compared to the control with direct feedback. The competitiveness depends mainly on the whole system and its mechanical time constant. The influence of the latency on the performance would be emphasized if the mechanical time constant of the system was shorter, and vice versa. The performance of the applied control method could probably be improved by applying modern and sophisticated control methods.

## Acknowledgement

## References

[1] Isao Takahashi, Toshihiko Noguchi, A New Quick-Response and High-Efficiency Control Strategy of an Induction Motor, IEEE Transactions on Industry Applications, Vol. 22, No. 5, pp. 820−827, Sep./Oct. 1986.

[2] F. Blaschke, The Principle of Field Orientation as Applied to the New TRANSVECTOR Closed Loop Control System for Rotating Field Machines, Siemens Review, Vol. 34, pp. 217−220, May 1972.

[3] J. Holtz, Sensorless Control of Induction Motors – Performance and Limitations, Proc. 2000 IEEE international Symposium on Industrial Electronics, Cholula, Puebla, Mexico, Dec. 2000, Vol 1, pp. PL12−PL20.

[4] Shaotang Chen, Erkuan Zhong, Thomas A. Lipo, A New Approach to Motor Condition Monitoring in Induction Motor Drives, IEEE Transactions on Industry Applications, Vol. 30, No. 4, pp. 905−911, Jul./Aug. 1994.

[5] J. Ahola, J. Toukonen, A. Kosonen, T. Lindh, V. Särkimäki, Electric Motor Cable Communication Overcomes the Biggest Obstacle in On-line Condition Monitoring, Proc. Condition Monitoring 2005 Conference, Cambridge, UK, Jul. 2005, pp.105−110.

[6] J. Ahola, J. Toukonen, A. Kosonen, T. Lindh, R. Tiainen, Ethernet to Electric Motor – via Mains Cable, Proc. 18th International Congress and Exhibition on Condition Monitoring and Diagnostic Engineering Management, Cranfield, UK, Aug./Sep. 2005, pp. 525−534.

[7] J. Ahola, A. Kosonen, J. Toukonen, T. Lindh, A New Approach to Data Transmission between an Electric Motor and an Inverter, to be published in Proc. International Symposium on Power Electronics, Electrical Drives, Automation and Motion, Taormina (Sicily), Italy, May 2006, pp. 126−130.

[8] Chun-Hung Liu, Eric Wade, H. Harry Asada, Reduced-Cable Smart Motors Using DC Power Line Communication, Proc. 2001 IEEE International Conference on Robotics & Automation, Seoul, Korea, May 2001, pp. 3831−3838.

[9] Eric Wade, H. Harry Asada, One-Wire Smart Motors Communicating over the DC Power Bus-Line with Application to Endless Rotary Joints, Proc. 2002 IEEE International Conference on Robotics & Automation, Washington, DC, USA, May 2002, pp. 2369−2374.

[10] Eric Wade, H. Harry Asada, Reduced Cable Smart Motors Communicating over the DC Power Bus-Line for High Degree of Freedom Systems, Proc. 2003 IEEE/RSJ International Conference on Intelligent Robots and Systems, Las Vegas, Nevada, USA, Oct. 2003, pp. 1987−1991.

[11] A. Kosonen, M. Jokinen, V. Särkimäki, J. Ahola, M. Niemelä, Motor Feedback Speed Control by Utilizing the Motor Feeder Cable as a Communication Channel, Proc. International Symposium on Power Electronics, Electrical Drives, Automation and Motion, Taormina (Sicily), Italy, May 2006, pp. 131−136.

[12] Antti Kosonen, Markku Jokinen, Jero Ahola, Markku Niemelä, Real-Time Induction Motor Speed Control with a Feedback Utilizing Power Line Communications and Motor Feeder Cable in Data Transmission, Proc. 32nd Annual Conference of the IEEE Industrial Electronics Society, Paris, France, Nov. 2006, pp. 638−643.

[13] Colin Schauder, Adaptive Speed Identification for Vector Control of Induction Motors without Rotational Transducers, IEEE Transactions on Industry Applications, Vol. 28, No. 5, pp. 1054−1061, Sep./Oct. 1992.

[14] Russel J. Kerkman, Gary L. Skibinski, David W. Schlegel, AC Drives: Year 2000 (Y2K) and Beyond, Proc. 14th Applied Power Electronics Conference and Exposition, Dallas, USA, Mar. 1999, pp. 28−39.

[15] M. K. Lee, R. E. Newman, H. A. Latchman, S. Katar, L. Yonge, HomePlug 1.0 Powerline Communication LANs – Protocol Description and Performance Results, version 5.4, International Journal of Communication Systems, pp. 1−25, 2000; 00:1-6

[16] HomePlug Powerline Alliance, Available at www.homeplug.org, Accessed on Sep. 2006.

[17] Product Overview, Intellon HomePlug® Family of Products, 2005. Available at www.intellon.com, Accessed on Sep. 2006.

[18] Lilantha Samaranayake, Sanath Alahakoon, Keerthi Walgama, Speed Controller Strategies for Distributed Motion Control via Ethernet, Proc. 18th IEEE International Symposium on Intelligent Control, Houston, USA, 2003, pp. 322−327.

[19] Dirk Jansen, Holger Büttner, Real-Time Ethernet the EtherCAT Solution, IEE Computing & Control Engineering Journal, Vol. 15, No. 1, pp. 16−21, Feb./Mar. 2004.

[20] Max Felser, Ethernet TCP/IP in Automation a Short Introduction to Real-Time Requirements, Proc. 8th IEEE International Conference on Emerging Technologies and Factory Automation, Antibes-Juan les Pins, France, 2001, pp. 501−504.

[21] L. Samaranayake, S. Alahakoon, Closed – loop Speed Control of a Brushless DC Motor via Ethernet, Proc. 9th Annual Technical Conference of IEEE, Colombo, Sri Lanka, 2002, 8 pages.

[22] J. D. Decotignie, A Perspective On Ethernet – TCP/IP as a Fieldbus, Proc. IFAC Int. Conf. Fieldbus Systems and their Applications, Nancy, France, 2001, pp. 138−143.

[23] Lilantha Samaranayake, Mats Leksell, Sanath Alahakoon, Real-Time Speed Control of a Brushless DC Motor via Ethernet, Proc. Nordic Workshop on Power and Industrial Electronics, Stockholm, Sweden, 2002, 6 pages, CD-ROM.

[24] K. Åström, T. Hägglund, PID Controllers: Theory, Design, and Tuning (2nd edition, 1995).

*A. Kosonen, M. Jokinen, J. Ahola, M. Niemelä*

# Authors' Information

Department of Electrical Engineering
Lappeenranta University of Technology
P.O. Box 20, FI-53851 LAPPEENRANTA
FINLAND
Tel: +358 5 621 6765
Fax: +358 5 621 6799
E-mail: antti.kosonen@lut.fi
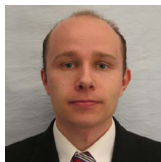
**Antti Kosonen,** was born in Imatra, Finland in 1980. He received M.Sc. degree in electrical engineering from Lappeenranta University of Technology in 2005.
He is currently preparing his doctoral dissertation at the Department of Electrical Engineering at Lappeenranta University of Technology. His current interests include power line communication and its industrial applications.

**Markku Jokinen,** was born in Joensuu, Finland in 1980. He received M.Sc. degree in electrical engineering from Lappeenranta University of Technology in 2004.
He is currently preparing his doctoral dissertation at the Department of Electrical Engineering at Lappeenranta University of Technology. His current interests include servo drive control systems and the possibility to utilize power line communication in a feedback channel.

**Jero Ahola,** was born in Lappeenranta, Finland in 1974. He received his Master of Science and Doctor of Science degrees in electrical engineering from Lappeenranta University of Technology, in Finland, in 1999 and 2003. He works currently as an acting professor at the Department of Electrical Engineering at Lappeenranta University of Technology. His main research interests are in power line communications and condition monitoring of electrical drives.

**Markku Niemelä,** was born in Mäntyharju, Finland in 1968. He received his B.Sc. degree in electrical engineering from Helsinki Institute of Technology in 1990. He obtained his M.Sc. degree in 1995 and his Doctor of Science degree in 1999 from Lappeenranta University of Technology. He is currently a senior researcher at the Carelian Drives and Motor Centre at Lappeenranta University of Technology. His current interests include motion control, control of line converters and design of synchronous machines.

# Publication VI

A. KOSONEN, J. AHOLA, AND P. SILVENTOINEN

**Measurements of HF Current Propagation to Low Voltage Grid through Frequency Converter**

*in Proceedings of the 12$^{th}$ European Conference on Power Electronics and Applications (EPE), Aalborg, Denmark, September 2007, 10 p., CD-ROM.*

# Measurements of HF Current Propagation to Low Voltage Grid through Frequency Converter

A. Kosonen, J. Ahola, and P. Silventoinen
LAPPEENRANTA UNIVERSITY OF TECHNOLOGY
P.O. Box 20, 53851 Lappeenranta
Finland
Tel.: +358 (0)5 621 6765
Fax: +358 (0)5 621 6799
E-Mail: antti.kosonen@lut.fi
URL: http://www.lut.fi

## Acknowledgements

## Keywords

«HomePlug 1.0», «EMI», «Power line communications», «Data transmission», «Adjustable-speed drive», «Industrial application».

## Abstract

It is known that frequency converters generate both conducted and radiated noise that spreads out to the low-voltage distribution network and disturbs victim devices. Nowadays, it is also possible to utilize the low-voltage motor power cable between a frequency converter and an electric motor as a medium for data transmission. In this study, conducted noise propagation generated by the data transmission is measured and analyzed in the frequency-domain.

## Introduction

Modern power line data transmission methods, such as HomePlug 1.0 and HomePlug AV, utilize the frequency band up to 30 MHz and OFDM (Orthogonal Frequency Division Multiplexing) in data transmission [1], [2]. These together with effective signal processing techniques have made it possible to transmit data also in the power cable between a frequency converter and an electric motor [3]. In general, it is known that frequency converters generate high frequency (HF) noise, both radiated and conducted, which spreads also out, for instance to low voltage distribution networks. These problems are commonly known as electromagnetic interference (EMI) [4]. According to [5], the main noise sources of a frequency converter are the output stage and the rectifier bridge. Several low-cost strategies to improve the electromagnetic compatibility (EMC) performance of these problems have been proposed in [6]. The most important source of EMI in the variable-speed drives is the currents that flow into the ground through the stray capacitors of the system elements, such as the grid, converter, power cable, and electric motor [7], [8]. Frequency-domain modelling methods of conducted EMI in electrical drives have been studied in [9].

The noise and its propagation produced by a frequency converter have been analyzed and modelled in numerous articles, while the HF noise produced in a motor power cable has received less attention. In this study, the propagation of HF current through a frequency converter to a low voltage grid is measured and analyzed. The results can be applied for example in the study of EMI and in evaluating the suitable coupling method for data transmission. The broadband HF current is produced by power line

communication (PLC) modems coupled to the motor feeder cable. The noise generated by the frequency converter is in a lower frequency band than the one generated by a HomePlug modem. The HomePlug 1.0 standard utilizes the frequency band of 4.49−20.7 MHz [1]. The transmit power of the HomePlug modems is approximately of the size of 10 mW. The effects of signal coupling on the conducted EMI are also studied. Two capacitive coupling interfaces for PLC in the motor cable are designed with couplings between a phase (L1) and the protective earth (PE), and between two phases (L1, L2). Both common-mode (CM) and differential-mode (DM) noise currents are measured from the output of the frequency converter and from the distribution network side in the frequency band of 150 kHz−30 MHz.

## EMI

Electromagnetic interferences can be divided into two classes: conducted and radiated noise emissions. These can be classified in further detail [5]. The conducted electromagnetic emissions are divided into CM and DM. The radiated emissions, in turn, are divided into near- and far-field emissions. In this study, only the conducted electromagnetic emissions are measured, because radiated emissions are generally measured only at frequencies above 30 MHz.

### Conducted Emissions

In CM, EMI noise is induced on signals with respect to a reference ground [4], and in DM, the noise is summed to the signal [5]. The basic idea of these according to [5] is illustrated in Fig. 1. In a three-phase motor cable, all three phase leads can be regarded as signal wires and the PE as a ground wire.
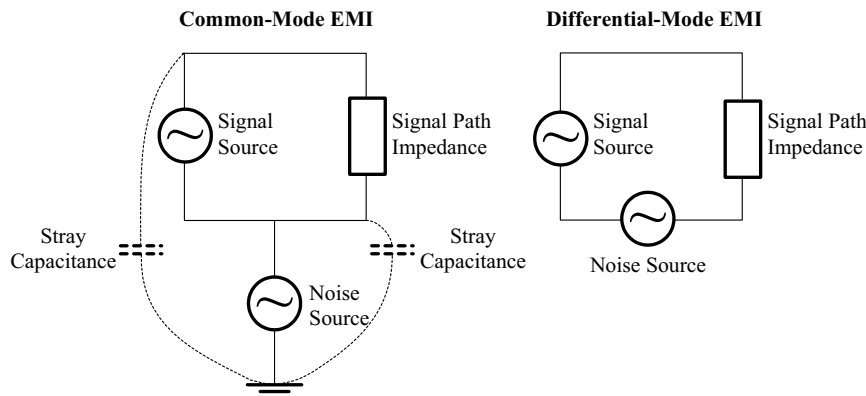


Fig. 1: CM and DM electromagnetic interferences

CM noise current is in all signal lines in the same phase [5]. Hence, the CM noise current is measured from all three phases (L1+L2+L3). The impedance of a CM loop is high at low frequencies, because the CM loops are usually closed via stray capacitances of different elements of the system (see Fig. 1). The DM noise is an extra current that flows in the signal path [5]. The noise is summed to the signal. Hence, the DM noise current is measured from a single phase in spite of the fact that it contains a CM component too. The DM loop can also be closed through the stray capacitances between two signal wires or between a signal wire and the ground. If the DM noise travels via the ground wire, it has to be passed through two stray capacitances back to the signal wire.

When identifying an effect of parasitic impedances on signal propagation, mutual inductances have to be taken into consideration. In addition to stray capacitances, they offer an alternative route for the HF signal between different conductors as illustrated in Fig. 2.
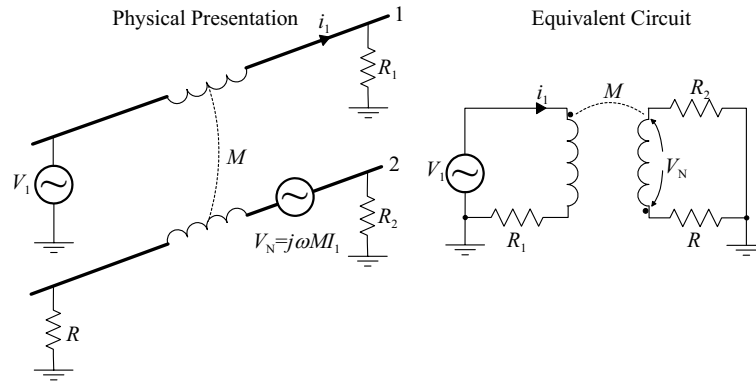
Fig. 2: Magnetic coupling between two conductors

In general, it is known that the magnetic coupling between two circuits can be described as follows:

$$u_{L1} = L_1 \frac{di_1}{dt} + M_{12} \frac{di_2}{dt} \tag{1}$$

$$u_{L2} = M_{12} \frac{di_1}{dt} + L_2 \frac{di_2}{dt}, \tag{2}$$

where $L_1$ and $L_2$ are the self inductances of the wires, $u_{L1}$ and $u_{L2}$ are the voltages over the inductances, $M_{12}$ is the mutual inductance between the source and the victim circuit, and $i_1$ and $i_2$ are the currents in the circuits, respectively.

According to Fig. 2, current $i_1$ flowing in a source circuit produces a flux $\varphi_{12}$ in a victim circuit due to the mutual inductance $M_{12}$ between the circuits 1 and 2 defined as [10]:

$$M_{12} = \frac{\varphi_{12}}{i_1} . \tag{3}$$

The mutual inductance can be approximated according to the Biot-Savart law, in which the magnetic flux density $B$ at a distance $r$ from a long current-carrying conductor can be written as follows:

$$B = \frac{\mu i}{2 \pi r} , \tag{4}$$

where $\mu$ is permeability of the medium, $i$ the current of a source conductor, and $r$ is greater than the radius of the conductor. The mutual inductance can be approximated using (3) and (4). In addition, it is known that:

$$\varphi = BA , \tag{5}$$

where $A$ is the area of closed loop that the magnetic flux penetrates.

## Adjustable-Speed Drive in EMI Sense

The data transmission used in motor cable communications utilizes a HF band (3−30 MHz). The signal can propagate from the motor cable to the low voltage grid via the capacitive or inductive coupling of an adjustable-speed drive; the stray capacitances cause capacitive coupling and the mutual inductances between two inductances inductive coupling. For magnetic and capacitive field couplings, a noise current is produced in series and parallel with the receptor conductor, respectively [10]. The main stray capacitances of an adjustable speed drive are illustrated in Fig. 3.
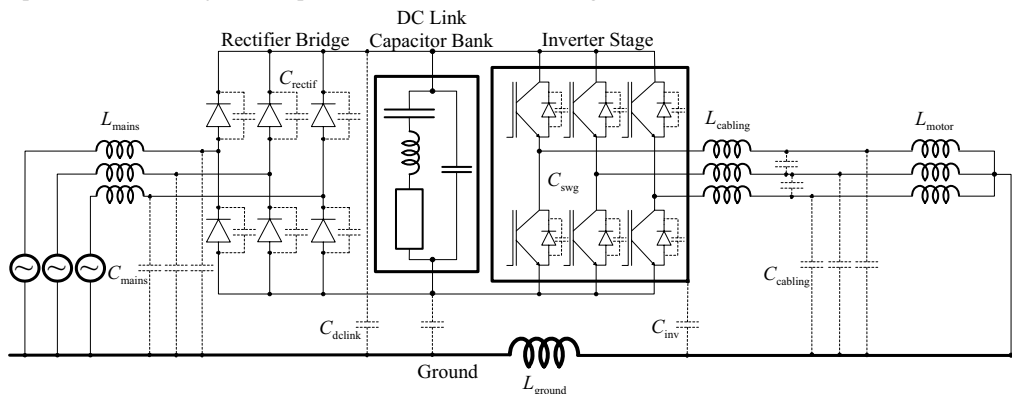


Fig. 3: Main stray capacitances for the path of the PLC signal from the motor cable to the mains network in an adjustable speed drive. The stray capacitances $C_{mains}$, $C_{rectif}$, $C_{dclink}$, $C_{swg}$, $C_{inv}$, $C_{cabling}$, and $C_{motor}$ are indicated with dashed lines. There are also many other stray capacitances, e.g. between the IGBTs or the DC bus and the heatsink. Between the heatsink and the ground, there is also a single stray capacitance

The rectifier bridge of a DC voltage link converter is both an EMI noise source and a coupling path to the low voltage grid. Generally, it acts as a low-frequency DM noise source [5]. The rectifier unit passes mainly CM noise current from the bridge to the ground or from a DC rail to another because of the stray capacitances, which are parallel with the rectifier diodes. In consequence, there are several different coupling paths. The DM signal propagation is a more complicated case: the signal can also propagate via the ground wire through the stray capacitances but it is more likely that it is attenuated because of the lower impedance between the DC rails than the impedance between DC rail−ground−DC rail in the HF band. However, signal attenuation depends mainly on the impedances of different coupling paths.

According to [5], a DC link capacitor with proper HF properties can be an effective DM noise attenuator. DM signal is short-circuited through the DC link capacitor. Practically, DC link capacitors of frequency converters are often aluminium electrolytic capacitors due to their high capacitance value proportion to the size. In general, electrolytic capacitors do not have good HF properties because of their high equivalent serial resistance (ESR) and high internal inductance, which is a consequence of the relatively large physical size, resulting in a low resonance frequency of about 10 kHz [6]. Hence, small and very fast capacitors are often installed parallel with the electrolytic capacitor both to ensure a fast energy storage and to short-circuit the DC rail from a rapid DM noise current in some instances.

Modern pulse width modulation (PWM) frequency converters use isolated gate bipolar transistors (IGBTs) with switching times ($t_r$) that can be lower than 80 ns in 400 V drives [9]. The inverter stage generates electromagnetic emissions of all forms [5]. In the viewpoint of communications at HF band, it is not the switching frequencies that are the most serious problem, but the short voltage rise times (du/dt) due to their high frequency and energy contents. The switching of the inverter output stage generates high-

frequency and high-energy pulses (~100 kHz−1 MHz) into the motor feeder cable [11]. The maximum voltage amplitude of these pulses between two phases may be even more than 1000 V at the motor end in low voltage inverter drives. According to [10], the maximum frequencies of a pulse can be related to its rise time as follows:

$$f_{\max} = \frac{1}{\pi t_{\mathrm{r}}},$$
(6)

where $t_r$ is the rise time of the current or voltage pulse. Evidently, a high switching frequency increases the number of switch transients, which in turn increase the sum of the total DM and CM noise current. HF noise can propagate through the inverter stage in a similar way as through the rectifier bridge via the stray capacitances (see Fig. 3). On the other hand, when the frequency converter is on the active mode, there are IGBTs that conduct, and thus the signal can flow freely through the transistors.

A motor cable termination to its characteristics impedance directly affects the reflections of the signal in the cable. Generally, terminations are not used in electrical drives and hence, this causes further EMI problems. The proper cable symmetry and shielding have also a remarkably effect on the EMI properties of a variable-speed electrical drive [12]. In this case, a symmetric and shielded motor power cable (MCCMK) is applied. In a cable of this kind, the core consists of three equal-size insulated power conductors cabled together in triangular form with the ground wire surrounding them.

In practice, an output filter is used to slow the du/dt times in adjustable-speed drives. Consequently, the stress effects on the motor insulation materials, bearing currents, and shaft voltages [13] are reduced. The output filter remarkably increases the impedance level to the frequency converter in the HF band due to the serial line inductances. A high impedance level complicates the propagation of both the CM and DM noise currents. The EMI noise can only pass the output filter through the stray capacitances or the mutual inductances, which do not have as low an impedance path as the direct path without the output filter. On the other hand, the output filter has single resonance frequencies, at which the impedance is extremely low. However, the output filter attenuates the CM and DM EMI noise currents.

Also a motor has its own stray capacitances. A simplified motor model is presented in Fig. 3. In practice, there are three motor windings, which have stray capacitances of their own between each other and between the ground in the similar way as in the cabling. The stray capacitances between the two stator windings are negligible, because the stray capacitance values between a stator winding and the motor frame are notably larger than between two stator windings, which is a consequence of the stator windings are embedded into slots of the stator core [8].

As shown previously, a frequency converter acts as an effective DM noise filter for the HF signal. It also filters the CM HF signal, but because of using protective earth in signalling, the frequency converter does not totally prevent it. An output filter may be the biggest obstacle for the CM noise current propagation. Filter characteristics are verified with the laboratory measurements. The HF signal propagation can be modelled for instance with a port model [14], [15].

## Power Line Communication in Motor Cable

To enable the data transmission in the motor cable, the communication signal level has to be higher than the noise in the data transmission frequencies produced by the frequency converter. On the other hand, in spread-spectrum technologies, such as direct-sequence spread spectrum (DSSS), the transmitted signal takes up more bandwidth than the information signal that is being modulated. In consequence, the system has a process gain, which is the ratio of the spread bandwidth to the original bandwidth. The process gain

makes it possible to use weaker signal levels compared to the noise levels. The process gain can be expressed as follows [16]:

$$G_{\mathrm{p}} = 10\log_{10}\left(\frac{\text{transmitted signal bandwidth}}{\text{original data bandwidth}}\right)(\text{dB}). \qquad (7)$$

In order to be able to couple the PLC modems to the motor cable of an adjustable-speed drive, coupling interfaces have to be developed. Two different capacitive coupling interfaces have been developed for PLC in a motor cable; one for the coupling between a single phase lead and the PE, and another differentially between two phase leads (patent pending). The couplings can be considered to be connected to the motor cable in the same way as the CM (L1, PE) or DM (L1, L2) noise sources illustrated in Fig. 1. Hence, it may be assumed that the EMI noise currents produced by the modems to be pure CM or DM noise current sources that are dependent only on the way of coupling. In practice, the couplings produce both CM and DM noise current, and the signal coupling determines which one is dominating. The advantage of the differential coupling over another method is that it does not use the PE in signalling at all. Next, the measurements are carried out to confirm the noise current levels on the motor cable and particularly on the low voltage grid.

## Laboratory Equipment and Tests

The conducted noise levels are measured with a Rohde & Schwarz EHSHS 30 EMI Test Receiver and with a Rohde & Schwarz EZ-17 current probe. The test receiver is set to peak detect mode and the intermediate filter of the receiver is set to the bandwidth of 10 kHz. To ensure the settling of the filter and the detector circuit in the test receiver, a measurement time of 20 ms was used for each 10 kHz measuring band. Due to the measurement method (peak detect mode), the situation can be regarded as the worst case of conducted noise levels. The test environment is constructed in the Laboratory of Power Electronics at Lappeenranta University of Technology. The test equipment structure and the current measurement locations are illustrated in Fig. 4. The electrical drive consists of a frequency converter, an output filter (du/dt filter), a 90-meter long low-voltage power cable (Pirelli MCCMK 3x35+16), and a 15 kW induction motor. The frequency converter uses IGBTs, and it has a fixed switching frequency of 4 kHz. The PLC modems are connected to the motor end and to the output filter terminals. The transmit power of the PLC modems is approximately 10 mW.
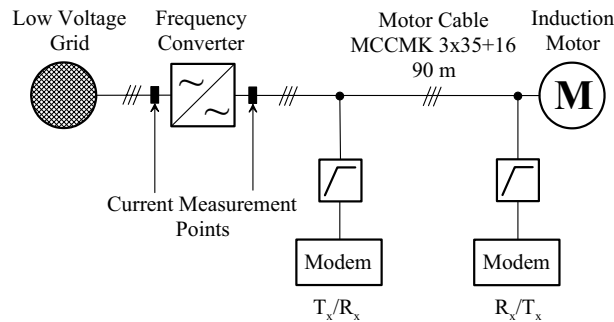
Fig. 4: Test equipment and the current measurement points

In Figs. 5 and 6, the measured DM and CM noise current spectrums produced by a frequency converter and a PLC modem are illustrated, respectively. The DM and CM currents are measured from a single phase conductor (L1) and from all three phase conductors (L1, L2, L3) of the du/dt filter output, respectively. The blue curve represents the situation when data is transmitted, while the red one indicates

the situation when the data transmission is not active. The frequency converter is active in both cases. The signal produced by the modems is coupled to the motor power cable differentially between two phases (L1, L2). According to Fig. 5, the modem increases the DM noise current level between 15−30 dB(μA) in the frequency band of approximately 4−21 MHz, which is the applied band in HomePlug 1.0. Fig. 5 shows deep notches that are the sub-bands, in which the carrier frequencies are permanently masked to avoid the amateur radio bands. All the available carrier frequencies are seemed to be in use. According to Fig. 6, the data transmission increases the CM noise current less than 10 dB(μA) in the frequency bands of approximately 5−12 MHz and 14−21 MHz. Hence, it is shown that data transmission does not produce a considerable CM noise current if the modems are coupled differentially to the power cable.



Fig. 5: DM noise currents produced by a frequency converter and a PLC modem. The noise current is measured from a single phase conductor (L1) of the output of the du/dt filter. The red curve is the noise current generated by the frequency converter and the blue one generated by the frequency converter and the HomePlug 1.0 modem with signal coupling (L1, L2)



Fig. 6: CM noise currents produced by a frequency converter and a PLC modem. The noise current is measured from all three phase conductors (L1+L2+L3) of the output of the du/dt filter. The red curve is

the noise current generated by the frequency converter and the blue one generated by the frequency converter and the HomePlug 1.0 modem with signal coupling (L1, L2)

In Figs. 7 and 8, the measured DM and CM noise current spectra produced by a frequency converter and a PLC modem are illustrated, respectively. The DM and CM currents are measured from a single phase conductor (L1) and from all three phase conductors (L1, L2, L3) of the frequency converter input on the supplying low voltage grid, respectively. The blue and green curves represent the situation when data is transmitted in the motor cable, while the red one illustrates the situation when the data transmission is not active. The frequency converter is active in all the cases. The blue curve is for the signal coupling (L1, L2) and the green one for the signal coupling (L1, PE). According to Fig. 7, differentially coupled power line communication modems do not produce apparently DM noise current to the supplying low voltage grid. The frequency converter effectively filters the communication signal. In addition, the du/dt filter used in the system assists the filtering. The situation is similar also for signal coupling (L1, PE). The erroneous illustration is caused by the measurement method, because it also measures the CM noise current in addition to the DM noise current. The situation is explained by Fig. 8, in which it can be seen that the signal coupling (L1, PE) produces a CM noise current to the low-voltage grid through the frequency converter; this increases CM noise current by 20 dB($\mu$A) at certain frequencies. This increase is due to the use of PE wire in signalling. The PE forms a low-impedance path for noise currents. The noise current also needs a return route that is formed through the stray capacitances, the impedances of which are low enough. Differentially coupled power line communication modems do not produce a CM noise current to the supplying low-voltage grid either.
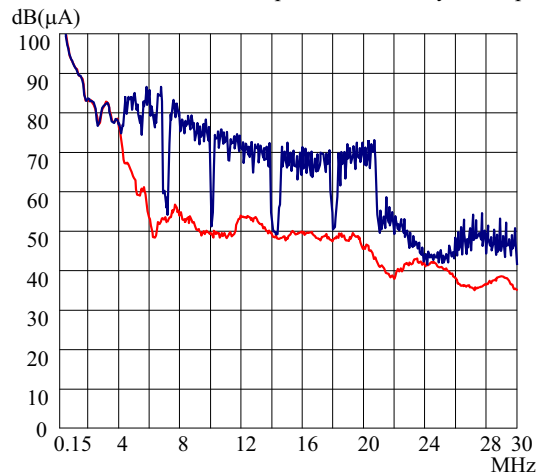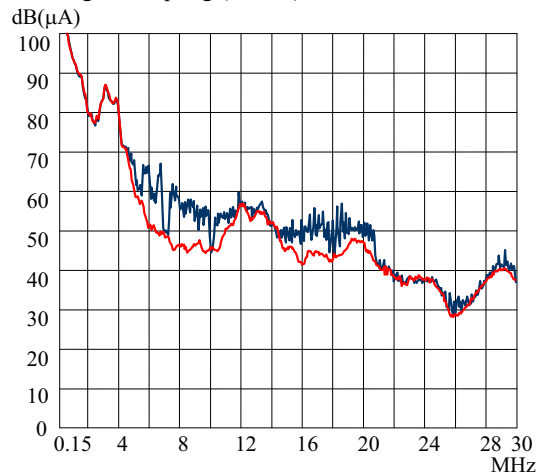


Fig. 7: DM noise currents produced by a frequency converter and a PLC modem. The noise current is measured from a single phase conductor (L1) of the input of the frequency converter on the supplying low voltage grid. The red curve is the noise current generated by the frequency converter. In other cases, data transmission is active in the motor power cable between a motor and a du/dt filter. The blue curve indicates the signal coupling (L1, L2) and the green one the signal coupling (L1, PE)
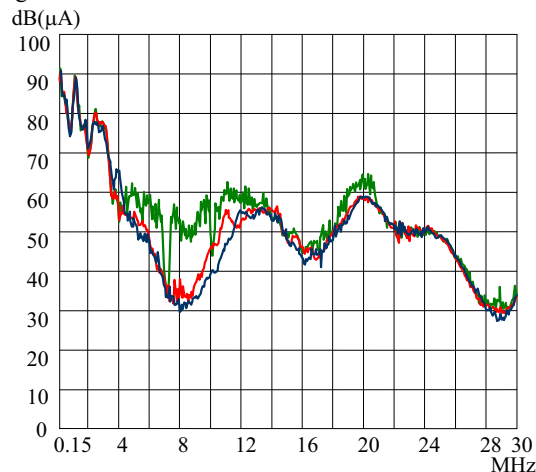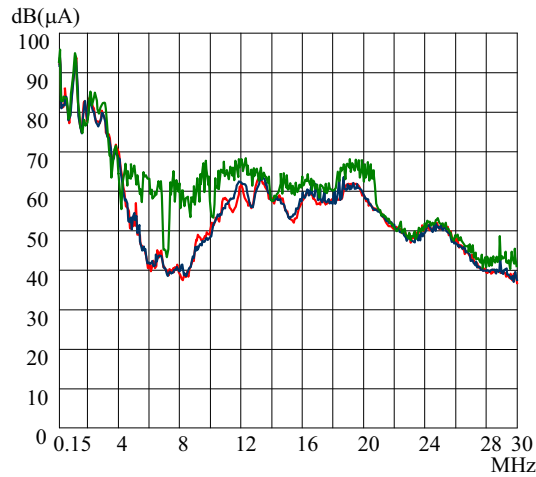
dB(μA)



Fig. 8: CM noise currents produced by a frequency converter and a PLC modem. The noise current is measured from all three phase conductors (L1+L2+L3) of the input of the frequency converter on the supplying low voltage grid. The red curve is the noise current generated by the frequency converter. In other cases, data transmission is active in the motor power cable between a motor and a du/dt filter. The blue curve indicates the signal coupling (L1, L2) and the green one the signal coupling (L1, PE)

According to the measurements, the differential signal coupling showed its strengths. In practice, if possible, it is advisable to bind the signal differentially between two phase leads. In the differential signal coupling, the PE conductor is not used for signalling at all, and hence the earth currents produced by other devices do not disturb communication. Yet another advantage is that the main route is not undefined, as it is when using PE conductor in signalling. In general, differential signal coupling is used in computer networks and in field buses, such as Profibus [17] and Modbus [18]. However, differential signal coupling produces a slight CM noise current to the motor power cable. Here, the most noteworthy point is that the communication signal does not propagate through the frequency converter to the low voltage grid at all. Hence, communication devices can cause no conducted noise to other devices in the low voltage network. A frequency converter can be regarded as a fire wall for motor cable communications. Using a PE wire in signalling, it causes CM mode noise to the low voltage grid. This may or may not disturb some victim devices. In the future, it is worth considering carrying out further measurements on the radiated HF noise produced by the PLC modems.

## Conclusion

Nowadays, data transmission is possible in a motor cable even in adjustable-speed drives. Data transmission utilizes frequencies up to 30 MHz. Adjustable-speed drives have always caused both conducted and radiated EMI problems to victim devices. This paper addresses the HF signal propagation from the motor power cable through a frequency converter to a low voltage grid. Conducted noise currents depend on the coupling of a noise source. Hence, two totally different coupling interfaces are studied in the viewpoint of conducted noise current; one is for coupling between two phase leads (DM) and the other between a phase and PE wire (CM). The HF signal is produced by standard HomePlug 1.0 modems. The modems produce DM signal only. The main parasitic impedances, which are vital for HF noise current propagation, are also discussed. According to the measurements, differentially coupled power line communication signal does not propagate to the low voltage grid. This is evident because the inverter stage, the DC link, and the rectifier bridge have multiple low-impedance paths for eliminating the HF DM

signal. The frequency converter and its output filter together are sufficient for block DM HF noise current. However, the CM noise current finds a path with a low enough impedance through the frequency converter, even if an output filter that has significant serial inductances is used; this phenomenon occurs when the PE conductor is used in signalling.

## References

[1] M. K. Lee, R. E. Newman, H. A. Latchman, S. Katar, and L. Yonge, "HomePlug 1.0 Powerline Communication LANs – Protocol Description and Performance Results, version 5.4," *International Journal of Communication Systems*, 2000, 00:1-6, pp. 1−25.

[2] HomePlug AV White Paper, HomePlug® Powerline Alliance, Available at www.homeplug.org, Accessed on Oct. 2006, Copyright© 2005, pp. 1−11.

[3] J. Ahola, A. Kosonen, J. Toukonen, and T. Lindh, "A New Approach to Data Transmission between an Electric Motor and an Inverter," in *Proc. of International Symposium on Power Electronics, Electrical Drives, Automation and Motion (SPEEDAM)*, Taormina (Sicily), Italy, May 2006, pp. 126−130.

[4] Gary L. Skibinski, Russel J. Kerkman, and Dave Schlegel, "EMI Emissions of Modern PWM ac Drives," *IEEE Industry Applications Magazine*, Vol. 5, No. 6, Nov./Dec. 1999, pp. 47−81.

[5] Pertti Silventoinen, *Electromagnetic Compatibility and EMC-Measurements in DC-Voltage Link Converters*, Dissertation, Lappeenranta University of Technology, Electrical Engineering, 2001, ISBN 951-764-588-0.

[6] Erkuan Zhong, and Thomas A. Lipo, "Improvements in EMC Performance of Inverter-Fed Motor Drives," *IEEE Transactions on Industry Applications*, Vol. 31, No. 2, Nov./Dec. 1995, pp. 1247−1256.

[7] Satoshi Ogasawara, and Hirofumi Akagi, "Analysis and Reduction of EMI Conducted by a PWM Inverted-Fed AC Motor Drive System Having Long Power Cables," in *Proc. of IEEE 31st Annual Power Electronics Specialists Conference (PESC'00)*, Vol. 2, 2000, pp. 928−933.

[8] Satoshi Ogasawara, Hideki Ayano, and Hirofumi Akagi, "Measurement and Reduction of EMI Radiated by a PWM Inverted-Fed AC Motor Drive System," *IEEE Transactions on Industry Applications*, Vol. 33, No. 4, Jul./Aug. 1997, pp. 1019−1026.

[9] Eugenio Gubia, Pablo Sanchis, Alfredo Ursúa, Jesús López, and Luis Marroyo, "Frequency Domain Model of Conducted EMI in Electrical Drives," *IEEE Power Electronics Letters*, Vol. 3, No. 2, Jun. 2005, pp. 45−49.

[10] Henry W. Ott, *Noise Reduction Techniques in Electronic Systems*, John Wiley & Sons, 2nd edition, Chichester, England, 1988, ISBN 0-471-85068-3.

[11] Jero Ahola, *Applicability of Power-Line Communications to Data Transfer of On-Line Condition Monitoring of Electrical Drives*, Dissertation, Lappeenranta University of Technology, Electrical Engineering, 2003, ISBN 951-764-783-2.

[12] Ettore J. Bartolucci, Bob H. Finke, "Cable Design for PWM Variable-Speed AC Drives," *IEEE Transactions on Industry Applications*, Vol. 37, No. 2, Mar./Apr. 2001, pp. 415−422.

[13] Shaotang Chen, and Thomas A. Lipo, "Bearing Currents and Shaft Voltages of an Induction Motor Under Hard- and Soft-Switching Inverter Excitation," *IEEE Transactions on Industry Applications*, Vol. 34, No. 5, Sep./Oct. 1998, pp. 1042−1048.

[14] T. C. Banwell, S. Galli, "A New Approach to the Modeling of the Transfer Function of the Power Line Channel," in *Proc. of the 5th International Symposium on Power-Line Communications and its Applications (ISPLC2001)*, Malmö, Sweden, Apr. 2001, pp. 319−324.

[15] T. Esmailian, F. R. Kschischang, and P. G. Gulak, "An In-building Power Line Channel Simulator," in *Proc. of the 6th International Symposium on Power-Line Communications and its Applications (ISPLC2002)*, Athens, Greece, Mar. 2002, 5 pages, CD-ROM.

[16] Ian A. Glover, and Peter M. Grant, *Digital Communications*, Pearson Education Ltd., 2nd edition, Harlow, England, 2004, ISBN 0-13-089399-4.

[17] Profibus, Available at http://www.profibus.com/pb/, Accessed on May 2007.

[18] Modbus, Available at http://www.modbus.org/, Accessed on May 2007.

# Publication VII

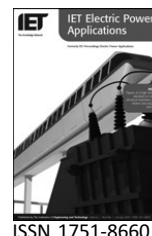A. Kosonen, M. Jokinen, J. Ahola, M. Niemelä, and J. Toukonen

**Ethernet-Based Broadband Power Line Communication between Motor and Inverter**

# Ethernet-based broadband power line communication between motor and inverter

A. Kosonen[1]   M. Jokinen[1]   J. Ahola[1]   M. Niemelä[1]
J. Toukonen[2]

[1]Department of Electrical Engineering, Lappeenranta University of Technology, PO Box 20, Lappeenranta FI-53851, Finland
[2]ABB Service, ABB Product and System Service, PO Box 52, FI-37101 Nokia, Finland
E-mail: antti.kosonen@lut.fi

**Abstract:** In variable-speed electrical drives, data transmission between an electric motor and an inverter is required because of sensors installed at the motor. Sensor information is used both in the motor control and in the diagnostics. For example, a data transmission medium can be implemented either by additional cabling or through the power cable. However, additional cabling is neither a cost-effective nor even a reliable solution. Previously, only a few application-specific solutions for data transmission via power cables have been presented. A general method to implement a broadband and Ethernet-based communication medium between a motor and an inverter is proposed here. The method forms an Ethernet-supported packet-based communication medium over the motor power cable. Ethernet supports all kind of protocols implemented above the link layer. The channel and noise characteristics are described. According to these, a coupling interface is developed that allows installing the communication device safely to a three-phase inverter-fed motor power cable. A channel capacity analysis is also performed. Laboratory measurements are carried out and analysed with the proposed method, and two possible applications are discussed.

## 1 Introduction

On-line condition monitoring is becoming a general feature in all kinds of industrial and consumer appliances, which requires sensors to be installed at the appliance. Traditionally, separate instrumentation cabling has been used for signalling, in which the cost can be from $60 up to $6000 per metre installed in an industrial environment [1]. In general, inverters are centralised in an industrial environment, and hence a 100-m-long motor power cable is not unusual in low-voltage drives. In addition to power delivery, the motor cable can be used as a communication medium. The costs of the implementation of the proposed method can be compared with the prices of any Ethernet-based consumer electronics and the number of components required in the coupling interfaces.

In the literature, only a few application-specific papers have focused on the application of a motor power cable as a communication medium in inverter-fed electrical drives.

These include only the physical-layer presentation. An on-line winding temperature monitoring system for an inverter-fed induction machine using its power cable as a communication medium is described in [2]. The communication bandwidth is 9600 b/s with 3.5 and 6.5 MHz frequency shift keying (FSK) modulation frequencies. A motor cable is also used as a feedback channel for an encoder signal in the real-time control of a servosystem [3]. Also an FSK modulator is applied at 15 V level on the transmitter side. According to [3], with this configuration it is possible to reach a communication rate above 40 kb/s, but the paper does not define the length of the motor cable. By the authors, broadband communication in an inverter-fed motor cable is presented in [4–6], and its utilisation in real-time induction motor control application in [7–9]. In addition, there are also a few papers that concern the power line communication (PLC) in a motor cable, but in these inverter-fed electrical drives are excluded. The normal low-voltage grid and CENELEC [10] frequencies (3–148.5 kHz) are applied in

[11]. Articles [12–14] concentrate merely on servosystems, in which the DC bus lines are utilised in communications.

In this paper, a broadband PLC method that offers a reliable communication medium is described and analysed. The method can be generally applied in the inverter-fed electrical drives. A coupling interface is developed, which filters the noise, but passes the communication signal with low attenuation. Laboratory experiments are carried out to verify the proposed method. Also two possible applications, on-line condition monitoring and real-time motor control, are presented and their requirements are discussed.

The structure of the paper is following. A motor cable as a communication channel and an inverter as a noise source are described in Section 2. Section 3 deals with the standardised broadband PLC method (HomePlug 1.0) and the designed coupling interface for a three-phase motor power cable. The results from the experimental tests carried out by the proposed PLC method are presented in Section 4. Two possible applications for the proposed method are presented in Section 5. The main contributions of the study are summarised in Section 6.

## 2 Communication channel

The proposed data transmission concept is illustrated in Fig. 1a. This can be simplified to the general model of a power line channel described in Fig. 1b. The model consists of a channel and noise model. According to the model, the received signal $r(t)$ is given by:

$$r(t) = s(t) * h(t) + n(t) \tag{1}$$

in which $s(t)$ is the injected signal to the channel by the transmitter, $h(t)$ the impulse response of the channel and
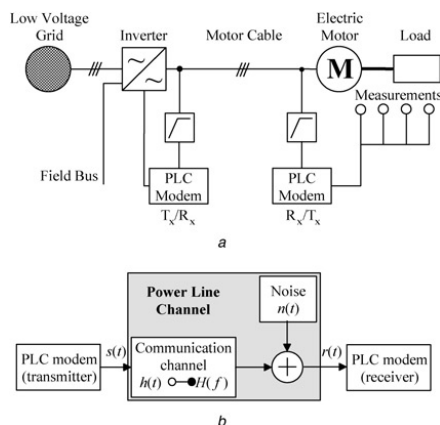


**Figure 1** *Data transmission concept and its channel model*
*a* Data transmission concept between an electric motor and inverter. The motor power cable is used as a medium for PLC
*b* General model of a power line channel

$n(t)$ the noise signal at the receiver end. Generally, signal attenuation and noise are important elements in a communication system. Hence, the channel and noise characteristics are studied next in detail.

### 2.1 Channel characteristics

The mains network is supplied by a transformer or a generator, whereas the output of a pulse width modulation (PWM) inverter-fed power cable is supplied by semiconductor switching components, which results in totally different impedance characteristics [2]. In this application, the motor power cable forms the medium for communications. Typically, the cables in variable-speed drives are three-phase symmetric ones and shielded because of electromagnetic interference (EMI) problems [15]. According to [6], the main cable parameters that affect the performance of PLC are the characteristic impedance $Z_0$, the attenuation coefficient $\alpha(f)$ and the cable length $L$. The cable attenuation is primarily caused by the polyvinyl chloride insulation material. Typical low-voltage power cable lengths are <100 m, but lengths above 200 m are also possible [11]. The cable is terminated at both cable ends. At the inverter end, the cable is terminated by either an output filter ($du/dt$) or the output stage of an inverter, which may consist of insulated gate bipolar transistors (IGBTs) or thyristors depending on the power rating of the electrical drive. Correspondingly, at the other end, the cable is terminated by an electric motor. Both of these can be considered as imperfect termination impedances, which lead to an impedance mismatch at the both cable ends. Also the PLC modems are coupled to the three-phase motor power cable at the both ends by coupling interfaces. The input impedances of electrical motors and the characteristic impedance of power cables are discussed in the frequency domain, for instance, in [11] and [16]. The impedance mismatches cause signal reflections, and thereby multi-path propagation. The reflection coefficient $\Gamma_R$ at the cable end can be written as:

$$\Gamma_R = \frac{Z_L - Z_0}{Z_L + Z_0} \tag{2}$$

where $Z_L$ is the load impedance and $Z_0$ the characteristic impedance of a cable.

In general, PLC channels are modelled in the frequency domain by an echo model, the parameters of which are obtained by measurements [17, 18]. However, in this application, the channel structure is simple, and thus the typical frequency characteristics of individual components can be parameterised and estimated. Therefore, it is convenient to model the channel attenuation by two-port models like done in [19].

In various electrical drives, the channel consists of similar components, and there are no branches. Some measurements of the channel voltage amplification with
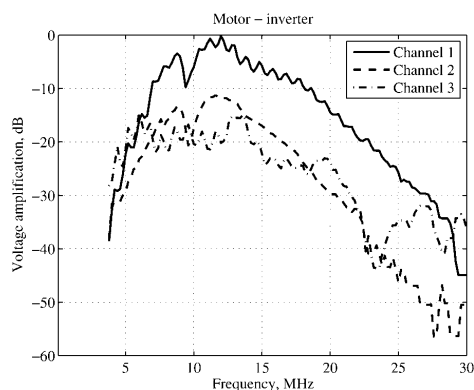
different components are illustrated in Fig. 2. The influence of cable length can be seen comparing the Channels 1 and 2.

## 2.2 Noise source

According to [20], power lines do not represent an additive white Gaussian noise (AWGN) channel. According to [21], the interference scenario of PLC is rather complicated, because the noise consists of five different variations: coloured background noise, narrowband noise, periodic impulsive noise asynchronous or synchronous to the network frequency (50/60 Hz) and asynchronous impulsive noise.

In this application, the main noise source is the output stage of an inverter, which can be considered an aperiodic impulsive noise source regardless of the implementation of the control method. The output voltage of an inverter basically consists of pulses or square waves with a variable frequency and duration [2]. In modern industrial PWM drives, the output voltage rise or fall times ($du/dt$) of IGBTs are in the range of $0.1-10 \mu s$, and the switching frequencies vary between 2 and 20 kHz [15]. Each switching injects a surge wave, the frequency content of which may reach to several megahertz, into the motor power cable. In practice, an output filter can be used to slow down the $du/dt$ times, and consequently, the stress effects on the motor insulation materials, bearing currents, and shaft voltages are reduced [22].

The amplitude of impulsive noise can be even twice the DC link voltage because of the result of the cable oscillation [11]. A measured inverter output voltage waveform is illustrated in Fig. 3, from where it can be

noticed that the power content is at highest around the output and switching frequencies. The power content of noise starts to lower after the cable oscillation frequency of 105 kHz, and the fall stops at 400 kHz. The peaks in the amplitude spectrum are mainly caused by the voltage rising edges. At megahertz frequencies, the power content is at a reasonable level, which makes it possible to use these frequencies for communication. In an inverter application, the frequency band of communication has to be chosen carefully, because it is always a compromise between the noise power at the lower frequency band and the signal attenuation at the higher frequency band.
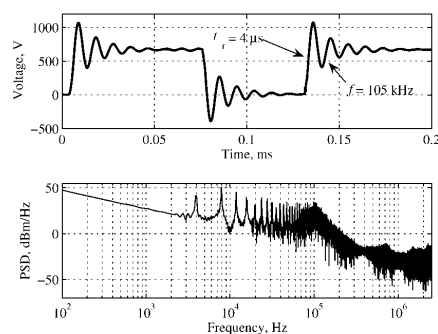
## 2.3 Channel capacity analysis

The information delivery capacity of the channel depends on the signal-to-noise ratio at the receiver end and the available frequency band for data transmission. According to the information theory by C. E. Shannon, the information delivery capacity of a communication channel is:

$$C = B \log_2 \left( 1 + \frac{S}{N} \right) \qquad (3)$$

where $C$ represents the information delivery capacity of the channel (in b/s), $B$ the available bandwidth and the symbols $S$ and $N$ are the signal and noise powers at the receiver end, respectively. The theory is not directly applicable to the analysis of a power line channel, because the signal-to-noise ratio is frequency dependent in a practical channel, and in Shannon's theory, the assumption is based on the AWGN channel. However, the main idea is to obtain the indicative estimate of the channel capacity.

According to [11], the output voltage of the transmitter $|U_{tx}(f)|$ can be presented by the output power of the



**Figure 2** Channel voltage amplification from the motor to the inverter with different components including the proposed coupling interface at the both ends

Channel 1: an inverter, output filter, 200 kW induction motor and 90 m motor cable. Channel 2: similar as Channel 1, but with a 200 m motor cable. Channel 3: an inverter, output filter, 15 kW induction motor and 90 m motor cable



**Figure 3** Measured voltage between phase leads (L1, L2) at the inverter end and its frequency content

The mains voltage is 500 V. The switching of an inverter output stage generates steeply rising ($t_r = 4 \mu s$) surge waves followed by the cable oscillation ($f = 105$ kHz). The energy content is at highest around the mains and switching frequencies, and also near the cable oscillation frequency. The noise includes frequency components up to several megahertz

transmitter $P_{\mathrm{tx}}(f)$ and the input impedance of the communication channel at the transmitter end $Z_{\mathrm{in,tx}}(f)$

$$|U_{\mathrm{tx}}(f)| = \left| \sqrt{\frac{P_{\mathrm{tx}}(f)}{\cos \varphi(f)} Z_{\mathrm{in,tx}}(f)} \right| \qquad (4)$$

where $\cos \varphi(f)$ is the phase angle of the input impedance $Z_{\mathrm{in,tx}}(f)$. The voltage of the received signal $|U_{\mathrm{rx}}(f)|$ can be written as follows

$$|U_{\mathrm{rx}}(f)| = |H(f)| \cdot |U_{\mathrm{tx}}(f)| \qquad (5)$$

where $|H(f)|$ is the transfer function of the communication channel. The noise voltage at the receiver end $|U_{\mathrm{n,rx}}(f)|$ can be measured in the time domain from the coupling interface at the receiver end and then filtered it by 84 narrow band pass filters similarly as implemented in HomePlug 1.0 described in Section 3.1. The root mean square value of the noise voltage can now be calculated individually for every sub-carrier. The information capacity of the power line channel can be described according to the signal and noise voltages

$$C = \int_{f_{\mathrm{l}}}^{f_{\mathrm{h}}} \log_2 \left[ 1 + \left( \frac{|U_{\mathrm{rx}}(f)|}{|U_{\mathrm{n,rx}}(f)|} \right)^2 \right] \mathrm{d}f \qquad (6)$$

where $f_{\mathrm{h}}$ and $f_{\mathrm{l}}$ are the highest and lowest frequency of the applied band, respectively, and $\mathrm{d}f$ the bandwidth of a single sub-carrier. An estimated channel capacity as a function of transmitted power for Channel 3 in the frequency band of 4.49–20.7 MHz is presented in Fig. 4, which indicates that the motor cable of an inverter drive offers a broadband communication channel for the frequency band used, even if the transmitted power is in the range of milliwatts. The
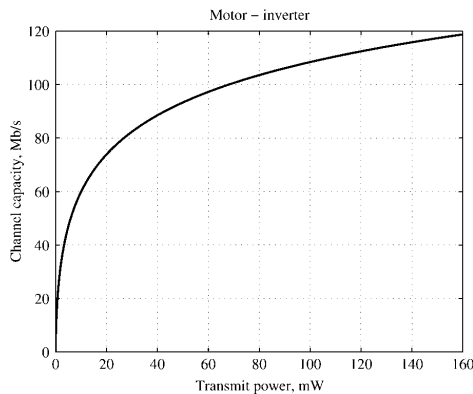


**Figure 4** *Estimated channel capacity as a function of transmitted power for Channel 3 in the frequency band of 4.49–20.7 MHz*

Distance between transmitter and receiver is 90 m and the signal coupling is (L1, L2). The transmitter is at the motor end and the receiver at the inverter end

transmitted power is distributed with a flat power spectrum even if the noise and channel characteristics are both frequency dependent.

# 3 Data transmission system

## 3.1 Overview for HomePlug 1.0 specification

The first broadband PLC specification, HomePlug 1.0 [23], was published in 2001 by the HomePlug® Powerline Alliance. The aim of the technology is to connect devices to each other through the power lines in a home. With the Ethernet connection, the protocol forms an Ethernet link over the power line. It encapsulates the Ethernet frames (IEEE 802.3) into its own protocol [24] and transmits them to the power line. From the viewpoint of Ethernet devices, the PLC modems are transparent. The HomePlug 1.0 specification defines both the physical (PHY) and medium access control (MAC) layers. The PHY of HomePlug 1.0 uses adaptive orthogonal frequency division multiplexing (OFDM) with a cyclic prefix (CP) in the band between $\sim$4.49 and 20.7 MHz. This band is divided into 84 sub-carriers, while eight of these are permanently masked to avoid amateur radio bands. The PHY of HomePlug 1.0 consists of forward error correction (FEC) coding, interleaving, error detection, automatic repeat request (ARQ) and three variants of phase shift keying modulation techniques. The PHY periodically adapts into the current channel conditions by avoiding poor sub-carriers and selecting an appropriate modulation method, and an FEC rate for the remaining sub-carriers. The data rates of the PHY may vary from 1 to 14.1 Mb/s, which corresponds to the rates in the MAC layer of 0.7 and 8.08 Mb/s, respectively [25]. Correspondingly, the maximum throughput at the transmission control protocol/internet protocol (TCP/IP) layer is 6.3 Mb/s. The transmission PSD is restricted to $-50$ dB m/Hz in HomePlug 1.0 [24]. This results in a total transmit power, injection losses excluded, of $\sim$10 mW. The total power consumption of a HomePlug compliant modem is about 5 W, which can be powered, for example, inductively from the motor power cable at the motor end.

## 3.2 Coupling interface

In this application, there is no point to completely attenuate the noise peaks caused by the inverter switching transients, because it would lead to an increased filter order, increased losses, complicated structure, and new resonant frequencies. Hence, it was decided to filter the noise to a certain level by a simple LC filter and then to clip the rest of the impulse voltage to a level that is not harmful to a communication circuit anymore. The OFDM symbol can last long enough to be received correctly even if a short impulse noise occurs during the data transmission. Also FEC coding can correct single and burst errors. The OFDM technique in PLC channels is analysed in [26].

There are two coupling methods available: capacitive and inductive. The coupling method depends on the way the isolation from the mains voltage is carried out. Approximately below the frequency of 100 MHz, a conventional coupling capacitor seems to be a suitable alternative, while only at frequencies of hundreds of megahertz a feed-through capacitor, which could be a foil that surrounds the conductor, is applicable because of its very low capacitance value. The main difference between these two capacitive couplings is that the latter one can be connected without interrupting the mains voltage. Inductive coupling has to be fitted according to the line current to avoid saturation, and it is not suitable for frequencies of hundreds of megahertz because of the collapse of magnetic properties, or for a low frequency band because of high cost. In medium voltage (over 1000 V) applications, it seems to be feasible to use inductive coupling because of the size and cost of the coupling capacitors.

The topology of the proposed capacitive coupling interface is illustrated in Fig. 5. It filters the voltage component of the mains frequency and impulsive noise generated by the switching of an inverter. It passes the frequencies used in communications with low attenuation at both the transmitter and receiver ends. In addition, the coupling interface protects a PLC device from overvoltage peaks and realises a galvanic isolation between the circuit of data transmission and the circuit of a motor cable. The coupling interface is coupled to a three-phase motor cable differentially between two phases, such as (L1, L2), (L1, L3) or (L2, L3).

The capacitors provide the isolation from the mains voltage of a motor cable and operate together with inductors, and the magnetizing inductance of the transformer as a high-pass filter. The galvanic isolation is carried out by the signal transformer. The middle point of
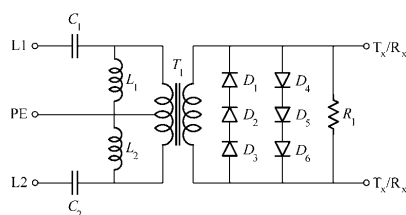


**Figure 5** *Proposed capacitive coupling interface for a three-phase inverter-fed motor cable*

PLC signal is coupled differentially between two phases. The coupling interfaces can be generally applied with modern PLC techniques that use megahertz frequencies at both the transmitter and receiver ends. The electrical parameters are as follows: $C_1 = C_2 = 680$ pF, $L_1 = L_2 = 0.7$ μH, the magnetising inductance of the transformer ($T_1$) $L_m = 3.5$ μH, $R_1 = 10$ kΩ. Diodes $D_1, \ldots, D_6$ are small signal diodes and they act as a transient protection

the transformer and the other sides of the inductors are bound together and connected to the protective earth (PE). Hence, the signal can be injected differentially between two phases of a three-phase motor cable. According to [27], differential signal coupling does not produce a visible common-mode voltage component, which would be seen as a current in the PE wire or in other earth loops. A small load impedance is problematic for the capacitive coupling, because it is connected in parallel to the grid.

The component selection plays an important role in this application. The maximum rating voltage of the capacitors has to be taken into account, because, for example, the voltage amplitudes can be even higher than 2 kV in an inverter-fed electrical drive connected to a 690 V mains network because of the cable oscillation. The transformer and inductors can be built by double aperture ferrite cores, because they are suitable for HF applications. In this application, the ferrite material has to be selected to minimise the imaginary part of the complex permeability at the selected frequencies. Complex permeability is defined as follows

$$\mu(f) = \mu'(f) + j\mu''(f) \quad (7)$$

where $\mu'$ is the real and $\mu''$ the imaginary part of permeability. The real and imaginary parts of permeability define the ability of a material to produce magnetising flux and its losses, respectively. Overvoltage protection is carried out by clipping the voltage peaks passing the coupling interface to a certain maximum level. The transient protection is implemented by small signal diodes that are divided into two parallel branches: one is forward biased and the other is reverse biased. The protection causes parallel capacitance of the magnitude of picofarads. Three small signal diodes are connected in series to increase the forward voltage, which is about 0.7 V for each diode.

The filtered inverter noise (Fig. 3) measured from the terminals of the proposed coupling interface is illustrated in Fig. 6. The noise pulse lasts about 6 μs, whereas 8.4 μs is reserved for a single OFDM symbol and for CP in HomePlug 1.0 [24]. This means in practice that the symbol may get broken and has to be re-transmitted (if it cannot be corrected by FEC coding) if these occur simultaneously.

## 4 Experimental results

The operation of the proposed data transmission method was verified by laboratory measurements. Extensive results and test setups are presented in [4–6]. The current spectra, which include noise and signal spectra, measured from a phase conductor are illustrated in Fig. 7. The HomePlug 1.0 modems were coupled to the motor cable by the proposed coupling interface. According to Fig. 7, the HomePlug 1.0 modems increase the peak current about 15–30 dB(μA) in the whole data transmission band they
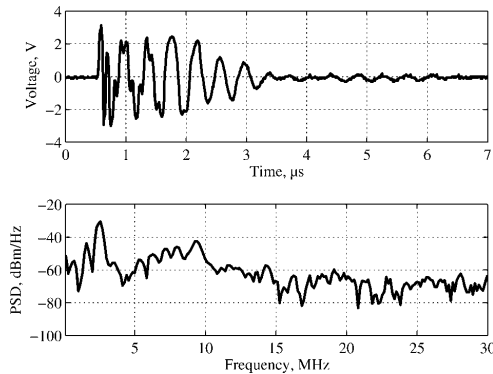
**Figure 6** *Filtered noise signal in the time- and frequency-domain produced by the switching of the inverter output stage (Figure 3)*

Frequency response approximation is computed by fast Fourier transform. The coupling interface is coupled between two phases (L1, L2) at the inverter end

used. The permanently masked amateur radio frequencies can be clearly seen in the band.

The bandwidth of the data transmission was tested by two laptops and file transmission protocol (FTP) software, which works above the TCP/IP layer. Modems were located at both ends of the motor power cable according to Fig. 1, and they were connected to the laptops by RJ-45 cables (Ethernet). The throughput was measured with different drives. The changeable parameters were the following: the type of an inverter, an output filter, a communication direction, the length of a motor power cable, a motor and an earth loop. The throughput results are presented in Fig. 8. For
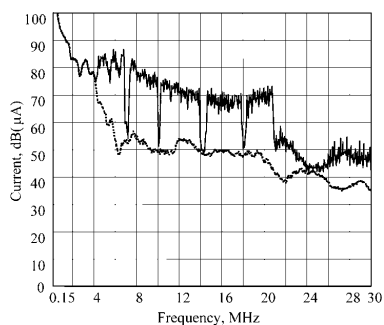


**Figure 7** *Current spectra measured from a phase conductor at the output of the du/dt filter*

Measurement is carried out by a Rohde & Schwarz EHSHS 30 EMI Test Receiver and a Rohde & Schwarz EZ-17 current probe. The measurement setup: 150 kHz−30 MHz frequency, 10 kHz bandwidth and 20 ms measurement time for each band, peak detect mode. The noise and signal + noise spectra are indicated with dashed and solid lines, respectively
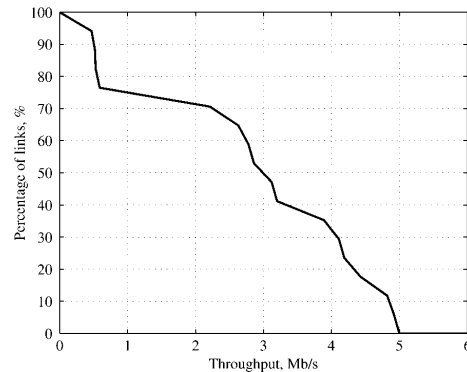


**Figure 8** *Percentage of links against throughput. The number of tested configurations was 16*

example, over 2 Mb/s transmission rates are reached in 70 % of the cases.

The latency of the proposed method is mainly caused by the processing time of the packet-based protocol. In this application, the data transmission is of point-to-point type, and hence the variation of the latency is mainly caused by the re-transmitted packet because of the lost or corrupted packets that cannot be reconstructed by the ARQ mechanism. According to [6], the channel quality directly affects the latency, and especially its variation in hostile channel conditions (<1 Mb/s). However, the average end-to-end data transmission delay remains still below 10 ms even if the data transmission rate is already below 1 Mb/s.

## 5 Applications

### 5.1 On-line condition monitoring

According to [4], the continuous evaluation of the healthiness of an appliance is known as on-line condition monitoring. Surprising damages of the system can be prevented by predictive maintenance, and hence expensive production losses can be avoided. According to [5], low-voltage electric motors and generators are usually sold without on-line self-diagnostics. The number of motors is vast in industry; for example a single wood processing plant may contain thousands of electric motors. Electric motors are not the only devices that can be monitored, but also appliances such as pumps, blowers and other machines driven by an electric drive. Condition monitoring of electric motors requires a data transmission medium between the motor and the inverter or the motor controller. The PLC is a competitive alternative to instrumentation cablings, because the installation cost of the instrumentation cabling may be as high as the power cabling. The instrumentation cabling also has to meet the same environmental requirements as the power cabling, which may further increase the cost.

According to [28], the vibration measurement that is used for envelope spectrum analysis produces about 500 kb of data, and hence the required average transmission rate for an interval of 4 h leads to the rate of 40 b/s. Other measurements used in the on-line induction motor condition monitoring produce less information than the vibration measurement. Therefore, the proposed method can be applied for transferring the information of several sensors without any problem. The proposed method can also be applied to improve the estimates of the sensorless control methods; for example, the inaccuracy of the motor model can be reduced by transmitting the temperature of the stator through the motor cable. This requires neither a wide bandwidth nor strict latency characteristics. In addition, even a real-time video can be transmitted via the motor cable; this is already verified by the authors.

## 5.2 Real-time motor control

The latency of Ethernet is non-deterministic because of the carrier sense multiple access with collision detection (CSMA/CD) bus reservation mechanism. This causes problems in real-time applications, which require deterministic response, such as in control applications. According to [29], in applications that require a time delay <1 ms, Ethernet is not a practical solution. The utilisation of Ethernet in industrial applications has been studied extensively, for instance, in [30–32]. The utilisation of Ethernet in distributed motion control is discussed in [33], in which the rotor feedback speed information of a brushless DC motor is delivered between the speed controller and the frequency converter by using a 10 Mb/s Ethernet local area network (LAN) and a frame size 64 bytes.

A real-time induction motor speed control applying the proposed method and the motor power cable as a feedback channel is discussed in [7–9]. The feedback information was sampled 500 times per second. The sampling frequency was limited by the computation power of a PLC modem. The frequency of the transmitted data packets is the problem, but not the data transmission bandwidth. According to [7], the test system, PLC excluded, causes a latency of 4 ms. The average latency of feedback information, $\tau_{avg} = 8$ ms, is small compared with the mechanical time constant of the test system, $\tau_{test} = 0.7$ s, but still some problems will occur in the real-time speed control of an induction motor. The delay varies between 6 and 12 ms. The PLC itself is not the problem, but the packet-based data transmission, and the fact that the packets, which cannot be corrected, are re-transmitted by the ARQ mechanism. The easiest way to compensate the feedback latency is to tune the gains of the speed controller experimentally. The performance of the test system is also compared with the commercial product with speed feedback and the sensorless control method discussed in [9]. The feedback information channel of the commercial product is implemented with a direct encoder cable, and there is almost no delay. The results showed clearly the potential of the proposed method, although the stiffness to load disturbances is decreased compared with the commercial product. Next, the authors implemented a disturbance observer in a control loop [34]. The disturbance observer significantly increased the stiffness to load disturbances, and there would not be any remarkable difference between the proposed and traditional feedback method to the load disturbances.

In the literature, there have been presented numerous methods, which take into account the delay of the process, such as internal model control tuning [35], and also methods, which compensate the delay, such as Smith predictor [36] and a model based on a predictive PI controller [37]. Common to these methods is that they assume the delay to be significant, constant and known. They are also sensitive to the accuracy of the estimated delay. When the estimate and the real delay of Smith predictor diverge by more than 20 % from each other, the response of the system is unacceptable [38].

## 6 Conclusion

A standard Ethernet-based communication method, which utilises the power cable between a motor and an inverter, is proposed. The channel and noise characteristics are described. Based on these, a coupling interface that filters the inverter noise, but passes the communication signal with a low attenuation, is developed. The coupling interface is designed for connecting the communication modem differentially between two phase to the three-phase power cables. The channel capacity analysis is also carried out. In addition, experimental results and two applications are presented.

## 7 Acknowledgments

## 8 References

[1] BROOKS T.: 'Wireless technology for industrial sensor and control networks'. Proc. ISA/IEEE Sensors for Industry Conf., Rosemont, IL, USA, November 2001, pp. 73–77

[2] CHEN S., ZHONG E., LIPO T.A.: 'A new approach to motor condition monitoring in induction motor drives', IEEE Trans. Ind. Appl., 1994, 30, (4), pp. 905–911

[3] COAKLEY N.G., KAVANAGH R.C.: 'Real-time control of a servosystem using the inverter-fed power lines to communicate sensor feedback', IEEE Trans. Ind. Electron., 1999, 46, (2), pp. 360–369

[4] AHOLA J., TOUKONEN J., KOSONEN A., LINDH T., SÄRKIMÄKI V.: 'Electric motor cable communication overcomes the biggest obstacle in on-line condition monitoring'. Proc. Condition Monitoring 2005 Conf. (COMADIT), Cambridge, UK, July 2005, pp. 105−110

[5] AHOLA J., TOUKONEN J., KOSONEN A., LINDH T., TIAINEN R.: 'Ethernet to electric motor − via mains cable'. Proc. Int. Congress and Exhibition on Condition Monitoring and Diagnostic Engineering Management (COMADEM), Cranfield, UK, August/September 2005, pp. 525−534

[6] AHOLA J., KOSONEN A., TOUKONEN J., LINDH T.: 'A new approach to data transmission between an electric motor and an inverter'. Proc. Int. Symp. on Power Electronics, Electrical Drives, Automation and Motion (SPEEDAM), Taormina (Sicily), Italy, May 2006, pp. 126−130

[7] KOSONEN A., JOKINEN M., SÄRKIMÄKI V., AHOLA J., NIEMELÄ M.: 'Motor feedback speed control by utilizing the motor feeder cable as a communication channel'. Proc. Int. Symp. on Power Electronics, Electrical Drives, Automation and Motion (SPEEDAM), Taormina (Sicily), Italy, May 2006, pp. 131−136

[8] KOSONEN A., JOKINEN M., AHOLA J., NIEMELÄ M.: 'Real-time induction motor speed control with a feedback utilizing power line communications and motor feeder cable in data transmission'. Proc. Ann. Conf. IEEE Industrial Electronics Society (IECON), Paris, France, November 2006, pp. 638−643

[9] KOSONEN A., JOKINEN M., AHOLA J., NIEMELÄ M.: 'Performance analysis of induction motor speed control method that utilizes power line communication', *Int. Rev. Electr. Eng.*, 2006, **1**, (5), pp. 684−694

[10] EN 50065-1 : 'Signaling on low voltage electrical installations in the frequency range from 3 kHz to 148.5 kHz' (GENELEC, Brussels, 1991)

[11] AHOLA J.: 'Applicability of power-line communications to data transfer of on-line condition monitoring of electrical drives', PhD Thesis, Lappeenranta University of Technology, Electrical Engineering, 2003

[12] LIU C., WADE E., ASADA H.H.: 'Reduced-cable smart motors using DC power line communication'. Proc. 2001 IEEE Int. Conf. on Robotics and Automation, Seoul, Korea, May 2001, pp. 3831−3838

[13] WADE E., ASADA H.H.: 'One-wire smart motors communicating over the DC power bus-line with application to endless rotary joints'. Proc. 2002 IEEE Int. Conf. on Robotics and Automation, Washington, DC, USA, May 2002, pp. 2369−2374

[14] WADE E., ASADA H.H.: 'Reduced cable smart motors communicating over the DC power bus-line for high degree of freedom systems'. Proc. 2003 IEEE/RSJ Int. Conf. on Intelligent Robots and Systems, Las Vegas, NE, USA, October 2003, pp. 1987−1991

[15] BARTOLUCCI E.J., FINKE B.H.: 'Cable design for PWM variable-speed AC drives', *IEEE Trans. Ind. Appl.*, 2001, **37**, (2), pp. 415−422

[16] SCHLEGEL D., WRATE G., KERKMAN R., SKIBINSKI G.: 'Resonant tank motor model for voltage reflection simulations with PWM drives'. Proc. IEEE Int. Electrical Machines and Drives Conf. (IEMD), Seattle, USA, May 1999, pp. 463−465

[17] PHILLIPS H.: 'Modelling of power-line communication channels'. Proc. Int. Symp. on Power-Line Communications and Its Applications (ISPLC), Lancaster, UK, March/April 1999, pp. 14−21

[18] ZIMMERMANN M., DOSTERT K.: 'A multipath model for the Powerline channel', *IEEE Trans. Commun.*, 2002, **50**, (4), pp. 553−559

[19] KOSONEN A., AHOLA J., JOKINEN M.: 'Modelling the RF signal propagation in the motor feeder cable'. Proc. Nordic Workshop on Power and Industrial Electronics (NORPIE), Lund, Sweden, June 2006, p. 5

[20] GÖTZ M., RAPP M., DOSTERT K.: 'Power line channel characteristics and their effect on communication system design', *IEEE Commun. Mag.*, 2004, **42**, (4), pp. 78−86

[21] ZIMMERMANN M., DOSTERT K.: 'Analysis and modeling of impulsive noise in broad-band Powerline communications', *IEEE Trans. Electromagn. Compat.*, 2002, **44**, (1), pp. 249−258

[22] CHEN S., LIPO T.A.: 'Bearing currents and shaft voltages of an induction motor under hard- and soft-switching inverter excitation', *IEEE Trans. Ind. Appl.*, 1998, **34**, (5), pp. 1042−1048

[23] HomePlug Powerline Alliance, available at: http://www.homeplug.org,accessed May 2007

[24] LEE M.K., NEWMAN R.E., LATCHMAN H.A., KATAR S., YONGE L.: 'HomePlug 1.0 Powerline communication LANs − protocol description and performance results', *Int. J. Commun. Syst. on Powerline Commun.*, 2003, **16**, (5), pp. 447−473

[25] LIN Y., LATCHMAN H.A., NEWMAN R.E., KATAR S.: 'A comparative performance study of wireless and power line networks', *IEEE Commun. Mag.*, 2003, **41**, (4), pp. 54−63

[26] BABIC M., BAUSCH J., KISTNER T., DOSTERT K.: 'Performance analysis of coded OFDM systems at statistically

representative PLC channels'. Proc. Int. Symp. on Power-Line Communications and Its Applications (ISPLC), Orlando, FL, USA, March 2006, pp. 104–109

[27] KOSONEN A., AHOLA J., SILVENTOINEN P.: 'Measurements of HF current propagation to low voltage grid through frequency converter'. Proc. European Conf. on Power Electronics and Applications (EPE), Aalborg, Denmark, September 2007, p. 10

[28] TIAINEN R., SÄRKIMÄKI V., LINDH T., AHOLA J.: 'Estimation of the data transfer requirements of vibration and temperature measurements in induction motor condition monitoring'. Proc. European Conf. on Power Electronics and Applications (EPE), Dresden, Germany, September 2005, p. 10

[29] SAMARANAYAKE L., ALAHAKOON S., WALGAMA K.: 'Speed controller strategies for distributed motion control via Ethernet'. Proc. IEEE Int. Symp. on Intelligent Control (ISIC), Houston, USA, October 2003, pp. 322–327

[30] FELSER M.: 'Ethernet TCP/IP in automation a short introduction to real-time requirements'. Proc. IEEE Int. Conf. on Emerging Technologies and Factory Automation, Antibes-Juan les Pins, France, October 2001, pp. 501–504

[31] SAMARANAYAKE L., ALAHAKOON S.: 'Closed-loop speed control of a brushless DC motor via Ethernet'. Proc. Ann.

Technical Conf. of IEEE, Colombo, Sri Lanka, September 2002, p. 8

[32] DECOTIGNIE J.D.: 'A perspective on Ethernet – TCP/IP as a Fieldbus'. Proc. IFAC Int. Conf. on Fieldbus Systems and Their Applications (FeT), Nancy, France, November 2001, pp. 138–143

[33] SAMARANAYAKE L., LEKSELL M., ALAHAKOON S.: 'Real-time speed control of a brushless DC motor via Ethernet'. Proc. Nordic Workshop on Power and Industrial Electronics (NORPIE), Stockholm, Sweden, August 2002, p. 6

[34] JOKINEN M., KOSONEN A., NIEMELÄ M., AHOLA J., PYRHÖNEN J.: 'Disturbance observer for speed controlled process with non-deterministic time delay of feedback information'. Proc. Ann. IEEE Power Electronics Specialists Conf. (PESC), Orlando, FL, USA, June 2007, pp. 2751–2756

[35] MORARI M., ZAFIRIOU E.: 'Robust process control' (Prentice Hall, Englewood Cliffs, NJ, 1986), p. 488

[36] SMITH O.J.M.: 'Closed control of loops with dead time', Chem. Eng. Progress, 1957, 53, pp. 217–219

[37] HÄGGLUND T.: 'An industrial dead-time compensating PI controller', Contr. Eng. Prac., 1996, 4, (6), pp. 749–756

[38] SCHNEIDER D.M.: 'Control of processes with time delays', IEEE Trans. Ind. Appl., 1988, 24, (2), pp. 186–191

**ACTA UNIVERSITATIS LAPPEENRANTAENSIS**

**283.**   BOTAR-JID, CLAUDIU CRISTIAN. Selective catalytic reduction of nitrogen oxides with ammonia in forced unsteady state reactors. Case based and mathematical model simulation reasoning.  2007.  Diss.

**284.**   KINNUNEN, JANNE. Direct-on-line axial flux permanent magnet synchronous generator static and dynamic performance.  2007.  Diss.

**285.**   VALTONEN, MIKKO. Performance characteristics of an axial-flux solid-rotor-core induction motor.  2007.  Diss.

**286.**   PUNNONEN, PEKKA. Impingement jet cooling of end windings in a high-speed electric machine.  2007.  Diss.

**287.**   KÄRRI, TIMO. Timing of capacity change: Models for capital intensive industry.  2007. Diss.

**288.**   TUPPURA, ANNI. Market entry order and competitive advantage of the firm.  2007.  Diss.

**289.**   TARKIAINEN, ANSSI. Field sales management control: Towards a multi-level theory. 2007.  Diss.

**290.**   HUANG, JUN. Analysis of industrial granular flow applications by using advanced collision models.  2007.  Diss.

**291.**   SJÖMAN, ELINA. Purification and fractionation by nanofiltration in dairy and sugar and sweetener industry applications.  2007.  Diss.

**292.**   AHO, TUOMO. Electromagnetic design of a solid steel rotor motor for demanding operation environments.  2007.  Diss.

**293.**   PURHONEN, HEIKKI. Experimental thermal hydraulic studies on the enhancement of safety of LWRs.  2007.  Diss.

**294.**   KENGPOL, ATHAKORN. An evalution of ICTs investment using decision support systems: Case applications from distributor's and end user's perspective group decision. 2007.  Diss.

**295.**   LASHKUL, ALEXANDER. Quantum transport phenomena and shallow impurity states in CdSb.  2007.  Diss.

**296.**   JASTRZĘBSKI, RAFAŁ PIOTR. Design and implementation of FPGA-based LQ control of active magnetic bearings.  2007.  Diss.

**297.**   GRÖNLUND, TANJA. Development of advanced silicon radiation detectors for harsh radiation environment.  2007.  Diss.

**298.**   RUOKONEN, MIKA. Market orientation in rapidly internationalizing small companies – evidence from the software industry.  2008.  Diss.

**299.**   OIKARINEN, TUIJA. Organisatorinen oppiminen – tapaustutkimus oppimisprosessien jännitteistä teollisuusyrityksessä.  2008.  Diss.

**300.** KARHULA, JUKKA. Cardan gear mechanism versus slider-crank mechanism in pumps and engines. 2008. Diss.

**301.** RAJAMÄKI, PEKKA. Fusion weld metal solidification: Continuum from weld interface to centerline. 2008. Diss.

**302.** KACHINA, ANNA. Gas-phase photocatalytic oxidation of volatile organic compounds. 2008. Diss.

**303.** VIRTANEN, PERTTU. Evolution, practice and theory of European database IP law. 2008.

**304.** TANNINEN, KATI. Diffusion of administrative innovation: TQM implementation and effectiveness in a global organization. 2008. Diss.

**305.** PUISTO, ANTTI. The initial oxidation of transition metal surfaces. 2008. Diss.

**306.** FELLMAN, ANNA. The effects of some variables on $CO_2$ laser-MAG hybrid welding. 2008. Diss.

**307.** KALLIOINEN, MARI. Regenerated cellulose ultrafiltration membranes in the treatment of pulp and paper mill process waters. 2008. Diss.

**308.** PELTOLA, SATU. Capability matrix – identifying and evaluating the key capabilities of purchasing and supply management. 2008. Diss.

**309.** HONKAPURO, SAMULI. Performance benchmarking and incentive regulation – considerations of directing signals for electricity distribution companies. 2008. Diss.

**310.** KORHONEN, KIRSI. Facilitating coordination improvement efforts in cross-functional process development programs. 2008. Diss.

**311.** RITVANEN, VIRPI. Purchasing and supply management capabilities in Finnish medium-sized enterprises. 2008. Diss.

**312.** PYNNÖNEN, MIKKO. Customer driven business model – connecting customer value to firm resources in ICT value networks. 2008. Diss.

**313.** AL-NAZER, RAMI. Flexible multibody simulation approach in the dynamic analysis of bone strains during physical activity. 2008. Diss.

**314.** The Proceedings of the 7th MiNEMA Workshop. Middleware for Network Eccentric and Mobile Applications. Ed. by Pekka Jäppinen, Jouni Ikonen and Jari Porras. 2008.

**315.** VÄÄTÄNEN, JUHA. Russian enterprise restructuring – the effect of privatisation and market liberalisation on the performance of large enterprises. 2008. Diss.

**316.** DABAGHMESHIN, MASHA. Modeling the transport phenomena within the arterial wall: Porous media approach. 2008. Diss.

**317.** HAIMALA, JUHA. Supplier's position in project marketing networks. 2008. Diss.

**318.** UOTILA, TUOMO. The use of future-oriented knowledge in regional innovation processes: Research on knowledge generation, transfer and conversion. 2008. Diss.